

High energy scattering in QCD

Tuomas Lappi

`tuomas.v.v.lappi@jyu.fi`

FYSS9000 lecture course, Jyväskylä, spring 2023

Contents

1	Introduction	3
1.1	Practicalities	3
1.2	Literature	3
1.3	Plan for classes	4
1.4	Preliminaries: high energy scattering	5
2	The diagrammatic way	14
2.1	The analytical S -matrix	14
2.2	One gluon exchange	21
2.3	Two gluon exchange	25
2.4	The Lipatov vertex	30
2.5	The BFKL equation	35
3	The eikonal way	44
3.1	Diffraction: scattering of scalar light off a plane	44
3.2	Eikonal scattering	49
3.3	Hybrid formalism for pA collisions	53
4	Deep inelastic scattering & high energy evolution	61
4.1	DIS in dipole picture	61
4.2	The photon light cone wave function	70
4.3	BK equation	78
5	Heavy ion collisions	86
5.1	Gluon saturation & CGC	86
5.2	Glasma	95
5.3	Bottom-up thermalization	102

Chapter 1

Introduction

1.1 Practicalities

Practicalities

<http://users.jyu.fi/~tulappi/heqcd23/>

Schedule We have 14 classes.

- Mostly blackboard lectures
- Will try to leave time to discuss exercises
- Exercises: question sheets handed out distributed in moodle, returned to moodle, graded by lecturer. Not every week: 4 sets.

Grading Exercises: 60%, final exam 40% (will be easy).

1.2 Literature

A large part of these lectures are based on courses lectured at the University of Jyväskylä: “High energy scattering in QCD” lectured in the spring of 2011, <http://users.jyu.fi/~tulappi/fysh560k111/> (original handwritten notes for the blackboard lectures are partly in Finnish.) and later a part of the course “QCD” lectured in the spring of 2014, <http://users.jyu.fi/~tulappi/fysh555k114/> (slides and handwritten lecture notes in English), and lectures on “Early stages of Heavy-Ion Collisions” at the 2018 ECT* Doctoral Training Program <https://indico.ectstar.eu/event/14/>

Literature

Mostly this course is based on the following books:

- [1] Y. V. Kovchegov and E. Levin, “Quantum chromodynamics at high energy,” [Camb. Monogr. Part. Phys. Nucl. Phys. Cosmol. 33 \(2012\)](#).
- [2] V. Barone and E. Predazzi, “High-Energy Particle Diffraction,” Springer 2002

An older book focusing on the BFKL equation is also a good reference for some parts of the lectures:

- [3] J. R. Forshaw and D. A. Ross, “Quantum Chromodynamics and the Pomeron,” Cambridge Lect. Notes Phys. **9** (1997), 1-248 Oxford University Press, 1998,

Potentially relevant are recent review articles:

- [4] F. Gelis, “Initial state and thermalization in the Color Glass Condensate framework,” Int. J. Mod. Phys. E **24** (2015) no.10, 1530008, [[arXiv:1508.07974](#) [[hep-ph](#)]]

- [5] J. L. Albacete and C. Marquet, “Gluon saturation and initial conditions for relativistic heavy ion collisions,” *Prog. Part. Nucl. Phys.* **76** (2014) 1 [[arXiv:1401.4866 \[hep-ph\]](#)]
- [6] S. Schlichting and D. Teaney, “The First fm/c of Heavy-Ion Collisions,” *Ann. Rev. Nucl. Part. Sci.* **69** (2019), 447-476, [[arXiv:1908.02113 \[nucl-th\]](#)].
- [7] J. Berges, M. P. Heller, A. Mazeliauskas and R. Venugopalan, “QCD thermalization: Ab initio approaches and interdisciplinary connections,” *Rev. Mod. Phys.* **93** (2021) no.3, 035003 [[arXiv:2005.12299 \[hep-th\]](#)].

and other slightly less new reviews and others:

- [8] E. Iancu and R. Venugopalan, “The Color glass condensate and high-energy scattering in QCD,” In *Hwa, R.C. (ed.) et al.: Quark gluon plasma* 249-3363 [[hep-ph/0303204](#)]
- [9] F. Gelis, E. Iancu, J. Jalilian-Marian and R. Venugopalan, “The Color Glass Condensate,” *Ann. Rev. Nucl. Part. Sci.* **60** (2010) 463 [[arXiv:1002.0333 \[hep-ph\]](#)]
- [10] T. Lappi, “Small x physics and RHIC data,” *Int. J. Mod. Phys. E* **20** (2011) no.1, 1 [[arXiv:1003.1852 \[hep-ph\]](#)]
- [11] H. Weigert, “Evolution at small x(bj): The Color glass condensate,” *Prog. Part. Nucl. Phys.* **55** (2005) 461 [[hep-ph/0501087](#)]
- [12] J. Jalilian-Marian and Y. V. Kovchegov, “Saturation physics and deuteron-Gold collisions at RHIC,” *Prog. Part. Nucl. Phys.* **56** (2006) 104 [[hep-ph/0505052](#)]
- [13] F. Gelis, T. Lappi and R. Venugopalan, “High energy scattering in Quantum Chromodynamics,” *Int. J. Mod. Phys. E* **16** (2007) 2595 [[arXiv:0708.0047 \[hep-ph\]](#)]
- [14] S. J. Brodsky, H. C. Pauli and S. S. Pinsky, “Quantum Chromodynamics and Other Field Theories on the Light Cone,” *Phys. Rept.* **301** (1998) 299 [[arXiv:hep-ph/9705477](#)].
- [15] C. Marquet, “Chromodynamique quantique à haute énergie, théorie et phénoménologie appliqué aux collisions de hadrons,” PhD thesis, in French (!) <http://tel.archives-ouvertes.fr/tel-00096416/fr/>
- [16] H. Hänninen, “Deep inelastic scattering in the dipole picture at next-to-leading order,” PhD thesis, [[arXiv:2112.08818 \[hep-ph\]](#)].

1.3 Plan for classes

Plan for classes

Note: lecture note in slightly different order. ...

1. Introduction: Sec. 1.4, 1-gluon exchange, eikonal vertex, Sec. 2.2
2. Diffraction of light, Sec. 3.1
3. The eikonal approximation in potential scattering, Sec. 3.2
4. “Hybrid formalism” of particle production in proton-nucleus collisions, Sec. 3.3
 - * Exercise set 1 until here
5. The analytical S-matrix, Sec. 2.1
6. 2-gluon exchange, Sec. 2.3
7. The Lipatov vertex, Sec. 2.4
8. The BFKL equation, Sec. 2.5

- * Exercise set 2 until here
- 9. Deep Inelastic scattering in the dipole picture, Sec. 4.1
- 10. Light Cone Perturbation theory and the photon wavefunction, Sec. 4.2
- 11. Soft gluon emission: the BK equation, Sec. 4.3
- * Exercise set 3 until here
- 12. Spacetime structure of the CGC color field, Sec. 5.1
- 13. The glasma, Sec. 5.2
- 14. Bottom-up thermalization in heavy ion collisions, Sec. 5.3
- * Exercise set 4 until here

1.4 Preliminaries: high energy scattering

1.4.1 Collider experiments

Collision systems

- $A+A \implies$ quark gluon plasma RHIC, LHC
- $p+p, p+A \implies$ particle production Tevatron, LHC
- $e+p, e+A$ (DIS) \implies p/A structure HERA, EIC

(Jargon: “A” = nucleus with mass number A, thus $p+A$ = proton-nucleus)

Building high energy colliders costs money, so there are not many experiments that are relevant for us. However, each of these has been and is a topic of interest for a large community of researchers.

Hadron colliders

- CERN SPS (Super Proton Synchrotron), started in 1976 with $p\bar{p}$ collisions, originally with $\sqrt{s} = 630\text{GeV}$, later upgraded to 900GeV . Notable collider experiments were UA1 and UA2. The SPS still continues its existence. It provides proton and nucleus beams to fixed target experiments (NA_{xx} , WA_{xx} with xx =some number, the acronyms stand for “North Area” and “West Area”). It is also a part of the LHC injector complex.
- Tevatron, at Fermilab, Illinois, near Chicago. Operated in 1983-2011, colliding $p\bar{p}$ originally at $\sqrt{s} \approx 1000\text{GeV}$, later improved to $\sqrt{s} \approx 1960\text{GeV}$
- RHIC (Relativistic Heavy Ion Collider) at Brookhaven, NY (near New York). RHIC collides different nuclei (the heaviest being Au) at $\sqrt{s} = 200A\text{GeV}$ (A is the mass number, for nuclei one always counts energies per nucleon). It also collides pp at energies up to $\sqrt{s} = 500\text{GeV}$ (could have easily done more, ask lecturer about politics), with a crucial element being the availability of spin-polarized proton beams.
- LHC: 2010 —
 - pp @ $\sqrt{s} = 7\text{TeV} \implies 14\text{TeV}$
 - $AuAu$ @ $\sqrt{s} = 2.76A\text{TeV} \implies 5.5\text{TeV}$

Lepton colliders

Lepton-lepton-colliders (less important for this course)

- SLAC SLD: e^+e^- @ $\sqrt{s} = 90\text{GeV}$

- LEP: 1989-2000: e^+e^- @ $\sqrt{s} = 91\text{GeV} \Rightarrow 209\text{GeV}$
- ILC $\sqrt{s} \sim \text{TeV}$ potentially in the future

Although the ILC is mainly meant to be a Higgs factory, it would also be interesting for high energy QCD. We will not discuss these processes in this course. What we will discuss, however, is that for QCD physics, a high energy lepton is primarily a source of photons, and high energy photons have an important hadronic component. In fact, for a theorist, a photon, especially a virtual one, is an ideal hadron, and its scattering is the perfect laboratory for QCD. One hint at this behavior is obtained by looking at the total cross sections in Fig. 1.1: the energy dependence of γ and p cross sections is very similar. They differ by a factor $\sim 1/137 = \alpha_{\text{e.m.}}$ from $p+p$ to $\gamma+p$ and another similar factor from $\gamma+p$ to $\gamma + \gamma$, because photon interactions always interact with the electric charge e , which is small ($e^2 = 4\pi\alpha_{\text{e.m.}}$ in natural units). But the energy dependence at high energy is similar, because it is dictated by similar QCD dynamics. Note that the $\gamma + \gamma$ cross sections in the plot are actually extracted from e^+e^- -collisions.

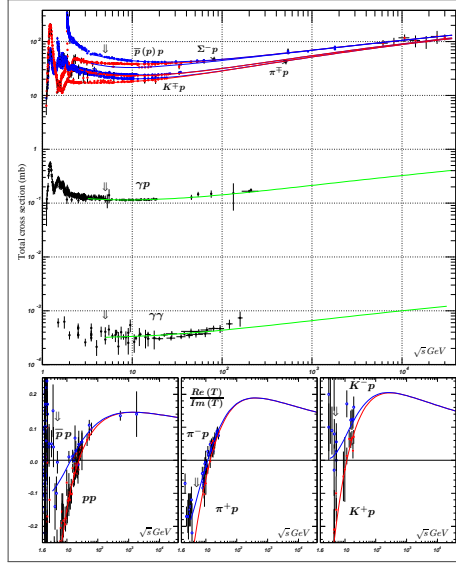


Figure 1.1: Total cross sections for different collision systems, from PDG [17]

Lepton-hadron colliders

Much more important for the purposes of this course are lepton-proton or lepton-nucleus collisions, i.e. Deep Inelastic Scattering (DIS) experiments. Relevant existing ones are

- Fixed target experiments, highest collision energies that have been achieved are $2\sqrt{1\text{GeV}} \times 465\sqrt{\text{GeV}} = 30\text{GeV}$ with a muon beam at Fermilab (these experiments have names like “the E665 experiment”).
- The HERA collider at DESY operated until 2007. In the final stage, after upgrades, it reached collision energies of $\sim 30\text{GeV}$ electrons on $\sim 900\text{GeV}$ protons, corresponding to $\sqrt{s} \sim 320\text{GeV}$

An important project for the future of QCD studies is the Electron-Ion Collider [18, 19] (EIC). It will have an electron beam of up to 18GeV colliding with the RHIC proton or heavy ion beam, with energies of up to 275GeV for protons or up to $\sim 100\text{AGeV}$ for ions. Thus the energy is lower than at HERA, but the EIC will have several other advantages:

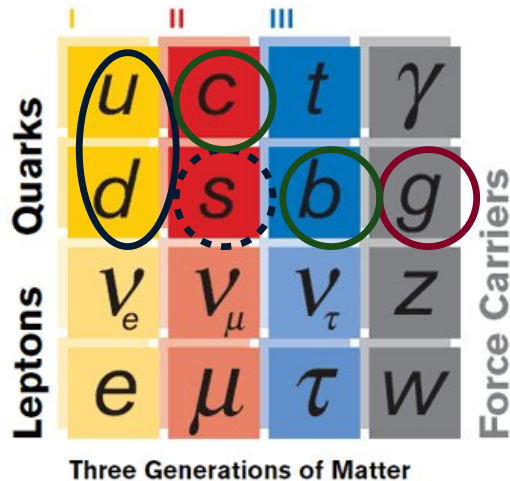
- Heavy ion beams
- Polarized (in spin) protons
- Much higher luminosity (i.e. more collisions, enabling the study of rarer processes)

There is also a proposal to build a Large Hadron-electron Collider (LHeC) by having the beam of a new electron accelerator colliding with the LHC beam. Such a machine could reach energies (for electron-proton collisions) of maybe even up to $\sqrt{s}_{pe} = 1.5\text{TeV}$ [20].

1.4.2 Partons and hadrons

Elementary particles

This is a course about quarks and gluons. We also care about photons, not for themselves, but because they can be used to study the quarks and, indirectly, gluons inside a proton and a nucleus.



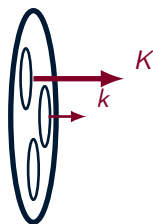
Important in this course

- Light quarks
- Heavy quarks
- gluons

(Top decays fast via weak interaction, different phenomenology)

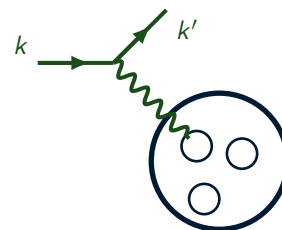
Bjorken's parton model is based on experimental observations of electron-proton scattering. As you might remember from Quantum Mechanics courses, the dependence of the cross section on momentum transfer can be understood as a Fourier-transform of the target. In low energy electron-proton elastic scattering, the cross section decreases exponentially (or as a Gaussian) in the momentum transfer. From this one can deduce that the proton has a finite size, roughly $\sim 10^{-15}\text{m}$. However, when one increases the scattering energy, the (inelastic) cross section starts to behave as a power in the momentum transfer, $\sim 1/Q^4$. This is indicative of scattering off point-like particles. In addition, from the angular dependence of the cross section one could deduce that these particles are spin 1/2. Bjorken postulated that when measured at high energies, i.e. short distances, the proton consists of almost free elementary pointlike constituents, and called them partons.

Partons, IMF



J.D. Bjorken: At high energy hadrons consist of pointlike constituents: "partons".

- Longit. momentum fraction x : $k = xK$
- Transverse momentum scale p_T or Q



Measured in *Deep Inelastic Scattering*

$$Q^2 = -(k - k')^2 = -q^2$$

$$x = \frac{Q^2}{2P \cdot (k - k')}$$

Bj scaling:

Q^2 -dependence is just like for a point-like particle.

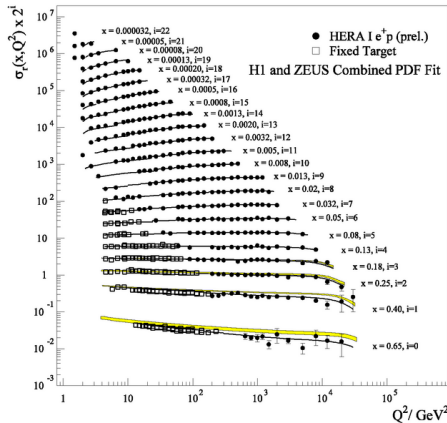
Here the “scale” Q can roughly be thought of as the inverse transverse size of the parton. In textbook calculations in the parton model, the partons are treated as collinear, i.e. they only have longitudinal but not transverse momentum, $k_T = 0$. The resolution scale Q is determined by the physical scattering process that one studies, for example for DIS it is given by the virtuality of the process. In fact it is better to really think of the parton, when measured in such a process as having $k_T \sim Q$. The feature that the parton really has $k_T \sim Q$, but nevertheless one can calculate as if it was collinear, as long as the parton distribution that the parton comes from depends on Q , is the magic of collinear factorization! In this course, we will go beyond collinear factorization: when discussing the CGC and the physics of gluon saturation it is essential to actually think and calculate of small- x gluons as having an intrinsic transverse momentum.

- Textbooks: partons collinear
- Now: partons have k_T

When Bjorken introduced the term “parton,” quarks and gluons were not yet known. Instead, Bjorken used the new word to describe some, so far unknown, elementary, pointlike constituents of the proton. Only later it became understood that partons are quarks and gluons. Today, one might consider the term “parton” to be a synonym of “quark and gluon”. But usually the term “parton” is used in a slightly more limited sense, meaning roughly “quarks and gluons as constituents of a proton or nucleus, especially one accelerated to near the speed of light.” If one is discussing e.g. the weak interaction, supersymmetry or the quark model for hadrons (i.e. with “constituent quarks”), one does not usually use the term “parton.”

Success of partonic picture

Bjorken scaling in inclusive ($ep \rightarrow \text{anything}$) DIS cross section:



- Free partons: horizontal lines
- Small deviations: understood in pQCD (= perturbative QCD)

However some things, like the total cross sections shown in Fig. 1.1, cannot be computed from the parton model. Also things like the complex phase of the scattering amplitude (also shown in the figure) matter in this course. This goes beyond a naive probabilistic interpretation of the parton model, which is only applicable at lowest order.

1.4.3 Perturbation theory: reminder from particle physics course

Cross section and scattering amplitude

- Initial state $|i\rangle$ is a multiparticle *Fock state*
- The time evolution operator from initial to final state is known as the “*S-matrix*”. Thus the final state of the system, after interactions (the collision) have taken place is $S|i\rangle$
- Usually one is interested in matrix elements of the *S-matrix* between specific states $S_{fi} \equiv \langle f|S|i\rangle$; while S is a Hilbert space operator, the matrix elements S_{fi} are just complex numbers.

- The square of the matrix element, i.e. the probability to transition from one state to the other, $P_{fi} = |S_{fi}|^2$ is related to the experimentally measurable quantity: the cross section $i \rightarrow f$

It is conventional to separate the case where nothing happens:

$$S = 1 + iT \quad (1.1)$$

(Separating the i is just a convention)

The 4-momentum is also always conserved. Thus it is also useful to separate

$$S_{fi} = \delta_{fi} + i(2\pi)^4 \delta^{(4)} \left(\sum p_f - \sum p_i \right) \underbrace{\mathcal{A}(i \rightarrow f)}_{\text{scattering amplitude}} \quad (1.2)$$

The cross section for a scattering process $a + b \rightarrow 1 + \dots + n$ with $s \equiv (p_a + p_b)^2$ is

$$d\sigma = \frac{1}{\Phi} |\mathcal{A}(i \rightarrow f)|^2 d\Pi_n \quad (1.3)$$

Here

- Φ is the flux factor; $\Phi \approx 2s$ when s is large (masses zero)
- $d\Pi_n$ is the n -particle invariant phase space

$$d\Pi_n = \prod_{m=1}^n \underbrace{\frac{d^4 p_m}{(2\pi)^4} (2\pi) \delta(p_m^2 - m_m^2)}_{\frac{d^3 p_m}{(2\pi)^3 2E_m}} (2\pi)^4 \delta^{(4)} \left(p_a + p_b - \sum_{i=1}^n p_i \right) \quad (1.4)$$

Note: 2π always follows the δ -function. Properties of the cross section

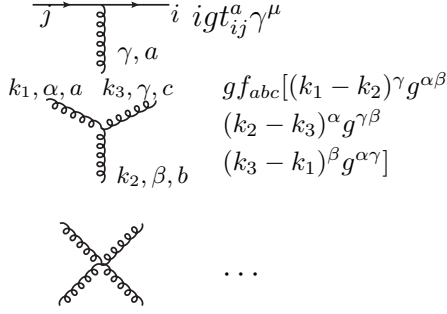
- Explicitly Lorentz-invariant
- The cross section is an *area* (it useful to check the dimensions from Eq. (1.3). It has a physical interpretation as probability to scatter integrated over transverse (with respect to the beam axis) *impact parameter* plane. Thus a cross section can be small either because the target is small, or because the interaction is weak.

Feynman rules

To get the scattering amplitude $i\mathcal{M}$, combine the following (i because $S = 1 + iT$)

- Propagators

.....	$\frac{i}{p^2 - m^2 + i\varepsilon}$ scalar
$\xrightarrow{\hspace{1cm}}$	$\frac{i}{\not{p} - m + i\varepsilon}$ fermion
$\sim\sim\sim\sim\sim\sim$	$\frac{-ig_{\mu\nu}}{p^2 + i\varepsilon}$ photon or gluon
$\circ\circ\circ\circ\circ\circ$	(Feynman gauge)
- Factors for external fermion or gauge boson lines
- Vertices



4. Internal lines

$$\int \frac{d^4 k}{(2\pi)^4} \quad (1.5)$$

Gauge theory

In this course we will be interested in QCD, which is a gauge theory. Many, but not all, of its features can be understood in terms of its simpler cousin QED.

QED

$$\text{Lagrangian } \mathcal{L} = -\frac{1}{4} F_{\mu\nu} F^{\mu\nu} + \bar{\psi} (i \not{\partial} - e \not{A} - m) \psi \quad (1.6)$$

QCD: add color $N_c = 3$

- Dirac matrix notation

$$\not{\partial} = a^\mu \gamma_\mu$$

- Field strength tensor

$$F_{\mu\nu} = \partial_\mu A_\nu - \partial_\nu A_\mu \text{ (linear in } A_\mu \text{)}$$

- Electric field

$$E^i = F^{i0} = F_{0i} \text{ (sign from } E^i = -\partial_i A^0 \text{)}$$

- Magnetic field

$$B^i = -\frac{1}{2} \varepsilon^{ijk} F^{jk}$$

- Quark color

$$\psi_i, i = 1, \dots, N_c$$

- Gluon color

$$A_\mu^a, a = 1, \dots, N_c^2 - 1 \equiv d_A$$

$$\mathcal{L} = -\frac{1}{4} F_{\mu\nu}^a F_a^{\mu\nu} + \bar{\psi}_i (i \not{\partial} \delta_{ij} + g \not{A}^a t_{ij}^a - m \delta_{ij}) \psi_j \quad (1.7)$$

Digression: Signs

In Peskin & Schröder, for QED, the covariant derivative is $i\partial_\mu - eA_\mu$, with $e = -|e|$ the charge of the particle, the electron. Then the Feynman rule for an electron vertex is $iQe\gamma^\mu = -iQ|e|\gamma^\mu$ with $Q = -1$ for the electron, i.e. for the electron the vertex is $i|e|\gamma^\mu$. We now use the rule $igt_{ij}^a\gamma^\mu$ and the covariant derivative $i\partial_\mu + gA_\mu$ for QCD in perturbative calculations, which is a little bit like saying that the quark color charge is negative (assuming $g > 0$). The lattice convention is $i\partial_\mu - gA_\mu$, which also appears in these notes.

Color matrices

Fundamental representation generators:

$$t_{ij}^a; i, j = 1, \dots, N_c; a = 1, \dots, N_c^2 - 1 \quad (1.8)$$

are $N_c^2 - 1$ traceless hermitian $N_c \times N_c$ matrices

$$\text{Normalization: } \text{tr } t^a t^b = \frac{1}{2} \delta^{ab} \quad (1.9)$$

$$\text{Structure constants } [t^a, t^b] = i f^{abc} t^c \quad (1.10)$$

$$\text{Matrix notation } A_\mu \equiv A_\mu^a t^a \quad ; \quad \mathcal{L} = -\frac{1}{2} \text{tr} F_{\mu\nu} F^{\mu\nu} + \bar{\psi} (i\cancel{\partial} + g\cancel{A} - m) \psi \quad (1.11)$$

Adjoint representation generators

$$(T^a)^{bc} = -if_{abc} \quad (1.12)$$

Adjoint and fundamental representation matrices:

$$V_F = \exp(i\alpha^a t^a) \quad \leftrightarrow \quad V_A = \exp(i\alpha^a T^a) \quad (1.13)$$

can be related by

$$(V_A)_{ab} = 2 \text{tr} t^a V_F t^b V_F^\dagger. \quad (1.14)$$

Often useful Fierz identity for summing over adjoint color indices

$$(t^a)_{ij} (t^a)_{kl} = \frac{1}{2} \delta_{il} \delta_{jk} - \frac{1}{2N_c} \delta_{ij} \delta_{kl} \quad (1.15)$$

Gauge invariance

Field strength tensor $F_{\mu\nu}$ cannot be as simple as QED, but has nonlinear part *gluon-gluon-interaction*

$$F_{\mu\nu} = \partial_\mu A_\nu - \partial_\nu A_\mu - ig[A_\mu, A_\nu] \quad (1.16)$$

Lagrangian is invariant under *gauge transformation*

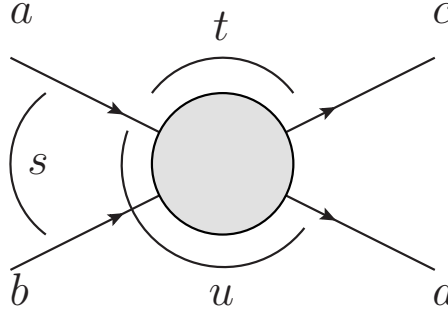
$$\Omega(x) \quad : \quad \mathbb{R}^4 \mapsto \text{SU}(N_c) \quad (1.17)$$

$$A^\mu(x) \rightarrow \Omega(x) A^\mu(x) \Omega^\dagger(x) + \frac{i}{g} \Omega(x) \partial^\mu \Omega^\dagger(x) \quad (1.18)$$

$$\psi(x) \rightarrow \Omega(x) \psi(x) \quad (1.19)$$

\mathcal{L} is invariant (exercise, particle physics course)

Mandelstam variables



(Remember $p_a + p_b = p_c + p_d$)

$$s = (p_a + p_b)^2 = (p_c + p_d)^2 \quad (1.20)$$

$$t = (p_a - p_c)^2 = (p_b - p_d)^2 \quad (1.21)$$

$$u = (p_a - p_d)^2 = (p_b - p_c)^2 \quad (1.22)$$

$$(1.23)$$

Only 2 independent:

$$s + t + u = m_a^2 + m_b^2 + m_c^2 + m_d^2 \quad (1.24)$$

Mandelstam variables are Lorentz-invariant

You can compute them from 4-vectors in any frame.

Differential cross section in manifestly Lorentz-invariant form

$$\frac{d\sigma_{ab \rightarrow cd}}{dt} = \frac{|\mathcal{M}_{ab \rightarrow cd}|^2}{16\pi s^2} \quad (m \approx 0) \quad (1.25)$$

Rapidity

Successive boosts in one direction with velocity v become easy if we define the *rapidity* ξ as $v = \tanh \xi$. Now for successive boosts $\xi = \xi_1 + \xi_2$. (exercise)

Momentum space rapidity y ; $v^z = \tanh y$

$$E = \sqrt{m^2 + p_T^2} \cosh y = m_T \cosh y \quad \mathbf{p}_T = (p^1, p^2) \quad (1.26)$$

$$p^3 = \sqrt{m^2 + p_T^2} \sinh y = m_T \sinh y \quad p_T^2 = \mathbf{p}_T^2 \quad (1.27)$$

When boosting with a boost ξ this behaves as you would expect ... (exercise)

The pseudorapidity η is defined by taking $m = 0$ in Eq. (1.27):

$$p^3 = p_T \sinh \eta \quad (1.28)$$

+ Pseudorapidity just depends on the scattering angle (different components of the 3-momentum), so it is easy to measure \Rightarrow it is the preferred quantity for experimentalists.

- Pseudorapidity is the same as rapidity y for massless particles.
- However, pseudorapidity does not Lorentz-transform easily for massive particles, it depends on the rest frame in a nontrivial way.

Light cone variables

We shall be interested in these lectures at particles traveling practically at the speed of light, at very high energy. In this case it is convenient to think of the scattering problem in a coordinate system well adapted to things traveling at the speed of light in the z - or 3-direction.

Light cone variables

For any 4-vector v^μ :

$$v^\pm = \frac{1}{\sqrt{2}} (v^0 \pm v^3) \quad (1.29)$$

Scalar product

$$x \cdot y = x^0 y^0 - x^3 y^3 - \mathbf{x} \cdot \mathbf{y} = x^+ y^- + x^- y^+ - \mathbf{x} \cdot \mathbf{y} \quad (1.30)$$

$$v^2 = (v^0)^2 - (v^3)^2 - \mathbf{v}^2 = 2v^+ v^- - \mathbf{v}^2 \quad (1.31)$$

Thus metric is

$$g_{\mu\nu} = \begin{pmatrix} 0 & 1 & 0 & 0 \\ 1 & 0 & 0 & 0 \\ 0 & 0 & -1 & 0 \\ 0 & 0 & 0 & -1 \end{pmatrix} = g^{\mu\nu} \quad (1.32)$$

Raising and lowering indices is not just a sign:

$$v^+ = v_- \quad v^- = v_+ \quad (1.33)$$

Be aware of the fact that there are two different conventions for the light cone variables. Here we use the Kogut-Soper (as in e.g. [21]) convention with factors $1/\sqrt{2}$. This is different from the Brodsky-Lepage convention (e.g. the review of Brodsky, Pauli and Pinsky [14] and the Kovchegov-Levin book [1]), where these factors are either 1 or 2 in various places. Also it is not 100% clear to me whether all authors associate the same meaning to indices being up or down.

High energy particle traveling in $+$ direction

$$p^+ \approx \sqrt{2}E \gg p^- = \frac{m^2 + \mathbf{p}^2}{2p^+} \quad (1.34)$$

Lorentz-invariant phase space

$$\frac{d^4 p}{(2\pi)^4} (2\pi) \delta(p^2 - m^2) = \frac{dp^+ dp^- d^2 \mathbf{p}}{(2\pi)^3} \delta(2p^+ p^- - \mathbf{p}^2 - m^2) = \frac{dp^+ d^2 \mathbf{p}}{(2\pi)^3} \frac{1}{2p^+} \quad (1.35)$$

Rapidity and light cone variables

$$k^+ = \frac{1}{\sqrt{2}} \sqrt{m^2 + k_T^2} e^y \quad (1.36)$$

$$k^- = \frac{1}{\sqrt{2}} \sqrt{m^2 + k_T^2} e^{-y} \quad (1.37)$$

Later in the course: Light cone quantization

Using light cone coordinates is just a change of variables and does not affect the physics in any way. However, the coordinate system is particularly useful in the context of light cone quantization [14, 1]. In ordinary (“instant form”) one quantizes the theory by imposing equal time ($t = t'$) commutation relations between Heisenberg theory time-dependent operators, and studies the evolution of the system in time t generated by a Hamiltonian H , which is the 0-component of a Lorentz 4-vector. In light-cone (or light front) quantization one treats instead the coordinate x^+ as the time coordinate (light cone time), and imposes canonical commutation relations at equal x^+ . The evolution of the Heisenberg picture operators is then generated by the light-cone Hamiltonian \hat{P}^- , which is the $-$ -component of a Lorentz 4-vector.

Chapter 2

The diagrammatic way

2.1 The analytical S -matrix

One concrete goal of this section is to learn what the energy-dependence of a total cross section (e.g. for $p + p \rightarrow X$ scattering) has to do with the real and imaginary parts of the elastic $p + p \rightarrow p + p$ scattering amplitude. We will also learn about unitarity-related techniques such as dispersion relations, that enable the calculation of the total scattering amplitude from just the imaginary part.

Before the discovery of QCD (1950's and especially 1960's) it was thought that the unitarity and analyticity of the S -matrix could be used to completely understand the structure of the strong interaction. Now we know that this is not the case, but an actual microscopical theory (QCD) is needed. This led to unitarity being relegated to a somewhat subsidiary role in the way quantum field theory is taught. Instead, the focus of most courses has been a more straightforward “draw all Feynman diagrams and calculate them” approach. However, more recently the most advanced high-order perturbative calculations again rely on unitarity: one calculates first imaginary parts of amplitudes which are easier to obtain (because they have less loop integrals) and then uses unitarity to obtain the total amplitude from them.

2.1.1 The S matrix as an analytical function

Let us consider a $2 \rightarrow 2$ scattering process. You recall that the kinematics for such a process is characterized by the 3 Mandelstam variables s, t, u (see Eqs. (1.20), (1.21) and (1.22)). Because of the linear relation between the variables (see Eq. (1.24)), only 2 of them can be treated as independent: we will choose these two to be s and t .

3 postulates

$$a + b \rightarrow c + d \quad (2.1)$$

- Lorentz-invariance $S(s, t)$
- Unitarity
- Analyticity

- Lorentz-invariance tells us that scattering amplitudes only depend on the Mandelstam variables, not on any single components of the momentum four-vectors.
- The unitarity of the S -matrix gives us relations between the real and imaginary parts of the scattering amplitudes, such as the optical theorem

$$\sigma_{\text{tot}} = \frac{1}{2s} 2 \text{Im } \mathcal{A}. \quad (2.2)$$

Here, unlike in Sec. 3.2, the $2 \rightarrow 2$ scattering amplitude \mathcal{A} is dimensionless, and there is a different overall factor in the optical theorem.

- Analyticity means that the S -matrix or scattering amplitudes are analytic functions of s and t treated as complex variables. This means that they can be analytically continued outside of the physically allowed area $s > 0, t < 0$ to different parts of the complex plane.

Digression: Cutkosky rules

The Cutkosky rules, based on the unitarity of the S -matrix, generalize the optical theorem. Let us briefly recall the basic idea. We start from the S -matrix for scattering from a state a to b :

$$S_{ba} = \delta_{ba} + i\mathcal{T}_{ba}. \quad (2.3)$$

Note the ordering of the indices: S is a matrix that operates on the incoming state $|a\rangle$ and gives an outgoing state $|b\rangle$, thus the indices are in the order “outgoing, incoming”. The matrix S is unitary:

$$\delta_{ca} = \sum_b S_{cb}^\dagger S_{ba} = \delta_{ca} + i\mathcal{T}_{ca} - i\mathcal{T}_{ca}^\dagger + \sum_b \mathcal{T}_{cb}^\dagger \mathcal{T}_{ba} \implies 2\text{Im } \mathcal{T}_{ca} = \sum_b \mathcal{T}_{cb}^\dagger \mathcal{T}_{ba} \quad (2.4)$$

For example the total cross section $a \rightarrow X$, summed over all final states, is obtained by setting $c = a$ as

$$\sigma_{a \rightarrow X} = \frac{1}{2s} \sum_b |\mathcal{T}_{ba}|^2 = \frac{1}{s} \text{Im } \mathcal{T}_{ca}, \quad (2.5)$$

where we have used the high energy approximation $2s$ for the flux factor. But we can use this relation more generally by taking $c \neq a$, and relate the imaginary part of the amplitude $a \rightarrow c$ to a sum over intermediate states b of amplitudes and complex conjugates $\mathcal{T}_{cb}^\dagger \mathcal{T}_{ba}$: this is calculating the “cut” of an amplitude.

In practice the sum over intermediate states b means the normal phase space integration. In generality one sums over all n -particle final states

$$\sum_b = \sum_n \int \prod_{i=1}^n \left[\frac{d^4 p_i}{(2\pi)^4} \delta(p_i^2 - m_i^2) \right] (2\pi) \delta^{(4)} \left(p_{\text{tot}} - \sum_i p_i \right) \quad (2.6)$$

where the total 4-momentum p_{tot} is the momentum of the multiparticle state a or c in Eq. (2.4). Because of energy-momentum conservation $p_{\text{tot}}^a = p_{\text{tot}}^c$. In practice of course at some given order in perturbation theory and for fixed states a and c , only a finite number of particles n are possible in the intermediate state.

So, let us now bravely go where no real physical particle has gone before, and consider the scattering amplitude \mathcal{A} for the process everywhere in the complex s plane. Assume for simplicity that all the particles a, b, c, d have the same mass m .

Now, the physical region for the process $a + b \rightarrow c + d$ is $s > 4m^2$; you can see this by going to the center of mass frame where $\vec{p}_a = -\vec{p}_b$ and $E_a = E_b > m$ so that $s = (E_a + E_b)^2 > 4m^2$. Thus, the total cross section, and consequently the imaginary part of the amplitude should be zero for $s < 4m^2$:

$$\begin{aligned} 0 < s < 4m^2 &\implies \text{no scattering} \implies \text{Im } \mathcal{A}(s, t) = 0 \\ &\implies (\mathcal{A}(s, t))^* = \mathcal{A}(s^*, t) \quad \text{“Schwartz reflection principle”} \end{aligned} \quad (2.7)$$

According to my sources (not all formulations of the Schwarz reflection principle are general enough, but see e.g. [here](#)), the actual statement for the Schwartz reflection principle is that if there are two domains that are reflections of each other around the real axis, and that have a common boundary formed by some interval of the real axis, then an analytical function on the union of these domains which has $\text{Im } f(z) = 0$ for z on this interval on the real axis satisfies $f(z)^* = f(z^*)$ on these domains in the complex plane.

Now let us look at some $s > 4m^2$, where the scattering is possible and thus the imaginary part of the scattering amplitude is nonzero. We’ll approach the real s axis from above, and express the imaginary part of the amplitude using $\text{Im } z = (z - z^*)/(2i)$ and the Schwarz reflection principle as

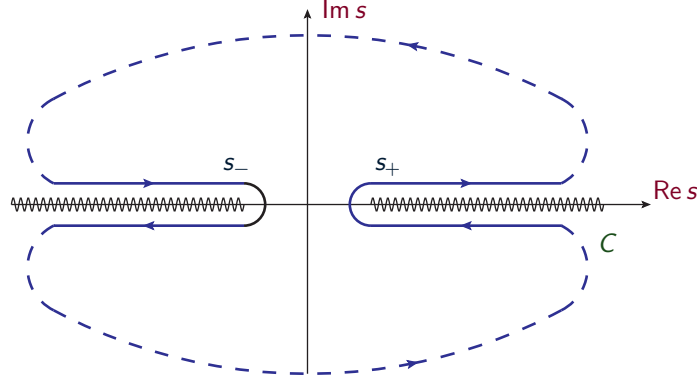
$$s > 4m^2 \implies 0 \neq \text{Im } \mathcal{A}(s + i\varepsilon, t) = \frac{1}{2i} (\mathcal{A}(s + i\varepsilon, t) - \mathcal{A}(s - i\varepsilon, t)) \quad (2.8)$$

Convention: physical $\mathcal{A}(s, t)$ is

$$\lim_{\varepsilon \rightarrow 0^+} \mathcal{A}(s + i\varepsilon, t) \quad (2.9)$$

Note that fact that the amplitude 1) does *not* have an imaginary part for $s < 4m^2$ (\rightarrow Schwarz) and 2) *does* have an imaginary part for $s > 4m^2$ together lead to the conclusion that the *amplitude is discontinuous on the real axis as a function of s !* In other words, the scattering amplitude has a branch cut on the positive s axis, precisely where the physical region is. This means that we have to choose whether the actual physical measurable scattering amplitude for $s > 4m^2$ is the value of the analytical function $\mathcal{A}(s, t)$ above or below the branch cut; the convention is that it is the value above it.

Now, as we will discuss below in Sec. 2.1.2, the imaginary part of the amplitude $\mathcal{A}(s, t)$ can also be nonzero for some $s < s_- < 0$, because this corresponds to the physical region in the u -channel process $a + \bar{d} \rightarrow \bar{b} + c$, where \bar{b}, \bar{d} are the antiparticles of b, d . Thus the structure of the amplitude in the complex plane will in general look like the following:



We can now, assuming that the amplitude is analytical (remember, this was one of our assumptions) express the value of the amplitude using the following Cauchy contour integral over the path C .

$$\mathcal{A}(s, t) = \frac{1}{2\pi i} \oint_C ds' \frac{\mathcal{A}(s', t)}{s' - s}. \quad (2.10)$$

Let us now *assume* that the contribution from the dashed semicircles vanishes (meaning that the amplitude is sufficiently small at large s). In fact we can also loosen this restriction somewhat, as we will discuss shortly. Now the integral turns into

$$\mathcal{A}(s, t) = \frac{1}{2\pi i} \left[\int_{-\infty}^{s_+} ds' \frac{\mathcal{A}(s' - i\varepsilon, t)}{s' - s - i\varepsilon} + \int_{s_+}^{\infty} ds' \frac{\mathcal{A}(s' + i\varepsilon, t)}{s' - s + i\varepsilon} + \int_{-\infty}^{s_-} ds' \frac{\mathcal{A}(s' + i\varepsilon, t)}{s' - s + i\varepsilon} + \int_{s_-}^{-\infty} ds' \frac{\mathcal{A}(s' - i\varepsilon, t)}{s' - s - i\varepsilon} \right] \quad (2.11)$$

Remembering the relation between the discontinuity and the imaginary part of the amplitude (2.8) this becomes

Dispersion relation

$$\mathcal{A}(s, t) = \frac{1}{\pi} \left[\int_{s_+}^{\infty} ds' \frac{\text{Im } \mathcal{A}(s', t)}{s' - s} + \int_{-\infty}^{s_-} ds' \frac{\text{Im } \mathcal{A}(s', t)}{s' - s} \right] \quad (2.12)$$

We threw away the $i\varepsilon$ in the denominators, but using

$$\frac{1}{x \pm i\varepsilon} = \mp i\pi\delta(x) + \mathcal{P} \frac{1}{x} \quad (2.13)$$

(where \mathcal{P} denotes the principal value) we can check that taking the imaginary part of (2.12) gives back the right thing (2.8)

$$\begin{aligned} \frac{1}{2i} [\mathcal{A}(s + i\varepsilon, t) - \mathcal{A}(s - i\varepsilon, t)] &= \frac{1}{2\pi i} \int_{s_+}^{\infty} ds' \text{Im } \mathcal{A}(s', t) \overbrace{\left[\frac{1}{s' - s - i} - \frac{1}{s' - s + i} \right]}^{2i\pi\delta(s' - s)} \\ &+ \frac{1}{2\pi i} \int_{-\infty}^{s_-} ds' \text{Im } \mathcal{A}(s', t) \overbrace{\left[\frac{1}{s' - s - i} - \frac{1}{s' - s + i} \right]}^{2i\pi\delta(s' - s)} = \text{Im } \mathcal{A}(s, t), \end{aligned} \quad (2.14)$$

where the limits s_-, s_+ must have been chosen so that they cover the part of the real s axis where $\text{Im } \mathcal{A}(s, t)$ is nonzero, so that one always hits the delta function.

The dispersion relation is, at least in principle, extremely powerful. It tells us that using just the imaginary part of the amplitude it is possible to fully reconstruct also the real part and thus the whole amplitude. While it is most powerful in analytical computations, dispersion relations can also be used to numerically manipulate experimentally measured amplitudes too.

Finally, let us discuss the situation when \mathcal{A} does not vanish sufficiently quickly as $|s| \rightarrow \infty$. In this case one can use a “subtracted” dispersion relation. This is done by calculating a similar integral as (2.10) for the function

$$\frac{\mathcal{A}(s, t)}{(s - s_1)(s - s_2) \cdots (s - s_n)}, \quad (2.15)$$

where n is chosen to be large enough that the integral converges. Now the Cauchy integral is

$$\begin{aligned} \frac{1}{2\pi i} \oint_C ds' \frac{\mathcal{A}(s', t)}{(s' - s)(s' - s_1)(s' - s_2) \cdots (s' - s_n)} &= \frac{\mathcal{A}(s, t)}{(s - s_1)(s - s_2) \cdots (s - s_n)} \\ &+ \frac{\mathcal{A}(s_1, t)}{(s_1 - s)(s_1 - s_2)(s_1 - s_3) \cdots (s_1 - s_n)} + \cdots + \frac{\mathcal{A}(s_n, t)}{(s_n - s)(s_n - s_1) \cdots (s_n - s_{n-1})} \end{aligned} \quad (2.16)$$

from which we solve

$$\begin{aligned} \mathcal{A}(s, t) &= \frac{(s - s_2) \cdots (s - s_n)}{(s_1 - s_2) \cdots (s_1 - s_n)} \mathcal{A}(s_1, t) + \cdots + \frac{(s - s_1) \cdots (s - s_{n-1})}{(s_n - s_1) \cdots (s_n - s_{n-1})} \mathcal{A}(s_n, t) \\ &+ \frac{(s - s_1) \cdots (s - s_n)}{\pi} \left[\int_{s_+}^{\infty} ds' \frac{\text{Im } \mathcal{A}(s', t)}{(s' - s)(s' - s_1) \cdots (s' - s_n)} + \int_{-\infty}^{s_-} ds' \frac{\text{Im } \mathcal{A}(s', t)}{(s' - s)(s' - s_1) \cdots (s' - s_n)} \right]. \end{aligned} \quad (2.17)$$

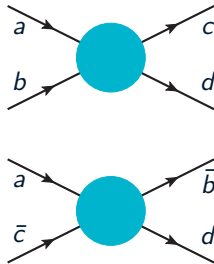
This is an “ n times subtracted” dispersion relation: now the dispersion relation only gives the amplitude up to n constants $\mathcal{A}(s_1, t), \dots, \mathcal{A}(s_n, t)$ that have to be determined from somewhere else. We can also think of these constants as the value and derivatives of $\mathcal{A}(s)$ at a single subtraction point s_0 . For example taking $n = 2$ and taking the limits $s_1 \rightarrow s_0$ and $s_2 \rightarrow s_0$ we can rewrite (2.17) in the perhaps easily interpreted form

$$\begin{aligned} \mathcal{A}(s, t) &= \mathcal{A}(s_0, t) + (s - s_0) \mathcal{A}'(s_0, t) \\ &+ \frac{(s - s_0)^2}{\pi} \left[\int_{s_+}^{\infty} ds' \frac{\text{Im } \mathcal{A}(s', t)}{(s' - s)(s' - s_0)^2} + \int_{-\infty}^{s_-} ds' \frac{\text{Im } \mathcal{A}(s', t)}{(s' - s)(s' - s_0)^2} \right]. \end{aligned} \quad (2.18)$$

For QCD, as we will see, imaginary parts of scattering amplitudes like to behave as $\text{Im } \mathcal{A}(s, t) \sim s$, so we will need a twice-subtracted form like (2.18) in the following.

2.1.2 Crossing symmetry

Strictly speaking crossing symmetry follows from Lorentz-invariance and CPT-symmetry (all laws of nature are invariant under the combined operation of a charge conjugation, a parity transformation and time reversal). We will not attempt to prove this here, but will just write down what this implies.

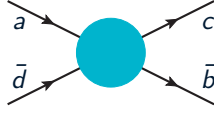


s -channel:

$$\mathcal{A}(\overbrace{s}^{ab}, \overbrace{t}^{ac}, \overbrace{u}^{ad}) \quad (2.19)$$

t -channel:

$$\mathcal{A}(\overbrace{t}^{ab}, \overbrace{s}^{ac}, \overbrace{u}^{ad}) \quad (2.20)$$



u -channel:

$$\mathcal{A}(\overbrace{u}^{ab}, \overbrace{t}^{ac}, \overbrace{s}^{ad}) \quad (2.21)$$

The point here is that the *same* analytical function \mathcal{A} describes all three “crossed” processes. The function has 2 arguments (remember that $s + t + u$ is fixed); what happens is that different regions for the values of these arguments are the physical regions for different processes. The same amplitude $\mathcal{A}(x, y)$ describes the “ s -channel” scattering $a + b \rightarrow c + d$ in the region $x = s_{a+b \rightarrow c+d} > 0, y = t_{a+b \rightarrow c+d} < 0$ and the “ t -channel” process $a + \bar{c} \rightarrow \bar{b} + d$ in the region $x = t_{a+\bar{c} \rightarrow \bar{b}+d} < 0, y = s_{a+\bar{c} \rightarrow \bar{b}+d} > 0$. These different regions in the complex planes of the two arguments of the function $\mathcal{A}(x, y)$ are related to each other, because the function is analytic.

The implication of this is that knowledge of one process, for example $a + b \rightarrow c + d$ can be used to obtain information on another one, say $a + \bar{c} \rightarrow \bar{b} + d$, if we have an analytical expression for the scattering amplitude.

2.1.3 Sommerfeld-Watson transform

You may have seen the concept of a *partial wave decomposition*. Here one writes the scattering amplitude as a series in orthonormal polynomials. The relevant functions are the ones that appear in all quantum mechanical problems with a 3-dimensionally rotationally invariant potential (e.g. the hydrogen atom): the Legendre polynomials $P_\ell(\cos \theta)$. To do such a decomposition in a Lorentz-invariant way we need to express the scattering angle θ (which is the *scattering angle in the center-of-mass frame*) in terms of the Mandelstam variables. To this end we need to recall the relation of between the scattering angle and the Mandelstam variables:

$$t = -\frac{s}{2}(1 - \cos(\theta)) \quad (m = 0) \quad (2.22)$$

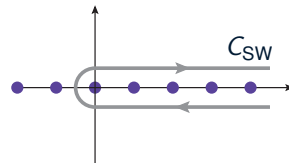
We now want to use crossing symmetry to learn something about the s -channel process. In order to do this, we start by writing down the partial wave decomposition of the amplitude for the t -channel process, which we then analytically continue to the s -channel

$$\mathcal{A}_{a\bar{c} \rightarrow \bar{b}d}(\overbrace{s}^{ac}, \overbrace{t}^{ab}) = \sum_{\ell=0}^{\infty} (2\ell + 1) a_\ell(s) P_\ell \left(1 + \frac{2t}{s} \right) \quad (2.23)$$

$$\mathcal{A}_{ab \rightarrow cd}(\overbrace{s}^{ab}, \overbrace{t}^{ac}) = \sum_{\ell=0}^{\infty} (2\ell + 1) a_\ell(t) P_\ell \left(1 + \frac{2s}{t} \right) \quad (2.24)$$

Here the coefficients a_ℓ are the partial wave amplitudes. For the t -channel process $-1 \leq 1 + 2t/s \leq 1$ as is appropriate for the cosine of a scattering amplitude. Then we have analytically continued this to the s -channel process, where the argument of the Legendre polynomial is < -1 ; since the Legendre polynomials are analytical functions these are perfectly reasonable, although unusual, values for the argument.

Now we perform a Sommerfeld-Watson transform. This is a trick that was first used for strong interactions by Tullio Regge in 1959 [22]. We transform the angular momentum quantum number ℓ from a discrete to a continuous variable, by writing the sum (2.24) as an integral of a function that has poles at integer values of ℓ . Such a function is conveniently provided by $1/\sin(\pi\ell)$



$$\mathcal{A}_{ab \rightarrow cd} = \frac{i}{2} \oint_{C_{SW}} d\ell (2\ell + 1) \overbrace{\frac{a(\ell, t)}{\sin(\pi\ell)}}^{\text{unique??}} P \left(\ell, 1 + \frac{2s}{t} \right) (-1)^\ell \quad (2.25)$$

Here note that the function $1/\sin(\pi\ell)$ has poles at all integer ℓ . The residue at these poles is $(-1)^\ell/\pi$. Since our contour is going clockwise (i.e. in the wrong direction), the residue theorem tells us that

$$\oint_{C_{\text{SW}}} = -2\pi i \sum_{\ell} (\text{res}_{\ell}), \quad (2.26)$$

and we indeed recover the sum (2.24).

We now must ask whether the function $a(\ell)$ of a continuous variable is uniquely determined for all $\ell \in \mathbb{C}$ by just its values at integer $\ell \in \mathbb{Z}$. Indeed it is not quite so, but apparently there is a theorem by Carlson (1914) saying that a function f_{ℓ} , $\ell \in \mathbb{N}$ has a unique continuation to all $\ell \in \mathbb{C}$ if one imposes a limit $|f(\ell)| < C e^{\pi|\ell|}$. But this leads to the possibility that we can add to our $a(\ell, t)$ some function proportional to $e^{i\pi\ell}$, which at integer values ℓ is just an alternating sign $(-1)^\ell$.

The easiest way to resolve this ambiguity is to introduce *two* functions of the complex variable ℓ . We split the partial wave amplitudes into even and odd values of ℓ . Then these the two functions of continuous variable ℓ are constructed so that

$$a^{(+)}(\ell, t) = a_{\ell}(t), \quad \ell \in 2\mathbb{Z} \quad (2.27)$$

$$a^{(-)}(\ell, t) = a_{\ell}(t), \quad \ell + 1 \in 2\mathbb{Z} \quad (2.28)$$

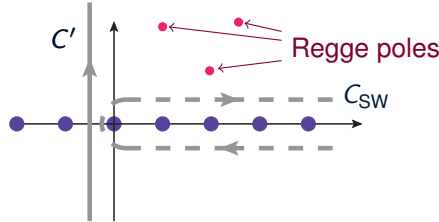
This allows us to explicitly separate out the possible $e^{i\pi\ell}$ -dependence, so that $a^{(\pm)}$ satisfy the condition of the Carlson theorem and do not grow faster than $e^{\pi|\ell|}$ for ℓ large and purely imaginary. The sign $\eta = \pm$ is called the *signature* of the amplitude. Note that in the t -channel process that we started with, even and odd ℓ values correspond to parity even and odd states for the particles $a\bar{c}$.

$$a(\ell, t) \Rightarrow \sum_{\eta=\pm 1} \frac{\eta + e^{-i\pi\ell}}{s} a^{(\eta)}(\ell, t) \quad (2.29)$$

$\eta = \pm 1$ =signature

Now we are ready to look at the high energy limit. For this we first look at the asymptotic behavior of the Legendre polynomials. Some clever mathematician has shown that for $\text{Re } \ell \geq -1/2$ we have a formula for the asymptotic values of the Legendre polynomials.

$$P\left(\ell, 1 + \frac{2s}{t}\right) \underset{s \rightarrow \infty}{\approx} \frac{1}{\sqrt{\pi}} \frac{\Gamma(\ell + 1/2)}{\Gamma(\ell + 1)} \left(\frac{4s}{t}\right)^{\ell} \quad (2.30)$$



$$\oint_{C_{\text{SW}}} = \int_{C'}^{\sim 1/\sqrt{s}} + (2\pi i) \sum_{\eta=\pm} \sum_{\text{pole } i_{\eta}} \text{res}(i_{\eta}) \quad (2.31)$$

We can now deform the integration contour from our original C_{SW} to the new contour C' running in the vertical direction along $\text{Re } \ell = -1/2$. On this contour the Legendre functions behave as $|P_{\ell=-1/2}| \sim 1/\sqrt{s}$, and the contribution does not contribute at high energy. In addition, there can be poles in the functions $a^{(\eta)}(\ell, t)$. Now the leading high energy behavior comes from the pole $\alpha(t)$ that has the largest real part

$$\mathcal{A}(s, t) \underset{s \rightarrow \infty}{\approx} \frac{\eta + e^{-i\pi\alpha(t)}}{2} \beta(t) s^{\alpha(t)} \quad (2.32)$$

Here $\alpha(t)$ and $\beta(t)$ are some functions of t that we do not know. But the essential thing at this point is that they do not depend on s .

Let us summarize our findings so far. We started from the assumption that partial wave amplitudes are analytical functions of angular momentum, with potentially simple poles in the complex angular momentum plane. This led us to a nontrivial result (2.32). What does this result tell us?

- We have a simple functional form for parametrizing scattering amplitudes as powers of s . Such a form really works very well, and is commonly used (most famously in the Donnachie&Landshoff parametrization [23]).
- One of the things our parametrization predicts is a nontrivial form for the relation between the real and imaginary parts of the scattering amplitude, whose ratio

$$\frac{\text{Re } \mathcal{A}}{\text{Im } \mathcal{A}} = -\frac{\eta + \cos(\pi\alpha(t))}{\sin(\pi\alpha(t))}, \quad \eta = \pm 1, \quad \alpha(t) = \frac{\partial \ln \mathcal{A}(s, t)}{\partial \ln s} \quad (2.33)$$

is related to the energy-dependence of the amplitude!

For example in elastic proton-proton collisions one can separately measure the absolute value and phase of the amplitude (for example using the interference with photon-mediated collisions which can be calculated). The total cross section grows with energy as $\sim s^{0.08}$, which would mean (see the optical theorem (2.2)) $\alpha \approx 1.08$, leading to

$$\frac{\text{Re } \mathcal{A}}{\text{Im } \mathcal{A}} \approx -\frac{1 + \cos(\pi + 0.08\pi)}{\sin(\pi + 0.08\pi)} \approx \frac{1 - \cos(0.08\pi)}{\sin(0.08\pi)} \approx \frac{\pi}{2} 0.08 \approx 0.13, \quad (2.34)$$

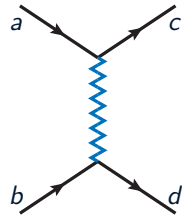
which is pretty close to what is measured. The other option $\eta = -1$ would not work at all. This leading high energy Regge pole is called the *pomeron*.

2.1.4 Regge trajectories

We have not parametrized the s -channel scattering amplitude in terms of t -dependent poles $\alpha(t)$. The natural next question is to then ask, what kind of physical objects do these poles correspond to. When do amplitudes have poles? Think for example of two cases

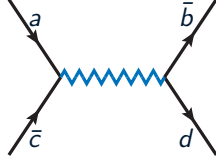
- In perturbative calculations, the propagator $i/(p^2 - m^2)$ has a pole when the particle is on mass shell
- In the Breit-Wigner form for a scattering amplitude $\mathcal{A}(E) \sim 1/(E - E_0 + i\gamma/2)$ there is a pole at $E = E_0 - i\Gamma/2$ corresponding to the scattering happening through a resonance, a shortlived particle with mass E and lifetime $1/\Gamma$

In general the idea is that a pole in an amplitude corresponds to a physical particle. To understand what the physical particles are in this case, we have to move back and forth between the t -channel and s -channel reactions. Now think of the s -channel scattering as happening through the exchange of some particle-like object. This same object appears as a resonance in the t -channel reaction.



$$\mathcal{A}_{ab \rightarrow cd} \sim \frac{s^{\alpha(t)}}{\sin(\pi\alpha(t))} \quad (2.35)$$

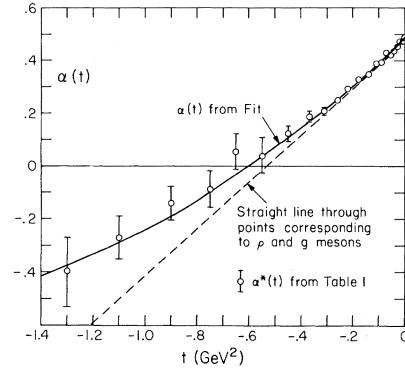
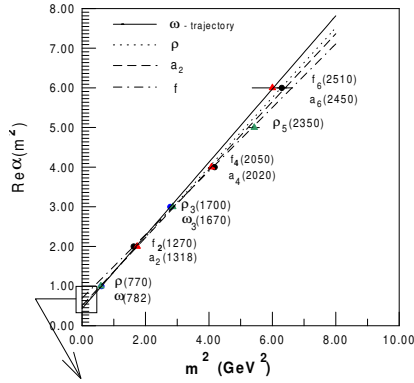
Here the interpretation is that the exponent of s corresponds to the spin of the exchanged particle (the jagged line): a scattering proceeding by the exchange of a spin- j particle is expected to have an amplitude $\mathcal{A} \sim s^j$ at $s \gg t$. The denominator has poles at integer values of $\alpha(t)$, but this function does not depend on s . For the s -channel process we do not usually expect to have $\alpha(t)$ close to an integer, and there are no resonance peaks in the cross section as a function of s . For the s -channel process any value of t is possible, $\alpha(t)$ takes on a continuum of values and different t 's correspond to a different “spin” of the exchanged particle.



$$\mathcal{A}_{a\bar{c} \rightarrow b d} \sim \frac{t^{\alpha(s)}}{\sin(\pi\alpha(s))} \quad (2.36)$$

In the crossed channel the interpretation is different. Now the amplitude has a pole, corresponding to a resonance, when $\alpha(s)$ is an integer, in this case $s = M^2$, the mass of the resonant particle. Resonances are actual particles, their spins need to be integers (or semi-integers, but mostly we are dealing with mesons here).

Experimentally, one observes that the functions (there are several for different quantum numbers, different poles, different signatures. . .) $\alpha(t)$ tend to be linear. This is demonstrated by the famous Chew-Frautschi plot (here is a newer version from [24]). Here one plots the spins of a group of mesons as a function of their squared masses; this is $\alpha(s)$ for the t -channel reaction. Then this plot can be put together with a measurement of the s -dependence of the scattering amplitude for the s -channel reaction for different t : this is the same function with a negative argument $\alpha(t)$ (Plot here is from Ref. [25]).



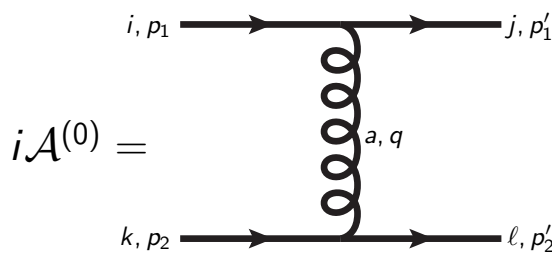
These groupings of meson masses, and the corresponding $\alpha(t)$ for the s -channel reaction, are known as Regge trajectories. The fact that the function $\alpha(t)$ is linear would occur naturally if mesons were excited states of strings. This led, back in the time, to the development of *string theory*, a nowadays abandoned attempt to understand the strong interaction before the discovery of QCD.

2.2 One gluon exchange

We will first try to compute the high energy behavior of scattering amplitudes in QCD from normal Feynman diagrams. For simplicity, we consider first $qq \rightarrow qq$ scattering. But I will try to convince you that the result we get is in fact much more general

2.2.1 One gluon exchange, high energy limit

As a warm-up exercise let's calculate the scattering amplitude for the process $qq \rightarrow qq$ via one gluon exchange. We first define the kinematical variables.



$i\mathcal{A}^{(0)} =$

$$p_1 = (p_1^+, 0, \mathbf{0}) \quad (2.37)$$

$$p_2 = (0, p_2^-, \mathbf{0}) \quad (2.38)$$

$$p_1' = (p_1^+ - q^+, -q^-, -\mathbf{q}) \quad (2.39)$$

$$p_2' = (q^+, p_2^- + q^-, \mathbf{q}) \quad (2.40)$$

$$s = (p_1 + p_2)^2 = 2p_1^+ p_2^- \quad (2.41)$$

$$t = q^2 \quad (2.42)$$

H. E. limit $s \gg t$

$$0 = (p_1')^2 = -2q^- p_1^+ - t \implies q^- = -\frac{t}{2p_1^+} = -\frac{t}{s} p_2^- \quad (2.43)$$

$$0 = (p_2')^2 = 2q^+ p_2^- + t \implies q^+ = -\frac{t}{2p_2^-} = -\frac{t}{s} p_1^+ \quad (2.44)$$

$$\implies p_1^+ \gg q^+ \quad p_2^- \gg q^- \quad , \quad t \approx \mathbf{q}^2. \quad (2.45)$$

This has some very typical features for scattering kinematics at high energy:

- We are considering momenta as ordered: the plus-going quark has a larger plus-momentum than the exchanged gluon.
- This kinematics is equivalent to the limit $s \gg t$
- This limit leads to the momentum transfer t being dominated by transverse momentum. Thus one can also think of the H.E. limit as the limit of *transverse momenta* \ll *longitudinal momenta*.
- If one thinks in terms of scattering angles this means that the scattering angle is very small. Thus the high energy limit is often also called the *forward limit*.

Now we want to calculate the square of the amplitude, and average over incoming and sum over outgoing colors and spins.

The color algebra can be done as follows

$$\mathcal{A}^{(0)} = g^2 t_{ji}^a t_{lk}^a \bar{u}(p_1') \gamma^\mu u(p_1) \bar{u}(p_2') \gamma_\mu u(p_2) \frac{1}{q^2} \quad (2.46)$$

$$\overline{|\mathcal{A}^{(0)}|^2} \sim \frac{1}{N_c^2} \overbrace{t_{ji}^a t_{lk}^a}^{\text{avg}} \underbrace{t_{ij}^b t_{kl}^b}_{\mathcal{A}^*} = \frac{1}{N_c^2} \text{tr}(t^a t^b) \text{tr}(t^a t^b) = \frac{1}{N_c^2} \frac{1}{2} \delta^{ab} \frac{1}{2} \delta^{ab} = \frac{N_c^2 - 1}{4N_c^2} \quad (2.47)$$

Note that the generators t_{ij}^a are Hermitian, ie. the complex conjugate of the transpose is the matrix itself, or equivalently complex conjugation is the same as taking the transpose. Thus if the amplitude \mathcal{A} has t_{ji}^a , the conjugate amplitude \mathcal{A}^* has $(t_{ji}^a)^* = t_{ij}^a$.

Now let us do the spin algebra as you would do it in the particle physics course, assuming massless quarks.

$$\overline{|\mathcal{A}^{(0)}|^2} \sim \frac{1}{2^2} \text{tr} \not{p}_1' \gamma^\mu \not{p}_1 \gamma^\nu \text{tr} \not{p}_2' \gamma_\mu \not{p}_2 \gamma_\nu \quad (2.48)$$

$$= \frac{1}{4} 4(p_1'^\mu p_1^\nu - g^{\mu\nu} p_1 \cdot p_1' + p_1'^\nu p_1^\mu) 4(p_{2\mu}' p_{2\nu} - g_{\mu\nu} p_2 \cdot p_2' + p_{2\nu}' p_{2\mu}') \quad (2.49)$$

$$= s^2 - t^2 + u^2 - t^2 + 4t^2 - t^2 + u^2 - t^2 + s^2 = 2s^2 + 2u^2 \quad (2.50)$$

$$s = (p_1 + p_2)^2 = 2p_1 \cdot p_2 = (p'_1 + p'_2)^2 = 2p'_1 \cdot p'_2 \quad (2.51)$$

$$t = (p_1 - p'_1)^2 = -2p_1 \cdot p'_1 = (p_2 - p'_2)^2 = -2p_2 \cdot p'_2 \quad (2.52)$$

$$t = (p_1 - p'_2)^2 = -2p_1 \cdot p'_2 = (p_2 - p'_1)^2 = -2p_2 \cdot p'_1 \quad (2.53)$$

$$|\overline{\mathcal{A}^{(0)}}|^2 = g^4 \frac{N_c^2 - 1}{4N_c} \frac{2s^2 + 2u^2}{t^2} \quad (2.54)$$

Very fine and good, this is the way one does amplitude computations in a normal particle physics or field theory course. With some practice this way of calculating becomes routine. But we want to do the same thing a little bit differently:

- We want to use the H.E. kinematical approximation to make our life simpler
- We want to look at the amplitude only, not have to square it.
- We want to understand what happens to individual spin states, now we just summed over the spin.

2.2.2 Eikonal vertex

We are interested in the interactions of spin-1 gauge bosons (gluons, also photons) with different kinds of matter. Very generically, a spin-1 particle is represented by a vector field A_μ , which couples in the Lagrangian to some 4-current carrying the appropriate charge: $J^\mu A_\mu$. For an elementary vertex particle \rightarrow particle + gauge boson in perturbation theory, the vector A_μ becomes the polarization vector of the gauge boson, i.e. the Lorentz-index in the gauge boson propagator. This polarization index then couples to some 4-vector, and the question is: which one?

We have basically two options. The 4-vector that the gauge boson couples to can be made up from 4-vectors of particle momenta, and from spins. Without proof, I claim that at in the high energy limit (when the momentum of the matter particle is much larger than that of the gauge boson), the spin does not matter. Thus, apart from the color factor, the interaction of a gauge boson with a high energy particle is always the same.

At high energy: spin does not matter

$$= 2igp^\mu \times [\text{color}]$$

Let us derive the eikonal vertex for some known interactions.

- Interaction with a scalar field. The standard vertex (with momenta as above) is

$$ig(p^\mu + (p - q)^\mu) \approx 2igp^\mu, \quad p \gg q \quad (2.55)$$

- Interaction with a fermion: the vertex is

$$ig\bar{u}_{\lambda'}(p - q)\gamma^\mu u_\lambda(p) \quad (2.56)$$

Here λ', λ are the quark spins, and we are not writing out the color factor). How does one treat this? One can always use the explicit forms, but a more straightforward option is to use the “Gordon identity”

$$ig\bar{u}_{\lambda'}(p - q)\gamma^\mu u_\lambda(p) = ig\bar{u}_{\lambda'}(p - q)[(p + (p - q))^\mu + i\sigma^{\mu\nu}(p - (p - q))_\nu]u_\lambda(p). \quad (2.57)$$

Now we see that explicitly the spin-dependent part ($\sigma^{\mu\nu} = \frac{i}{2}[\gamma^\mu, \gamma^\nu]$ is the generator of Lorentz-transformations, including rotations, and thus related to the spin) is proportional to the small momentum q . Neglecting terms proportional to q and using the spinor normalization

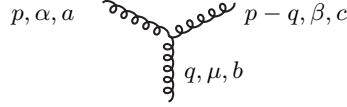
$$\bar{u}_{\lambda'}(p)u_\lambda(p) = \delta_{\lambda'\lambda} \quad (2.58)$$

we arrive at the eikonal vertex. At this point the reader might wonder why we say that the vertex has the spinors \bar{u} and u which, in the usual Feynman rules, are only attached to external lines. To see why also internal quark lines entering a vertex can be thought of as contributing a similar factor, one can write the quark propagator as

$$\frac{i}{\not{p} - m + i\varepsilon} = i \frac{\not{p} + m}{p^2 - m^2 + i\varepsilon} = i \sum_{\sigma} \frac{u_{\sigma}(p) \bar{u}_{\sigma}(p)}{p^2 - m^2 + i\varepsilon}. \quad (2.59)$$

The first u is then associated with the vertex at the beginning of the propagator (following the fermion line), and the \bar{u} with the one at the end.

- Gluon: we start from the elementary vertex (note that now p is incoming, $p - q$ and q outgoing momenta)



menta)

$$gf^{abc} [g^{\alpha\mu}(p+q)^{\beta} + g^{\mu\beta}(-q+(p-q))^{\alpha} + g^{\beta\alpha}(-(p-q)-p)^{\mu}] \quad (2.60)$$

We first neglect the small momentum components $q \ll p$, and this becomes

$$gf^{abc} [g^{\alpha\mu}p^{\beta} + g^{\mu\beta}p^{\alpha} - 2g^{\beta\alpha}p^{\mu}] \quad (2.61)$$

Now we must, in a way that is similar to the insertion of the spinors needed for the fermionic vertex, discuss the polarization states of the gluons. If the incoming (p) and outgoing ($p - q$) hard gluons are external, on-shell particles, the vertex must be contracted with their polarization vectors $\varepsilon_{\alpha}(p)$ and $\varepsilon_{\beta}^{*}(p - q) \approx \varepsilon_{\beta}^{*}(p)$. These polarization vectors are transverse, i.e. $k^{\mu}\varepsilon_{\mu}(k) = 0$. Thus, in this case at least, the terms $\sim p^{\alpha}$ and $\sim p^{\beta}$ do not contribute. Also if these gluons are internal lines, we can do the calculation assuming that they are transverse (i.e. taking the propagators in Landau gauge); we know that the result for a scattering amplitude is gauge invariant. Finally, relating the structure constant to the generator of the adjoint representation of $SU(3)$ $(T^c)_{ba} = if_{abc}$ we can write the vertex as

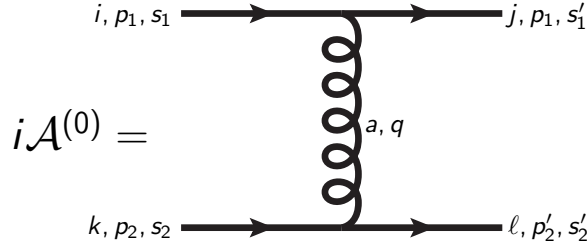
$$2igp^{\mu}g^{\beta\alpha}(T^c)_{ba} \quad (2.62)$$

(signs $\sim \dots$). The way to read this is that the eikonal 3-gluon vertex has the universal eikonal coupling of a color charged particle to gluons, $2igp^{\mu}$. This is multiplied by a color factor $(T^c)_{ba}$ (reading the color indices starting from the end of the diagram) corresponding to the adjoint representation color charge. There is also a polarization delta function $g^{\beta\alpha}$ which ensures that the polarization of the fast particle does not change, just like the spin of a quark does not change in the eikonal interaction.

Notes:

- This eikonal vertex should only be used in covariant gauge, where the polarization vector of the gauge particle $\varepsilon^{\mu}(q)$ has all 4 components. Later in this course we will also work in light cone gauge, where one chooses the gauge in such a way that $\varepsilon^{\mu}(q)p_{\mu} = 0$, i.e. so that the component of the polarization vector that couples to the eikonal vertex vanished by a gauge choice. In this case the interaction cannot be taken to be given by the same eikonal vertex, and one needs to take into account the other components.
- The eikonal interaction conserves the spin/helicity/polarization of the “matter” particle.
- Note that the two approximations: neglecting the momentum of the gauge particle from the point of view of the matter particle $p^{+} \approx p^{+} - q^{+}$ and the interaction not depending on the spin of the matter particle together mean that we are neglecting the *quantum* nature of the radiation. The eikonal approximation or eikonal vertex corresponds to the classical interaction with charged matter with a gauge field: acceleration or deceleration of the matter due to the Lorentz force, and potential classical radiation due to this acceleration or deceleration. Thus physics in the leading high energy limit can, if one does it carefully, be represented by classical (color) charges interacting with classical gauge fields.

2.2.3 One gluon exchange with the eikonal vertex



Now let us calculate the scattering amplitude again using the eikonal vertex. We write out the spins of the quarks s_1, s_2, s'_1, s'_2 explicitly and use the eikonal vertex for the gluon coupling. Now the amplitude is

$$\mathcal{A}^{(0)} \approx -i [\delta_{s_1, s'_1} 2ip_1^\mu t_{ji}^a] \frac{-ig_{\mu\nu}}{q^2} [\delta_{s_2, s'_2} 2ip_2^\nu t_{lk}^a] = g^2 t_{ji}^a t_{lk}^a \frac{2s}{t} \delta_{s_1, s'_1} \delta_{s_2, s'_2}, \quad (2.63)$$

remembering that $p_1 \cdot p_2 = s/2$. (I think that even the sign is right. In the Abelian limit the potential is repulsive, and the scattering amplitude should be negative.) We can square this and sum or average over the spins and colors to get the squared amplitude as

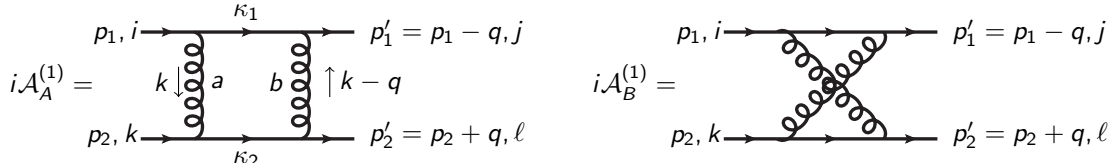
$$|\overline{\mathcal{A}^{(0)}}|^2 = \left(\frac{2sg^2}{t}\right)^2 \left[\frac{1}{2} \sum_{s_1=\pm, s'_1=\pm} (\delta_{s_1, s'_1})^2\right] \left[\frac{1}{2} \sum_{s_2=\pm, s'_2=\pm} (\delta_{s_2, s'_2})^2\right] \frac{N_c^2 - 1}{4N_c^2} = g^4 \frac{N_c^2 - 1}{4N_c^2} \frac{4s^2}{t^2}, \quad (2.64)$$

where the color sum is done just as before. We notice that this is exactly the same as the full expression (2.54) in the H.E: limit $s \approx -u \gg |t|$, obtained with a lot less effort.

2.3 Two gluon exchange

2.3.1 Two gluon exchange

Now, let us move to quark-quark scattering at next to leading order. The leading high energy behavior is given by the following two loop diagrams [3]:



There are of course many other diagrams also contributing at the same order in α_s , but they are subleading at large collision energy s . For example vertex correction diagrams to the quark-gluon vertex will have the same s -dependence as the leading order one gluon exchange diagram. Likewise there are propagator correction diagrams for the gluon propagator, which again have the same energy dependence as the leading order one-gluon exchange diagram. Another way to deduce that these two loop diagrams are the leading ones at high energy is to realize that in order to have the biggest large s contribution one needs to have the maximum number (4) of big eikonal couplings of gluons to the high energy quark lines. One also needs internal gluon propagators to *not* have any large longitudinal momentum components, so that they don't suppress the diagram at high s . This basically leaves the two diagrams A and B , where in the high energy limit it is possible for the gluon momenta k and $k - q$ to not have large longitudinal components. Concretely, we expect that the region:

$$\sqrt{s} \sim p_1^+ \gg k^+ \sim q^+ \quad (2.65)$$

$$\sqrt{s} \sim p_2^- \gg k^- \sim q^- \quad (2.66)$$

will provide the dominant contribution to the value of these integrals at large s . As we will see, in this region $k^2 \approx -\mathbf{k}^2$ and $(k - q)^2 \approx -(\mathbf{k} - \mathbf{q})^2$, so the gluon propagators do not bring in large longitudinal momenta. There are only 2 propagators that do: κ_1 and κ_2 , but they are compensated by the vertices with large eikonal couplings.

These diagrams are *loop diagrams*, which means that we have to integrate over an internal momentum (k) circulating in the loop. Such loop integrals are in general quite some work to calculate in the full generality. Our purpose here is not to take the significant effort required to do them in full glory. In stead, we will proceed straight to the result by a *dispersive* technique that appears completely magical but is nevertheless correct.

Our starting point is the Cutkosky cutting rule (2.4) (a generalization of the optical theorem) which relates the imaginary part of the scattering amplitude to the “cut,” a sum of all intermediate states that can have all particles on shell while satisfying 4-momentum conservation. Here the amplitudes going to the intermediate states are lower order in perturbation theory and thus easier to calculate. In this case it means that we can construct the imaginary part of a one-loop amplitude by gluing together tree-level amplitudes with on-shell external legs (in our case the tree-level amplitude Eq. (2.63)). Let us apply the rule to diagram A, expressing its imaginary part in terms of a *cut diagram*

$$\text{Im } \mathcal{A}_A^{(1)} = \frac{1}{2} \int d\mathcal{P}_2(\kappa_1, \kappa_2) \mathcal{A}^{(0)}(s, k) \left(\mathcal{A}^{(0)}(s, k - q) \right)^\dagger, \quad (2.67)$$

2-particle phase space

$$\begin{aligned} \int d\mathcal{P}_2(\kappa_1, \kappa_2) &= \int \frac{d^4 \kappa_1}{(2\pi)^4} \frac{d^4 \kappa_2}{(2\pi)^4} (2\pi)^2 \delta(\kappa_1^2) \delta(\kappa_2^2) (2\pi)^4 \delta^{(4)}(p_1 + p_2 - \kappa_1 - \kappa_2) \\ &= \int \frac{d^4 k}{(2\pi)^2} \delta((p_1 - k)^2) \delta((p_2 + k)^2) \end{aligned} \quad (2.68)$$

Here $\mathcal{A}^{(0)}(s, k)$ is the tree-level amplitude with center of mass energy s and momentum transfer k . While this would not be strictly speaking necessary for our calculation here, we will next introduce the *Sudakov variables* α, β , which provide a Lorentz-invariant notation for what are, essentially, just the light cone variables p^\pm . In some parts of the literature the Sudakov variables are often used, so it is useful to have some familiarity with the concept.

Sudakov variables

$$k^\mu = \alpha p_1^\mu - \beta p_2^\mu + k_\perp^\mu \quad (2.69)$$

$$k = (\alpha p_1^+, -\beta p_2^-, \mathbf{k}) \quad (2.70)$$

$$\int d^4 k = \overbrace{p_1^+ p_2^-}^{=s/2} \int d\alpha d\beta d^2 \mathbf{k} \quad (2.71)$$

Digression: General Sudakov-decomposition

In general the Sudakov variables are defined by taking two light-like vectors n^μ, \bar{n}^μ with $n^2 = \bar{n}^2 = 0$. We also choose these vectors to have a positive 0-component $n^0 > 0, \bar{n}^0 > 0$; note that the sign of the 0-component of a vector does not change in any Lorentz boost or rotation so the statement $n^0 > 0, \bar{n}^0 > 0$ is independent of the Lorentz frame. By going to the center-of-mass frame of the lightlike vectors (with $n = (n_0, \vec{n}), \bar{n} = (n_0, -\vec{n})$) one can show that $2n \cdot \bar{n} = (n + \bar{n})^2 > 0$. The light-like vectors are usually normalized so that $n \cdot \bar{n} = 1$. We then decompose any vector k^μ into three parts: the components parallel to these n^μ and \bar{n}^μ and the remainder k_\perp^μ that is orthogonal to both n^μ and \bar{n}^μ : $k_\perp \cdot n = k \cdot \bar{n} = 0$.

In these notes we just work in a fixed coordinate system where the incoming particle momenta are in opposite directions along the z -axis. This implies that their momenta p_1 and p_2 only have a plus- and minus-component, respectively. Thus the natural choice is $n^\mu = (n^+ = 1, 0, \mathbf{0}), \bar{n}^\mu = (0, \bar{n}^- = 1, \mathbf{0})$.

Now we can use the delta functions that set the intermediate state fermions on shell to eliminate the Sudakov variables.

$$(p_1 - k)^2 = (1 - \alpha)\beta s - \mathbf{k}^2 = 0 \quad (2.72)$$

$$(p_2 + k)^2 = \alpha(1 - \beta)s - \mathbf{k}^2 = 0 \quad (2.73)$$

$$\Rightarrow \alpha \approx \beta \approx \frac{\mathbf{k}^2}{s} \ll 1 \quad (2.74)$$

$$\delta((p_1 - k)^2) \approx \frac{1}{s} \delta(\beta - \frac{\mathbf{k}^2}{s}) \quad (2.75)$$

$$\delta((p_2 + k)^2) \approx \frac{1}{s} \delta(\alpha - \frac{\mathbf{k}^2}{s}) \quad (2.76)$$

$$\Rightarrow \int d\Omega_2 \approx \frac{1}{2s} \int \frac{d^2 \mathbf{k}}{(2\pi)^2} \quad (2.77)$$

This is very typical for the high energy limit. Everything that is longitudinal (\pm components) is separated out and dealt with separately, in this case just yielding the appropriate power of s . What remains are transverse momentum integrals.

We can now put the pieces together. We want to write the expressions in terms of the Mandelstam variables s, t as much as possible, because in the following stage we want to invoke the analyticity of the amplitude in terms of s, t . To that end, note that $t = (p_1 - (p_1 - q))^2 = q^2$. In a similar way as we above used the on-shell condition for κ_1, κ_2 to deduce that $k^+ = \alpha p_1^+ \approx p_1^+ \mathbf{k}^2/s$ and $k^- = -\beta p_2^- \approx -p_2^- \mathbf{k}^2/s$, we can use the on-shellness of $p'_1 = p_1 - q$ and $p'_2 = p_2 + q$ to deduce that

$$q^+ \approx p_1^+ \frac{\mathbf{q}^2}{s} \quad (2.78)$$

$$q^- \approx -p_2^- \frac{\mathbf{q}^2}{s} \quad (2.79)$$

$$t = q^2 \approx -2p_1^+ p_2^- \left(\frac{\mathbf{q}^2}{s} \right)^2 - \mathbf{q}^2 \approx -\mathbf{q}^2 \left(\frac{\mathbf{q}^2}{s} + 1 \right) \approx -\mathbf{q}^2, \quad (2.80)$$

remembering that s is always larger than any transverse momentum, such as \mathbf{q}^2 .

$$\text{Im } \mathcal{A}_A^{(1)} = \frac{1}{4s} \int \frac{d^2 \mathbf{k}}{(2\pi)^2} (t^b t^a)_{ji} (t^b t^a)_{\ell k} \overbrace{\frac{2g^2 s}{-\mathbf{k}^2}}^{\mathcal{A}^{(0)}(k)} \overbrace{\frac{2g^2 s}{-(\mathbf{k} - \mathbf{q})^2}}^{(\mathcal{A}^{(0)}(k - \mathbf{q}))^\dagger} \quad (2.81)$$

$$= 16\pi^2 \alpha_s^2 (t^b t^a)_{ji} (t^b t^a)_{\ell k} \frac{1}{N_c \alpha_s} \frac{s}{t} \overbrace{\int \frac{d^2 \mathbf{k}}{(2\pi)^2} \frac{-\mathbf{q}^2}{\mathbf{k}^2 (\mathbf{q} - \mathbf{k})^2}}^{\equiv \varepsilon(\mathbf{q}^2) \sim \ln \mathbf{q}^2} \quad (2.82)$$

Here we have factored out some parts of the expression to define $\varepsilon(\mathbf{q}^2)$, this notation will be useful later when we combine these one-loop corrections with the real emission contributions to arrive at a resummed BFKL ladder diagram. Note that the integral

$$\varepsilon(\mathbf{q}^2) = N_c \alpha_s \int \frac{d^2 \mathbf{k}}{(2\pi)^2} \frac{-\mathbf{q}^2}{\mathbf{k}^2 (\mathbf{q} - \mathbf{k})^2} \quad (2.83)$$

is dimensionless and logarithmically infrared divergent. Thus, to make sense of the calculation, it properly speaking needs to be regularized with some cutoff, which then has to cancel later if one calculates some physical observable.

Now comes the magic. We know the real part of the scattering amplitude from the imaginary part using dispersion relations, as discussed in Sec. 2.1. Since the imaginary part of the amplitude behaves as $\text{Im } \mathcal{A} \sim s$, we will need to do this using a “twice-subtracted” dispersion relation in order for the dispersion relation integral to converge. This means that we separate out two integration constants; the value of the amplitude

at $s = s_0$ and its derivative. Then our dispersion relation becomes

$$\mathcal{A}(s, t) = \mathcal{A}(s_0, t) + (s - s_0)\mathcal{A}'(s_0, t) + \frac{1}{\pi}(s - s_0)^2 \int ds' \frac{\text{Im } \mathcal{A}(s', t)}{(s' - s_0)^2 (s' - (s + i\varepsilon))} \quad (2.84)$$

Here s is the real, positive Mandelstam variable, and the combination appearing in the dispersion relation $s + i\varepsilon$ corresponds to the convention that the physical scattering amplitude is obtained by approaching the real s axis from above in the complex plane. Often in the literature, e.g. [2], this is written just as s , with the understanding that then s has a small positive imaginary part. Now the imaginary part of our scattering amplitude (2.82) is s times some function of t which factorizes out from the dispersion relation integral. Inserting $\mathcal{A}(s', t) = s'$ in the (2.84) and choosing, for simplicity, $s_0 = 0$ and putting the lower limit of the integration to $-t$ (changing the lower limit will to something else will just contribute something that does not affect the large s behavior) our dispersion integral becomes

$$\frac{s^2}{\pi} \int_{-t}^{\infty} ds' \frac{s'}{(s')^2 (s' - (s + i\varepsilon))} \quad (2.85)$$

Using

$$\frac{1}{x - i\varepsilon} = i\pi\delta(x) + \mathcal{P}\frac{1}{x}, \quad (2.86)$$

where \mathcal{P} denotes the fact that the integral over this variable must be treated as a principal value integral, we can evaluate the dispersion integral (2.85) as

$$is - \frac{s}{\pi} \ln \frac{s}{-t} = -\frac{s}{\pi} \ln \frac{s}{t} \quad (2.87)$$

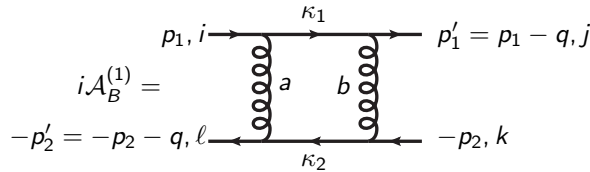
Two notes on this:

1. The convention is that s has a small positive imaginary part: $s = |s|e^{i\delta}$, which means that $-s = |s|e^{-i(\pi-\delta)}$. Now we use, as is conventional, the principle branch of the logarithm that has a branch cut on the negative real axis, this means that the imaginary part of $\ln(-s)$ is $-i\pi$.
2. A good consistency check for the signs is of course that we get back the same imaginary part of the amplitude that we started with.

To summarize, what the dispersion relation approach tells us is that the whole amplitude can be reconstructed from the imaginary part by interpreting our result in (2.82) in the following way

$$\frac{s}{t} = \text{Im} \left(-\frac{1}{\pi} \frac{s}{t} \ln \frac{s}{t} \right) \quad (2.88)$$

Now let us look at the other diagram, $\mathcal{A}_B^{(1)}$. We can actually relate it to the diagram A by *crossing* symmetry: we pull the final state quark with momentum p'_2 into the initial state on the left, where it becomes an incoming antiquark with momentum $-p'_2$. Likewise the incoming quark with momentum p_2 becomes an outgoing antiquark with momentum $-p_2$. Now the diagram looks like this:



We now notice that it is exactly the same as diagram A, except for the interchanges:

- The lower line is now an antiquark instead of a quark. This does not make any difference for us now that we are not caring about the particle mass, since the polarization sums will be the same

$$\sum_s u_s(p) \bar{u}_s(p) = \not{p} = \sum_s v_s(p) \bar{v}_s(p) \quad (2.89)$$

In fact crossing symmetry implies that thing will work by just exchanging the Mandelstams s, t, u in the appropriate way also for massive particles, but to get the signs correctly at the amplitude level even for massive particle one has to treat separately how the different helicity states of the quarks map into antiquarks.

- The incoming and outgoing lower momenta are exchanged $p_2 \leftrightarrow -p'_2$. This leaves $t = (p_1 - p'_1)^2$ unchanged but exchanges $s = 2p_1 \cdot p_2 = 2p'_1 \cdot p'_2$ and $u = -2p_1 \cdot p'_2 = -2p'_1 \cdot p_2$ with each other
- The color ℓ associated with the outgoing quark p'_2 is now associated with the incoming antiquark $-p'_2$. But since the color indices are read against the direction of the fermion arrow, the color factor for the lower line is still read from ℓ to k . This color factor is now $(t^a t^b)_{\ell k}$ (instead of $(t^b t^a)_{\ell k}$ for diagram A in (2.82).

Thus we get the result for diagram B from diagram A by just exchanging $s \leftrightarrow u \approx -s$. Note that this eliminates the imaginary part, because $\ln(s/t)$ becomes $\ln -s/t$.

We finally get

$$\mathcal{A}_A^{(1)} = 16\pi\alpha_s^2 (t^b t^a)_{ji} (t^b t^a)_{\ell k} \frac{1}{N_c \alpha_s} \left(-\frac{s}{t}\right) \ln \frac{s}{t} \varepsilon(\mathbf{q}^2) \quad (2.90)$$

$$\mathcal{A}_B^{(1)} = 16\pi\alpha_s^2 (t^b t^a)_{ji} (t^a t^b)_{\ell k} \frac{1}{N_c \alpha_s} \left(\frac{s}{t}\right) \ln \frac{s}{-t} \varepsilon(\mathbf{q}^2) \quad (2.91)$$

2.3.2 Color projections

The color structure of the amplitude is now a little bit complicated. We want to decompose it into two possible structures. The first one is a color octet exchange, the part of the two gluon exchange whose color structure is similar to one gluon exchange. This part of the amplitude can be put together with the one-gluon exchange from Eq. (2.63), which we write in the form

$$\mathcal{A}^{(0)} = 8\pi\alpha_s t_{ji}^a t_{\ell k}^a \frac{s}{t} \quad (2.92)$$

The second one is a color singlet exchange, where the color of the colliding quarks does not change: the color taken away by one gluon is fully compensated by the other.

- Singlet

$$\sim \delta_{ij} \delta_{k\ell} \quad (2.93)$$

- Octet

$$\sim t_{ji}^a t_{\ell k}^a \quad (2.94)$$

We also split the amplitude into the real and imaginary part. Note that the real part gets a contribution from both diagrams A and B , noting the sign change

$$\text{Re } \mathcal{A}^{(1)} \sim (t^b t^a)_{ji} [t^b, t^a]_{\ell k}, \quad (2.95)$$

while the imaginary part only comes from the diagram A , and has a color structure

$$\text{Im } \mathcal{A}^{(1)} \sim (t^b t^a)_{ji} (t^b t^a)_{\ell k}. \quad (2.96)$$

Using e.g. the Fierz identity (1.15) we can decompose these into terms proportional to the singlet (2.93) and octet (2.94) color structures. We then combine the singlet and octet channels together with the leading order amplitudes as

$$\mathcal{A}_{\underline{1}} = 16i\pi\alpha_s \delta_{ij} \delta_{k\ell} \frac{N_c^2 - 1}{4N_c^2} \pi \frac{s}{t} \varepsilon(\mathbf{q}^2) \quad (2.97)$$

$$\mathcal{A}_{\underline{8}} = 8\pi\alpha_s t_{ji}^a t_{\ell k}^a \frac{s}{t} \left[1 + \varepsilon(\mathbf{q}^2) \ln \frac{s}{|t|} - \frac{2i}{N_c^2} \pi \varepsilon(\mathbf{q}^2) + \dots \right] \quad (2.98)$$

The singlet (2.97) is basically what we would expect. It only starts at this order in perturbation theory, and starts as being imaginary, because the imaginary part of the elastic amplitude is the cross section, which at this order is the square of the single gluon exchange amplitude. Note that for a scattering to be elastic in the sense of the optical theorem, the outgoing particles must be in the same color state as the incoming ones,

i.e. only the singlet channel is elastic. In terms of the language of Regge trajectories, the singlet amplitude is consistent with a Regge trajectory with a signature $\eta_{\mathbb{P}} = +$ and a residue $\alpha(t) \sim 1 + \varepsilon(-t)$:

$$\mathcal{A}_{\mathbb{P}} \approx -(1 + e^{-i\pi(1+\varepsilon(-t))})s^{1+\varepsilon} \approx i\pi s \quad (2.99)$$

This “particle” is the perturbative QCD pomeron (this is what \mathbb{P} stands for), it is the Regge trajectory with vacuum quantum numbers, associated with the leading high energy behavior of the elastic cross section. Now of course the exponent $\varepsilon(\mathbf{q}^2)$ is really the logarithmically IR-divergent integral (2.83). This is because we are trying to calculate a total cross section for the scattering of two colored particles via the exchange of a massless gauge boson. In this case the total cross section is in fact infinite, just like it is for e^-e^- scattering to lowest order in QED. If we would consider color neutral composite objects made of several quarks, this IR divergence would eventually cancel in the end.

At leading logarithmic accuracy in s , or also at leading order in $1/N_c$, we can neglect the imaginary part of the octet amplitude (2.98). Then we approximate it as

$$\mathcal{A}_{\underline{8}} \approx -8\pi\alpha_s t_{ji}^a t_{\ell k}^a \left(\frac{s}{|t|} \right)^{1+\varepsilon(\mathbf{q}^2)} \quad (2.100)$$

In the language of Regge trajectories, this looks like the real part of what one would get from a signature $\eta_{\mathbb{R}} = -1$ Regge trajectory:

$$(-1 + e^{-i\pi(1+\varepsilon(-t))})s^{1+\varepsilon(-t)} = (-2 - i\pi\varepsilon(-t) + \dots)s^{1+\varepsilon(-t)} \approx -2s^{1+\varepsilon(-t)} \quad (2.101)$$

So this would be another “particle” with the same residue $\alpha(t) \sim 1 + \varepsilon(-t)$ as the pomeron. This “particle” is known as the *reggeized gluon*; it includes the leading high energy correction to gluon exchanges. The imaginary part of the octet channel (2.98), however, does not match what one would get from the Regge form (2.101) (it is suppressed by $1/N_c^2$). Thus overall the analytic structure of the amplitude is not quite that of a Regge pole.

2.4 The Lipatov vertex

2.4.1 Multi-Regge kinematics

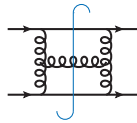
Now we have calculated the $q + q \rightarrow q + q$ scattering amplitude in the high energy $s \gg t$ limit to order α_s^2 . We saw that it can be interpreted in terms of two different kinds of exchanges:

- Color singlet *pomeron*, which could be a Regge trajectory with signature $\eta_{\mathbb{P}} = 1$ and residue $\alpha(t) \approx 1 + \varepsilon(-t)$.
- Color octet *reggeized gluon* with signature $\eta_{\mathbb{R}} = -1$ and the same residue $\alpha(t) \approx 1 + \varepsilon(-t)$.

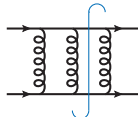
At this point these are still of course just conjectures. In order to understand whether this structure really is true, we need to go to higher order $\sim \alpha_s^3$. In particular, the α_s^2 calculation only gives us the leading order contribution to color singlet exchange, and the energy dependence is a pure conjecture at this point.

We will still want to calculate the next order corrections only in the leading large s limit, and using dispersive techniques just like at α_s^2 . This means that we will calculate cut diagrams to obtain the imaginary part of the amplitude. There are of course a large number of two-loop diagrams. We will not calculate all of them, but focus on ones that give the leading large s contribution, and have an imaginary part (i.e. an intermediate state that can consist of on-shell particles). These can be classified into two kinds of contributions, depending on whether we are cutting both the quark lines and a gluon line, or only the two quark lines like at α_s^2 .

- Real: cut $2q + g$, e.g.

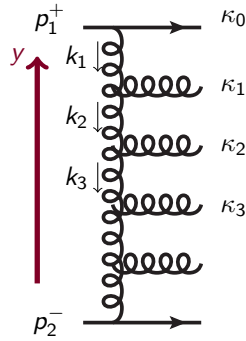


- Virtual: cut $2q$, e.g.



As one sees from the diagram, the virtual contributions are put together from pieces that we already know: the $q + q \rightarrow q + q$ amplitudes. The real or radiative contributions are new, they are the ones that we will now calculate. Before embarking on the calculation, let us state a bit more explicitly the kinematical approximation we are using, which will give us the leading high energy contribution. We want to calculate things at leading $s \gg |t|$. It is useful to think of this limit in terms of transverse and longitudinal momenta. The scale t is the scale of transverse momenta, which we will assume to be parametrically of similar size to each other. Then the longitudinal momenta are characterized by a large p^+ momentum of one incoming particle (drawn at the top of the diagram) and a large p^- of the other (drawn at the bottom). In the multi-Regge kinematics (MRK) all the longitudinal momenta of any intermediate particles are *strongly ordered* in longitudinal momenta: all the longitudinal momenta of the particles lines are either much larger, or much smaller than those of other particles. Since transverse momenta are similar and $p^- \sim \mathbf{p}^2/p^+$, strong ordering in p^+ implies strong ordering in p^- , just in the other direction. In drawing diagrams the convention is that the vertical dimension should be thought of as a rapidity axis, with p^+ increasing when moving up, and p^- increasing when moving down.

Multi-Regge kinematics



Strongly ordered

$$p_1^+ \gg \kappa_1^+ \approx k_1^+ \gg \dots \gg \kappa_n^+ \approx k_n^+ \gg p_2^+ \approx 0 \quad (2.102)$$

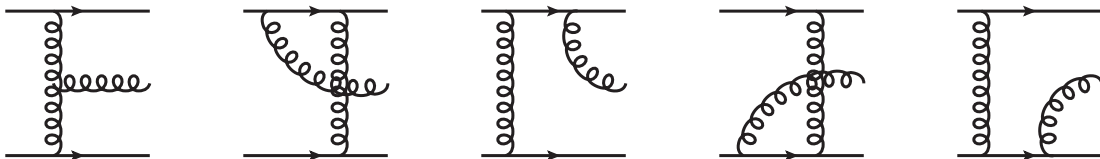
$$p_2^- \gg \kappa_n^- \approx -k_{n+1}^- \gg \dots \gg \kappa_1^- \approx -k_2^- \gg \kappa_0^- \approx -k_1^- \gg p_1^- \approx 0 \quad (2.103)$$

$$k_n^2 \approx 2\kappa_n^+ \kappa_{n-1}^- - \mathbf{k}_1^2 = \frac{\kappa_n^+}{\kappa_{n-1}^+} \kappa_{n-1,\perp}^2 - \mathbf{k}_1^2 \approx -\mathbf{k}_1^2 \quad (2.104)$$

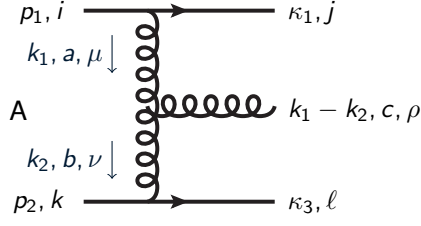
If (as they will be) the horizontal gluon lines are on mass-shell, the virtuality (four-momentum squared) of the vertical lines is dominated by the transverse momentum. This is one way of seeing why the MRK limit is the leading one at high energy: if the strong ordering of longitudinal momenta is violated, the (vertical) off shell propagators will give a power-law suppression (with a large longitudinal momentum) for the whole diagram.

2.4.2 Lipatov vertex

Now let us start calculating the gluon emission diagrams, which are needed for the real part of the α_s^3 scattering amplitude. There are 5 diagrams that we need to consider:



Let us start calculating these one by one.



$$\mathcal{A}_A = -i(2igp_{1\mu})t_{ji}^a \left(\frac{-i}{k_1^2} \right) f_{abc} [(k_1 + k_2)^\rho g^{\mu\nu} + (-k_2 - (-k_1 + k_2))^\mu g^{\rho\nu} + (-(k_1 - k_2) - k_1)^\nu g^{\mu\rho}] \times \left(\frac{-i}{k_2^2} \right) (2igp_{2\nu})t_{lk}^b \quad (2.105)$$

Now we will make approximations in the MRK kinematics, which allows several simplifications:

- Recall that $p_{1\mu}$ only has a p_1^+ -component. Thus the dot product with the middle one of the three terms in the 3-gluon vertex $p_1 \cdot (k_1 - 2k_2) = 2p_1^+(k_1^- - 2k_2^-) \approx -2p_1^- k_2^-$, because in the MRK the minus momenta are ordered, so that $k_2^- \gg k_1^-$. Similarly, since $p_{2\nu}$ only has a p_2^- -component, $p_2 \cdot (k_2 - 2k_1) \approx -2p_2^- k_1^+ = -2p_2 \cdot k_1$.
- Also because $p_{1\mu}$ and $p_{2\nu}$ only have p_1^+ and p_2^- -components, it is convenient to express k_1^+ and k_2^- in terms of the Sudakov variables:

$$k_1^+ = \alpha_1 p_1^+ \quad (2.106)$$

$$k_2^- = -\beta_2 p_2^- \quad (2.107)$$

Using these we can then write $p_1 \cdot k_2 = -\beta_2 p_1 \cdot p_1$ and $p_2 \cdot k_1 = \alpha_1 p_2 \cdot p_1$. Thus we make the k 's disappear in favor of the p 's, which we pull out as common factors

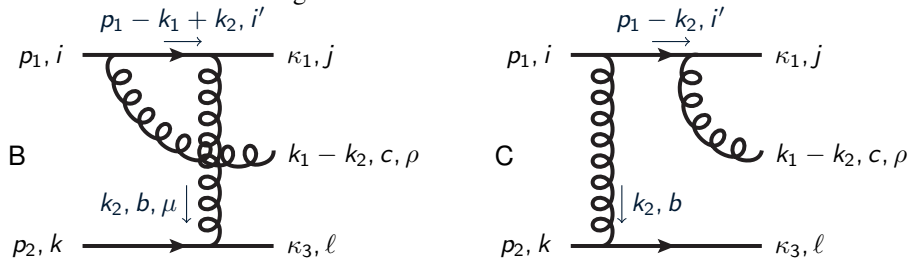
- In the second and third term of the 3-gluon vertex we contract $p_{2\nu} g^{\rho\nu} = p_2^\rho$ and $p_{1\mu} g^{\mu\rho} = p_1^\rho$, and pull the factors from the eikonal vertices inside the square bracket.

Putting these together we get

$$\mathcal{A}_A = \frac{-4if_{abc}t_{ji}^a t_{lk}^b}{\mathbf{k}_1^2 \mathbf{k}_2^2} p_{1\mu} p_{2\nu} g^{\mu\nu} [(k_1 + k_2)^\rho + 2\beta_2 p_2^\rho - 2\alpha_1 p_1^\rho]. \quad (2.108)$$

Here we have also explicitly replaced the t -channel (vertical) propagators by just the transverse momenta following the MRK, see Eq. (2.104).

Then let us move to the other diagrams, starting with the two where the gluon is emitted from the upper line. Note that we label the momenta and colors in all five diagrams in such a way that the external particle momenta and colors are the same in all diagrams.



Let us first look at the off-shell intermediate quark propagator in diagram B, which simplifies in the high energy limit. We first write it in a way that separates out the fermion spin and the scalar propagator, using $\not{p}\not{p} = p^2$, as

$$\frac{i}{\not{p}_1 - \not{k}_1 + \not{k}_2} = \frac{i(\not{p}_1 - \not{k}_1 + \not{k}_2)}{(p_1 - k_1 + k_2)^2}. \quad (2.109)$$

Now the numerator can be rewritten as a polarization sum:

$$p_1' - k_1' + k_2' = \sum_{\sigma} u_{\sigma}(p_1 - k_1 + k_2) \bar{u}_{\sigma}(p_1 - k_1 + k_2) \quad (2.110)$$

These spinors are combined into forming the eikonal vertices for both gluons attaching to the top line:

$$\bar{u}_{\lambda}(\kappa_1) i g \gamma^{\mu} u_{\sigma}(p_1 - k_1 + k_2) \approx 2 i g p_1^{\mu} \delta_{\sigma, \lambda} \quad (2.111)$$

$$\bar{u}_{\sigma}(p_1 - k_1 + k_2) i g \gamma^{\rho} u_{\lambda'}(p_1) \approx 2 i g p_1^{\rho} \delta_{\sigma, \lambda'}, \quad (2.112)$$

with, exceptionally, the polarizations of the quarks $\lambda = \sigma = \lambda'$ written explicitly. The scalar propagator becomes:

$$(p_1 - k_1 + k_2)^2 = \overbrace{p_1^2}^{=0} - 2 p_1 \cdot (k_1 - k_2) + \overbrace{(k_1 - k_2)^2}^{=0} = -2 p_1^+ (k_1^- - k_2^-) \approx 2 p_1^+ k_2^- = -\beta_2 s \approx -(p_1 - k_2)^2, \quad (2.113)$$

where we have used the MRK kinematics and the fact that the outgoing particles are on mass shell. We notice that the same thing happens to the scalar part of the fermion propagator of diagram B, $(p_1 - k_2)^2$, except for the sign. In fact the only difference between diagrams B and C is this sign, and the fact that the color matrices are in different order:

$$\mathcal{A}_B = (-i)(2 i g p_1^{\mu})(2 i g p_1^{\rho}) \frac{i}{\beta_2 s} (t^b t^c)_{ji} \frac{-i g_{\mu\nu}}{k_2^2} t_{\ell k}^b (2 i g p_2^{\nu}) \quad (2.114)$$

$$\mathcal{A}_C = (-i)(2 i g p_1^{\rho})(2 i g p_1^{\mu}) \frac{-i}{\beta_2 s} (t^c t^b)_{ji} \frac{-i g_{\mu\nu}}{k_2^2} t_{\ell k}^b (2 i g p_2^{\nu}) \quad (2.115)$$

We can sum them up using the commutator

$$[t^b, t^c] = i f^{abc} t^a \quad (2.116)$$

into a single form that has the same color structure as diagram A with the 3-gluon vertex.

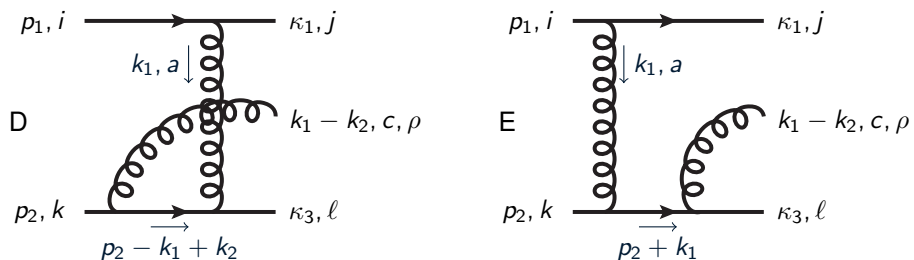
$$\mathcal{A}_B + \mathcal{A}_C = \frac{8 p_1^{\rho} p_1^{\mu} p_2^{\nu}}{\beta_2 s (-\mathbf{k}_2^2)} g_{\mu\nu} i g^3 f^{abc} t_{ji}^a t_{\ell k}^b \quad (2.117)$$

The essential thing in this manipulation was the fact that we have two diagrams where the gluons with color b and c are attached to the quark in the opposite order. The intermediate propagator of the quark that is emitting them has a different sign for the two orderings: in diagram B the quark first emits the gluon (color c) and ends up with a negative minus-momentum ($k_2^+ < 0$), which is then compensated by the second gluon, while in diagram C it first gets minus momentum from the first gluon ($-k_2^+ > 0$) which then goes away with the emitted second gluon (color c).

The same manipulations can be done to combine diagrams D and E,

$$\mathcal{A}_D + \mathcal{A}_E = \frac{8 p_2^{\rho} p_1^{\mu} p_2^{\nu}}{-\alpha_1 s (-\mathbf{k}_1^2)} g_{\mu\nu} i g^3 f^{abc} t_{ji}^a t_{\ell k}^b \quad (2.118)$$

and the whole result combined into



$$\mathcal{A}_A + \mathcal{A}_B + \mathcal{A}_C + \mathcal{A}_D + \mathcal{A}_E = (-i) \frac{i}{\mathbf{k}_1^2} \frac{i}{\mathbf{k}_2^2} (2igp_1^\mu)(2igp_2^\nu) g f^{abc} t_{ji}^a t_{\ell k}^b g_{\mu\nu} \times \underbrace{\left[(k_1 + k_2)^\rho + 2\beta_2 p_2^\rho - 2\alpha_1 p_1^\rho + \frac{2p_1^\rho \mathbf{k}_1^2}{\beta_2 s} - \frac{2p_2^\rho \mathbf{k}_2^2}{\alpha_1 s} \right]}_{C_\rho(k_1, k_2)}. \quad (2.119)$$

Using

$$k_1^+ + k_2^- \underbrace{2\alpha_1 p_1^+}_{=k_1^+} + \underbrace{\frac{2p_1^+ \mathbf{k}_1^2}{2\beta_2 p_1^+ p_2^-}}_{=-k_2^-} \approx -k_1^+ - \frac{\mathbf{k}_1^2}{k_2^-} \quad (2.120)$$

$$k_1^- + k_2^- + 2 \underbrace{\beta_2 p_2^-}_{=-k_2^-} - \underbrace{\frac{2p_2^- \mathbf{k}_2^2}{2\alpha_1 p_1^+ p_2^-}}_{=k_1^+} \approx -k_2^- - \frac{\mathbf{k}_2^2}{k_1^+} \quad (2.121)$$

we can simplify this into

The Lipatov effective vertex

$$C^+ = -k_1^+ - \frac{\mathbf{k}_1^2}{k_2^-} \quad (2.122)$$

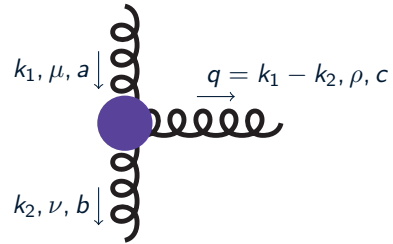
$$C^- = -k_2^- - \frac{\mathbf{k}_2^2}{k_1^+} \quad (2.123)$$

$$\mathbf{C} = \mathbf{k}_1 + \mathbf{k}_2 \quad (2.124)$$

$$q \cdot \mathbf{C} = 0 \quad (2.125)$$

$$C^2 = -4 \frac{\mathbf{k}_1^2 \mathbf{k}_2^2}{q^2} \quad (2.126)$$

$$g f^{abc} g_{\mu\nu} C^\rho(k_1, k_2) \quad (2.127)$$



The Lipatov effective vertex is a way to combine the effect of these five diagrams into one vertex, in the MRK limit. In stead of five diagrams, we only have one, but with a more complicated Feynman rule. The Lipatov vertex is *nonlocal*: in coordinate space the inverse momenta $1/k_2^-$, $1/k_1^+$ are nonlocal operators (unlike momenta, which are derivatives, and local operators). The Lipatov vertex is an essential building block in resumming all the diagrams that contribute to cross section in the leading high energy limit. Although here we calculated the scattering of two quarks, the Lipatov vertex does not know about the quarks. The color structure of the 4 diagrams B, C, D and E is written in terms of the same color structure f^{abc} as the three gluon vertex. The same thing happens if we replace the quarks by any colored particles in any representation: one always gets the commutator of two color matrices from the two diagrams B, C (or D, E) that differ only by a sign and the ordering of the color matrices, thus this becomes a commutator that is written in terms of a single matrix in that representation, and a structure constant. The Lipatov vertex therefore describes the scattering of any two colored particles, in the high energy limit.

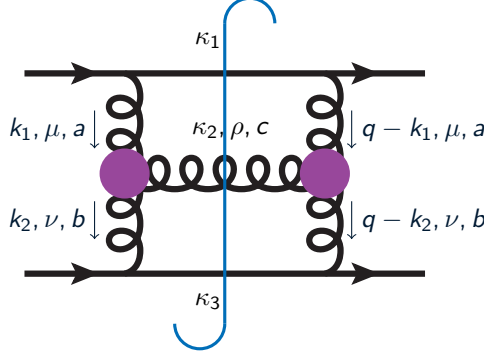
Digression: Comparison to QED

Note that none of these leading high energy contributions exist in QED. There is no three photon vertex. Also the photon emissions before and after the exchanged photon (diagrams B and C) cancel in the MRK approximation, because there is only a relative minus sign, not a commutator $[t^b, t^c]$. The same feature can be seen in for example the calculation of brehmsstrahlung, where an electron scatters of the Coulomb field of e.g. a heavy atomic nucleus: the leading (soft+collinear) infrared divergence cancels in a destructive interference between diagrams with an emission before and an emission after the interaction with the Coulomb field.

2.5 The BFKL equation

2.5.1 Scattering at α_s^3

To see how this happens, let us first look at the radiative α_s^3 -contribution to the imaginary part of the scattering amplitude. This is the square of the amplitude that we used to derive the Lipatov vertex, together with the 3-particle phase space:



$$\text{Im } \mathcal{A}_{\text{rad}}^{(2)} = \frac{1}{2} \int d\Pi_3 \frac{g^6 (s/2)^2 f^{abc} f^{a'b'c} t_{ji'}^{a'} t_{ji}^a t_{ek'}^{b'} t_{ek}^b (-C^\rho(k_1, k_2) C^\rho(k_1 - q, k_2 - q))}{\mathbf{k}_1^2 \mathbf{k}_2^2 (\mathbf{k}_1 - \mathbf{q})^2 (\mathbf{k}_2 - \mathbf{q})^2} \quad (2.128)$$

$$\int d\Pi_3 = \frac{1}{8\pi s} \int \frac{d^2 \mathbf{k}_1}{(2\pi)^2} \frac{d^2 \mathbf{k}_2}{(2\pi)^2} \underbrace{\int_{|t|/s}^1 \frac{d\alpha_1}{\alpha_1}}_{\sim \ln s} \quad (k_1^+ = \alpha_1 p_1^+) \quad (2.129)$$

$$\text{Im } \mathcal{A}_{\text{rad}}^{(2)} \sim \frac{s}{t} \ln \frac{s}{|t|} \implies \mathcal{A}_{\text{rad}}^{(2)} \sim \frac{s}{t} \ln^2 \frac{s}{|t|} \quad (2.130)$$

Let's calculate the phase space a bit more carefully

$$\begin{aligned} \int d\Pi_3 &= \int \frac{d^4 k_1}{(2\pi)^4} \frac{d^4 k_2}{(2\pi)^4} (2\pi) \delta((p_1 - k_1)^2) (2\pi) \delta((p_2 - k_2)^2) (2\pi) \delta((k_1 - k_2)^2) \\ &= \frac{s^2}{4(2\pi)^5} \int d^2 \mathbf{k}_1 d^2 \mathbf{k}_2 \int_0^1 d\alpha_1 d\alpha_2 d\beta_1 d\beta_2 \\ &\quad \times \delta(\beta_1(1 - \alpha_1)s - \mathbf{k}_1^2) \delta(\alpha_2(1 - \beta_2)s - \mathbf{k}_2^2) \delta((\alpha_1 - \alpha_2)(\beta_2 - \beta_1)s - (\mathbf{k}_1 - \mathbf{k}_2)^2), \end{aligned} \quad (2.131)$$

recalling the Sudakov variables $0 < \alpha_i, \beta_i < 1$ defined as

$$k_i^+ = \alpha_i p_1^+ \quad (2.132)$$

$$k_i^- = -\beta_i p_2^-. \quad (2.133)$$

Now the delta function constraints can be satisfied with $1 - \alpha_1 \approx 1$, which leads to $\beta_1 \approx \mathbf{k}_1^2/s$ and $1 - \beta_2 \approx 1$, which leads to $\alpha_2 \approx \mathbf{k}_2^2/s$ and $(\alpha_1 - \alpha_2)(\beta_2 - \beta_1) \approx \alpha_1 \beta_2 \approx (\mathbf{k}_1 - \mathbf{k}_2)^2/s$ (which again is consistent with $\alpha_1 \ll 1, \beta_2 \ll 1$ which was what we assumed to more easily find these solutions). Now we can use the delta functions to integrate over β_1, α_2 and β_2 , with the last one of these leaving us with the restriction $\beta_2 = (\mathbf{k}_1 - \mathbf{k}_2)^2/(\alpha_1 s) < 1$, i.e. $\alpha_1 > (\mathbf{k}_1 - \mathbf{k}_2)^2/s$. In writing the lower limit in Eq. (2.129) we have, since we are just interested in the leading large s behavior, replaced $(\mathbf{k}_1 - \mathbf{k}_2)^2$ by $|t|$.

In terms of rapidity; the gluon κ_2 can be anywhere between p_1 and p_2 in rapidity, with a production spectrum that is independent of this rapidity (because all the propagators are just transverse momenta). Then the integral over the rapidity of this gluon gives a logarithm of s . Remembering that this logarithm is the imaginary part of the amplitude, we know that the real part of the amplitude will go like $\ln^2 s$. The integral in the dispersion relation will go like

$$\mathcal{A} \sim s^2 \int_{|t|}^{\infty} \frac{ds' \ln s'}{(s')^2 (s' - s)} \sim s \ln^2 s, \quad (2.134)$$

i.e. give an additional logarithm just like in the one-loop case.

One now needs to do a calculation that we will not go through in these lectures, but is possible starting from the ingredients that we have:

- Evaluate the squared Lipatov vertex in Eq. (2.128).
- Reconstruct the real part of the amplitude for this diagram starting from the imaginary part using the dispersion relation.
- Use crossing symmetry to reconstruct the crossed diagram, which will only have a real part.
- Decompose the amplitude into color octet and color singlet parts.

In addition to this, one needs to consider the “virtual” cut diagrams. These give contributions like

$$\begin{aligned}
& 2 \operatorname{Im} \mathcal{A}_{\text{virt}}^{(2)} \\
&= \int d\mathcal{P}_2(k_2) \left[\begin{array}{c} \text{Diagram 1: Two vertical gluon lines with momenta } k_1 \text{ and } k_2 - k_1. \\ \text{Diagram 2: Two crossed gluon lines.} \end{array} \right] \times \left[\begin{array}{c} \text{Diagram 3: A single vertical gluon line with momentum } q - k_2. \end{array} \right]^\dagger \\
&+ \left[\begin{array}{c} \text{Diagram 4: A single vertical gluon line.} \end{array} \right] \times \left[\begin{array}{c} \text{Diagram 5: Two vertical gluon lines.} \\ \text{Diagram 6: Two crossed gluon lines.} \end{array} \right]^\dagger \quad (2.135)
\end{aligned}$$

The first bracket we calculated in Sec. 2.3, with the result that the leading high energy part is a real color octet amplitude, proportional to $s \ln s$ and to the transverse momentum integral:

$$\sim \varepsilon(\mathbf{k}_2^2) \sim \int \frac{d^2 \mathbf{k}_1 \mathbf{k}_2^2}{\mathbf{k}_1^2 (\mathbf{k}_1 - \mathbf{k}_2)^2} \quad (2.136)$$

Together with the two-particle phase space integral in Eq. (2.135) this becomes also an integral over two transverse momenta, just like Eq. (2.128), and the two can be combined into a single expression. For the octet color channel, these combine into a form that confirms at this order the reggeized gluon structure that starts to emerge in Eq. (2.98):

$$\mathcal{A}_{\underline{8}}^{(0)+(1)+(2)} = 8\pi\alpha_s t_{ji}^a t_{\ell k}^a \frac{s}{t} \left[1 + \varepsilon(\mathbf{q}^2) \ln \frac{s}{|t|} + \frac{1}{2} \varepsilon^2(\mathbf{q}^2) \ln^2 \frac{s}{|t|} + \dots \right] \quad (2.137)$$

For the singlet color channel, the situation is more complicated. Together with the one loop order contribution from Eq. (2.97) we now get

$$\begin{aligned}
\mathcal{A}_{\underline{1}}^{(1)+(2)} &= 16i\pi^2 \alpha_s^2 \delta_{ij} \delta_{k\ell} \frac{N_c^2 - 1}{4N_c^2} \frac{s}{t} \left\{ \int \frac{d^2 \mathbf{k}_1}{(2\pi)^2} \frac{-\mathbf{q}^2}{\mathbf{k}^2 (\mathbf{q} - \mathbf{k})^2} \right. \\
&+ 2\alpha_s \ln \frac{s}{|t|} (-\mathbf{q}^2) \int \frac{d^2 \mathbf{k}_1}{(2\pi)^2} \frac{d^2 \mathbf{k}_2}{(2\pi)^2} \left[\frac{\mathbf{q}^2}{\mathbf{k}_1^2 \mathbf{k}_2^2 (\mathbf{k}_1 - \mathbf{q})^2 (\mathbf{k}_2 - \mathbf{q})^2} \right. \\
&\quad \left. \left. - \frac{1}{2} \frac{1}{\mathbf{k}_2^2 (\mathbf{k}_1 - \mathbf{q})^2 (\mathbf{k}_1 - \mathbf{k}_2)^2} - \frac{1}{2} \frac{1}{\mathbf{k}_1^2 (\mathbf{k}_2 - \mathbf{q})^2 (\mathbf{k}_1 - \mathbf{k}_2)^2} \right] \right\} \quad (2.138)
\end{aligned}$$

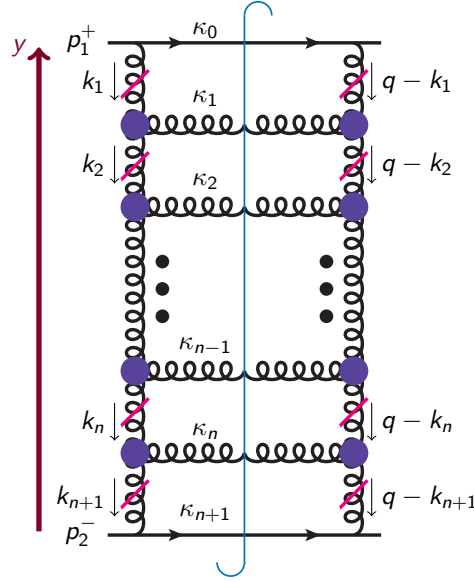
Here the first out of the three terms inside the square bracket is a term like $\varepsilon^2(\mathbf{q}^2)$ just like the one in the octet channel. The second two cancel between the radiative and the virtual terms for the octet channel, but survive for the color singlet.

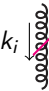
- Octet: confirm reggeized gluon
- Singlet: more complicated integral

Clearly something more sophisticated must be done to resum the pomeron exchange cross section to all orders in $\alpha_s \ln s$. This more sophisticated approximation is provided by the BFKL equation.

2.5.2 Ladder diagrams

Now we are in a position to resum all the leading high energy contributions to QCD scattering cross sections, a calculation that is attributed to Balitsky, Fadin, Kuraev and Lipatov [26, 27]. This can be done by resumming so called BFKL ladder diagrams by the way of the BFKL equation. We will not try to give a general “proof” that this is indeed the case, but we are by now familiar with all the ingredients needed to put together these ladder diagrams and this equation.



- Reggeized gluon k_i  $\sim \frac{i g^{4\nu}}{k_i^2} \left(\frac{s_i}{k_i^2} \right) \varepsilon(k_i^2)$

- Lipatov vertex , (2.127).

- MRK = Multi-Regge Kinematics:

$$\kappa_0^+ \gg \kappa_1^+ \gg \dots \gg \kappa_n^+ \gg \kappa_{n+1}^+, \quad \kappa_0^- \ll \kappa_1^- \ll \dots \ll \kappa_n^- \ll \kappa_{n+1}^-,$$

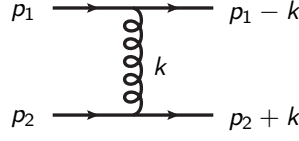
$$\Rightarrow y_0 > y_1 > \dots > y_{n+1} \quad (2.139)$$

- BFKL equation: recursion equation, solution = sum of ladders

Now, let's go through these aspects in order. We start with the reggeized gluon propagator. We derived it in a way that involved a total center of mass energy of a $2 \rightarrow 2$ scattering, but now we have to express it in a way that can be applied to our ladder diagram. We wrote the propagator in terms of a center-of-mass energy s_i . This should be interpreted as the total center-of-mass energy of the $2 \rightarrow 2$ system attached to the ends of this propagator. So let us look at a simple $2 \rightarrow 2$ scattering $p_1 + p_2 \rightarrow (p_1 - k) + (p_2 + k)$. Using the fact that the outgoing particle with momentum $p_2 + k$ is on shell, we can express the transverse momentum \mathbf{k} that is carried by the exchanged gluon in terms of the longitudinal momenta. Then the minus-momentum at the lower end cancels, and the factor $\frac{s_i}{k_i^2}$ can be expressed as a ratio of the longitudinal momentum carried

by the exchanged gluon to the momentum of the parent. This should be interpreted as the exponential of the rapidity interval corresponding to the exchanged gluon.

Reggeized gluon



$$(p_2 + k)^2 = 2p_2^- k^+ - \mathbf{k}^2 = 0 \implies \frac{s}{\mathbf{k}^2} = \frac{2p_1^+ p_2^-}{2p_2^- k^+} \quad (2.140)$$

$$\frac{s_i}{\mathbf{k}_i^2} \approx \frac{k_{i-1}^+}{k_1^+} \sim e^{y_i - y_{i-1}} \quad (2.141)$$

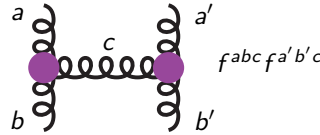
The pair of Lipatov vertices at the end of each of each rung of the ladder can be summed over the spin of the gluon crossing the cut. Because the Lipatov vertex is gauge invariant (Eq. (2.125)), this can be done with the metric tensor $(-g_{\rho\rho'})C^\rho(k_i, k_{i+1})C_\rho(q - k_i, q - k_{i+1})$ with a straightforward, if not very intuitive result.

Lipatov vertex

$$C^\rho(k_i, k_{i+1})C_\rho(q - k_i, q - k_{i+1}) = -2 \left[\mathbf{q}^2 - \frac{\mathbf{k}_i^2(\mathbf{q} - \mathbf{k}_{i+1})^2}{(\mathbf{k}_i - \mathbf{k}_{i+1})^2} - \frac{\mathbf{k}_{i+1}^2(\mathbf{q} - \mathbf{k}_i)^2}{(\mathbf{k}_i - \mathbf{k}_{i+1})^2} \right] \quad (2.142)$$

The color structure is more important, although tricky. Until now we have been dealing with the explicit colors of the quarks, but now the quarks are at the end of the ladder and we need to be able to decompose the color state of a two-gluon system propagating along the ladder to find the color singlet and octet contributions. To make a long story short, this has the following result for the effective color factor associated with a pair of Lipatov vertices, i.e. the contribution from a single rung of the ladder:

Color structure



- Octet: $N_c/2$
- Singlet: N_c

Let us derive these color factors. We can start by defining projection operators that take a two-gluon state (colors a, a') and project out its color singlet and octet components. (More group theory minded readers will note that $8 \otimes 8 = 1 \oplus 8 \oplus 8 \oplus 10 \oplus \bar{10} \oplus 27$, i.e. there are two possible color octets. We are only interested in one of them the antisymmetric one, that can be thought of as a correction to the leading order single gluon exchange. The symmetric octet will have a different parity.)

$$P_{\underline{1}}^{bb',aa'} = \frac{1}{N_c^2 - 1} \delta^{aa'} \delta^{bb'} \quad (2.143)$$

$$P_{\underline{8}}^{bb',aa'} = \frac{1}{N_c} f^{aa'e} f^{bb'e}. \quad (2.144)$$

We can easily check that these projection operators are normalized

$$P_{\underline{1}}^{bb',aa'} P_{\underline{1}}^{aa',cc'} = P_{\underline{1}}^{bb',cc'} \quad (2.145)$$

$$P_{\underline{8}}^{bb',aa'} P_{\underline{8}}^{aa',cc'} = P_{\underline{8}}^{bb',cc'}, \quad (2.146)$$

$$P_{\underline{8}}^{bb',aa'} P_{\underline{1}}^{aa',cc'} = 0, \quad (2.147)$$

using the adjoint representation Casimir

$$f^{abc} f^{abd} = N_c \delta^{cd}. \quad (2.148)$$

If the singlet/octet projection operators act on a singlet/octet state of a two gluon system with colors a, a' , they just give that state back:

$$P_{\underline{1}}^{bb',aa'} \delta^{aa'} = \delta^{bb'} \quad (2.149)$$

$$P_{\underline{1}}^{bb',aa'} f^{aa'd} = f^{bb'd}. \quad (2.150)$$

Now let us see what happens when these states exchange a gluon, described by a pair of Lipatov vertices. Let us start from a singlet $\delta^{dd'}$, which we let exchange a gluon (with color c) and then project out back to the singlet state:

$$P_{\underline{1}}^{bb',aa'} (f^{adc} f^{a'd'c}) (\delta^{dd'}) = \left(\frac{1}{N_c^2 - 1} \delta^{aa'} \delta^{bb'} \right) \overbrace{f^{adc} f^{a'd'c}}^{N_c \delta^{aa'}} = N_c \delta^{bb'} \quad (2.151)$$

Thus N_c is the color factor when a singlet pair of gluons exchanges a gluon.

Then let us look at a two gluon system (gluon colors dd') which is in a color octet state with color e . Such a system is described by $f^{dd'e}$. We let it interact by exchanging a gluon of color c and project out the color octet part from the final state:

$$O^{bb'e} \equiv P_{\underline{8}}^{bb',aa'} (f^{adc} f^{a'd'c}) f^{dd'e} = \frac{1}{N_c} f^{aa'f} f^{bb'f} (f^{adc} f^{a'd'c}) f^{dd'e} \quad (2.152)$$

We now use the fact that $f^{aa'f}$ is antisymmetric in $a \leftrightarrow a'$. Thus we can antisymmetrize the squared Lipatov vertex with respect to a, a' , with an associated factor $\frac{1}{2}$:

$$f^{aa'f} f^{adc} f^{a'd'c} = f^{aa'f} \frac{1}{2} (f^{adc} f^{a'd'c} - f^{a'dc} f^{ad'c}) \quad (2.153)$$

We can now use the Jacobi identity satisfied by the structure constants (following from the Jacobi identity for commutators) to rearrange the part in parenthesis as

$$f^{adc} f^{a'd'c} - f^{a'dc} f^{ad'c} = f^{aa'c} f^{dd'c}. \quad (2.154)$$

Now a repeated use of the adjoint representation Casimir relation gives us the result:

$$O^{bb'e} = \frac{1}{N_c} \frac{1}{2} (N_c \delta^{fc}) (N_c \delta^{ec}) = \frac{N_c}{2} f^{bb'e}. \quad (2.155)$$

Thus the color factor associated with a gluon exchange in the octet channel is $\frac{N_c}{2}$.

n -particle phase space

$$\mathcal{A}_n(y = \ln(s/|t|)) \sim \int d\Omega_{n+2} = \frac{1}{2s} \prod_{i=1}^n \frac{d^2 \mathbf{k}_i}{(2\pi)^2} \prod_{i=1}^n \overbrace{\frac{dy_i}{4\pi}}^{\sim \ln s} \quad (2.156)$$

We can calculate the n -particle phase space in more detail

$$\int d\Pi_{n+2} = \prod_{i=0}^{n+1} \left[\frac{d^4 \kappa_i}{(2\pi)^4} (2\pi) \delta(\kappa_i^2) \right] (2\pi)^4 \delta^{(4)} \left(p_1 + p_2 - \sum_{i=0}^{n+1} \kappa_i \right) \quad (2.157)$$

We first get rid of the overall momentum conservation. In the MRK approximation we have $p_1^+ \sim \kappa_0^+ \gg \kappa_1^+ \gg \dots$. Thus we can approximate the plus momentum conservation delta function as

$$\delta \left(p_1^+ - \sum_{i=0}^{n+1} \kappa_i^+ \right) \approx \delta(p_1^+ - \kappa_0^+) \quad (2.158)$$

and use it to integrate over κ_0^+ . Similarly we eliminate $\kappa_{n+1}^- \approx p_2^-$ with the minus-momentum conservation delta function. For transverse momenta, we have $n+2$ momenta κ that have to sum up to zero, and we can replace them by the $n+1$ transverse momenta \mathbf{k}_i that are unconstrained by momentum conservation.

$$\int \prod_{i=0}^{n+1} \left[\frac{d^2 \kappa_i}{(2\pi)^2} \right] (2\pi)^2 \delta^{(2)} \left(\sum_{i=0}^{n+1} \kappa_i \right) = \int \prod_{i=1}^{n+1} \frac{d^2 \mathbf{k}_i}{(2\pi)^2} \quad (2.159)$$

Now we still have $n+1$ κ_i^- -integrals ($i = 0, \dots, n$) and $n+1$ κ_i^+ -integrals ($i = 1, \dots, n+1$), with $n+2$ on-shell conditions. We integrate over all the κ_i^- -variables using the on-shell conditions

$$\int \frac{d\kappa_i^-}{(2\pi)} (2\pi) \delta(2\kappa_i^+ \kappa_i^- - \kappa_i^2) = \frac{1}{2\kappa_i^+}, \quad i = 0, \dots, n \quad (\kappa_0^+ = p_1^+). \quad (2.160)$$

The single remaining on-shell delta function is taken care of with the κ_{n+1}^+ -integral

$$\int \frac{d\kappa_{n+1}^+}{(2\pi)} (2\pi) \delta(2\kappa_{n+1}^+ p_2^- - \kappa_{n+1}^2) = \frac{1}{2p_2^-}. \quad (2.161)$$

This leaves us with the $n+1$ transverse integrals, and n plus-momentum integrals, with extra factors from the $i=0$ and $i=n+1$ on-shell delta functions

$$\overbrace{\frac{1}{2p_1^+} \frac{1}{2p_2^-}}^{\frac{1}{2s}} \int \prod_{i=1}^n \overbrace{\left[\frac{d\kappa_i^+}{2\pi} \frac{1}{2\kappa_i^+} \right]}^{\frac{dy_i}{4\pi}}. \quad (2.162)$$

So in total we have:

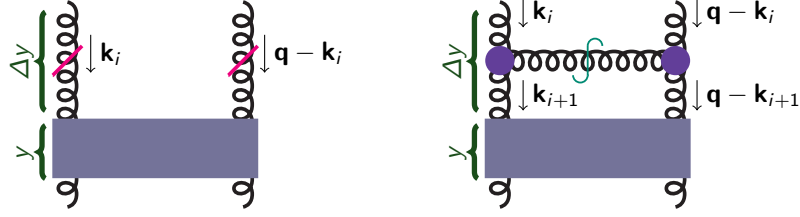
- An overall factor $\frac{1}{2s}$
- $n+1$ transverse integrals, which can taken to be those of the vertical gluon lines.
- n rapidities, integrated with an integration measure $dy/(4\pi)$.

It is good to check that our earlier 2- and 3-particle phase spaces from Eqs. (2.68) and (2.129) conform to this.

Now let us put together everything that happens when we add one rung to the ladder. We start from a situation where we already have a bunch of gluon exchanges and reggeized gluons filling the rapidities from the lower end of the ladder at $y = 0$ up to y . The gluons attached to this already formed partial ladder will have momenta k_{i+1} and $q - k_{i+1}$ going down to the ladder. Now we consider the addition of a new rapidity interval from y to $y + \Delta y$. Two things can happen in this rapidity interval. We can get an additional contribution from the Reggeized gluon propagators, which when expanded for a small interval in rapidity give a contribution $\sim \Delta y (\varepsilon(\mathbf{k}_i^2) + \varepsilon((\mathbf{q} - \mathbf{k}_i)^2))$. The definition of ε (see Eq. (2.83)) involves an integration over some dummy variable: we can choose to call this variable \mathbf{k}_{i+1} .

On the other hand we also can exchange a gluon, which is associated with a factor $\Delta y/(4\pi)$ from the phase space integration, a color factor N_c or $N_c/2$ and the square of C^ρ from the Lipatov vertices. Now the gluon crossing the cut can carry some momentum, so we have to differentiate between the momenta $\mathbf{k}_i, \mathbf{q} - \mathbf{k}_i$ at the upper end of the line and the momenta below the Lipatov vertices $\mathbf{k}_{i+1}, \mathbf{q} - \mathbf{k}_{i+1}$. We are interested in the new slightly more resummed ladder with $\mathbf{k}_i, \mathbf{q} - \mathbf{k}_i$, so we integrate over \mathbf{k}_{i+1} .

One step



$$\begin{aligned}
 & N_c \alpha_s \Delta y \int \frac{d^2 \mathbf{k}_{i+1}}{(2\pi)^2} \left[\frac{-\mathbf{k}_i^2}{\mathbf{k}_{i+1}^2 (\mathbf{k}_{i+1} - \mathbf{k}_i)^2} + \frac{-(\mathbf{q} - \mathbf{k}_i)^2}{(\mathbf{q} - \mathbf{k}_{i+1})^2 (\mathbf{k}_{i+1} - \mathbf{k}_i)^2} \right] \text{Im } \mathcal{A}(\mathbf{k}_i, \mathbf{q}) \\
 & + \frac{\Delta y}{4\pi} g^2 \underbrace{\overbrace{G_R}^{8:N_c/2}}_{\underline{1}:N_c} \int \frac{d^2 \mathbf{k}_{i+1}}{(2\pi)^2} \frac{i}{\mathbf{k}_{i+1}^2} \frac{i}{(\mathbf{q} - \mathbf{k}_{i+1})^2} \left[\mathbf{q}^2 - \frac{\mathbf{k}_{i+1}^2 (\mathbf{q} - \mathbf{k}_i)^2}{(\mathbf{k}_i - \mathbf{k}_{i+1})^2} - \frac{\mathbf{k}_i^2 (\mathbf{q} - \mathbf{k}_{i+1})^2}{(\mathbf{k}_i - \mathbf{k}_{i+1})^2} \right] \text{Im } \mathcal{A}(\mathbf{k}_{i+1}, \mathbf{q})
 \end{aligned} \tag{2.163}$$

In the second term coming from the reggeized gluon propagators, we have $\varepsilon(\mathbf{q} - \mathbf{k}_i)^2$ where originally the denominator is $(\mathbf{k}_{i+1})^2 (\mathbf{q} - \mathbf{k}_{i+1} - \mathbf{k}_i)^2$, but it can be brought into the form $(\mathbf{q} - \mathbf{k}_{i+1})^2 (\mathbf{k}_{i+1} - \mathbf{k}_i)^2$ by a change in the integration variable. The square of the Lipatov vertex from Eq. (2.142) is multiplied by a minus sign, because the polarization sum is $-g_{\rho\rho'}$. There are also the two propagators with the (transverse only in the MRK approximation) momenta $\mathbf{k}_i, \mathbf{q} - \mathbf{k}_i$. Note that $g^2/(4\pi) = \alpha_s$. Note that for the octet, the terms in the first square bracket are exactly the same as the last two terms in the second square bracket. For the singlet they are not, as we already saw in Eq. (2.138).

2.5.3 Resumming the ladder: Mellin space

Now let us discuss how all the ladder diagrams can be summed together. The traditional way to do this is to deconvolute the MRK ordered rapidities by a Laplace transformation in rapidity, i.e. a Mellin transform in s .

Laplace/Mellin

$$\text{Im } \mathcal{A}_n(y = \ln(s/|t|), \mathbf{q}) \sim \int_0^y dy_1 \int_0^{y_1} dy_2 \cdots \int_0^{y_{n-1}} dy_n e^{(y-y_1)\varepsilon_1} \times \cdots \times e^{(y_n-0)\varepsilon_{n+1}} \tag{2.164}$$

$$\mathcal{A}_n(\omega, \mathbf{q}) = \int_0^\infty dy e^{-\omega y} \mathcal{A}(y) = G_R \prod_{i=1}^{n+1} \frac{1}{\mathbf{k}_i^2} \frac{1}{(\mathbf{q} - \mathbf{k}_i)^2} \frac{K_{i,i+1}}{\omega - \varepsilon_i} \tag{2.165}$$

$$\varepsilon_i \equiv \varepsilon(\mathbf{k}_i^2) + \varepsilon((\mathbf{q} - \mathbf{k}_i)^2) \quad K_{i,i+1} \equiv C_R \alpha_s N_c C^\rho(k_i, k_{i+1}) C_\rho(q - k_i, q - k_{i+1}). \tag{2.166}$$

Here $C_R = 1$ for $R = \underline{8}$ and $C_R = 1/2$ for $R = \underline{1}$ and there is a separate representation-dependent prefactor G_R for the leading-order amplitude.

Now all the ladder diagrams can be resummed. This can be done by first defining a little bit of auxiliary notation:

$$\text{Im } \mathcal{A}_R(\omega, \mathbf{q}) = \sum_{n=0}^{\infty} \text{Im } \mathcal{A}_n(\omega, \mathbf{q}) = G_R \int d^2 \mathbf{k} \frac{\mathcal{F}}{\mathbf{k}^2 (\mathbf{q} - \mathbf{k}^2)} \equiv \int_1 \mathcal{F}_1, \tag{2.167}$$

With the help of this auxiliary function, the ladder diagrams are summed by solving the recursive equation

BFKL equation in momentum space

$$\omega \mathcal{F}_1 = 1 - \int_2 K_{12} \mathcal{F}_2 + \varepsilon_1 \mathcal{F}_1 \quad (2.168)$$

This equation is the momentum space BFKL equation. We can check that it indeed reproduces the sum of the n -rung ladder amplitudes by solving it recursively:

$$\begin{aligned} \int_1 \mathcal{F}_1 &= \int_1 \frac{1 - \int_2 K_{12} \mathcal{F}_2}{\omega - \varepsilon_1} = \int_1 \frac{1}{\omega - \varepsilon_1} - \int_{1,2} \frac{K_{12} \mathcal{F}_2}{\omega - \varepsilon_1} \\ &= \int_1 \frac{1}{\omega - \varepsilon_1} - \int_{1,2} \frac{K_{12}}{(\omega - \varepsilon_1)(\omega - \varepsilon_2)} \left(1 - \int_3 K_{23} \mathcal{F}_3 \right) = \dots, \end{aligned} \quad (2.169)$$

where continuing the expansion reproduces the terms in the sum

$$\text{Im } \mathcal{A}_R(\omega, \mathbf{q}) = \sum_n \mathcal{A}_n(\omega, \mathbf{q}). \quad (2.170)$$

To solve the equation (2.168) we write it more explicitly in an integral equation form, by introducing a delta function so that we can write the right hand side as an integral operator acting on \mathcal{F}_2 :

$$\varepsilon_1 \mathcal{F}_1 = \int_2 K_{12}^{\text{virt}} \mathcal{F}_2, \quad (2.171)$$

where K_{12}^{virt} is proportional to $\delta^{(2)}(\mathbf{k}_1 - \mathbf{k}_2)$. Now we can write (2.168) as

$$\omega \mathcal{F}_1 = 1 - \int_2 (K_{12} - K_{12}^{\text{virt}}) \mathcal{F}_2 \quad (2.172)$$

Now one needs to find the eigenfunctions of the integral kernel $K_{12} + K_{12}^{\text{virt}}$, which can be used to express the solution. In fact the eigenfunctions of the kernel are just powers of transverse momentum. Thus in fact the calculation is done by Mellin transforming, in addition to the energy s , also the transverse momentum. This is the calculation originally done by Lipatov et al.

2.5.4 Resumming the ladder: differential equation

From a modern point of view it is perhaps better to write the BFKL equation (2.168) as a differential equation in rapidity. This is also the form in which we will rederive it later in this course, as a dilute limit of the BK equation.

We think of all the ladder diagrams with gluons bwtween $y = 0$ and y as being represented by a function, the *BFKL Green's function* $\mathcal{F}_y(\mathbf{q}, \mathbf{k}, \mathbf{p})$

Differential equation

$$\mathcal{F}_{y+\Delta y}(\mathbf{q}, \mathbf{k}, \mathbf{p}) = (1 + \Delta y \varepsilon(\mathbf{q}, \mathbf{k})) \mathcal{F}_y(\mathbf{q}, \mathbf{k}, \mathbf{p}) - \int_{\kappa} K(\mathbf{q}, \mathbf{k}, \kappa) \mathcal{F}_2(\mathbf{q}, \kappa, \mathbf{p}) \quad (2.173)$$

$$\mathcal{F}_{y+\Delta y}(\mathbf{q}, \mathbf{k}, \mathbf{p}) = (1 + \Delta y \varepsilon(\mathbf{q}, \mathbf{k})) \mathcal{F}_y(\mathbf{q}, \mathbf{k}, \mathbf{p}) - \int_{\kappa} K(\mathbf{q}, \mathbf{k}, \kappa) \mathcal{F}_2(\mathbf{q}, \kappa, \mathbf{p}) \quad (2.174)$$

Thinking about Δy as an infinitesimal variable, this becomes a differential equation

$$\partial_y \mathcal{F}_y(\mathbf{q}, \mathbf{k}, \mathbf{p}) = - \int_{\kappa} (K(\mathbf{q}, \mathbf{k}, \kappa) - K^{\text{virt}}(\mathbf{q}, \mathbf{k}, \kappa)) \mathcal{F}_y(\mathbf{q}, \kappa, \mathbf{p}), \quad (2.175)$$

where again $K^{\text{virt}}(\mathbf{q}, \mathbf{k}, \boldsymbol{\kappa})$ is proportional to $\delta^{(2)}(\mathbf{k} - \boldsymbol{\kappa})$. The initial condition (corresponding to the identity 1 in Eq. (2.168)) corresponds to the lowest order scattering amplitude, where s is so small that powers of $\alpha_s \ln s$ do not need to be resummed. Solving this differential equation with such an initial condition then performs the resummation of these large logarithms. For concreteness let me quote explicitly the differential form of the color singlet BFKL equation for $\mathbf{q} = 0$:

$$\partial_y \mathcal{G}_y(\mathbf{0}, \mathbf{k}, \mathbf{p}) = \frac{N_c \alpha_s}{\pi^2} \int d^2 \boldsymbol{\kappa} \left[\frac{1}{(\boldsymbol{\kappa} - \mathbf{k})^2} \mathcal{G}_y(\mathbf{0}, \boldsymbol{\kappa}, \mathbf{p}) - \frac{1}{2} \frac{\mathbf{k}^2}{(\boldsymbol{\kappa} - \mathbf{k})^2 \boldsymbol{\kappa}^2} \mathcal{G}_y(\mathbf{0}, \mathbf{k}, \mathbf{p}) \right], \quad (2.176)$$

where $\mathcal{G}(\mathbf{0}, \mathbf{k}, \mathbf{p}) = \mathbf{k}^2 \mathbf{p}^2 \mathcal{F}(\mathbf{0}, \mathbf{k}, \mathbf{p})$. Unfortunately the BFKL equation appears in the literature in many forms, and it sometimes takes some work to relate the different expressions to each other; I am not a 100% sure that this is the right relation between \mathcal{G} and \mathcal{F} . A few manipulations of this equation can show that, in spite of the IR divergences present in $\varepsilon(\mathbf{q})$, this equation (and thus the singlet solution to the BFKL equation, unlike the octet) is perfectly IR finite: the IR divergences cancel between the two (“real” and “virtual”) terms of the equation.

To summarize:

- We have managed to resum all the leading large energy contributions to QCD cross sections, resumming powers of $\alpha_s \ln s$.
- The solution to the color octet exchange is the reggeized gluon: the color octet amplitude behaves as

$$\mathcal{A}_{\underline{8}} = -2\pi\alpha_s \left[1 - e^{-i\pi(1+\varepsilon(t))} \right] \left(\frac{s}{|t|} \right)^{1+\varepsilon(t)}, \quad (2.177)$$

with a logarithmically IR divergent function $\varepsilon(t)$. Because of the IR divergence, this solution cannot give any physically meaningful cross sections by itself, but it is a key ingredient in building measurable cross sections in a calculation where the IR divergence eventually cancels.

- The singlet solution (the “QCD pomeron”) can be obtained by solving the BFKL equation. This happens by finding the eigenfunctions of the BFKL kernel appearing in an integral equation describing the energy dependence of the cross section. The solution with the largest eigenvalue determines the asymptotic high energy behavior. Because of the continuum of eigenfunctions contributing, the analytical structure of the singlet amplitude is not a simple pole (as in Regge theory), but rather a branch cut.
- The result of solving the color singlet BFKL equation (which we have not done here) tells us that the singlet cross section behaves as

$$\mathcal{A}_{\underline{1}} \sim s^{1 + \frac{N_c \alpha_s}{\pi} 4 \ln 2} \approx s^{1+0.5} \quad (2.178)$$

This is a much faster energy dependence than observed in things like the total proton-proton cross section, which rather grows like $s^{1.08}$. But the solution will work better for processes where there is some transverse momentum scale that is large enough that the weak coupling calculation we have made here works better.

Chapter 3

The eikonal way

3.1 Diffraction: scattering of scalar light off a plane

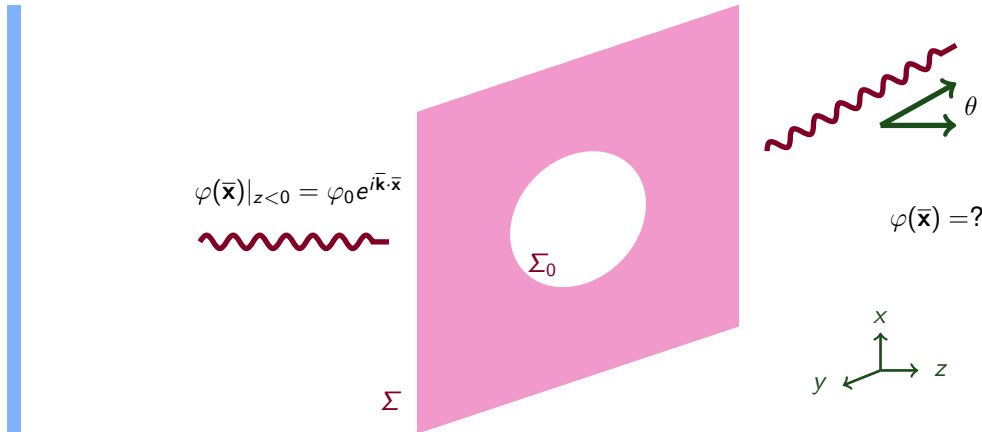
The discussion here follows very closely the one in Barone & Predazzi, sec 2.1. Also Kovchegov & Levin, Sec 7.1 has a very similar discussion.

Aim We start familiarizing ourselves with high energy scattering in an “old-fashioned” way by looking at the simplest possible relativistic problem: the scattering of light off a planar (semi)absorbing target. This will help us illustrate in a simple context several concepts that are essential for understanding the scattering of hadrons and nuclei at high energies, such as:

- the impact parameter
- the optical theorem
- elastic and total cross sections
- the scattering amplitude, its phase and unitarity constraints

3.1.1 Scattering from a hole

Before discussing scattering off a disk, we start with the opposite situation of scattering off a hole in an infinite opaque plane. The experimental situation at first is the following: we have an absorbing sheet on the xy plane (surface Σ), with a hole (denoted Σ_0) in the middle. Upon this whole we have an incoming ray of light with momentum (wave vector) \vec{k} along the z -direction, which we measure behind the hole at $z \rightarrow \infty$, keeping track of the pattern of light far away from the whole as a function of the angle θ with respect to the z -axis.



We look at “scalar light” (forgetting the polarization/spin) for now, so our ray of light obeys a relativistic Klein-Gordon wave equation. Since the disk is static (does not depend on time), the time dependence of the

wave function can be described by a single frequency¹ $\omega = k$, and we can factorize the solution of the wave equation as

$$\square \Phi(x) \equiv \partial_\mu \partial^\mu \Phi(x) = 0, \quad \Phi(t, \bar{x}) = e^{-ikt} \varphi(\bar{x}) \implies (k^2 + \nabla^2) \varphi(\bar{x}) = 0, \quad k \equiv |\bar{k}| \quad (3.1)$$

We now want to find the scattered wave after it has gone through the hole, $\varphi(\bar{x})|_{z>0}$. The way we will do this is physically known as the *Huygens principle*: every point on Σ_0 is itself a source of spherical light waves. In terms of mathematics we will do this using a Green function and Green's theorem:

Green function G :

$$(k^2 + \nabla_{\bar{x}}^2) G(\bar{x}, \bar{y}) = -\delta^{(3)}(\bar{x} - \bar{y}) \quad (3.2)$$

$$\implies G(\bar{x}, \bar{y}) = \frac{e^{ik|\bar{x}-\bar{y}|}}{4\pi|\bar{x}-\bar{y}|} \quad (3.3)$$

Green's theorem

$$\varphi(\bar{x}) = \int_{\bar{y} \in \Sigma_0} d\mathbf{S} \cdot [(\nabla_{\bar{y}} G(\bar{x} - \bar{y})) \varphi(\bar{y}) - G(\bar{x} - \bar{y}) \nabla_{\bar{y}} \varphi(\bar{y})] \quad (3.4)$$

The Green function (3.3) can be derived by taking a Fourier-transform of equation (3.2). This is a good exercise to go through and is presented below in more detail. An important thing to recall is that the solution to the second order differential equation (3.2) is not unique, because from one solution one can always obtain another solution by adding to it a solution of the homogenous equation

$$(k^2 + \nabla_{\bar{x}}^2) h(\bar{x}, \bar{y}) = 0 \implies (k^2 + \nabla_{\bar{x}}^2)(G(\bar{x}, \bar{y}) + h(\bar{x}, \bar{y})) = -\delta^{(3)}(\bar{x} - \bar{y}). \quad (3.5)$$

The solution becomes unique when one supplements it with a *boundary condition*. Here we have chosed a boundary condition that corresponds to the physical situation: we want to have an outgoing plane wave $e^{i\bar{k} \cdot \bar{x}}$ at large \bar{x} .

The Green's theorem is a way to somewhat formally construct a solution to the wave equation (3.1) that satisfies a desired boundary condition in the hole Σ_0 ; the first term guarantees that $\varphi(\bar{x})$ has the correct value at Σ_0 , and the second term that the derivative with respect to z also does so. Recall that we know the solution at $z < 0$, it is just the incoming plane wave; thus we also know the solution on Σ_0 .

Digression: Green function

To derive the Green function (3.3) we represent it as a Fourier-transform. Note that since the r.h.s. of equation (3.2) only depends on the difference $\bar{x} - \bar{y}$, the solution must also be a function of just the difference.

$$G(\bar{x}, \bar{y}) = \int \frac{d^3 \bar{\mathbf{p}}}{(2\pi)^3} e^{i\bar{\mathbf{p}} \cdot (\bar{x} - \bar{y})} G(\bar{\mathbf{p}}) \quad (3.6)$$

We now insert this into the defining equation (3.2) to get

$$(k^2 + \nabla_{\bar{x}}^2) G(\bar{x}, \bar{y}) = \int \frac{d^3 \bar{\mathbf{p}}}{(2\pi)^3} e^{i\bar{\mathbf{p}} \cdot (\bar{x} - \bar{y})} (k^2 - \bar{\mathbf{p}}^2) G(\bar{\mathbf{p}}) \quad (3.7)$$

$$= -\delta^{(3)}(\bar{x} - \bar{y}) = - \int \frac{d^3 \bar{\mathbf{p}}}{(2\pi)^3} e^{i\bar{\mathbf{p}} \cdot (\bar{x} - \bar{y})} \quad (3.8)$$

We know that Fourier-transforms are invertible, so we can deduce that

$$(\bar{\mathbf{p}}^2 - k^2) G(\bar{\mathbf{p}}) = 1 \quad (3.9)$$

Now we should divide both sides of this equation with $(\bar{\mathbf{p}}^2 - k^2)$ to solve for $G(\bar{\mathbf{p}})$. This is fine except at the point $k^2 = \bar{\mathbf{p}}^2$: where we have to regularize the expression somehow. In fact there are several ways of doing this, which correspond to several different possible boundary conditions for the original equation. We will here replace k^2 by

¹More precisely, a general solution of the wave equation can always be expressed as a linear superposition of these oscillations, and because the wave equation is linear these oscillations are not coupled to each other

$(k + i\varepsilon)^2$ to get the correct result (outgoing wave), other possible options would be $(k - i\varepsilon)^2$ or $k^2 \pm i\varepsilon$, which would correspond to an incoming wave, or a linear combination between incoming and outgoing ones. We now get

$$G(\vec{p}) = \frac{1}{\vec{p}^2 - (k + i\varepsilon)^2}, \quad (3.10)$$

and can invert the Fourier-transform as

$$G(\vec{x}, \vec{y}) = \int \frac{d^3\vec{p}}{(2\pi)^3} \frac{e^{i\vec{p} \cdot (\vec{x} - \vec{y})}}{\vec{p}^2 - (k + i\varepsilon)^2} \quad (3.11)$$

$$= \frac{1}{(2\pi)^2} \int_0^\infty dp p^2 \int_{-1}^1 d\cos\theta \frac{e^{ip|\vec{x} - \vec{y}| \cos\theta}}{\vec{p}^2 - (k + i\varepsilon)^2} \quad (3.12)$$

$$= \frac{1}{(2\pi)^2} \int_0^\infty dp p^2 \frac{1}{ip|\vec{x} - \vec{y}|} \frac{e^{ip|\vec{x} - \vec{y}|} - e^{-ip|\vec{x} - \vec{y}|}}{\vec{p}^2 - (k + i\varepsilon)^2} \quad (3.13)$$

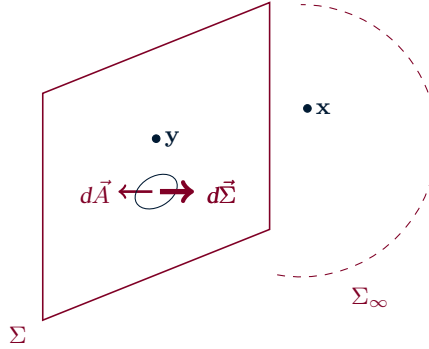
$$= \frac{-i}{(2\pi)^2 |\vec{x} - \vec{y}|} \int_{-\infty}^\infty dp p \frac{e^{ip|\vec{x} - \vec{y}|}}{(p + k + i\varepsilon)(p - k - i\varepsilon)} \quad (3.14)$$

This integral is performed by the theorem of residues, closing the contour in the upper complex p -plane, where one picks up the pole at $p = k + i\varepsilon$, with residue $e^{ik|\vec{x} - \vec{y}|}/2$. Together with the factor $2\pi i$ from the residue theorem this gives the result

$$G(\vec{x}, \vec{y}) = \frac{e^{ik|\vec{x} - \vec{y}|}}{4\pi |\vec{x} - \vec{y}|} \quad (3.15)$$

Digression: Green's theorem

See e.g. Jackson, Classical Electrodynamics, sec 10.5.



Let us look at the volume V , defined as the half-space with very large radius, on the positive side of the z -axis, i.e. $z > 0, |x^2 + y^2 + z^2| < R^2, R \rightarrow \infty$. Recalling the definition of the Green function (3.2), we can write the value of the wave function $\varphi(\vec{x})$ within this sphere as

$$\varphi(\vec{x})|_{\vec{x} \in V} = - \int_V d^3\vec{y} \overbrace{[(\nabla_{\vec{y}}^2 + k^2) G(\vec{x}, \vec{y})]}^{-\delta^{(3)}(\vec{x} - \vec{y})} \varphi(\vec{y}) \quad (3.16)$$

$$= - \int_V d^3\vec{y} \nabla_{\vec{y}} \cdot [(\nabla_{\vec{y}} G(\vec{x}, \vec{y})) \varphi(\vec{y}) - G(\vec{x}, \vec{y}) \nabla_{\vec{y}} \varphi(\vec{y})], \quad (3.17)$$

where we used the equation of motion $(\nabla_{\vec{y}}^2 + k^2)\varphi(\vec{y}) = 0$. Now we can transform the volume integral into a surface integral, neglecting the half-sphere at infinity where the wave function (and Green function) vanish. Denoting by $d\vec{\Sigma}$ the directed surface element pointing in the positive z -direction (towards the inside of the volume V , i.e. opposite to the conventional direction of a surface element) we now have

$$\varphi(\vec{x})|_{\vec{x} \in V} = \int_{\Sigma} d\vec{\Sigma} \cdot [(\nabla_{\vec{y}} G(\vec{x}, \vec{y})) \varphi(\vec{y}) - G(\vec{x}, \vec{y}) \nabla_{\vec{y}} \varphi(\vec{y})] \quad (3.18)$$

In order to apply Green's theorem to our scattering problem, we need to calculate the required quantities on the boundary Σ , which we will parametrize now with the 2-dimensional coordinate known as the *impact parameter* \mathbf{b} .

$$\partial_{y^3} \varphi(\bar{\mathbf{y}}) \Big|_{\bar{\mathbf{y}}=(\mathbf{b},0)} = ik\varphi_0 \quad (3.19)$$

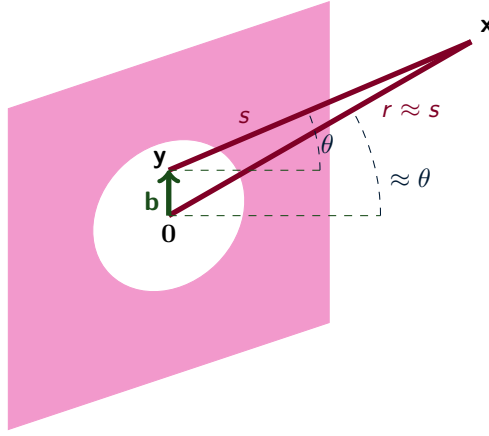
$$\partial_{y^3} \frac{e^{ik|\bar{\mathbf{x}}-\bar{\mathbf{y}}|}}{4\pi|\bar{\mathbf{x}}-\bar{\mathbf{y}}|} \Big|_{\bar{\mathbf{y}}=(\mathbf{b},0)} = -\varphi_0 \cos \theta \left(ik - \frac{1}{|\bar{\mathbf{x}}-\bar{\mathbf{y}}|} \right), \quad (3.20)$$

where θ is the angle between the z -axis and the vector $\bar{\mathbf{x}} - \bar{\mathbf{y}}$ connecting the point $\bar{\mathbf{y}}$ on the $z = 0$ -plane Σ that is the target of our scattering, and the far away location $\bar{\mathbf{x}}$ where we are observing the outcoming wave. here we have used

$$\begin{aligned} \partial_{y^3} |\bar{\mathbf{y}} - \bar{\mathbf{x}}| &= \partial_{y^3} \sqrt{(x^1 - y^1)^2 + (x^2 - y^2)^2 + (x^3 - y^3)^2} \\ &= \frac{2(y^3 - x^3)}{2\sqrt{(x^1 - y^1)^2 + (x^2 - y^2)^2 + (x^3 - y^3)^2}} = -\cos(\theta), \end{aligned} \quad (3.21)$$

with

$$\cos(\theta) = \frac{(x^3 - y^3)}{|\bar{\mathbf{y}} - \bar{\mathbf{x}}|}. \quad (3.22)$$



$$\varphi(\bar{\mathbf{x}}) = \varphi \int_{\Sigma_0} d^2\mathbf{b} \left[-\cos(\theta) \left(ik - \frac{1}{|\bar{\mathbf{y}} - \bar{\mathbf{x}}|} \right) - ik \right] \frac{e^{ik|\bar{\mathbf{x}}-\bar{\mathbf{y}}|}}{4\pi|\bar{\mathbf{x}}-\bar{\mathbf{y}}|} \quad (3.23)$$

This is an exact result. Now we are going to make certain approximations that limit our interest to a detector that is far from the scattering compared to the wavelength of the wave $|\bar{\mathbf{y}} - \bar{\mathbf{x}}| \gg 1/k$, and to scattering at small angles: $\theta \ll 1$

- $|\bar{\mathbf{y}} - \bar{\mathbf{x}}| \gg 1/k$
- $\theta \ll 1 \implies \cos \theta \approx 1$

$$k|\bar{\mathbf{y}} - \bar{\mathbf{x}}| = k\sqrt{(x^3)^2 + (\mathbf{x} - \mathbf{b})^2} \approx kr \left(1 - \frac{\mathbf{x} \cdot \mathbf{b}}{r^2} \right) \approx kr - \mathbf{q} \cdot \mathbf{b} \quad r \equiv |\bar{\mathbf{x}}| \quad (3.24)$$

$$\bar{\mathbf{q}} = \bar{\mathbf{k}}' - \bar{\mathbf{k}}, \quad \frac{\mathbf{q}}{k} = \frac{\mathbf{x}}{r} \sim \theta \quad q^3 \sim k(1 - \cos \theta) \sim k\theta^2 \ll |\mathbf{q}| \quad (3.25)$$

$$\varphi(\bar{\mathbf{x}}) = -ik\varphi_0 \frac{e^{ikr}}{2\pi r} \int_{\Sigma} d^2\mathbf{b} \Gamma(\mathbf{b}) e^{-i\mathbf{q} \cdot \mathbf{b}} \quad (3.26)$$

$$\Gamma(\mathbf{b}) = \begin{cases} 1, & \mathbf{b} \in \Sigma_0 \\ 0, & \mathbf{b} \notin \Sigma_0 \end{cases} \quad (3.27)$$

To be specific: here $\bar{\mathbf{k}}'$ is defined as a vector of absolute value k , pointing in the direction of $\bar{\mathbf{x}}$, i.e. from the origin of our coordinate system (which is somewhere inside the target hole) to our detector.

Digression: Energy conservation check

We made several small angle approximations in this process. It can be useful to check to what extent energy is still conserved in our scattering. We can do this by comparing the radiation power (= intensity times area) incoming on the hole, and the power going out. The incoming power is (up to a factor of k) the intensity of the incoming wave $|\varphi_0|^2$ integrated over the area of the hole

$$P_{in} = |\varphi_0|^2 \int_{\Sigma_0} d^2\mathbf{b}. \quad (3.28)$$

The outgoing power is obtained by integrating, at a distance $r = R$ from the target, the intensity $|\varphi(\bar{\mathbf{x}})|^2$ over the area, where the area element is the solid angle times the squared radius: $dS = R^2 d\Omega = R^2 d^2\mathbf{q}/k^2$

$$P_{out} = R^2 \int \frac{d^2\mathbf{q}}{k^2} |\varphi(\bar{\mathbf{x}})|^2 \quad (3.29)$$

$$= R^2 |\varphi_0|^2 \int \frac{d^2\mathbf{q}}{k^2} \frac{1}{(2\pi r)^2} \int_{\Sigma_0} d^2\mathbf{b} \int_{\Sigma_0} d^2\mathbf{b}' \Gamma(\mathbf{b}) \Gamma(\mathbf{b}') e^{-i\mathbf{q} \cdot (\mathbf{b} - \mathbf{b}')} \quad (3.30)$$

Integrating first over \mathbf{q} gives a δ -function in $\mathbf{b} - \mathbf{b}'$, which can be used to do the \mathbf{b}' -integral, resulting in $P_{out} = P_{in}$. This is of course not exact, because the identification $d\Omega = d^2\mathbf{q}/k^2$ is only valid for small angles.

3.1.2 Scattering off disk

So far we have been looking at light going through a hole in an opaque plane. Let us now switch to a situation that is closer to the case of high energy particle, and replace the hole by an opaque disk of the same shape Σ_0 . Because the wave equation is linear, the waves scattered off the hole and the disk should add up to the original wave. We can therefore obtain the wave scattered from the disk by simply subtracting from the original incoming wave the wave scattered off a hole, i.e. replacing our profile function $\Gamma(\mathbf{b})$ by $1 - \Gamma(\mathbf{b})$

Babinet: hole + disk = original wave

\Rightarrow Scattering off disk Σ_0

$$\varphi(\bar{\mathbf{x}}) = -ik\varphi_0 \frac{e^{ikr}}{2\pi r} \int_{\Sigma_0} d^2\mathbf{b} (1 - \Gamma(\mathbf{b})) e^{-i\mathbf{q} \cdot \mathbf{b}} \approx \varphi(\bar{\mathbf{x}}) + \varphi_0 f(\mathbf{q}) \frac{e^{ikr}}{r} \quad (3.31)$$

$f(\mathbf{q})$ = QM scattering amplitude, cross section:

$$\frac{d\sigma}{d^2\mathbf{q}} = \frac{1}{k^2} \frac{d\sigma}{d\Omega} = \frac{1}{k^2} |f(\mathbf{q})|^2 = \left| \frac{i}{2\pi} \int_{\Sigma_0} d^2\mathbf{b} \Gamma(\mathbf{b}) e^{-i\mathbf{q} \cdot \mathbf{b}} \right|^2 \quad (3.32)$$

Note that because we have written the outgoing wave as a spherical one, it is a bit tricky to directly mathematically reconstruct the original wave by taking just the “1” in the $1 - \Gamma$. The physical interpretation should however be clear: the 1 corresponds to no target, and the Γ to the opaque disk.

Here we constantly pass between the solid angle $d\Omega$ and the momentum transfer $d\Omega \approx d^2\mathbf{q}/k^2$. For an azimuthally symmetric target we can write this in terms of the scalar momentum transfer (the usual Mandelstam variable t) using $d^2\mathbf{q} = 2\pi d\mathbf{q}^2 = -2\pi dt$.

Note that the quantum mechanical scattering amplitude f in this case is imaginary. This corresponds, in the usual conventions, to a purely absorptive potential, as is our target of a fully opaque disk. Mathematically it follows from the derivatives acting on the plane wave and the Green function in the Green’s theorem formula. It is, however, easy to generalize this to a scattering amplitude that has both absorptive and non-absorptive parts by just assuming that the function Γ can take arbitrary complex values. In this case the expression (3.32) must be interpreted as *elastic* scattering, since what comes out is the same ray of light that went in, just bent in a different direction. We can also calculate an *absorptive* cross section by taking the difference between incoming intensity (the 1) and the outgoing one (the $1 - \Gamma$) and integrating over the momentum \mathbf{q} (which now is not directly an observable quantity, but is rather interpreted as the momentum that the outgoing wave would have had if it not been absorbed). The sum of the elastic and absorptive cross sections is the total cross section. Integrating over \mathbf{q} gives a delta function that sets the impact parameter \mathbf{b} to be the same in the amplitude and the conjugate amplitude and also absorbs the factors $1/2\pi$. Thus the integrated absorptive and elastic cross sections have particularly simple expressions in as integrals over the transverse area of the target:

Generalization: $\Gamma(\mathbf{b}) \in \mathbb{C}$

- Elastic

$$\frac{d\sigma_{\text{el}}}{d^2\mathbf{q}} = \left| \frac{i}{2\pi} \int_{\Sigma_0} d^2\mathbf{b} \Gamma(\mathbf{b}) e^{-i\mathbf{q}\cdot\mathbf{b}} \right|^2 \Rightarrow \sigma_{\text{el}} = \int_{\Sigma_0} d^2\mathbf{b} |\Gamma(\mathbf{b})|^2 \quad (3.33)$$

- Absorptive

$$\begin{aligned} \frac{d\sigma_{\text{abs}}}{d^2\mathbf{q}} &= \left| \frac{i}{2\pi} \int_{\Sigma_0} d^2\mathbf{b} 1 e^{-i\mathbf{q}\cdot\mathbf{b}} \right|^2 - \left| \frac{i}{2\pi} \int_{\Sigma_0} d^2\mathbf{b} (1 - \Gamma(\mathbf{b})) e^{-i\mathbf{q}\cdot\mathbf{b}} \right|^2 \\ &\Rightarrow \sigma_{\text{abs}} = \int_{\Sigma_0} d^2\mathbf{b} [2 \operatorname{Re}(\Gamma(\mathbf{b})) - |\Gamma(\mathbf{b})|^2] \end{aligned} \quad (3.34)$$

- Total

$$\sigma_{\text{tot}} = \sigma_{\text{el}} + \sigma_{\text{abs}} = \sigma_{\text{abs}} = 2 \int_{\Sigma} d^2\mathbf{b} [\operatorname{Re} \Gamma(\mathbf{b})] = \frac{4\pi}{k} \operatorname{Im}(f(\mathbf{q} = 0)) \quad (3.35)$$

\Rightarrow optical theorem

- Black disk= $\Gamma = 1 \Rightarrow \sigma_{\text{el}} = \sigma_{\text{abs}}$

This is a concrete and explicit demonstration of the optical theorem, which of course is constantly used in scattering theory. In fact it is so frequent that one often does not explicitly mention it when using it. Note that there is a difference of i between our opacity function Γ and the scattering amplitude f , i.e. when f is purely imaginary, Γ is purely real.

Note that contrary to the usual relativistic field theory expressions, we have not derived these in terms of Lorentz-invariant matrix elements and flux factors; the flux factor is absorbed into the normalization of Γ , see [1]. In stead we have a very good physical interpretation of what the cross section means: it is a quantity with the dimensions of area that results from integrating over the surface of the target the dimensionless probability that the probe will scatter if it hits the specific impact parameter \mathbf{b} . This wording might sound classical, but the importance of interference and the complex phase of Γ should serve as reminders that these results reflect the wave nature of quantum particles.

3.2 Eikonal scattering

3.2.1 Eikonal approximation

Scattering at high energy becomes much simpler with the *eikonal approximation*. Many textbooks, (e.g. Barone & Predazzi (Sec 2.3) start by describing the eikonal approximation for nonrelativistic scattering off a classical potential). A more formal field theoretic derivation for gauge theory (e.g. [13]) follows the important work of Bjorken et al [21] by starting from the operator definition of the scattering amplitude and looking at its properties when the incoming state is boosted to a very high energy. We will here follow an approach that is between these in the sense that we look just at solutions of wave equation, but inspect a situation that is

- relativistic and
- involves a vector potential (for the Abelian theory at first)

Klein-Gordon eq. in external vector potential:

$$[(i\partial_\mu + eA_\mu(x))(i\partial^\mu + eA^\mu(x)) - m^2] \phi(x) = 0 \quad (3.36)$$

We are now interested in the scattering problem where the boundary condition is that of a high energy particle approaching the target (represented by the gauge potential A_μ). Thus the boundary condition for the equation is a plane wave $e^{-ik\cdot x}$ at $x^+ \rightarrow -\infty$. The assumption that we are interested in high energy means that k^+ is much larger than any other momentum scale in the problem, in particular any gradients of the potential A_μ . It is natural to make this assumption about the momentum scales explicit and to separate

out the rapidly oscillating behavior of the wave function from the smoother scales by using an ansatz where it is explicitly factorized. We can also assume that we are in Lorenz gauge $\partial_\mu A^\mu = 0$.

Ansatz

$$\phi(x) \rightarrow e^{-ik \cdot x}, \quad x^+ \rightarrow -\infty \quad (3.37)$$

$$\phi(x) = e^{-ik \cdot x} \varphi(x) \quad (3.38)$$

$$k^+ \gg \frac{\partial_\mu \varphi(x)}{\varphi(x)} \quad (3.39)$$

$$\partial_\mu A^\mu = 0 \quad (3.40)$$

Inserting the ansatz (3.38) into the original equation (3.36) leads to

$$e^{-ik \cdot x} \left[\overbrace{k^2 - m^2}^{=0} + \underline{2ek^\mu A_\mu} + \underline{2ik^\mu \partial_\mu} - \partial_\mu \partial^\mu + 2ieA^\mu \partial_\mu + e^2 A_\mu A^\mu \right] \varphi(x) = 0 \quad (3.41)$$

Now comes the crux of the eikonal approximation. We are assuming that k^+ is a large variable, thus at leading order we only need to keep the terms proportional to k^+ in equation (3.41). These only appear in the terms that are underlined in the equation. Thus, and recalling that now the initial condition is $\varphi(x) \rightarrow 1, \quad x^+ \rightarrow -\infty$, and factoring out the $2ik^\mu$ we end up with

$$[\partial_+ - ieA^-(x)] \varphi(x) = 0 \implies \varphi(x) = \exp \left\{ ie \int_{-\infty}^{x^+} dy^+ A^-(y^+, x^-, \mathbf{x}) \right\} \quad (3.42)$$

Note that at this point only the A^- component of the target gauge potential matters, due to the large k^+ momentum of the probe. In the far future after the target, $x^+ \rightarrow \infty$, the outgoing wave is written in terms of the incoming one in terms of the

Eikonal phase

$$\chi(\mathbf{x}) = e \int_{-\infty}^{\infty} dy^+ A^-(y^+, x^-, \mathbf{x}) \quad (3.43)$$

$$\phi(x)|_{x^+ \rightarrow \infty} \approx e^{-ik \cdot x} \left[1 - \left(1 - e^{i\chi(\mathbf{x})} \right) \right] \quad (3.44)$$

At this point we will just state, without trying to go through a formal derivation, that one minus the exponential of the eikonal phase is analogous to the opacity/transparency of the optical problem, and that the elastic cross section is given (see equation (3.33)) by

$$1 - e^{i\chi(\mathbf{x})} \iff \Gamma(\mathbf{x}) \implies \frac{d\sigma_{\text{el.}}}{d^2\mathbf{q}} = \left| \frac{-i}{2\pi} \int d^2\mathbf{x} e^{-i\mathbf{q} \cdot \mathbf{x}} \left(1 - e^{i\chi(\mathbf{x})} \right) \right|^2 \quad (3.45)$$

We can also try to just directly calculate the cross section starting from the outgoing wavefunction (3.44) in terms of the definition of the cross section. In the outgoing wavefunction (3.44) we clearly see which wave is the incoming wave and which one the scattered one:

$$\phi(x)|_{x^+ \rightarrow \infty} = \phi_{\text{in}} + \phi_{\text{scat}} \quad (3.46)$$

with

$$\phi_{\text{in}} = e^{-ik \cdot x} \quad (3.47)$$

$$\phi_{\text{scat}} = e^{-ik \cdot x} \left(1 - e^{i\chi(\mathbf{x})} \right) \quad (3.48)$$

This derivation follows the way a cross section is calculated from a scattering amplitude in nonrelativistic quantum mechanics. A cross section is defined as

$$d\sigma = \frac{d(\text{number of particle in phase space})/\text{time}}{\text{flux in}} \quad (3.49)$$

Now the square of our wavefunction in coordinate space is related to the probability density of particles. Let us calculate the flux:

$$\text{flux} = \frac{\text{number}}{\text{time} \times \text{area}} = \frac{\text{number length}}{\text{volume time}}, = |\phi_{\text{in}}|^2 \times \frac{k}{E(k)} = |e^{-ik \cdot x}|^2 \times \frac{k}{E(k)} = \frac{k}{E(k)} \quad (3.50)$$

where the length (= volume/area) is some distance in the direction of the incoming particles which, divided by the unit of time that it takes the particles to travel this distance, gives us the velocity. The velocity of a relativistic particle is its momentum divided by energy. Now, for the outgoing particles, we do not want to measure the density as a function of transverse coordinate, but rather transverse momentum. Thus we need to Fourier-transform the wavefunction to transverse momentum, to get the number of outgoing particles. Define the mixed space wavefunction as

$$\phi(\mathbf{q}, z, t) = \int d^2\mathbf{x} e^{i\mathbf{q} \cdot \mathbf{x}} \phi(\mathbf{x}, z, t) \quad (3.51)$$

Now the square of this quantity gives the number of particles per unit length and unit transverse momentum, with a $(2\pi)^2$ that always goes with the Fourier transform²

$$|\phi(\mathbf{q}, z, t)|^2 = (2\pi)^2 \frac{dN}{dz} \quad (3.52)$$

Again we need to change this from a number of particles per unit length to a number of particles per unit time. This involves the velocity of the particle. Here, we need to again evoke the fact that we are working in the high energy limit, where the scattering angle is very small. Thus, even if the particle does acquire some transverse momentum \mathbf{q} in the scattering, we consider that the longitudinal momentum k is still much larger, $k \gg |\mathbf{q}|$, and the velocity (in the z -direction) is given by $k/E(k)$. Then we get the elastic cross section as

$$\begin{aligned} \frac{d\sigma_{\text{el.}}}{d^2\mathbf{q}} &= \frac{\frac{dN}{d^2\mathbf{q} dz} \times \frac{k}{E(k)}}{\text{flux}} = \frac{1}{(2\pi)^2} |\phi_{\text{scat}}(\mathbf{q}, z, t)|^2 = \frac{1}{(2\pi)^2} \left| \int d^2\mathbf{x} e^{i\mathbf{q} \cdot \mathbf{x}} e^{ik \cdot x} (1 - e^{i\chi(\mathbf{x})}) \right|^2 \\ &= \left| \frac{-i}{2\pi} \int d^2\mathbf{x} e^{i\mathbf{q} \cdot \mathbf{x}} (1 - e^{i\chi(\mathbf{x})}) \right|^2, \quad (3.53) \end{aligned}$$

using the fact that $\mathbf{k} = 0$ and thus $e^{ik \cdot x}$ just cancels in the absolute value. The final $-i$ of course inside the integral just gives one in the absolute value. We scale it out so that we recover the conventional complex phase of the scattering amplitude.

Summary

This was a sketchy derivation. Some points of interest:

- We haven't specified anything about x^- : we will come back to this later
- The outgoing wave does not appear to expand spherically as was the case for our optical problem. This is mainly an artefact of the coordinate system; and a result of the eikonal approximation that assumes small angle scattering.
- If we do expand to leading order in the eikonal phase χ , we see that Γ is imaginary, i.e. the scattering amplitude real. But when expanded to second order, the scattering amplitude develops an imaginary phase. The eikonal approximation builds in a relation between the real and complex parts of the scattering amplitude, i.e. between elastic and inelastic (absorptive) scattering, that is consistent with unitarity of the scattering S -matrix.

²You can check this by checking that the total number of particles is

$$N = \int d^2\mathbf{x} dz |\phi(\mathbf{x}, z, t)|^2 = \int \frac{d^2\mathbf{q}}{(2\pi)^2} dz |\phi(\mathbf{q}, z, t)|^2.$$

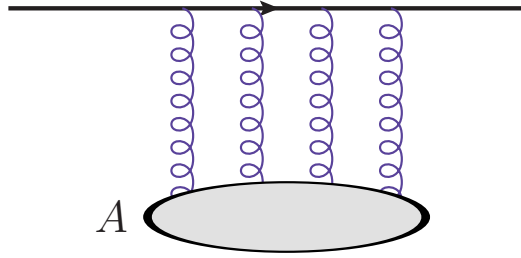
3.2.2 Eikonal scattering off target of glue

So far we have only been discussing Abelian theory. Let us now move to QCD in the high energy limit. We will, however still stay within the eikonal picture of scattering. In particular, we will assume that QCD scattering is dominated by scattering off the gluon field of the target. This is in fact not just an assumption, but a consequence of the spin of the gluons: the coupling strength of a high energy particle to the gluon field is proportional to the momentum of the particle. The coupling to the fermion field of the target, on the other hand, is proportional to the square root of the high energy, because the fermion field has spin half.

We also know from experiment, and can show in perturbative QCD (BFKL evolution), that the number of gluons in the proton or nucleus grows at higher energy (i.e. smaller x). We may therefore assume that there are many of these gluons, in fact so many that eventually at some point the gluon field becomes nonperturbatively strong.

Color Glass Condensate (CGC)

Target has many gluons: $A_\mu \gg 1/g \Rightarrow$ described as classical gluon field



To see how a colored particle interacts with such a target color field, we can follow the same procedure as previously, by solving the Dirac equation of a colored fermion in this field. The work essentially the same as previously in the abelian theory. The only difference with respect to eq. (3.42) is that now the field is a matrix in color space, and does not commute with the field at a different coordinate x^+ . Thus, when multiplying or exponentiating matrices, one naturally ends up with a path ordered exponential.

Quark in color field, Dirac:

$$(i\cancel{\partial} - g\cancel{A})\psi(x) = 0 \quad (3.54)$$

Ansatz $\psi(x) = V(x)e^{-ip \cdot x}u(p) + \text{eikonal approx.}$

$$\partial_+ V(x^+, x^-, \mathbf{x}) = -igA^-(x^+, x^-, \mathbf{x})V(x^+, x^-, \mathbf{x}) \quad (3.55)$$

Inserting the ansatz, with $p^\mu = (p^+, 0, \mathbf{0})$ into the Dirac equation we get

$$e^{-ip \cdot x}(\cancel{p} + i\cancel{\partial} - g\cancel{A})V(x)u(p) = 0 \quad (3.56)$$

We now use the massless Dirac equation $\cancel{p}u(p) = 0$. From this equation it follows, since $p^\mu = (p^+, 0, \mathbf{0})$, that $\gamma^- u(p) = 0$. We can now multiply the remaining equation from the left by γ^- to get

$$\gamma^-(i\cancel{\partial} - g\cancel{A})V(x)u(p) = 0 \quad (3.57)$$

Since

$$\gamma^- \cancel{a} = \gamma^- (a^+ \gamma^- + a^- \gamma^+ - \mathbf{a} \cdot \boldsymbol{\gamma}) = - (a^- \gamma^+ - \mathbf{a} \cdot \boldsymbol{\gamma}) \gamma^- + a^-, \quad (3.58)$$

this implies

$$(i\partial_+ - gA^-)V = 0. \quad (3.59)$$

Wilson line = path-ordered exponential

$$V(x^+, x^-, \mathbf{x}) = \mathbb{P} \exp \left\{ -ig \int_{x^-}^{x^+} dy^+ A^-(y^+, x^-, \mathbf{x}) \right\} \quad (3.60)$$

$$\mathbb{P} [A(y^+)A(x^+)] \equiv \theta(y^+ - x^+)A(y^+)A(x^+) + \theta(x^+ - y^+)A(x^+)A(y^+) \quad (3.61)$$

These path ordered exponentials are the same quantities that one uses to formulate lattice field theory (the link matrices). The difference is that now, we are following a light-like path, whereas in lattice field theory

the links are in the spatial or imaginary time (also \sim spatial) direction. This is because we are interested in the propagation of a very energetic particle moving at the speed of light instead of a static equilibrium system.

Recap

- We used an eikonal approximation: assume that longitudinal momentum is larger than other momenta involved
- Our result is not perturbative, i.e. it sums a series of different powers of the external field A_μ
- Only one component of the vector field A^- matters. This is related to the high energy approximation: the current of charged particles with a large momentum k^+ has a J^+ -component that is larger than all others, and this component of the current only couples to the A^- -component of the gauge field. Incidentally, this feature is independent of the spin of the probe, and is thus the same also if we replace our incoming charged scalar particles by fermions or charged vector bosons. On the other hand, this feature does very much depend on the fact that we are scattering off a spin-1 field (a vector field), it is this feature that causes the strength of the interaction to be proportional to the momentum of the incoming particle. The graviton field would couple to the momentum squared, whereas a scalar field does not couple to the momentum. The same feature can easily be seen by calculating some tree level Feynman diagrams for such scattering [exercise]. In terms of Feynman diagrams one can state the eikonal approximation in terms of the “eikonal vertex”. The fact that only A^- matters indicates that there is a gauge dependence in our result. It should be possible to do a gauge transformation that changes A^- , but leaves the cross section invariant. Thus there are gauges where obtaining the correct result requires taking into account other components of the gauge field, which in some gauge might be large enough to compensate the lack of an explicit enhancement by the large component k^+ .

Digression: Probe and target light cone gauges

If we wanted to count the photons of the target in a rigorous well-defined quantum mechanical way, we would want to go to the light-cone gauge of the leftmoving target, $A^- = 0$. Then our interaction would look very different from what we have now. Thus, even the perturbative limit (power series expansion in A_μ) of our result is a perturbation series in the interaction with a Coulomb field of the target, not really with a specific number of actual radiation quanta (photons) in it.

3.3 Hybrid formalism for pA collisions

3.3.1 Forward rapidity in proton-nucleus collisions

Now we have developed the concept of measuring the gluon field in a dense target by measuring the scattering amplitude of a simple elementary colored probe going through this target. What would be a possible scattering experiments for doing this? It will turn out in the end that, in many ways, the cleanest such a process is deep inelastic scattering. However, it is easier for us to start with another process that looks even simpler at first, which is single inclusive hadron production in proton-nucleus collisions at forward rapidity. For the purposes of our discussion here this is indeed the simplest process. When doing actual phenomenology or higher order calculations it has complications that DIS does not have (collinear divergences, parton distributions, fragmentation functions, real-virtual cancellations, ...), but we will not encounter them in this first, introductory discussion.

Experimental data that we might want to address could be something like the nuclear modification ratio R_{pA} . Some experimental measurements for this quantity from ALICE [28] and LHCb [29, 30] are shown in Fig. 3.1.

The nuclear modification ratio R_{pA} is the ratio of a cross section for something in proton-nucleus collisions, divided by the mass number A times the corresponding cross section in proton-proton collisions. We expect saturation effects to be more important in nuclei than in protons and more important at small x than at large x . Thus a suitable place to look for them is in a collision system where a large x parton, preferably a quark, collides with small- x degrees of freedom. This, very generically, happens at forward rapidity (i.e.

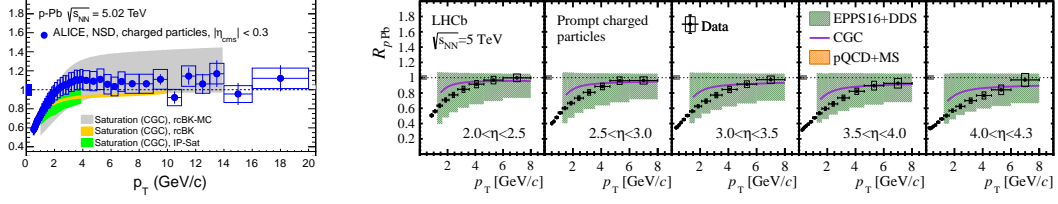
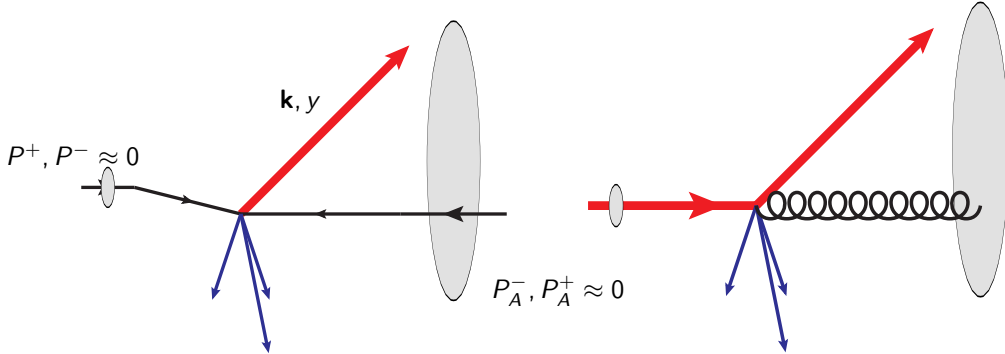


Figure 3.1: Nuclear modification ratio R_{pA} from ALICE [28] at midrapidity $y \approx 0$ and LHCb [29, 30] at forward rapidities.

in the proton-going direction) in a proton-nucleus collision. To see this let us take a quick look at the kinematics. We consider a proton moving in the positive z direction, with a large momentum P^+ and very small $P^- = m_p^2/(2P^+)$. It collides with a heavy ion in the negative z direction, with a large P_A^- and a small $P_A^+ = m_A^2/(2P_A^-)$. Usually with nuclear collisions one calculates energies per nucleon, and thus the center of mass collision energy per nucleon is $s = (P_A + P)^2/A \approx 2P \cdot (P_A/A) = 2P^+ P_A^-/A$. For simplicity let us assume that we are in the proton-nucleon center of mass frame. This means that the longitudinal momentum of the proton (P^+) is the same as the longitudinal momentum per nucleon in the nucleus (P_A^-/A). At the LHC, this is not exactly the frame where the detectors sit, but close enough for the purposes of this discussion; for a more careful calculation for LHC data one needs to take this small difference into account better.

We now produce and measure a particle with transverse momentum k at rapidity y , with y large. Four-momentum must be conserved. Since the proton has very little p^- , all the k^- of the produced particle must come from the nucleus. Similarly all the k^+ of the produced particle must come from the proton. If the produced particle is massless, we calculate its plus and minus momenta as follows.



$$\text{C.M.S} \implies P^+ = \frac{P_A^-}{A} = \sqrt{\frac{s}{2}} \quad (3.62)$$

$$k^+ = \frac{1}{\sqrt{2}} k_T e^y = \frac{k_T e^y}{\sqrt{2} P^+} P^+ = \frac{\overbrace{k_T e^y}^{x_p \lesssim 1}}{\sqrt{s}} P^+ \quad (3.63)$$

$$k^- = \frac{1}{\sqrt{2}} k_T e^{-y} = \frac{k_T e^{-y}}{\sqrt{2} (P_A^-/A)} \frac{P_A^-}{A} = \frac{k_T e^{-y}}{\underbrace{\sqrt{s}}_{x_A \ll 1}} \frac{P_A^-}{A} \quad (3.64)$$

The fractions x_p and x_A are the fractions of the proton and nucleus longitudinal momenta carried by the produced particle. We see that when one is looking in the proton-going direction, where y is large, the process requires a large x_p and a small x_A . To a first approximation, the degrees of freedom at large x_p in the proton are valence quarks, and the ones at small x_A in the nucleus gluons. Thus, the process of particle production at forward rapidity in proton-nucleus collisions provides us a simple example of a dilute probe interacting with the color field of a dense nucleus. We shall next proceed to calculating the cross section for such a process.

3.3.2 Quark-nucleus scattering

To quantify the scattering of dilute probes on a dense gluon field target in a systematical way, we need to specify more precisely the theoretical framework that we use. In this context, the best way to do this is to use Light Cone Perturbation theory. A classic review is provided by the review of Brodsky, Pauli and Pinsky [14]. This review is not, however, very convenient for the kind of calculations we do here: the notations are different, and the discussion does not systematically use the concept of the Light Cone Wave Function (LCWF). A more useful reference for our calculation is the Kovchegov-Levin book [1], and the papers on DIS in the dipole picture [31, 32, 33, 34, 35, 36, 37]. We will, as in these papers, use a covariant normalization for the states (unlike the review [14]) and the Kogut-Soper metric for light cone variables introduced in Sec.1.4 (unlike the book [1]). A classic paper where the treatment of scattering off a classical background field is introduced is [21], which provides the more formal field theoretical justification for what we are doing here.

In our conventions, quark momentum eigenstates are normalized as

$$\langle q(\mathbf{p}, p^+, \lambda_p, i_p) | q(\mathbf{q}, q^+, \lambda_q, i_q) \rangle = 2p^+ (2\pi)^3 \delta(p^+ - q^+) \delta^{(2)}(\mathbf{p} - \mathbf{q}) \delta_{i_p, i_q} \delta_{\lambda_p, \lambda_q}, \quad (3.65)$$

where $\lambda_{p,q}$ is the *light front helicity* (spin, for the purposes of our discussion here), and $i_{p,q}$ the color, in the fundamental representation. For brevity of notation we will not write out the helicity explicitly for now. Because the eikonal interaction with the target preserves helicity, we will not write it out explicitly from now on.

Our incoming state for the quark is a single quark in a specific momentum state. The eikonal interaction, as we recall, preserves the transverse coordinate of the particle. We therefore need to Fourier transform to coordinate space. The Fourier-transforms and coordinate space states are defined as

$$|q(\mathbf{p}, p^+, i)\rangle = \int d^2\mathbf{x} e^{i\mathbf{p}\cdot\mathbf{x}} |q(\mathbf{x}, p^+, i)\rangle \quad (3.66)$$

$$|q(\mathbf{x}, p^+, i)\rangle = \int \frac{d^2\mathbf{p}}{(2\pi)^2} e^{-i\mathbf{p}\cdot\mathbf{x}} |q(\mathbf{p}, p^+, i)\rangle \quad (3.67)$$

$$\langle q(\mathbf{x}, p^+, i_p) | q(\mathbf{y}, q^+, i_q) \rangle = 2p^+ (2\pi) \delta(p^+ - q^+) \delta^{(2)}(\mathbf{x} - \mathbf{y}) \delta_{i_p, i_q} \quad (3.68)$$

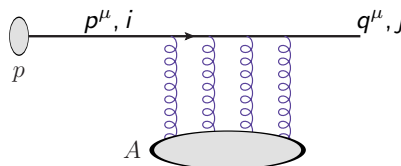
The state $|\text{in}\rangle = |q(\mathbf{p}, p^+, i)\rangle$ is the state of the incoming particle just before the shockwave of the target color field, i.e. at light cone time $x^+ \rightarrow 0^-$. As we have discussed, the effect of the color field shock wave is to color rotate the particle. This means that the state vector (bra) of the scattered particle in coordinate space is rotated by the Wilson line. We denote this rotation as the effect of the “scattering operator” \hat{S} .

Digression: Interaction picture

To be more specific, we are, as is common in scattering theory, using the Interaction or Dirac picture of time evolution. This means that we split the Hamiltonian of our system into two parts. The free part, corresponding to the kinetic energy k^- of the partons in the probe, causes a time evolution of the operators of the theory. The interaction part of the Hamiltonian, on the other hand, generates a time dependence in the state vector of the system. In this case, the interaction part consists of the interaction with the background field. Later, we will also include the interactions between different Fock states of the probe, most importantly gluon emission, in the interaction part of the Hamiltonian.

$$|\text{in}\rangle = |q(\mathbf{p}, p^+, i)\rangle = \int d^2\mathbf{x} e^{i\mathbf{p}\cdot\mathbf{x}} |q(\mathbf{x}, p^+, i)\rangle \quad x^+ < 0 \quad (3.69)$$

$$\hat{S} |q(\mathbf{x}, q^+, i)\rangle = \sum_j [V(\mathbf{x})]_{ji} |q(\mathbf{x}, q^+, j)\rangle \quad x^+ > 0 \quad (3.70)$$



Now we know what is the quantum state of the outgoing particle. To calculate the scattering amplitude, we need to project out the final state that we are measuring from the outgoing particle state. Now, because our

background field does not (in the eikonal approximation) depend on x^- , it does not carry any longitudinal momentum p^+ . Thus the scattering amplitude will be proportional to a delta function $\delta(p^+ + q^+)$. As is customary in all field theory calculations, this delta function is factorized out. This is done because to calculate the cross section we will need to square the amplitude. The square of the delta function becomes, in the calculation relating the square of the matrix element to the cross section, a single delta function the cross section level times a dimensional factor that is needed to match the correct interpretation of the cross section as a number of scatterings per unit time. It is also customary to factor out a factor $2q^+(2\pi)$ and an imaginary unit together with the delta function. This is just a convention (in field theory one writes $S = 1 + iT$), but helps to keep the terminology straight, since one often ends up discussing the meaning of the “real” and “imaginary” parts of the scattering amplitude separately. We also need to subtract the original incoming state, i.e. subtract identity from the interaction operator \hat{S} : when there is no background field and $\hat{S} = \hat{1}$, the scattering amplitude should be zero.

This leads us to define the invariant scattering amplitude \mathcal{M} in the following way from the matrix element between the incoming and outgoing states. Given the explicit expression (3.70) it is straightforward to calculate the amplitude for our particular case of quark-color field scattering.

$$2q^+(2\pi)\delta(p^+ - q^+)i \overbrace{\mathcal{M}(i, \mathbf{p} \rightarrow j, \mathbf{q})}^{\text{invariant amplitude}} \equiv \langle q(\mathbf{q}, q^+, j) | (\hat{S} - 1) | q(\mathbf{p}, p^+, i) \rangle \quad (3.71)$$

$$\begin{aligned} & \langle q(\mathbf{q}, q^+, j) | (\hat{S} - 1) | q(\mathbf{p}, p^+, i) \rangle \\ &= \int d^2\mathbf{x} d^2\mathbf{y} e^{i\mathbf{p}\cdot\mathbf{x} - i\mathbf{q}\cdot\mathbf{y}} \langle q(\mathbf{y}, q^+, j) | (\hat{S} - 1) | q(\mathbf{x}, p^+, i) \rangle \\ &= \int d^2\mathbf{x} d^2\mathbf{y} e^{i\mathbf{p}\cdot\mathbf{x} - i\mathbf{q}\cdot\mathbf{y}} ([V(\mathbf{x})]_{ji} - \delta_{ij}) 2p^+(2\pi)\delta(p^+ - q^+)\delta^{(2)}(\mathbf{x} - \mathbf{y}) \quad (3.72) \end{aligned}$$

$$\mathcal{M}(i, \mathbf{p} \rightarrow j, \mathbf{q}) = \int d^2\mathbf{x} e^{i(\mathbf{p}-\mathbf{q})\cdot\mathbf{x}} ([V(\mathbf{x})]_{ji} - \delta_{ij}) \quad (3.73)$$

Note that we now, again, have the interpretation of the Wilson line V as the *eikonal scattering amplitude of a dilute probe off the target color field*.

Now, the square of the invariant amplitude, multiplied by the invariant phase space element and a momentum conserving delta function, is just the cross section. There are some factors of (2π) that, conventionally, go along with the momenta. In the case of light cone coordinates, there are additional factors of $2p^+$ that always go together with integrals or delta functions in p^+ to turn them into Lorentz-invariant phase space integrals (see Eq. (1.35)). To make a properly normalized cross section, we have to average over incoming colors i and sum over outgoing ones j . At this point let us also take the transverse momentum of the incoming quark to be zero, since we are interested in collinear high- x quarks coming from a high energy proton.

(Set $\mathbf{p} = 0$)

$$d\sigma = \frac{1}{N_c} \sum_{i,j} 2p^+(2\pi)\delta(p^+ - q^+) |\mathcal{M}(i, \mathbf{p} \rightarrow j, \mathbf{q})|^2 \frac{d^2\mathbf{q}}{(2\pi)^2} \frac{dq^+}{4\pi q^+} \quad (3.74)$$

$$\begin{aligned} & \frac{1}{N_c} \sum_{i,j} |\mathcal{M}(i, \mathbf{0} \rightarrow j, \mathbf{q})|^2 = \int d^2\mathbf{x} d^2\mathbf{y} e^{-i\mathbf{q}\cdot(\mathbf{x}-\mathbf{y})} \\ & \times \frac{1}{N_c} \left[\text{tr } V(\mathbf{x}) V^\dagger(\mathbf{y}) - \overbrace{\text{tr } V(\mathbf{x}) - \text{tr } V^\dagger(\mathbf{y}) + N_c}^{\sim \delta^{(2)}(\mathbf{q})} \right] \quad (3.75) \end{aligned}$$

In simplifying the Wilson lines it is useful to note that $[V(\mathbf{x})]_{ji}^* = [V^\dagger(\mathbf{x})]_{ij}$. Note that out of the four terms resulting from the square of the amplitude, the last three will give a delta function in the produced quark transverse momentum, after integration over \mathbf{x} or \mathbf{y} . While they need to be there to preserve unitarity, we shall promptly disregard these terms as not physically interesting, since in the experimental situation we

will be measuring quarks that actually scatter off the transverse plane

The crucial, general formulae here are Eq. (3.71) defining the invariant amplitude in terms of the incoming and outgoing states, and Eq. (3.74) which tells us how to calculate the cross section from this amplitude. These equations are valid for any process, the other equations just for the particular case of quark-nucleus scattering. These general formulae look quite similar to the corresponding ones in covariant field theory (“instant form,” i.e. equal- t quantization), apart from the fact that only longitudinal momentum is conserved and some factors $2p^+$ are needed to make things Lorentz-covariant. Contrary to conventional Feynman perturbation theory, transverse momentum, and consequently k^- , are now not conserved for the “particles” that we are quantizing, because these particles are scattering off an external classical field that can also contribute momentum. To my knowledge, these general expressions were first written down in the very important paper of Bjorken, Kogut and Soper [21].

Let us now perform a final step and see how one goes from quark-nucleus scattering to proton-nucleus scattering. The quarks come from a collinear distribution in the proton $q(x, Q^2)$, and we must integrate over the momentum fraction x . The energy of the incoming quark is $p^+ = xP^+$, and we can insert an identity in terms of an integral over p^+ with a delta function. We change the variable for the longitudinal momentum from q^+ to the rapidity by $dy = dq^+/q^+$. This leads us to

$$\begin{aligned} \frac{d\sigma^{p+A \rightarrow q+A}}{d^2\mathbf{q} dy} &= \int dx q(x, Q^2) \int dp^+ \delta(p^+ - xP^+) q^+ \overbrace{\frac{d\sigma^{q+A \rightarrow q+A}}{d^2\mathbf{q} dq^+}}^{\sim \delta(q^+ - p^+)} \\ &= \int dx q(x, Q^2) \int dp^+ \delta(p^+ - xP^+) \overbrace{q^+ \delta(p^+ - q^+)}^{q^+ \delta(q^+ - xP^+) = x \delta(x - q^+/P^+)} \\ &\quad \times \frac{1}{(2\pi)^2} \int d^2\mathbf{x} d^2\mathbf{y} e^{-i\mathbf{q} \cdot (\mathbf{x} - \mathbf{y})} \frac{1}{N_c} \text{tr} V(\mathbf{x}) V^\dagger(\mathbf{y}) \quad (3.76) \end{aligned}$$

Hybrid formula for quark production

$$\frac{d\sigma}{d^2\mathbf{q} dy} = \frac{1}{(2\pi)^2} x q(x, \mu^2) \int d^2\mathbf{x} d^2\mathbf{y} e^{-i\mathbf{q} \cdot (\mathbf{x} - \mathbf{y})} \overbrace{\left(\frac{1}{N_c} \text{tr} V(\mathbf{x}) V^\dagger(\mathbf{y}) \right)}^{\text{dipole operator}} \quad (3.77)$$

Now we have obtained a key result! This is our first example of how to measure the gluon field of a dense target. Of course, there are caveats. Firstly, one does of course not measure quarks in a collider experiment. There are typically two things one could do to actually connect (3.77) to experiment.

1. Measure jets. Experimentally, a jet is a collimated (close in angle) set of high-ish momentum particles. These are then “clustered” together into jets, and one is interested in the total momentum of the jet. One should think of a jet a direct product of a high momentum parton being produced in the primary collision. Jets are where perturbation theory and experiment meet, jets cross sections are well defined (infrared and collinear safe) observables. In a theory calculation a jet is a leading order a one-parton state, and at higher orders in perturbation theory also a 2-, 3- etc particle state. Thus a jet is in some sense the closest one can get experimentally to single quark production, but with the understanding that the relation between a jet and the quarks and gluons that create it must be systematically improved order by order in perturbation theory. The inconvenient thing about jets for our purpose is that experimentally identifying a jet as being separate from the background of the other particles produced in a hadronic collision, the jet must have a sufficiently high transverse momentum. This means that it will be typically at higher x and, more importantly, removed from the saturation region of $p_T \sim Q_s$.
2. The other option is to measure individual hadrons. In this case one needs a way to calculate the transformation of the produced quark to hadrons. Typically this is done by using “fragmentation functions,” which are extracted from data (in particular $e^+e^- \rightarrow \text{hadrons}$) and satisfy their own version of the DGLAP evolution equation.

In addition to relating the quark to a measurable observable, one of course also needs to know where

to get the dipole amplitude. One option for this is to use a model: later in these lectures we will discuss the McLerran-Venugopalan (MV) model [38, 39, 40] for the classical color fields, and calculate the dipole amplitude from this model. We can also derive renormalization group equations that allow one to predict, from a weak coupling QCD calculation, the dependence of the dipole amplitude on the collision energy. These go by the name of the Balitsky-Kovchegov (BK) [41, 42, 43] or JIMWLK [44, 45, 46, 47, 48, 49, 50, 51] equations. One can also, together with a model, parametrization of the BK/JIMWLK equations, extract the dipole cross amplitude from Deep Inelastic Scattering data.

To address the nuclear modification ratio R_{pA} we need to have a dipole operator separately for protons and for nuclei. We then calculate the cross sections using our hybrid formula, and take the ratio. This is the way the “CGC” curves in the LHCb plot have been obtained.

We will do an explicit calculation of the dipole operator in a specific model, the MV model, later. But even without such a calculation, it is possible to discuss the physics of gluon saturation in terms of the dipole operator.

Gluon saturation

- $\mathbf{x} = \mathbf{y} \implies \frac{1}{N_c} \langle \text{tr } V(\mathbf{x}) V^\dagger(\mathbf{y}) \rangle = 1$
- $|\mathbf{x} - \mathbf{y}| \rightarrow \infty \implies \frac{1}{N_c} \langle \text{tr } V(\mathbf{x}) V^\dagger(\mathbf{y}) \rangle \rightarrow 0$

$\implies \exists \text{ length scale } |\mathbf{x} - \mathbf{y}| \sim 1/Q_s \text{ s.t. } \frac{1}{N_c} \langle \text{tr } V(\mathbf{x}) V^\dagger(\mathbf{y}) \rangle \sim \frac{1}{2} \quad Q_s = \text{Saturation scale}$

Perturbation theory in a theory with point-like particles (partons in the target) would always give you a power-law dependence. But a power law dependence on $|\mathbf{x} - \mathbf{y}|$ cannot be true at all values: it is not possible to satisfy the group theory constraints on possible values of the trace of an $SU(N_c)$ matrix with a pure power law. Here the expectation values $\langle \rangle$ refer to some, quantum or classical, average over the states of the target.

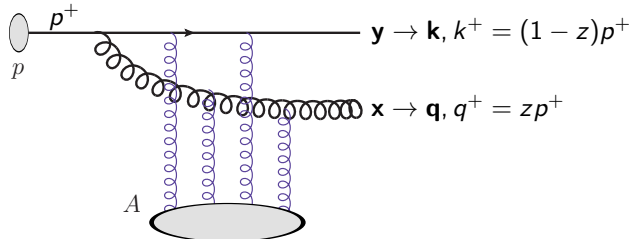
3.3.3 Going to higher orders

Without doing an actual calculation here, let us discuss what happens when we go to higher order in perturbation theory. Recall that we are already working to all orders in the classical field. Our probe, the quark, on the other hand is a quantum mechanical particle that we understand in perturbation theory. Starting from the single quark state, the next order in perturbation theory is when this quark emits a gluon. The emission can then happen either before or after the target. In the former case the quark-gluon system must pass through the target color field. In stead of a single fundamental representation Wilson line this process will result in the product of an adjoint representation Wilson line for the gluon and a fundamental one for the quark. The adjoint representation Wilson line can be related to the fundamental one by

$$(V_{\text{adj}})^{ab} = 2 \text{tr } t^a V t^b V^\dagger. \quad (3.78)$$

If one uses this relation to express everything in terms of the fundamental representation, one ends up with three Wilson lines in the scattering amplitude. Squaring the amplitude, this means that we have operators made up of up to six Wilson lines in the cross section. We can express the result in terms of a $q + A \rightarrow q + g + X$ cross section, first derived in this formalism in Ref. [52]. Schematically, the expression looks like this:

Emit a gluon



$$\frac{d\sigma^{qA \rightarrow qgX}}{d^3\mathbf{q} d^3\mathbf{k}} \propto \int_{\mathbf{x}, \bar{\mathbf{x}}_\perp, \mathbf{y}, \bar{\mathbf{y}}_\perp} e^{-i\mathbf{q} \cdot (\mathbf{x} - \bar{\mathbf{x}}_\perp)} e^{-i\mathbf{k} \cdot (\mathbf{y} - \bar{\mathbf{y}}_\perp)} \mathcal{F}(\bar{\mathbf{x}}_\perp - \bar{\mathbf{y}}_\perp, \mathbf{x} - \mathbf{y})$$

$$\left\langle \hat{Q}(\mathbf{y}, \bar{\mathbf{y}}_\perp, \bar{\mathbf{x}}_\perp, \mathbf{x}) \hat{D}(\mathbf{x}, \bar{\mathbf{x}}_\perp) - \hat{D}(\mathbf{y}, \mathbf{x}) \hat{D}(\mathbf{x}, \bar{\mathbf{z}}_\perp) - \hat{D}(\mathbf{z}, \bar{\mathbf{x}}_\perp) \hat{D}(\bar{\mathbf{x}}_\perp, \bar{\mathbf{y}}_\perp) \right.$$

$$\left. + \frac{C_F}{N_c} \hat{D}(\mathbf{z}, \bar{\mathbf{z}}_\perp) + \frac{1}{N_c^2} \left(\hat{D}(\mathbf{y}, \bar{\mathbf{z}}_\perp) + \hat{D}(\mathbf{z}, \bar{\mathbf{y}}_\perp) - \hat{D}(\mathbf{y}, \bar{\mathbf{y}}_\perp) \right) \right\rangle_{\text{target}} \quad (3.79)$$

$$(\mathbf{z} = z\mathbf{x} + (1-z)\mathbf{y}, \bar{\mathbf{z}}_\perp = z\bar{\mathbf{x}}_\perp + (1-z)\bar{\mathbf{y}}_\perp.)$$

$$\hat{D}(\mathbf{x} - \mathbf{y}) \equiv \frac{1}{N_c} \text{tr} V(\mathbf{x}) V^\dagger(\mathbf{y}) \quad \hat{Q}(\mathbf{x}, \mathbf{y}, \mathbf{u}, \mathbf{v}) \equiv \frac{1}{N_c} \text{tr} V(\mathbf{x}) V^\dagger(\mathbf{y}) V(\mathbf{u}) V^\dagger(\mathbf{v}) \quad (3.80)$$

Some things can be pointed out about these equations. The function $\mathcal{F}(\bar{\mathbf{x}}_\perp - \bar{\mathbf{y}}_\perp, \mathbf{x} - \mathbf{y})$ includes the dynamics of the vertex of gluon emission from the quark. We could calculate it from LCPT even in these lectures, if we had a bit more time. The transverse coordinates \mathbf{y} and \mathbf{x} are the coordinates of the quark and the gluon in the amplitude (remember that in the eikonal approach the coordinates stay fixed when propagating through the background field). Correspondingly, $\bar{\mathbf{y}}_\perp$ and $\bar{\mathbf{x}}_\perp$ are the coordinates of the quark and the gluon in the conjugate amplitude. The difference between the coordinates in the amplitude and the conjugate, e.g. $\mathbf{x} - \bar{\mathbf{x}}_\perp$ is Fourier-conjugate to the momentum of the produced particle. There are diagrams where the gluon is emitted either before or after the classical gluon field. This sum of two diagrams in the amplitude is then squared, yielding even more terms. The gluon emission vertex includes a fundamental representation generator t^a . When expressing the adjoint Wilson lines in terms of fundamental ones, one gets more fundamental representation generators. One then sums over all colors of final state particles, and averages over colors of the incoming quark. These color summations turn into traces of Wilson lines. One then finally gets rid of the generators t^a by the Fierz identity:

$$(t^a)_{ij} (t^a)_{kl} = \frac{1}{2} \left(\delta_{il} \delta_{jk} - \frac{1}{N_c} \delta_{ij} \delta_{kl} \right), \quad (3.81)$$

which still increases the number of terms.

This is a wonderful result, that leads to further kinds of physics in two different ways.

- One can use it to study correlations between produced hadrons or jets. Particularly interesting are correlations in the azimuthal angle, between particles that have relatively low momenta, not too much larger than the saturation scale. Here, the essential thing for the physics is that the produced particles receive, in addition to the back-to-back momentum that they have in recoiling against each other, intrinsic momentum from the classical field. In this case the larger saturation scale of the nucleus leads to a larger momentum being transferred from the target, which leads to a washing out of the back-to-back azimuthal correlation dictated by momentum conservation if there is no momentum transfer from the target. Observing such an effect in two-particle correlations would be a direct probe of the nature of the saturation scale as a transverse momentum scale, and thus very valuable. There are hints of such a nuclear effect in the dihadron correlations observed at RHIC, but there is not yet a unanimity of the interpretation of these observations.
- One can also take the qg cross section result and integrate over the momentum of one of the particles. This procedure gives a part of the NLO correction to single particle production. Note that an integration over a momentum sets the coordinates of the corresponding particle in the amplitude and the conjugate amplitude to be equal. This significantly simplifies the Wilson line operator expression. A particularly important class of NLO corrections are the ones that are enhanced by some large logarithm. In this case, there are two relevant ones:
 - Collinear divergences: there can be an infrared divergence in the integral over the transverse momentum of either of the two partons. This divergence can be regularized, and then absorbed into the DGLAP-evolution of the quark distribution in the leading order cross section. To my knowledge, this was first demonstrated in [53]. The fact that there is a collinear divergence at NLO that can be absorbed into DGLAP evolution of the parton distribution function in the LO

cross section expression is the real “proof” of the hybrid factorization formula, at least at this order.

- Rapidity divergences (or soft divergences). There is also a divergence in the limit of $z \rightarrow 0$. This divergence has to be absorbed into the BK/JIMWLK evolution of the Wilson lines of the target. That this happens was demonstrated in [54, 55] (see also [56, 57]).

Taking into account not only the logarithmically enhanced contributions but the full expression is needed for the full NLO calculation of single inclusive particle production in the hybrid formalism.

Chapter 4

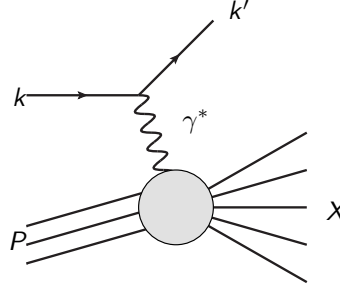
Deep inelastic scattering & high energy evolution

4.1 DIS in dipole picture

4.1.1 DIS introduction

Before understanding what happens when two nuclei collide at high energy, we have to know what the nuclei are made of. We know that they consist of quarks and gluons, but how many of these are there? We know that the nuclei are nonperturbative objects, so we cannot understand them from first principles at weak coupling alone. We can, however, *measure* the content of the hadron experimentally, by studying it with a simple probe: an electron. This experimental situation is known as deep inelastic scattering.

DIS kinematics



$$s = (k + P)^2 \quad (4.1)$$

$$q = k - k' \quad q^2 \equiv -Q^2 \quad (4.2)$$

$$W^2 = (P + q)^2 \quad (4.3)$$

$$x = \frac{Q^2}{2P \cdot q} = \frac{Q^2}{W^2 + Q^2 - m_N^2} \quad (4.4)$$

High energy limit

$$x \rightarrow 0 \quad W^2 \rightarrow \infty \quad (4.5)$$

In addition to the variables above, one also conventionally defines the following Lorentz-invariant variables

$$y = \frac{2P \cdot q}{2P \cdot k} = \frac{W^2 + Q^2 - m_N^2}{s - m_N^2} \quad (4.6)$$

$$\nu = P \cdot q / m_N = \frac{W^2 + Q^2 - m_N^2}{2m_N} \quad (4.7)$$

Before moving on let us discuss a little the physical interpretation of the kinematical variables.

- The total e^-p center of mass energy s is of course important for an experimentalist. For the QCD part of the scattering process it is, completely irrelevant; its only practical consequence is that kinematically it sets the upper limit for the quantity we are really interested in, which is
- W^2 , the c.m.s. energy of the γ^*p -system. This is the collision energy that is relevant for the QCD part of the scattering, and the high W^2 is what defines the high energy limit that we are interested in. The collision energy W^2 is practically the same as
- ν , which is the energy of the γ^* , i.e. the energy lost by the electron, in the target rest frame. This is important historically when most experiments are done at fixed targets, but W^2 is nicer for a theorist since it is Lorentz-invariant.
- The “inelasticity” y is really related to the electron-photon vertex kinematics. It determines how much of the electron energy is taken by the photon, i.e. the relation between the uninteresting variable s and the interesting one W^2 , and is thus uninteresting for us here.¹
- Q^2 should be thought of as the spatial resolution scale, it tells us what is the wavelength of the space-like virtual photon and therefore the resolution scale at which we can probe the contents of the target. Unless we have heavy quarks, Q^2 has to be large enough to justify weak coupling. As we will see later, it is useful to think of Q^2 as a transverse momentum scale, and W^2 as a longitudinal momentum, or energy scale.
- Finally there is x ; which for the purposes of these lectures is mostly just a way of parametrizing W^2 . However, it is conventionally thought of as a momentum fraction of the struck parton, and we will first take a short detour to see why this is the case.

Let us look at the diagram in a bit more detail, and introduce the concept of the *leptonic tensor*, the *hadronic tensor* and the structure functions F_1 and F_2 . In general the cross section is

$$d\sigma = \frac{1}{2(s-m^2)} \frac{1}{2} \sum_{s_e, s_{e'}} \frac{1}{2} \sum_{s_p, s_X} \sum_X \int d\Pi_X |\mathcal{M}|^2 \frac{d^3\vec{k}'}{2E'(2\pi)^3} \quad (4.8)$$

Here we have even kept the full proton mass dependence, just for fun (m is the proton mass). The electron is massless ($m_e = 0$). The spins of the incoming electron and proton s_e and s_p are averaged over, and we sum over the spin of the outgoing electron $s_{e'}$ and all the spins of all the outgoing particles in the final state X . We all summing over all possible final states X of the proton system X , and integrating over their phase spaces $d\Pi_X$. There is a separate integration over the phase space of the outgoing electron, whose momentum is \vec{k}' and energy $E' = |\vec{k}'|$. We have included the overall momentum conservation delta function in the phase space of the system X , with the idea that it should be thought of as restricting the total four-momentum of the system X to $P^\mu + q^\mu = P^\mu + k^\mu - k'^\mu$. Now let us split out of the scattering amplitude \mathcal{M} all the ingredients that we know. The amplitude will be, in Feynman gauge,

$$\mathcal{M} = e^2 \bar{u}_{s_{e'}}(k') \gamma^\mu u_{s_e}(k) \frac{-ig_{\mu\nu}}{q^2} \langle X, P+q | J^\nu(0) | P \rangle, \quad (4.9)$$

where all the unknown QCD physics of the target is in the matrix element of the electric current operator J^μ in the target state.

Digression: Why current operator?

It might not be obvious why the electric current operator expectation value is the one that appears. One way to think about it is in the field theory language: the interaction term between photons and charged particles in the Lagrangian is $e \int d^4x A_\mu(x) J^\mu(x)$, where we have scaled out the coupling, so that the current J^μ is really a number current and not a charge current. For example for an elementary charged fermion field, the current operator is $J^\mu(x) = \bar{\psi}(x) \gamma^\mu \psi(x)$,

¹Of course, if you are building a detector for DIS experiments at the Electron-Ion Collider, y is the most important variable for you: it determines what direction the electron flies in, and you really have to measure very precisely this electron.

with fermion field operators $\bar{\psi}(x), \psi(x)$. When doing perturbation theory, the Lagrangian is in the exponent, and at each order one power of the interaction term drops down: we therefore calculate expectation values of $e \int d^4x A_\mu(x) J^\mu(x)$ between the incoming and outgoing states. The photon field A_μ becomes a part of the photon propagator (which is $\langle A_\mu A_\nu \rangle$) and the integral over coordinates x becomes a four-momentum conserving delta function. What is left is the QCD part: the expectation value of the current-current correlator in the hadronic state.

Now we split this into a few parts. First is the

Leptonic tensor

$$L_{\mu\nu} = \frac{1}{2} \sum_{s_e, s_{e'}} \bar{u}_{s_{e'}}(k') \gamma_\mu u_{s_e}(k) [\bar{u}_{s_e}(k') \gamma_\nu u_{s_{e'}}(k)]^\dagger = 2(k_\mu k'_\nu + k'_\mu k_\nu - g_{\mu\nu} k \cdot k') \quad (4.10)$$

Remember that we are not squaring the lepton tensor with the same index in the amplitude and the conjugate amplitude: instead each index (μ for the amplitude and ν for the conjugate) is separately contracted with the respective indices in the hadron, via the photon propagator).

The structure of the hadron is encoded in the

Hadronic tensor

$$W_{\mu'\nu'} \quad (4.11)$$

Gauge invariance:

$$q^\mu L_{\mu\nu} = q^\nu L_{\mu\nu} = q^{\mu'} W_{\mu'\nu'} = q^{\nu'} W_{\mu'\nu'} = 0 \quad (4.12)$$

Electromagnetic gauge invariance is encoded in the Ward identities, which lead to the leptonic and hadronic tensors being transverse to the photon momentum. This follows from the fact that both $L_{\mu\nu}$ and $W_{\mu\nu}$ are expectation values of electromagnetic current operators, and the current is conserved: $\partial_\mu J^\mu(x) = 0$. If we are not measuring spin (of any of the particles), the hadronic tensor can only depend on two Lorentz four-vectors: q^μ and P^μ . Out of these two vectors, it is possible to construct only two independent symmetric ($W_{\mu\nu} = W_{\nu\mu}$) Lorentz structures. The coefficients of these Lorentz tensors are known as the structure functions F_1 and F_2 .

Structure functions

$$W_{\mu\nu} = 2 \left(-g_{\mu\nu} + \frac{q_\mu q_\nu}{q^2} \right) F_1(x, Q^2) + \frac{2}{P \cdot q} \left[\left(P_\mu - \frac{P \cdot q}{q^2} q_\mu \right) \left(P_\nu - \frac{P \cdot q}{q^2} q_\nu \right) \right] F_2(x, Q^2) \quad (4.13)$$

The way one should read this is relation is that

- F_2 is the structure corresponding to the current (remember $W_{\mu\nu} \sim \langle J_\mu J_\nu \rangle$) in the direction of the proton, but removing the part that is parallel to the photon q_μ .
- F_1 is the rest, so in some appropriately Lorentz and gauge invariant sense both the part parallel to P_μ and orthogonal to it.

Let us now simplify our cross section (4.8) with the help of the structure functions. We also will write it as differentially in Lorentz-invariant variables (for this also there are several different options). We start by contracting the leptonic and hadronic tensors. Since we have expressions for all the scalar products in terms of the Lorentz-invariants, we can, after some algebra, easily see that

$$L_{\mu\nu} W^{\mu\nu} = 4Q^2 F_1(x, Q^2) + \frac{4Q^2}{xy^2} \left[1 - y - \frac{x^2 m^2 y^2}{Q^2} \right] F_2(x, Q^2) \quad (4.14)$$

Let us then treat the phase space integration for the final state electron in the cross section (4.8). These manipulations are easiest to do in the target (proton) rest frame, but the final result will be Lorentz-invariant. We first write the electron phase space in polar coordinates: $d^3\vec{k}' = (E')^2 d\Omega dE'$, with $E' = |\vec{k}'|$ for a

massless electron. We also have $s - m^2 = 2mE$ with $E = |\vec{k}|$ for the incoming electron. Our cross section is now

$$\frac{d\sigma}{dE' d\Omega} = \frac{\alpha_{\text{e.m.}}^2}{2mQ^4} \frac{E'}{E} L_{\mu\nu} W^{\mu\nu}. \quad (4.15)$$

This is the useful form if you actually want to measure this, assuming your detector is in the target rest frame. But we can do some changes in the integration variables. First integrate over the azimuthal angle of the electron (assuming the cross section does not depend on it, which it will not if we are averaging over spins and averaging over the azimuthal angle of the scattered electron, as we will discuss in a moment), which leads to $d\Omega = 2\pi d\cos\theta$. We then replace $\cos\theta$ with Q^2 (you remember already from nonrelativistic scattering theory that the momentum transfer is closely tied in with the scattering angle). This is done with the help of

$$Q^2 = 2EE'(1 - \cos\theta) \implies d\sigma = \frac{2\pi\alpha_{\text{e.m.}}^2}{Q^4} L_{\mu\nu} W^{\mu\nu} \frac{dQ^2 dE'}{4mE^2} \quad (4.16)$$

We then also want to get rid of the scattered electron energy E' . We can exchange this to the Lorentz-invariant variable x with the help of the relation (now for fixed Q^2 , because Q^2 is at this point our other integration variable:

$$E' = \frac{1}{2m} \left(s - \frac{Q^2}{x} - Q^2 \right) \implies dE' = \frac{Q^2}{2mx^2} dx \implies d\sigma = \frac{2\pi\alpha_{\text{e.m.}}^2}{Q^4} L_{\mu\nu} W^{\mu\nu} \frac{Q^2 dQ^2 dx}{8m^2 E^2 x^2} \quad (4.17)$$

Using $Q^2 = xy(s - m^2) = 2mExy$ this leads to another commonly seen form

$$\frac{d\sigma}{dx dQ^2} = \frac{2\pi\alpha_{\text{e.m.}}^2}{Q^4} L_{\mu\nu} W^{\mu\nu} \frac{y}{4mEx}, \quad (4.18)$$

where using (4.14)

$$\frac{d\sigma}{dx dQ^2} = \frac{4\pi\alpha_{\text{e.m.}}}{xQ^4} \left[\left(1 - y - \frac{xm^2y^2}{Q^2} \right) F_2(x, Q^2) + xy^2 F_1(x, Q^2) \right]. \quad (4.19)$$

We can still go further and change the variable from Q^2 to y using $Q^2 = xy(s - m^2) = 2mExy$ and thus $dQ^2 = 2xmE dy$, remembering that now x is fixed. This leads to

$$d\sigma = \frac{2\pi\alpha_{\text{e.m.}}^2}{Q^4} L_{\mu\nu} W^{\mu\nu} \frac{y dy dx}{2}, \quad (4.20)$$

and to

$$\frac{d\sigma}{dx dy} = \frac{4\pi\alpha_{\text{e.m.}}^2 (s - m^2)}{Q^4} \left[\left(1 - y - \frac{xm^2y^2}{Q^2} \right) F_2(x, Q^2) + xy^2 F_1(x, Q^2) \right], \quad (4.21)$$

where for example in [58] this is written with $s - m^2 = 2mE$.

4.1.2 Partons

Usually the textbook description of DIS is done in the infinite momentum frame, where the hadron is moving fast. One then makes the *parton model* assumption that the hadron consists of partons, quarks and gluons, whose momenta are parallel to that of the hadron (since the hadron momentum is very high, the transverse momenta of the partons with respect to the large longitudinal momenta are small). The physical picture of a DIS process is then that the virtual photon strikes one of these partons (at LO it has to be a quark, since photons couple to gluons only through a higher order process with intermediate quarks).

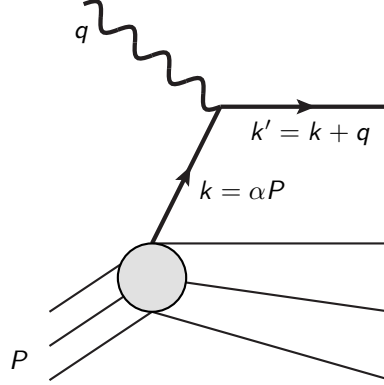
Let us now assume that

1. the 4-momentum of the quark before it hits the photon is parallel to the hadron and carries a fraction α of the momentum of the hadron P ,
2. the quark after it is struck by the photon is an asymptotic final state particle and thus on shell (this is certainly always the case in inclusive cross sections, because there one is summing over all possible final states, and this can be done using any complete set of states, including of course the free particle states)

3. we can neglect the mass of the hadron (we always do in these lectures whenever we can).

This allows us to show that actually the momentum fraction α is *with these assumptions* is actually the same as the kinematical variable x :

Infinite momentum frame IMF



$$0 = (q + \alpha P)^2 = -Q^2 + 2\alpha P \cdot q + \underbrace{\alpha^2 m_N^2}_{\approx 0} \Rightarrow \alpha = \frac{Q^2}{2P \cdot q} = x \quad (4.22)$$

$x = \text{momentum fraction}$

The identification of the kinematical variable x (or Bjorken x , i.e. x_{Bj}), which is a well defined Lorentz-invariant constructed from the 4-momenta of the incoming and outgoing electron and the incoming proton, with the momentum fraction of the quark that is struck is so common, that the two concepts are often used completely interchangeably. It is good to remember, however, that x and the momentum fraction are conceptually separate things and identifying them requires a certain physical picture, that of the quarks as completely collinear to the hadron moving at infinite velocity.

One can with relative ease show that if the scattering happens off spin-1/2 quarks only, and these quark behave like free particles like the electrons, one has a relation between the structure functions

Callan-Gross

Free spin- $\frac{1}{2}$ quarks

$$F_2 = 2xF_1 \quad (4.23)$$

This is easy to show by checking that if this condition is true, the decomposition (4.13) reduces to the same form as the leptonic tensor. If the Callan-Gross relation is satisfied, quarks are free, and there are no gluons. Consequently in QCD the violation

$$F_L = F_2 - 2xF_1 \sim \alpha_s x g(x, Q^2) \quad (4.24)$$

only arises at higher order in perturbation theory, and is directly sensitive to gluons. We will see why this is called the “longitudinal structure function” shortly.

4.1.3 Virtual photon scattering

We can use the gauge invariance relation (4.12) to replace in the photon propagator

$$-g_{\mu\mu'} \rightarrow -\left(g_{\mu\mu'} - \frac{q_\mu q_{\mu'}}{q^2}\right). \quad (4.25)$$

The propagator with this replacement is called the Landau gauge propagator. Now $q^2 < 0$, i.e. the virtual photon is spacelike and off shell. Thus we can go to a frame where it does not have an energy component: this is the *Breit frame* with

$$q^\mu = (0, 0, 0, Q) \quad (= (q^0, q^1, q^2, q^3)). \quad (4.26)$$

Now let us introduce three polarization vectors

$$\varepsilon_1^\mu = (0, 1, 0, 0) \quad \varepsilon_2^\mu = (0, 0, 1, 0) \quad \varepsilon_L^\mu = (1, 0, 0, 0) \quad (4.27)$$

The first two are (linear) transverse polarizations, and the third one a longitudinal one. The usual transverse polarization states with a specific angular momentum are linear combinations of our polarization states $\varepsilon_1^\mu, \varepsilon_2^\mu$. They satisfy

$$q \cdot \varepsilon_\lambda(q) = 0. \quad (4.28)$$

With the help of these polarization vectors we can write the transverse polarization projection operator

$$-\left(g_{\mu\mu'} - \frac{q_\mu q_{\mu'}}{q^2}\right) = -\varepsilon_L^{*\mu} \varepsilon_L^{\mu'} + \varepsilon_1^{*\mu} \varepsilon_1^{\mu'} + \varepsilon_2^{*\mu} \varepsilon_2^{\mu'} = \sum_{\lambda=0}^2 (\eta_\lambda) \varepsilon_\lambda^{*\mu} \varepsilon_\lambda^{\mu'}, \quad (4.29)$$

with $\eta_{L=0} = -1, \eta_1 = \eta_2 = 1$.

Note the sign of the longitudinal polarization vector squared in this expression. Because the virtual photon is spacelike, it is impossible to have a Lorentz-covariant form for the the transverse projection operator Eq. (4.25) in terms of a sum of squares (which are positive) of polarization vectors with equal signs. In the frame (4.26) the projection operator (4.25) is $\text{diag}(-1, 1, 1, 0)$; this is not a positive definite tensor that could be a sum of squared polarization vectors with positive coefficients. Nevertheless, it is useful to think of the propagator as being a sum of polarization states. Now we can write our DIS cross section (in the original Lorentz-covariant form) as

$$d\sigma = \frac{1}{2(s-m^2)} \sum_{\lambda, \lambda'=0}^2 (\eta_\lambda \eta_{\lambda'}) \varepsilon_\lambda^{*\mu} \varepsilon_\lambda^{\mu'} \varepsilon_{\lambda'}^{\nu} \varepsilon_{\lambda'}^{*\nu'} L_{\mu\nu}(2\pi) W_{\mu'\nu'} \frac{d^3\vec{k}'}{2E'(2\pi)^3}. \quad (4.30)$$

The electron momentum only appears in the leptonic tensor $L_{\mu\nu}$. Let us now integrate over the angle of the electron, for fixed values of the Lorentz-invariants s, x, y, Q^2 . It is convenient to do this in the Breit frame, where we can choose the momenta as:

$$k = (E_B, \kappa \cos \varphi, \kappa \sin \varphi, Q/2) \quad (4.31)$$

$$k' = (E_B, \kappa \cos \varphi, \kappa \sin \varphi, -Q/2) \quad (4.32)$$

$$q = (0, 0, 0, Q) \quad (4.33)$$

$$P = (\sqrt{m^2 + Q^2/(4x^2)}, 0, 0, -Q/(2x)) \quad (4.34)$$

The value of the incoming electron energy E_B can be fixed from $s = (k + P)^2 = Q^2/(xy) + m^2$ and the value of κ from $k^2 = 0$. In this frame it is easy to take the dot products of the photon polarization vectors with the leptonic tensor, integrate them over the outgoing electron angle φ and see that

$$\varepsilon_\lambda^{*\mu} \varepsilon_{\lambda'}^{\nu} L_{\mu\nu} \propto \delta_{\lambda, \lambda'}. \quad (4.35)$$

Although we did this calculation in a specific frame, our expression for the cross section is Lorentz-invariant, and thus this result is completely general. This leads to an important result that very commonly used:

■ $\int d\varphi_{e'} (Q^2, x = \text{cst.}) \implies \gamma^* \text{ polarizations do not interfere.}$

If we do not measure or track (i.e. we integrate over) the scattered electron angle, the polarization of the virtual photon in the amplitude and the conjugate amplitude is the same. This means that we can write the electron-proton cross section as an (“incoherent”) sum of cross sections that are mediated by different polarization states, with

$$\frac{d\sigma}{dy dx} = \frac{2\pi\alpha_{\text{e.m.}}^2 y}{Q^4} \sum_{\lambda=0}^2 [\varepsilon_\lambda^{*\mu} \varepsilon_\lambda^{\nu} L_{\mu\nu}] [\varepsilon_\lambda^{\mu'} \varepsilon_\lambda^{*\nu'} (2\pi) W_{\mu'\nu'}] \quad (4.36)$$

Note that now there is only one sum over polarizations, at the cross section level, not any more in the amplitude and conjugate separately. With a little bit more time we would evaluate these integrals and calculate $[\varepsilon_\lambda^{*\mu} \varepsilon_\lambda^{\nu} L_{\mu\nu}]$.

We can think of this as a photon flux from the electron, multiplied by a virtual photon-target cross section. Which parts of the expression one actually factorizes into the cross section and which part into the photon flux. My convention, as in [2], is to define

$$\sigma^{\gamma^* + p \rightarrow X} = \frac{2\pi^2 \alpha_{\text{e.m.}}}{4mK} [\varepsilon_\lambda^{\mu'} \varepsilon_\lambda^{*\nu'} W_{\mu'\nu'}], \quad (4.37)$$

with

- $K = \sqrt{\nu^2 + Q^2}$ (Gilman convention), which is the photon momentum in the target rest frame
- $K = \nu - Q^2/(2m) = \nu(1 - x)$ (Hand convention), which is constructed such that the $\gamma^* + p$ center of mass energy $W^2 = 2m\nu - Q^2 + m^2$ satisfies the relation that it would for a scattering of a proton at rest with a real photon with energy K , namely $W^2 = m^2 + 2mK$.

All of these conventions become the same in the high energy, i.e. $x \rightarrow 0$ limit.

With a little bit more time, we would derive the virtual photon cross sections more carefully, some of this is done as an exercise. Here, I will just quote the result (flux convention $K = \nu$ and proton mass neglected $m = 0$ here):

Define

$$\sigma_L^{\gamma^*+p \rightarrow X} = \frac{4\pi^2\alpha_{\text{e.m.}}}{Q^2} (F_2 - 2xF_1) \quad (4.38)$$

$$\sigma_T^{\gamma^*+p \rightarrow X} = \frac{4\pi^2\alpha_{\text{e.m.}}}{Q^2} 2xF_1 \quad (4.39)$$

$$\sigma_{\text{tot}}^{\gamma^*+p \rightarrow X} = \sigma_L^{\gamma^*+p \rightarrow X} + \sigma_T^{\gamma^*+p \rightarrow X} = \frac{4\pi^2\alpha_{\text{e.m.}}}{Q^2} F_2 \quad (4.40)$$

This finally explains why the combination $F_2 - 2xF_1$ is called the longitudinal structure function F_L . Correspondingly $2xF_1$ can be called F_T . Note that the transverse cross section is defined as an average *per polarization*, not the sum of two polarizations. Thinking about this as a γ^*p scattering such a definition does not really make sense. However, this is the natural convention for the ep scattering. A single transverse polarization state of the photon contributes to the total DIS cross section with a factor 1/2 compared to a longitudinal one, because the integral over the scattered electron angle gives a factor 1/2: although there are 2 transverse polarizations, the “total cross section” (appropriate for ep) is approximately the sum of one “average” transverse and one longitudinal photon polarization.

In Eq. (4.21) we can see that the total *electron-proton* cross section is proportional to just F_2 in the limit $y \rightarrow 0$. This is the limit of the electron emitting a *soft* photon (we will discuss soft gluons in Sec.4.3), which carries only a small fraction of its momentum. In this limit, the photon does not really know about the spin of the electron, and the DIS cross section truly factorizes into a photon emission and a photon-proton cross section. For large y the spin of the electron matters, and the total ep cross section is not just proportional to the γ^*p cross section, but the dependence is a bit more complicated. However, to a first approximation it is useful to think that the total DIS cross section measures F_2 .

Experimentally this leads to the following situation

- $\sigma(e + p) \Rightarrow \sim F_2(x, Q^2)$
- Vary y (i.e. s) for fixed $x, Q^2 \Rightarrow F_L$

The easy thing to measure, and therefore much more precisely known, is the “reduced cross section” which is, to a first approximation ($y \ll 1$) essentially F_2 . For this it is enough to measure the ep cross section with one collision energy s . To disentangle F_2 and F_L (i.e. F_2 and F_1 separately), one needs to vary the beam energy s in order measure cross sections at the same x, Q^2 and different y , and then extract F_L from the (not particularly strong) y dependence. This is known as the *Rosenbluth separation*, and is more difficult to perform: both because it requires more statistics, and because for different y at the same x, Q^2 the electron goes into a different parts of the detector with resulting different systematical uncertainties.

4.1.4 Dipole picture

Now let us move to a different Lorentz frame, i.e. the target (hadron/nucleus) rest frame. Cross sections are Lorentz-invariant, but the physical picture of the scattering is not. In fact, in this frame, and at small x , we think of the γ^* as a kind of a hadron, which itself consists of quarks and gluons. DIS (and even $\gamma\gamma$ -scattering) are now hadronic processes. In particular one would expect the high energy behavior of the cross sections to be similar to hadronic scattering, just scaled by a factor of 1/137 (or $(1/137)^2$) (see Fig. 4.1) because at some point γp (and respectively $\gamma\gamma$) involve one (or two) additional electromagnetic vertices. In

fact I want to convince you that the γ^* with a largish Q^2 is the theorist's favorite hadron it is a QCD bound state; but unlike the proton, its partonic structure can be fully understood in perturbation theory!

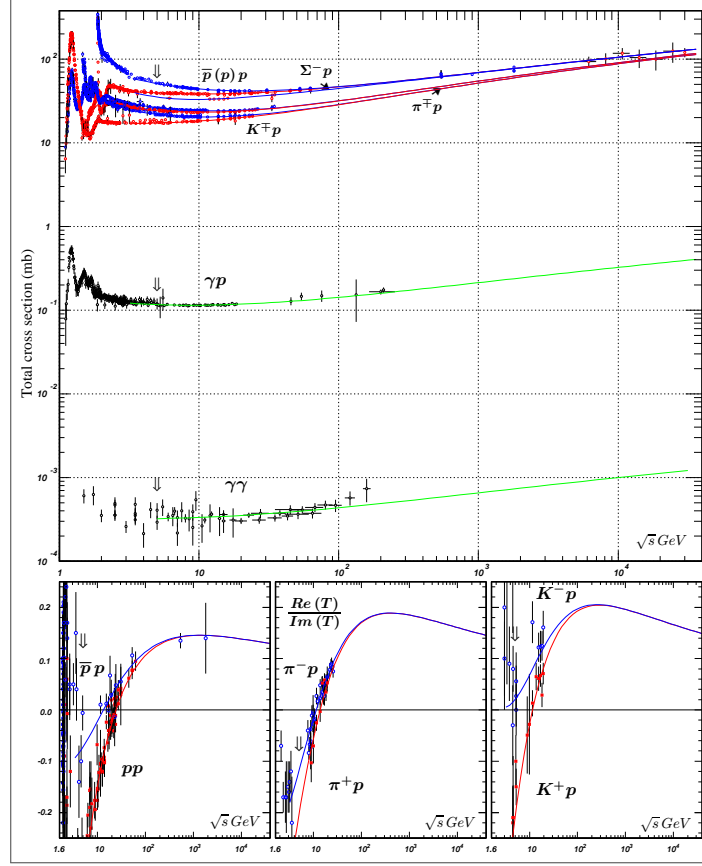


Figure 4.1: pp , γp , and $\gamma\gamma$ total cross sections vs \sqrt{s} .

Let us now look at the kinematics of DIS in the target rest frame

Target Rest Frame TRF

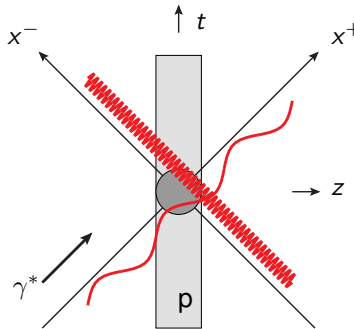
$$x^\pm = \frac{1}{\sqrt{2}}(t \pm z)$$

$$P^\mu = \begin{pmatrix} m \\ \vec{0} \end{pmatrix} \Rightarrow \begin{pmatrix} m/\sqrt{2} \\ m/\sqrt{2}, \vec{0} \end{pmatrix} \quad (4.41)$$

$$q^\mu \approx \begin{pmatrix} W^2/(2m) \\ \vec{0} \end{pmatrix}, \frac{z}{\sqrt{(W^2/2m)^2 + Q^2}} \Rightarrow \begin{pmatrix} q^+ \\ -Q^2/(2q^+), \vec{0} \end{pmatrix} \quad (4.42)$$

High energy: $q^+ \approx W^2/(\sqrt{2}m) \rightarrow \infty$

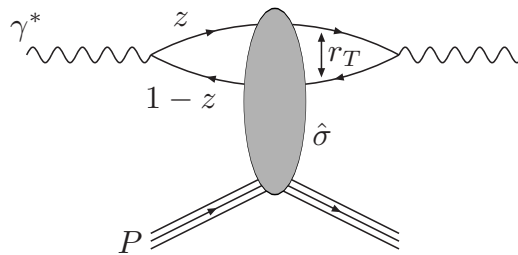
γ^* wave $e^{-i(q^+x^- + q^-x^+)}$



- 1000000

pl
ir
di

100



1003

$$\sigma_{T,L}^{\gamma^*p} = \int d^2\mathbf{r} d\mathbf{z} \left| \psi^{\gamma^* \rightarrow q\bar{q}}(\mathbf{r}, \mathbf{z})_{T,L} \right|^2 2 \int d^2\mathbf{b} \mathcal{N} \quad (4.43)$$

- 100%

is
ta

pa
th
re
th

$$\sigma_{q\bar{q}} = 2 \int d^2\mathbf{b} \mathcal{N} \quad (4.44)$$

R

 ic

$$S_{fi} = \langle f | \hat{S} | i \rangle = 1 + iT_{fi} \quad (4.45)$$

T

$$\sigma_{\text{tot}} = 2\text{Im}T_{ii} \quad (4.46)$$

N
ex
 Λ

$$\mathcal{N} \equiv \text{Im}T_{ii} \quad (4.47)$$

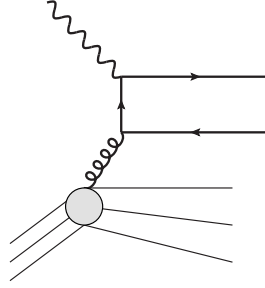
and the diagonal element of the S -matrix is given by

$$S_{ii} = \delta_{ii} - \mathcal{N} + \text{imag}, \quad (4.48)$$

where we are all the time neglecting the imaginary part of the diagonal elements of the S -matrix, i.e. the real part of the diagonal element of the T -matrix.

In the infinite momentum frame, in the case scattering off a dilute gluon field that can be pictured as one gluon exchange, the same process would look like this:

Same process in IMF:



In the usual parton model/IMF thinking this process is formally higher order in α_s . It can however be argued to dominate at small x since the gluon distribution $xg(x, Q^2)$ is so large compared to the quark distribution. However, this kind of a picture cannot describe valence quarks, or large x physics more generally.

Without any more detailed calculation right now we will just state that the information of the target color field in the CGC picture is built from two Wilson lines, one for the quark and another one, hermitian conjugate, for the gluon. In the eikonal approximation the quark and antiquark stay at the same coordinate when passing through the target color field. Thus the dipole cross section is needed in coordinate space, it depends on the transverse coordinate separation of the quark and the antiquark. In general the Wilson lines in (3.60) depend also on the longitudinal coordinate x^- (they do not depend on x^+ since this is a quantity that is integrated over). However, here we again refer to the timescale argument above: since the probe has a high q^+ , it has a very high resolution in x^- . In the strict high energy limit this means that we are probing the degrees of freedom in the target at a fixed, instantaneous x^- , which we can take to be 0 here. Thus in practice we do not worry about an x^- -dependence in the Wilson line, and instead consider it as a function of only the transverse coordinate.

Dipole amplitude in the CGC

$$\mathcal{N}_{q\bar{q}} = 1 - \frac{1}{N_c} \text{tr} V(\mathbf{x}) V^\dagger(\mathbf{y}) \quad (4.49)$$

$V(\mathbf{x})$ = familiar Wilson line (3.60)

Next, we will try to understand how to calculate the “virtual photon light cone wavefunction.”

4.2 The photon light cone wave function

4.2.1 Light Cone Perturbation Theory

The classic reference is the Brodsky, Pauli, Pinsky review [14]. For a slightly shorter review of the basics see [59]. The introduction of the Kovchegov&Levin book [1] provides a concise introduction to what we really need, unfortunately with a different metric. We use here the covariant normalization (unlike Brodsky et al. [14]), to understand the normalization it is better to look at [33] (for loop calculations see however the remark in Sec. II D of Ref. [34]) or [35]. The terms “instant form” (for ordinary equal-time quantization), “front form” (for light cone, i.e. light front, quantization) and “point form” (quantization with a proper time as time coordinate) date back to P. Dirac [60].

In the Heisenberg picture of time evolution in Quantum Mechanics, the operators are time dependent, with a time dependence generated by the Hamiltonian operator. Their quantum nature is expressed by the commutation relations of operators

Usual QM

$$\left[\hat{A}(t), \hat{B}(t') \right] \Big|_{t=t'} = \dots \quad (4.50)$$

The essential point is that we know these commutation relations (like $[\hat{x}(t), \hat{p}(t)] = i\hbar$) at *equal time*. Being able to calculate the commutation relations at unequal time $t \neq t'$ is something that can only be done once one has solved the time dependence of the theory, not something that is known from the start.

Since quantum field theory is Lorentz-covariant, one can boost to any coordinate system moving at a velocity $v < 1$. The commutation relations, equations of motion etc. will look the same in this new frame with a different time coordinate. However, one cannot boost to exactly light velocity $v = 1$. For high energy scattering problem the physical situation is such that the natural “time” coordinate would be a lightlike variable corresponding to the trajectory of a massless particle. But formulating quantum field theory for such a variable can not be obtained by a continuous transformation from the normal “instant form” quantum mechanics. In stead, one has to start from the begining and separately *define* a quantization where the “time” coordinate is a light-like variable, conventionally taken to be x^+ :

LC quantization QM

$$\left[\hat{A}(x^+), \hat{B}(y^+) \right] \Big|_{x^+=y^+} = \dots \quad (4.51)$$

LC Hamiltonian \hat{P}^-

The Hamiltonian of the theory is, by definition, the operator that generates translations in time. Since x^+ is now “time,” the conjugate operator \hat{P}^- is the light cone Hamiltonian.

Digression: Poincaré generators

The Poincaré group is 10 dimensional, generated by the 4 generators of translations \hat{P}^μ and the 6 rotations and Lorentz boosts (the 6 elements of the antisymmetric matrix $\hat{J}^{\mu\nu}$). These generators are divided into *kinematical* and *dynamical* ones. Kinematical generators are “easy,” they do not change the time coordinate (leave the equal-time hypersurface intact); thus in Lorentz-invariant theory they are symmetries that are conserved in time. The generators that do mix different equal-time hypersurfaces are called “dynamical;” they are related to how the system changes in time and are much more complicated to understand. In instant form quantization there are 6 kinematical generators: 3 spatial translations \hat{P}^i and 3 spatial rotations \hat{J}^{ij} with $i, j = 1, 2, 3$. States of a Lorentz-invariant quantum mechanical system (like bound states that can otherwise have complicated interactions) are all eigenstates of these generators (momentum and angular momentum eigenstates). The 4 other generators are dynamical (the Hamiltonian \hat{P}^0 and the 3 boosts \hat{J}^{0i}), and for example the behavior of a bound state under a boost is very complicated. In light cone quantization, on the other hand, there are 7 kinematical generators ($\hat{P}^+, \hat{P}^j, \hat{J}^{ij}, \hat{J}^{i+}$ and \hat{J}^{+-} with $i, j = 1, 2$). Strictly speaking the longitudinal boost \hat{J}^{+-} acts on the LC time as $x^+ \rightarrow e^\omega x^+$, so it does not leave constant x^+ hyperplanes invariant. Nevertheless it does leave the $x^+ = 0$ hyperplane invariant so in practice it behaves as a kinematical generator. This leaves only 3 dynamical generators: the Hamiltonian \hat{P}^- and \hat{J}^{i-} . Just counting generators LCPT is “more symmetric” than instant form quantization. The downside is that these symmetries are somewhat nontrivial combinations of rotations and boosts.

Consider for example a simple bound state of positronium e^+e^- in QED. In instant form quantization it is described by a total 3-momentum of the bound state and the spins of the particles. The Hamiltonian is nontrivial, and boosting in any of the 3 dimensions mixes up the spins, angular momenta and different Fock states in complicated ways, e.g. what in the rest frame just looks like an interacting e^+e^- state will in a boosted frame also have a $e^+e^-\gamma$ component. The same positronium in light front quantization will be characterized by a total 3-momentum \hat{P}^+, \hat{P}^j , and the angular momentum in the longitudinal direction \hat{J}^{ij} . It will be invariant under “Galileian” boosts in the 2 transverse directions \hat{J}^{i+} and transform trivially under longitudinal boosts \hat{J}^{+-} . The two rotations \hat{J}^{i-} that mix transverse and longitudinal directions will, however, be very complicated just like Lorentz-boosts are for instant form quantization.

Let us discuss (without all the details) what actually happens when one starts to quantize field theory. One of main advantage of LCPT is that it is possible to canonically quantize even nonabelian gauge theory. Thus we will here stick with canonical quantization, starting with a scalar field. We write the field operator for the noninteracting theory as a linear superposition of creation and annihilation operators. There are two equivalent ways to approach canonical quantization. We could start from the Lagrangian, derive the canonical conjugates to the fields (generalized coordinates) of the theory, and then impose Heisenberg commutation operators between the field operators and the conjugate operators. Or we could just write down

a momentum mode decomposition of the fields, and impose the commutation/anticommutation operators on the coefficients, which become creation and annihilation operators. These are equivalent and we use them interchangeably. I am here assuming that the reader is familiar with classical Lagrangian/Hamiltonian mechanics and how their concepts are used to quantize the theory.

Scalar field

$$\hat{\phi}(x) = \int \overbrace{\frac{d^2 \mathbf{k} dk^+}{2p^+(2\pi)^3}}^{\equiv \widetilde{d}\mathbf{k}} [e^{ik \cdot x} a^\dagger(\bar{k}) + e^{-ik \cdot x} a(\bar{k})] \quad (4.52)$$

$$\bar{k} \equiv (k^+, \mathbf{k}) \quad k^- \equiv \frac{\mathbf{k}^2 + m^2}{2k^+} \quad (4.53)$$

$$[a(\bar{p}), a^\dagger(\bar{q})] = 2p^+(2\pi)^2 \delta^{(3)}(\bar{p} - \bar{q}) \iff [\hat{\phi}(x), \overbrace{\partial_- \hat{\phi}(y)}^{=\Pi(y)}] \Big|_{x^+=y^+} = i\delta^{(3)}(\bar{x} - \bar{y}) \quad \bar{x} \equiv (x^-, \mathbf{x}) \quad (4.54)$$

This is just the normal commutation relation

$$[\hat{\phi}(x^+, \bar{x}), \hat{\Pi}(x^+, \bar{y})] = i\delta^{(3)}(\bar{x} - \bar{y}) \quad (4.55)$$

between a field and its conjugate variable, which is obtained by taking a derivative of the action (which is the integral of the Lagrangian density) with respect to the time derivative of the field:

$$\Pi(x) \equiv \frac{\delta \mathcal{S}}{\delta(\partial_+ \phi(x))} = \frac{\delta}{\delta(\partial_+ \phi(x))} \int d^4 y \{ \partial_+ \phi \partial_- \phi - \partial_i \phi \partial_i \phi - V(\phi) \} = \partial_- \phi(x). \quad (4.56)$$

The difference with respect to equal time quantization is that now the conjugate variable to the field is not the time derivative of the field, but a spatial derivative (x^+ is the time coordinate, x^- is a spatial coordinate). Now let us see what happens to fermions. The field operator in terms of creation and annihilation operators is the usual

$$\sum_s \int \widetilde{d}\mathbf{k} [\overbrace{d^\dagger(\bar{k})}^{\text{creates antifermion}} v_s(k) e^{ik \cdot x} + \overbrace{b(\bar{k})}^{\text{annihilates fermion}} u_s(k) e^{-ik \cdot x}] \quad (4.57)$$

$$\{b(\bar{p}), b^\dagger(\bar{q})\} = \{d(\bar{p}), d^\dagger(\bar{q})\} = 2p^+(2\pi)^2 \delta^{(3)}(\bar{p} - \bar{q}) \quad (4.58)$$

These are the normal anticommutation relations for the particle and antiparticle creation and annihilation operators. So far this looks just like in usual equal time quantization. Now let us ask the same question as for the scalar field: what is the conjugate momentum for the fermion field ψ ? In instant form quantization it is

$$\Pi(x) = \frac{\delta}{\delta(\partial_0 \psi)} \int d^4 x (i\bar{\psi} \not{\partial} \psi + \dots) = \frac{\delta}{\delta(\partial_0 \psi)} \int d^4 x (i\psi^\dagger \partial_0 \psi + \dots) = i\psi^\dagger(x). \quad (4.59)$$

Here we use $\bar{\psi} \equiv \psi^\dagger \gamma^0$ and $(\gamma^0)^2 = 1$. So there is a perfectly nice conjugate variable for all spinor components of the field. Also all spinor components of the field have a nice equation of motion:

$$\partial_0 \Pi(x) = i\partial_0 \psi^\dagger(x) = \frac{\delta}{\delta \psi(x)} \int d^4 y (i\bar{\psi}(y) \not{\partial} \psi(y) + \dots) = \dots, \quad (4.60)$$

which is just (the Hermitian conjugate of) the Dirac equation.

For light cone quantization, on the other hand, the conjugate to the fermion field is

Fermion

$$\begin{aligned} \Pi(x) &= \frac{\delta}{\delta(\partial_+ \psi(x))} \int d^4 y (i \bar{\psi} \not{\partial} \psi + \dots) = \frac{\delta}{\delta(\partial_+ \psi(x))} \int d^4 y (i \psi^\dagger \gamma^0 \gamma^+ \partial_+ \psi + \dots) \\ &= i \psi^\dagger(x) \gamma^0 \gamma^+ = i(\gamma^0 \gamma^+ \psi(x))^\dagger. \end{aligned} \quad (4.61)$$

$$\gamma^+ \gamma^+ = \frac{1}{2} \{\gamma^+, \gamma^+\} = 0 \quad (4.62)$$

$$1 = \frac{1}{\sqrt{2}} \left[\frac{1}{\sqrt{2}} (1 + \gamma^0 \gamma^3) + \frac{1}{\sqrt{2}} (1 - \gamma^0 \gamma^3) \right] = \overbrace{\frac{\gamma^0}{\sqrt{2}} \gamma^+}^{=\mathbb{P}^+} + \overbrace{\frac{\gamma^0}{\sqrt{2}} \gamma^-}^{=\mathbb{P}^-} \quad (4.63)$$

- Good component $\mathbb{P}^+ \psi$, has $\partial_+ \mathbb{P}^+ \psi$
- Bad component $\mathbb{P}^- \psi \implies$ constraint $\mathbb{P}^- \psi = \frac{1}{\partial_-} (\dots) \mathbb{P}^+ \psi$

$$\not{\partial} = i \gamma^+ \partial_+ + \dots \quad (4.64)$$

One can easily check that \mathbb{P}^\pm are *projection operators*, i.e. they satisfy $\mathbb{P}^+ \mathbb{P}^+ = \mathbb{P}^+$, $\mathbb{P}^- \mathbb{P}^- = \mathbb{P}^-$ and $\mathbb{P}^+ \mathbb{P}^- = 0$. This means that they divide the 4-dimensional complex space of Dirac spinors into two subspaces. Only one of these subspaces is an actual dynamical variable that has an equation of motion: this can in fact be seen directly from the Dirac equation, where only $\gamma^+ \psi$ has a time derivative.

Now the problem is that while our original Dirac spinor had 4 components, there are only 2 conjugate variables. Another way of saying the same thing is to notice that in the Dirac equation the derivative operator $\not{\partial}$ only has a time derivative in the combination $\gamma^+ \partial_+$, which does not act on the component $\mathbb{P}^- \psi$. The two components of a Dirac spinor are called:

- The good component $\mathbb{P}^+ \psi = \psi^+$. The good component is a proper time-dependent variable. Classically it has an equation of motion, and quantum mechanically it is described by a field operator that has a Heisenberg equation of motion.
- The bad component $\mathbb{P}^- \psi = \psi^-$. It does not have an equation of motion that would tell us how it evolves in time, thus it is not a dynamical variable. Instead, its Dirac equation is a constraint equation: at every value of time we can always solve this constraint equation to obtain ψ^- as a function of the actual dynamical field ψ^+ . Because the Dirac operator is $\not{\partial} = \gamma^- \partial_- + \dots$, the constraint equation is a differential equation $\partial_- \psi^- = \dots$ and must be solved by inverting the (spatial) derivative ∂_- . Much ink has been spilled over the boundary conditions necessary for performing this inversion, but we will not dwell on this further here [61]. In the diagrammatical rules of LCPT, this results in rules that have inverse powers of the momentum k^+ .

To obtain the Hamiltonian of the theory, which we will write down in a moment, one must eliminate the dependent, non-independent, degree of freedom ψ^- . Thus, it will only involve good components of the field ψ , including in terms with inverse powers of the spatial derivative ∂_- . These terms are known as *instantaneous interactions*. A peculiarity is that in loop calculations, the field strength renormalization is different for the two components [62].

A very similar thing happens with gauge bosons, although in contrast to fermions there are not only complications but also advantages from light cone quantization.

Gauge boson

$$\mathcal{L} = -\frac{1}{4} F_{\mu\nu} F^{\mu\nu} \quad (4.65)$$

$$E^\mu = \frac{\delta}{\delta(\partial_+ A^\mu)} \mathcal{L} \implies \text{no } \partial_+ A^- \quad (4.66)$$

So for gauge fields we face an analogous situation as for the quarks, and one component of the gauge field does not have a conjugate variable, or an equation of motion that would give its time dependence. It should therefore be solved in terms of the other components by a constraint equation. To get this equation, let us look at the $+$ component of the equation of motion for the gauge field

$$[D_-, F^{-+}] + [D_i, F^{i+}] = J^+. \quad (4.67)$$

$$\underbrace{A^+ = 0}_{\text{choice}} \implies \underbrace{(\partial_-)^2 A^- = [D_i, F^{i+}] - J^+}_{\text{constraint}}, \quad (4.68)$$

Here J^+ is the color current from the fermions and possible other colored particles in the theory. The important point is that in general it is difficult to solve the constrained field component A^- from Eq. (4.67) because of the nonlinear terms like $[A^+, [A^-, A^+]]$. However, in the specific gauge $A^+ = 0$ there are no such terms, and A^- can be solved. Similarly as for the fermions, we now solve A^- from Eq. (4.68), and substitute it back into the Lagrangian/Hamiltonian, which will then only depend on the transverse components of the gauge field A_i , $i = 1, 2$.

- If we look at $--$ -component of equation of motion, it has more complicated nonlinear terms in A^- , e.g. $[A^-, \partial_- A^-] \sim J^-$. However, the J^+ current is the one corresponding to a conserved charge (it is the time component of a charge current 4-vector), and it is the one that is expressed in terms of the good components of the spinors: $J_a^+ = \bar{\psi} \gamma^+ t^a \psi$.
- The textbook quantization of QED in Coulomb gauge is done in a similar way. One chooses the gauge $\nabla \cdot \vec{A} = 0$, and then expresses the non-dynamical degree of freedom A^0 as a constraint equation. Here one problem is that for nonabelian theory it is in fact in general not possible to fix the gauge $\nabla \cdot \vec{A} = 0$. Also in nonabelian gauge theory the constraint, which should come from the time- i.e. 0-component of the equation of motion $[D_\mu, F^{\mu 0}] = J^0$ has terms like $[A^i, [A^i, A^0]] \sim J^0$ which make it much more difficult to try to solve the constraint A_0 in terms of the dynamical fields of the theory. Thus canonical quantization is usually only done for QED, and QCD is quantized by path integrals.

In summary, we have a light cone gauge light cone quantized theory, where there are only two physical polarization states, expressed (or at least expressible) in terms of two transverse component of the gauge potential. We can write for them a decomposition in terms of creation and annihilation operators

$$A^i(x) = \sum_{\lambda=\pm} \int \tilde{d}k [(\varepsilon_{(\lambda)}^i)^* e^{ik \cdot x} a_{(\lambda)}^\dagger(\vec{k}) + \varepsilon_{(\lambda)}^i e^{-ik \cdot x} a_{(\lambda)}(\vec{k})]. \quad (4.69)$$

If one uses circular polarization states (which is convenient), the polarization vectors $\varepsilon_{(\lambda)}^i$ can be taken as given in Eq. (4.82).

We can now also write down the Hamiltonian of the theory. Let us do this for QED, for simplicity. It is

$$\hat{P}^- = \hat{P}_0^- + \hat{P}_{\text{int}}^- \quad (4.70)$$

$$\hat{P}_0^- = \int d^3 \vec{x} \left[\bar{\psi} \frac{m^2 + (i \nabla_\perp)^2}{2i \partial_-} \gamma^+ \psi + \frac{1}{2} A^i \nabla_\perp^2 A^i \right] \quad (4.71)$$

$$\hat{P}_{\text{int}}^- = \int d^3 \vec{x} \left[e \bar{\psi} \tilde{A} \psi + e^2 \bar{\psi} \gamma^+ \psi \frac{1}{(i \partial_-)^2} \bar{\psi} \gamma^+ \psi + e^2 \bar{\psi} \tilde{A} \frac{\gamma^+}{i \partial_-} \tilde{A} \psi \right] \quad (4.72)$$

$$\tilde{A}^\mu = (0, \tilde{A}^- = -\frac{1}{\partial_-} \partial_i A^i, \mathbf{A}) \quad (4.73)$$

Here we have introduced the notation \tilde{A}^μ for the vector potential in the $A^+ = 0$ gauge and with a A^- given by the the gauge field part of the constraint equation (4.68). The current part of the constraint equation (4.68) ($A^- \sim J^+ / (\partial_-)^2$) is written separately as the second term in the interaction (4.72): it generates a four-fermion interaction (mediated by an “instantaneous photon” exchange, a Coulomb-like photon with only the A^- polarization). In the third term we write $\tilde{A} \gamma^+ \tilde{A}$, but because $A^+ = 0$ and $\gamma^+ \gamma^+ = 0$, in fact only the transverse components of the vector potential appear. This term is a fermion-antifermion-2-photon interaction, mediated by an “instantaneous fermion”. It comes from the term $\bar{\psi} \gamma^- \partial_- \psi \sim \bar{\psi}^- \gamma^- \partial_- \psi^-$ part

of the fermion Lagrangian, with both ψ^- and $\bar{\psi}^-$ expressed in terms of the good component ψ^+ via the Dirac equation, which also involves the gauge field.

In the Hamiltonian (4.70) the spinor and gauge fields should be thought of as linear superpositions of creation and annihilation operators according to Eqs. (4.57) and (4.69). Now in principle we are ready to start calculating light cone wave functions.

4.2.2 Virtual photon light cone wave function

Let us now go through the calculation of the wave function $\psi^{\gamma^* \rightarrow q\bar{q}}(\mathbf{r}, z)$ needed for the DIS cross section in the dipole picture, Eq. (4.43). The most important thing to remember is that this is a purely QED process, and therefore very well understood.

The concept of a light cone wave function makes sense in the framework of Light Cone Perturbation Theory (LCPT). In LCPT one starts from the standard Lagrangian of the theory, and quantizes it by postulating canonical commutation relations at equal light cone time x^+ among interaction picture (i.e. time-dependent) field operators. One then works in “old fashioned” quantum mechanical perturbation theory (in stead of the “modern” covariant theory of Feynman et al). This is a framework that is used to understand the partonic structure of hadronic bound (or more generally composite) states as they are measured in high energy scattering processes. In the case of the dipole picture of DIS the “bound state” that we are quantizing is the virtual photon. We will not go into any details here, for a review see [14, 1] and for the notations and technical details of the calculation done here (and its extension to NLO) see [34].

The basic idea of the LCPT calculations here is that in perturbation theory we know the free particle Fock states, for a photon $|\gamma^*\rangle_0$, $|q\bar{q}\rangle_0$, $|q\bar{q}g\rangle_0$ etc. Physical particles are eigenstates of the interacting theory; they can always be written as linear superpositions of the free particle states

$$|\gamma^*\rangle = (1 + \dots)|\gamma^*\rangle_0 + \psi^{\gamma^* \rightarrow q\bar{q}} \otimes |q\bar{q}\rangle_0 + \psi^{\gamma^* \rightarrow q\bar{q}g} \otimes |q\bar{q}g\rangle_0 + \dots \quad (4.74)$$

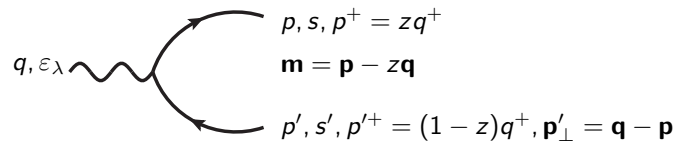
It is the coefficient functions of this expansion that are called *light cone wave functions*. In quantum mechanical perturbation theory the first perturbative correction to the ground state $|0\rangle$ wavefunction is

$$|0\rangle \implies |0\rangle + \sum_n \frac{\langle n | \hat{V} | 0 \rangle}{E_0 - E_n} |n\rangle, \quad (4.75)$$

LCPT: $E \implies k^-$

Here V is the interaction part of the Hamiltonian. The energy denominator $1/\Delta E$ is \sim the lifetime of the quantum fluctuation from 0 to n ; it suppresses short-lived fluctuations whose energy differs by a large amount from the unperturbed state. The LCPT “energy” is the operator generating translations in light cone time x^+ , i.e. k^- . The energy denominator corresponds to the propagator of covariant theory, integrated over the k^- momentum using the pole. The matrix elements $\langle n | \hat{V} | 0 \rangle$ are vertices in Feynman rules: the interaction terms in field theory are operators that change the number of particles.

Now let us briefly review what goes into the calculation of the virtual photon to quark-antiquark wavefunction. For this we need to evaluate the energy denominator and the matrix element in Eq. (4.75). This can be represented by the following diagram:



The matrix element in the general perturbation theory formula (4.75) is (now the state “ $|0\rangle$ ” is the leading order state: the virtual photon)

$$\langle q(\bar{p}), \bar{q}(\bar{p}') | \left[\int d^3\bar{x} e^{i\bar{p}\bar{x}} \bar{\psi} \hat{A} \psi \right] | \gamma(\bar{q}, \lambda) \rangle \quad (4.76)$$

At this order we just need the first, “normal interaction,” term from the Hamiltonian (4.72). The incoming and outgoing states are obtained by acting on the vacuum with creation operators:

$$|\gamma(\bar{q}, \lambda)\rangle = a_\lambda^\dagger(\bar{q}) |0\rangle \quad (4.77)$$

$$\langle q(\bar{p}, s), \bar{q}(\bar{p}', s') | = d_{s'}^\dagger(\bar{p}') b_s^\dagger(\bar{p}) |0\rangle \quad (4.78)$$

Now all we need is the field operators in terms of the creation and annihilation operators, Eqs. (4.57) and (4.69), and the commutators of these operators. When the creation/annihilation operators act on the in/outgoing state, they just give momentum delta functions setting the momenta in the integrals (4.57) and (4.69) to be the same as the incoming/outgoing particle momenta. What is left over is the photon polarization vector in (4.69) and the spinors in (4.57). The integral over space in the interaction matrix element (4.76) gives an overall momentum conservation delta function. We are left with

$$\langle q(\vec{p}), \bar{q}(\vec{p}') | \hat{P}_{\text{int}}^- | \gamma(\vec{q}, \lambda) \rangle = (2\pi)^3 \delta^{(3)}(\vec{q} - \vec{p} - \vec{p}') e e_f \bar{u}_s(p) \not{\epsilon}_\lambda v_{s'}(p') \quad (4.79)$$

$$s, s' = \pm \frac{1}{2}; \quad \lambda = 0 = L, \quad \lambda = \pm 1 = T \quad (4.80)$$

Here e is the electromagnetic coupling constant and e_f the fractional charge of the quarks, $e_d = -1/3$ for down and $e_u = 2/3$ for up quarks. The spinor matrix element $\bar{u}_s(p) \not{\epsilon}_\lambda v_{s'}(p')$ can be evaluated explicitly. For this we need in principle the explicit expressions for the spinors and the transversely polarized virtual photon polarization vector in the LC gauge is given by

$$\epsilon_{\lambda=\pm}^\mu(q) = (0, \frac{\mathbf{q} \cdot \epsilon_\lambda}{q^+}, \epsilon_\lambda) = (0, 0, \epsilon_\lambda), \quad (4.81)$$

where the circularly polarized transverse polarization vectors can be taken as

$$\epsilon_\pm = \frac{1}{\sqrt{2}} \begin{pmatrix} \mp 1 \\ -i \end{pmatrix} \quad (4.82)$$

In practice one does not need to do these by hand, the needed elements can be found e.g. in [63]). Explicitly evaluating the matrix elements between the Dirac spinors (these are independent of the representation of the γ -matrices,

$$\bar{u}_s(p) \not{\epsilon}_{\lambda=\pm 1} v_{s'}(p') = \delta_{s,-s'} \frac{2}{\sqrt{z(1-z)}} (z \delta_{\lambda,2s} - (1-z) \delta_{\lambda,-2s}) \epsilon_\lambda \cdot \mathbf{m} + \delta_{s,s'} \delta_{\lambda,2s} \frac{\sqrt{2}m}{\sqrt{z(1-z)}}. \quad (4.83)$$

Here we clearly have the separated quark helicity conserving vertex which is independent of the mass, and the helicity-flip matrix element that is proportional to the mass.

A longitudinally polarized virtual photon is strictly speaking not a part of the Fock space of the theory. In stead it is part of an additional “instantaneous” vertex that arises from explicitly solving non-dynamical constraints in light cone quantization. However, for the purposes of this calculation we can in practice define a longitudinal polarization vector for a virtual photon in the $\epsilon^+ = 0$ light cone gauge

$$\epsilon_{\lambda=0}^\mu(q) = (0, \frac{\sqrt{Q^2 - \mathbf{q}^2}}{q^+}, \frac{\mathbf{q}}{\sqrt{Q^2 - \mathbf{q}^2}}) \stackrel{\mathbf{q}=0}{=} (0, \frac{Q}{q^+}, 0), \quad (4.84)$$

where we chose $\mathbf{q} = 0$. Using this we get

$$\bar{u}_s(p) \not{\epsilon}_{\lambda=0} v_{s'}(p') = -2Q \sqrt{z(1-z)} \delta_{s,-s'} \quad (4.85)$$

The other ingredient needed is the energy denominator: the difference between the (on-shell!) energies of the incoming and the outgoing states $(q^- - p^- - p'^-)^{-1}$. It can be simplified as

$$q^- - p^- - p'^- = - \left(\frac{Q^2}{2q^+} + \frac{\mathbf{p}^2 + m^2}{2zq^+} + \frac{(\mathbf{p} - \mathbf{q})^2 + m^2}{2(1-z)q^+} \right) = \frac{\overbrace{Q^2 z(1-z) + m^2}^{\equiv \epsilon^2} + m^2}{-2q^+ z(1-z)}. \quad (4.86)$$

Note how the momentum conservation delta function in (4.79) nicely combines with the $2q^+$ from the energy denominator into a Lorentz-invariant combination $2q^+ (2\pi)^3 \delta^{(3)}(\vec{q} - \dots)$.

Note that neither the energy denominator nor the vertex do not depend on $\mathbf{p}, \mathbf{p}', \mathbf{q} = \mathbf{p} + \mathbf{p}'$ separately, but only through the combination $\mathbf{m} \equiv \mathbf{p} - z\mathbf{q}$. From now on we will take $\mathbf{q} = 0$ so that $\mathbf{m} = \mathbf{p}$. This is a general and crucial fact that significantly helps simplify the calculations. This momentum should be understood as the appropriate relative transverse momentum between the quark and the antiquark. It has an

interpretation in terms of the 2 + 1-dimensional Galileian invariance of the theory, which we will not go into here. So now we have our final result:

$$\psi^{\gamma^* \rightarrow q\bar{q}}(\mathbf{p}, \mathbf{p}'_{\perp}, z) = -2q^+(2\pi)^3 \delta^{(3)}(\bar{q} - \dots) \frac{z(1-z) e e_f \bar{u}_s(p) \not{\epsilon}_{\lambda} v_{s'}(p')}{\varepsilon^2 + \mathbf{m}^2}. \quad (4.87)$$

The eikonal scattering with the target happens such that the transverse *coordinates* of the quark and antiquark stay constant. Thus we need the Fourier transforms of the wave functions from transverse momenta to transverse coordinates. The transformed wavefunction is called the *mixed space* wavefunction: it is in transverse coordinate and longitudinal momentum space.

Mixed space wave function

$$\psi^{\gamma^* \rightarrow q\bar{q}}(\mathbf{x}, \mathbf{y}, z) = \int \frac{d^2 \mathbf{p}}{(2\pi)^2} \int \frac{d^2 \mathbf{p}'_{\perp}}{(2\pi)^2} \psi^{\gamma^* \rightarrow q\bar{q}}(\mathbf{p}, \mathbf{p}'_{\perp}, z) e^{i\mathbf{p} \cdot \mathbf{x}} e^{i\mathbf{p}'_{\perp} \cdot \mathbf{y}} \quad (4.88)$$

Note that due to the transverse momentum conserving delta function in the full momentum space wavefunction (4.87), one of the two momentum integrals in the wave function is trivial. The Fourier-transforms of polynomials in \mathbf{p} divided by the energy denominator (4.86) are modified Bessel functions (exercise).

We then leave out the overall longitudinal momentum conservation $2q^+(2\pi)\delta(q^+ - \dots)$ (see discussion in Sec. 3.3) to form what is called the “reduced wave function”. By then squaring, and summing over spins and colors we can write (see e.g. Sec. III of [34])

$$\left| \psi_T^{\gamma^* \rightarrow q\bar{q}} \right|^2 = \frac{\alpha_{\text{e.m.}}}{4\pi^2} N_c e_f^2 2 \left([z^2 + (1-z)^2] K_1^2(\varepsilon r) + m_f^2 K_0^2(\varepsilon r) \right) \quad (4.89)$$

$$\left| \psi_L^{\gamma^* \rightarrow q\bar{q}} \right|^2 = \frac{\alpha_{\text{e.m.}}}{4\pi^2} 2 N_c e_f^2 4 Q^2 z^2 (1-z)^2 K_0^2(\varepsilon r), \quad (4.90)$$

$$\varepsilon^2 = Q^2 z(1-z) + m^2 \quad (4.91)$$

Here $r = |\mathbf{x} - \mathbf{y}|$. These are now squares of the wave functions needed to calculate the dipole picture DIS cross section in Eq. (4.43).

Unfortunately there are a couple of different conventions for different factors. The overall $2q^+$ can be in different places, but it is easier to spot because it must vanish from the final result (the cross section is boost invariant but q^+ is not, so it must vanish). More tricky are factors of 4π . The result here requires an integration over the final phase space (see Eq. (3.74))

$$\int \frac{dp^+}{4\pi p^+} \frac{dp'^+}{4\pi p'^+} 2q^+(2\pi)\delta(2q^+ - p^+ - p'^+) = \int_0^1 \frac{dz}{4\pi} \frac{1}{z(1-z)}, \quad (4.92)$$

where we absorb the 4π into $\alpha_{\text{e.m.}} = e^2/(4\pi)$. This comes with a $1/(2\pi)^2$ coming together with the Bessel function squared, and an N_c from the sum over colors. For the longitudinal case there is a 2 for the sum over spins with $(2Q)^2 z(1-z)$ from the vertex (4.85) squared and $(z(1-z))^2$ originating from the energy denominator squared. For the transverse case the $1/(z(1-z))$ from the vertex squared cancels a part of the $(z(1-z))^2$ from the energy denominator squared, and the phase space (4.92) cancels the rest. There is a 2^2 from the prefactor of the vertex (4.83), together with a $1/2$ because we are averaging over polarizations (see Sec. 4.1), and the rest of the vertex (4.83) summed over polarizations gives $z^2 + (1-z)^2$.

To summarize, we have understood the DIS process as a virtual photon γ^* scattering on target at rest. In the high energy limit this process factorizes into two parts:

- γ^* fluctuates into $q\bar{q}$: this is a well understood QED process
- The $q\bar{q}$ scatters off the color field of the target: this is the part that tells us about the color field of the target.

Some side remarks about this process:

- The modified Bessel function K_n decreases exponentially in its argument. This means that the typical dipole transverse size contributing to the scattering process is $r \sim 1/Q$. This gives a concrete meaning

to our earlier statement that Q should be thought of as a transverse momentum or resolution scale in the scattering.

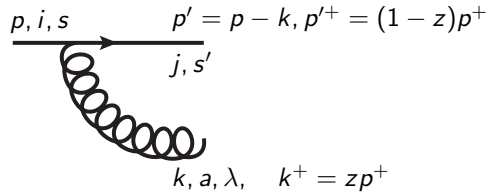
- We used, in Eq. (4.43), the optical theorem expressing the total cross section as $2\mathcal{N}$, where \mathcal{N} is, in our notation, the imaginary part of the scattering amplitude. But the quantity that we really are using to describe the target is the elastic scattering amplitude. Thus we get a direct connection between inclusive scattering (total cross section) and exclusive scattering, where the target indeed stays intact. In DIS the exclusive scattering process is referred to as Diffractive DIS, and it can be independently measured. In the parton picture inclusive and exclusive DIS are different processes described by independent, separate parton distributions. But in the dipole picture one calculates the cross sections for both from the same scattering amplitude, i.e. Wilson line correlator. This enables one to make nontrivial predictions for DIS cross sections that are not possible in the parton model.
- Another way to state the content of the eikonal approximation is that we are assuming that fixed-size dipoles are the basis of states that diagonalizes the imaginary part of the T -matrix. In general, the fact that in the high energy/eikonal approximation particles fly through target at fixed \mathbf{x} does not imply zero momentum transfer! Rather it should be understood that even if they do get a momentum transfer, their energy is so high (and/or the longitudinal extent of the target so short, these statements are Lorentz-transforms of each other) that the transverse momentum transfer is not enough to modify the transverse position of the particle during the time that it spends inside the target.

4.3 BK equation

4.3.1 Soft gluon radiation

As discussed above, the dipole picture of DIS represents just the leading order in a QCD perturbation theory expansion. The next correction comes in, when one adds a gluon, either to make a loop correction, or to interact with the target. We shall here consider the kinematical limit of these processes where the gluon is very soft because, as we will see, it contributes to the cross section as a large logarithm of the energy or x . When we want to study what happens at very small x , we have to resum these logarithms of $\alpha_s \ln 1/x$. This resummation is performed using the Balitsky-Kovchegov (BK) equation. Our purpose here is to derive this equation. In order to do this it is enough to consider the radiative correction, where the dipole emits a gluon, and this gluon then interacts with the target nucleus. The loop corrections can, in the soft gluon limit but not generally, be deduced indirectly from a unitarity argument.

NLO: radiate soft gluon $z \ll 1$



Light cone wavefunction

$$\psi^{q \rightarrow qg}(z, \mathbf{k}) = \frac{1}{\frac{\mathbf{p}^2}{2p^+} - \frac{\mathbf{k}^2}{2k^+} - \frac{\mathbf{p}'^2}{2p'^+}} \bar{u}_{s'}(p') (-g) t_{ji}^a \not{\epsilon}^*(k) u_s(p) \quad (4.93)$$

Similarly as for the $\gamma^* \rightarrow q\bar{q}$ wavefunction in Sec. 4.1, we need the matrix element, which can be calculated in any representation of the γ -matrices. The full matrix element (now for massless quarks for simplicity) is

$$\bar{u}_{s'}(p') (-g) t_{ji}^a \not{\epsilon}^*(k) u_s(p) = \frac{-2gt_{ji}^a}{z\sqrt{1-z}} (\delta_{\lambda, 2s} + (1-z)\delta_{\lambda, -2s}) \mathbf{q} \cdot \boldsymbol{\epsilon}_\lambda^*, \quad \mathbf{q} = \mathbf{k} - z\mathbf{p} \quad (4.94)$$

We will here be interested only in the high energy limit where the quark longitudinal momentum p^+ is large, so that there is a lot of phase space for emission of gluons with a much smaller k^+ . We will therefore assume that the emitted gluon is soft, and take $z \rightarrow 0$. In this limit the emitted gluon light cone energy k^- is large and dominates the energy denominator in (4.93). Also the emission vertex simplifies, in particular we see that it becomes the same for both of the gluon polarization states $\lambda = \pm 2s$. This is very general feature at

high energy limit and related to what we have already discussed in the context of the eikonal approximation: the interaction of the gauge soft gauge field with the hard particles cares only about one vector: that of the hard particle, and not e.g. the spin states of the quark or gluon. In the soft limit also the relative momentum $\mathbf{q} = \mathbf{k} - z\mathbf{p} \rightarrow \mathbf{k}$

In *soft* limit $z \rightarrow 0$:

$$\psi^{q \rightarrow qg}(k^+, \mathbf{k}) \approx \frac{-2zp^+}{\mathbf{k}^2} \frac{-2gt_{ji}^a}{z} \mathbf{k} \cdot \boldsymbol{\varepsilon}_\lambda^* = \frac{4gt_{ji}^a p^+}{\mathbf{k}^2} \mathbf{k} \cdot \boldsymbol{\varepsilon}_\lambda^* \quad (4.95)$$

From this one can calculate (somewhat sketchily) a “probability to emit a gluon” by squaring the wave-function and integrating over a Lorentz-invariant phase space for gluon emission, which exhibits the typical gauge theory logarithmic divergences for both soft $z \rightarrow 0$ and collinear $\mathbf{k} \rightarrow \mathbf{0}$ gluon emission.

$$dP_{q \rightarrow qg} = |\psi^{q \rightarrow qg}(k^+, \mathbf{k})|^2 \frac{d^4k}{2k^+ (2\pi)^3} \sim \frac{dz}{z} \frac{d^2\mathbf{k}}{\mathbf{k}^2} \left(\sum_{\lambda=\pm 1} \varepsilon_i \varepsilon_j^* = \delta_{ij} \right) \quad (4.96)$$

soft $\frac{dz}{z}$

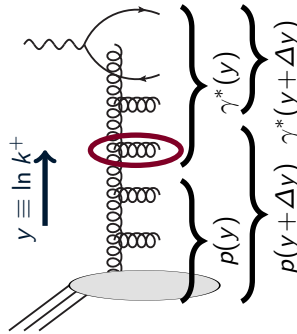
collinear $\frac{d^2\mathbf{k}}{\mathbf{k}^2}$

Out of these divergences the collinear one, corresponding to the emission of very large (transverse) wavelength gluons will cancel when we consider the emission from a color neutral dipole, because the emissions from the quark and the gluon must destructively interfere in this limit. (In fact, in the calculation we are going to do, the collinear divergence is an artefact of taking $z \rightarrow 0$ and is not actually there at finite z . Nevertheless there is a cancellation between the emission from the quark and the antiquark, and in some sense the physics becomes more transparent if we take $z \rightarrow 0$ here and let this spurious divergence appear, to be then canceled later...)

The soft divergence, on the other hand, does not cancel. In stead it is something that we must absorb into a redefinition of what exactly we mean by the target. To visualize this it is conventional to draw diagrams where the vertical axis corresponds to rapidity. At the top is the probe photon with a large q^+ and at the bottom the target, with the smallest p^+ , i.e. the largest p^- , with the small momentum fraction $x \sim p^+/q^+$. The large logarithmic contributions come from integrating over the longitudinal momentum of the emitted gluons over the whole rapidity interval. Since the phase space integral is logarithmic, each gluon contributes a factor $\sim \alpha_s \ln 1/x$, which we are assuming to be of order one. Therefore we must resum the emission of arbitrary numbers of these gluons.

4.3.2 Idea of a renormalization group equation

This resummation is done by using a renormalization group equation, in this case the BK equation. To start with, we have to introduce some separation scale in rapidity $y \sim \ln k^+$. Now whatever is at a higher k^+ will be called a part of the probe photon, and all that is at a lower p^+ we decide to call a part of the target. The separation scale now appears as a cutoff in the integral over the longitudinal momentum fraction z . Now the smart thing to do is to choose in the end the separation scale so close to the rapidity of the probe q^+ that the integral $\sim \alpha_s \int_{z_{\text{cutoff}}} dz/z$ is small. Then we do not have a large logarithm left, but this comes at the expense of our parametrization of target depending on this cutoff. The advantage is that now we can calculate how exactly the target depends on this cutoff: this dependence is precisely the RGE equation that tells us how the cross section depends on the energy.



If we now look at an individual gluon (at y) the cross section has to be the same whether this gluon is a part of the probe γ^* Fock state, or a part of the target p . The equality of the cross section gives us an equation, which is the BK evolution equation.

$$\begin{aligned} \sigma^{\gamma^* p} &= \overbrace{\left| \psi^{\gamma^* \rightarrow q\bar{q}} \right|_y^2 \otimes 2\mathcal{N}_y^{q\bar{q}p} + \left| \psi^{\gamma^* \rightarrow q\bar{q}g} \right|_y^2 \otimes 2\mathcal{N}_y^{q\bar{q}gp} + \dots}^{\text{gluons up to } y \text{ part of proton}} \\ &= \underbrace{\left| \psi^{\gamma^* \rightarrow q\bar{q}} \right|_{y+\Delta y}^2 \otimes 2\mathcal{N}_{y+\Delta y}^{q\bar{q}p} + \left| \psi^{\gamma^* \rightarrow q\bar{q}g} \right|_{y+\Delta y}^2 \otimes 2\mathcal{N}_{y+\Delta y}^{q\bar{q}gp} + \dots}_{\text{gluons up to } y+\Delta y \text{ part of proton}} \end{aligned} \quad (4.97)$$

4.3.3 The Balitsky-Kovchegov equation: a short derivation

Let us now put this idea into practice. To derive the BK equation one needs to

- Calculate $\psi^{\gamma^* \rightarrow q\bar{q}g}(z)$
- Take soft gluon limit $z \rightarrow 0$;
- Reabsorb the gluon to become a part of the target
- Get evolution equation for $q\bar{q}$ cross section

The full $\psi^{\gamma^* \rightarrow q\bar{q}g}(z)$ wavefunction is a rather complicated object (see e.g. [34]), because we need to go to second order in perturbation theory. Somewhat schematically, it will be

$$\psi^{\gamma^* \rightarrow q\bar{q}g} = \frac{\langle q\bar{q}g | \hat{P}_{\text{int}}^- | q\bar{q} \rangle}{k^-(\gamma^*) - k^-(q\bar{q}g)} \frac{\langle q\bar{q} | \hat{P}_{\text{int}}^- | \gamma \rangle}{k^-(\gamma^*) - k^-(q\bar{q})}. \quad (4.98)$$

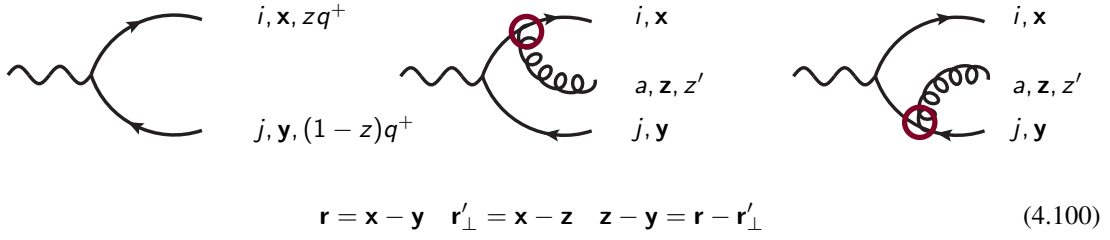
The complicated thing is that the energy denominators are always calculated with respect to the incoming γ^* state. Thus the wavefunction does not actually factorize into a product of a $\gamma^* \rightarrow q\bar{q}$ and a $q/\bar{q} \rightarrow q/\bar{q} + g$ wavefunction. However, we do not need to deal with all this complication here, due to two things.

- In a somewhat miraculous manner, when one Fourier-transforms to transverse coordinate space, the $\gamma^* \rightarrow q\bar{q}g$ LCWF *does* in fact factorize into a somewhat modified $\gamma^* \rightarrow q\bar{q}$ wavefunction (that knows about the gluon emission), and a completely unmodified $q/\bar{q} \rightarrow q/\bar{q} + g$ wavefunction. I have yet to find a clear interpretation for why this is the case. Somehow, in momentum space information propagates forward: later splittings know about the earlier ones because the energy denominators are always calculated with respect to the original incoming state. In transverse coordinate space this information propagates backwards: the last splitting (the gluon emission) does not know about the history (the $\gamma^* \rightarrow q\bar{q}$ splitting), but the earlier splittings know about the future (the part of the wavefunction related to the $\gamma^* \rightarrow q\bar{q}$ splitting knows that a gluon will be emitted later).
- The soft gluon limit $z \rightarrow 0$ makes things even simpler. As we discussed (see Eq. (4.95)) in this limit the energy denominator is completely dominated by the energy of the gluon $k^-(\gamma^*) - k^-(q\bar{q}g) \approx -k^-(g)$ and therefore does not care about what the gluon was emitted from. In this limit the wavefunction factorizes in both momentum and coordinate space.

Let us now move on with the calculation in coordinate space. We need to Fourier-transform the gluon emission wave function, which becomes:

$$\psi^{q \rightarrow qg}(k^+, \mathbf{r}) = \int \frac{d^2 \mathbf{k}}{(2\pi)^2} e^{i\mathbf{k} \cdot \mathbf{r}} \psi^{q \rightarrow qg}(k^+, \mathbf{k}) = -i2p^+ \frac{2gt_{ji}^a}{2\pi} \frac{\boldsymbol{\varepsilon} \cdot \mathbf{r}}{\mathbf{r}^2} \delta_{s,s'} \quad (4.99)$$

Now we need to coherently sum the emissions from the quark and the antiquark, where for the latter there is a relative minus sign in the emission vertex.



$$\mathbf{r} = \mathbf{x} - \mathbf{y} \quad \mathbf{r}'_\perp = \mathbf{x} - \mathbf{z} \quad \mathbf{z} - \mathbf{y} = \mathbf{r} - \mathbf{r}'_\perp \quad (4.100)$$

We are being sloppy with the exact factors from the phase space. However, up to overall constants we can now write the Fock state wavefunction of the virtual photon as

$$\begin{aligned} |\gamma^*\rangle_{\text{int}} = & |\gamma^*\rangle + \int_{z, \mathbf{x}, \mathbf{y}} C(\mathbf{r} = \mathbf{x} - \mathbf{y}) \psi^{\gamma^* \rightarrow q\bar{q}}(z, \mathbf{r}) |q_i(\mathbf{x}, z) \bar{q}_i(\mathbf{y}, 1-z)\rangle \\ & + \int_{z, \mathbf{x}, \mathbf{y}, \mathbf{z}} \psi^{\gamma^* \rightarrow q\bar{q}}(z, \mathbf{r}) \int \frac{dz'}{4\pi z'} \frac{-i2g}{2\pi} t_{ji}^a \left[\frac{(\mathbf{x} - \mathbf{z}) \cdot \boldsymbol{\varepsilon}}{(\mathbf{x} - \mathbf{z})^2} - \frac{(\mathbf{y} - \mathbf{z}) \cdot \boldsymbol{\varepsilon}}{(\mathbf{y} - \mathbf{z})^2} \right] \\ & \times |q_i(\mathbf{x}, z) \bar{q}_j(\mathbf{y}, 1-z) g_a(\mathbf{z}, z')\rangle, \quad (4.101) \end{aligned}$$

Here we have, as discussed above, taken the $\gamma^* \rightarrow a\bar{q}g$ wavefunction to be just a product of photon splitting and gluon emission wavefunctions, which is only true because we are taking the gluon longitudinal momentum z' to be small.

To be a bit more precise let us also write the exact expressions for the longitudinal phase space integrals here. These require a bit of care to be done correctly. The Lorentz-invariant phase space element for the integrations is

$$\frac{dk^+}{4\pi k^+}, \quad (4.102)$$

but the factor $2k^+$ is not there in the momentum conservation delta function: each vertex yields a

$$2\pi\delta\left(\sum p^+\right). \quad (4.103)$$

For the quark-antiquark dipole the phase exact expression for the phase space integral is

$$“\int_z” \equiv \int \frac{dp^+}{4\pi p^+} \frac{dp'^+}{4\pi p'^+} (2\pi)\delta(p^+ + p'^+ - q^+) = \frac{1}{2q^+} \int \frac{dz}{4\pi z(1-z)}. \quad (4.104)$$

For the quark-antiquark-gluon state we have in (4.101) already assumed that the gluon is soft $k^+ = z'q^+ \ll p^+, p'^+, q^+$. This has enabled us to factor out the kinematics of the leading order vertex; this is possible only in the soft limit. For the full kinematics the whole expressions are a bit more complicated [34]. For the term where the gluon is emitted from the quark, the phase space integral (denoting p'' the momentum of the quark before emitting the gluon) is

$$\begin{aligned} “\int_{z, z'}” & \equiv \int \frac{dp^+}{4\pi p^+} \frac{dp'^+}{4\pi p'^+} \frac{dp''^+}{4\pi p''^+} \frac{dk^+}{4\pi k^+} (2\pi)\delta(p''^+ + p'^+ - q^+) (2\pi)\delta(p^+ + k^+ - p''^+) \\ & = \frac{1}{(q^+)^2} \int \frac{dz}{4\pi} \frac{dz'}{4\pi} \frac{1}{z} \frac{1}{1-z-z'} \frac{1}{z+z'} \frac{1}{z'} \approx \frac{1}{q^+} \int \frac{dz}{8\pi z(1-z)} \frac{1}{zq^+} \int \frac{dz'}{8\pi z'}. \\ & = “\int_z” \times \frac{1}{2p^+} \int \frac{dz'}{4\pi z'}, \quad (4.105) \end{aligned}$$

where we separated out an explicit $1/2p^+$ to recover the normal Lorentz-invariant phase space $dz'/(4\pi z')$. Likewise, when the gluon is emitted from the antiquark we get, using this time p'' for the momentum of the

antiquark before the emission

$$\begin{aligned}
\text{“} \int_{z,z'} \text{”} &\equiv \int \frac{dp^+}{4\pi p^+} \frac{dp'^+}{4\pi p'^+} \frac{dp''^+}{4\pi p''^+} \frac{dk^+}{4\pi k^+} (2\pi)\delta(p^+ + p''^+ - q^+) (2\pi)\delta(p'^+ + k^+ - p''^+) \\
&= \frac{1}{(q^+)^2} \int \frac{dz}{4\pi} \frac{dz'}{4\pi} \frac{1}{z} \frac{1}{1-z-z'} \frac{1}{1-z} \frac{1}{z'} \approx \frac{1}{q^+} \int \frac{dz}{8\pi z(1-z)} \frac{1}{(1-z)q^+} \int \frac{dz'}{8\pi z'}. \\
&= \text{“} \int_z \text{”} \times \frac{1}{2p'^+} \int \frac{dz'}{4\pi z'}, \quad (4.106)
\end{aligned}$$

Here the explicit factors $\frac{1}{2p^+}$, $\frac{1}{2p'^+}$ in Eqs. (4.106) and (4.105) cancel against the $2p^+$ in Eq. (4.99) and the corresponding $2p'^+$ in the emission wavefunction from the antiquark, and therefore do not appear in Eq. (4.101).

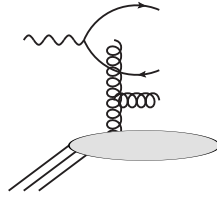
It is important to note that the $\int_{z'}$ -integral is divergent because of the phase space $\int_{z'} \sim \int dz'/z'$. We have also added a coefficient $C(\mathbf{r})$ in front of the leading order term, because the normalization of this term needs to be adjusted in order to keep the wavefunction normalized. We can determine this coefficient from the requirement that the normalization of the wave function with the extra gluon, i.e. square of the dipole term with the normalization constant plus the square of the $q\bar{q}g$ term, are the same as the square of the dipole term at lowest order. Note that here squaring involves also one sum over the colors of the quarks, which yields a factor N_c for the dipoles. We get the condition

$$N_c |C(\mathbf{r})|^2 = N_c - \frac{(2g)^2}{(2\pi)^2} \frac{1}{4\pi} t_{ij}^a t_{ji}^a \int \frac{dz'}{z'} \int d^2\mathbf{r}'_{\perp} \sum_{\lambda=\pm 1} \left| \frac{(\mathbf{x}-\mathbf{z}) \cdot \boldsymbol{\varepsilon}_{\lambda}}{(\mathbf{x}-\mathbf{z})^2} - \frac{(\mathbf{y}-\mathbf{z}) \cdot \boldsymbol{\varepsilon}_{\lambda}}{(\mathbf{y}-\mathbf{z})^2} \right|^2 \quad (4.107)$$

$$= N_c - \frac{\alpha_s}{\pi^2} \frac{N_c^2 - 1}{2} \Delta y \int d^2\mathbf{r}'_{\perp} \frac{\mathbf{r}^2}{\mathbf{r}'_{\perp}{}^2 (\mathbf{r} - \mathbf{r}'_{\perp})^2} \sum_{\lambda=\pm 1} \varepsilon_i^{(\lambda)} \varepsilon_j^{(\lambda)*} = \delta_{ij} \quad (4.108)$$

Putting these together, and remembering that we now redefine our scattering amplitude so that the scattering off the dipole and the dipole-gluon system from the old target becomes the same as the scattering of just a dipole off a new, renormalized, target.

$$\mathcal{N}_{q\bar{q}}^{y+\Delta y} = \mathcal{N}_{q\bar{q}}^y + \frac{\alpha_s}{\pi^2} \frac{N_c^2 - 1}{2N_c} \int_y^{y+\Delta y} d \ln 1/z' \int d^2\mathbf{r}'_{\perp} \frac{\mathbf{r}^2}{\mathbf{r}'_{\perp}{}^2 (\mathbf{r} - \mathbf{r}'_{\perp})^2} \left[\mathcal{N}_{q\bar{q}g}^{\ln 1/z'} - \mathcal{N}_{q\bar{q}}^{\ln 1/z'} \right] \quad (4.109)$$

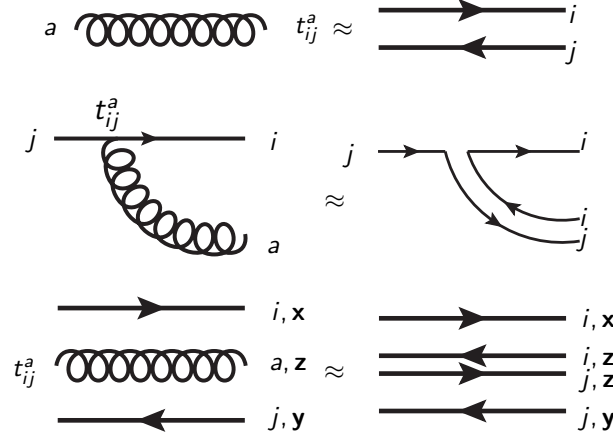


What this equation now tells us is that the dipole scattering on new target $\mathcal{N}_{q\bar{q}}^{y+\Delta y}$ consists of

- A dipole scattering off original target $\mathcal{N}_{q\bar{q}}^y$
- A contribution where the dipole emits a gluon into rapidity interval $[y, y + \Delta y]$, which scatters off the target and
- A correction to the normalization of original dipole (There are now less dipoles in γ^*)

Now we are almost there. We are looking for an evolution equation for the scattering amplitude $\mathcal{N}_{q\bar{q}}$: but encountered new quantity $\mathcal{N}_{q\bar{q}g}$, which needs to be related to $\mathcal{N}_{q\bar{q}}$. Let us do this in the large N_c approximation. At large N_c a gluon is approximately the same as a quark-antiquark pair (note: not a color neutral dipole, in fact a general quark-antiquark pair is $1/N_c^2$ parts dipole and $(N_c^2 - 1)/N_c^2$ parts octet, i.e. gluon, and at large N_c we can forget the color neutral dipole). So when we have a quantum state $|q(\mathbf{x})\bar{q}(\mathbf{y})g(\mathbf{z})\rangle$, we can approximate it by $|q(\mathbf{x})\bar{q}(\mathbf{z})q(\mathbf{z})\bar{q}(\mathbf{y})\rangle$

- $N_c \rightarrow \infty \implies g \approx q\bar{q}$ (not dipole!)
- $N_c^2 - 1$ gluon colors $\approx N_c^2$ $q\bar{q}$ colors.



Now, instead of $\mathcal{N}_{q\bar{q}g}$, we need $\mathcal{N}_{q\bar{q}q\bar{q}}$; the amplitude for the simultaneous scattering of two dipoles. We can obtain it with the following argument:

- \mathcal{N} is a really a *scattering probability*;
- $S = 1 - \mathcal{N}$ is a probability *not to scatter*

For two dipoles no scattering means that neither dipole scatters, from which we deduce

$$S_{q\bar{q}q\bar{q}} = S_{q\bar{q}}S_{q\bar{q}} \quad (4.110)$$

In order to justify this argument we need to make an additional *mean field* approximation, namely that the scattering probabilities of the two dipoles are independent of each other, which enables the factorized form (4.110). In fact this mean field approximation can be argued to hold in the large N_c limit, which we are already assuming here.

Thus the scattering probability for a two-gluon system is

$$\mathcal{N}_{q\bar{q}q\bar{q}} = 1 - S_{q\bar{q}q\bar{q}} = 1 - (1 - \mathcal{N}_{q\bar{q}})(1 - \mathcal{N}_{q\bar{q}}) \quad (4.111)$$

With this argument we end up with the approximation

$$S = 1 - \mathcal{N} \quad \& \quad S_{q\bar{q}q\bar{q}} = S_{q\bar{q}}S_{q\bar{q}} \quad (4.112)$$

$$\implies \mathcal{N}(q(\mathbf{x})\bar{q}(\mathbf{y})g(\mathbf{z})) \approx \mathcal{N}(q(\mathbf{x})\bar{q}(\mathbf{z})) + \mathcal{N}(q(\mathbf{z})\bar{q}(\mathbf{y})) - \mathcal{N}(q(\mathbf{x})\bar{q}(\mathbf{z}))\mathcal{N}(q(\mathbf{z})\bar{q}(\mathbf{y})). \quad (4.113)$$

The argument leading to this can also be stated in another way: in order to calculate the probability for a scattering to happen, one must add the probabilities that one of the two dipoles scatters, and then subtract the case that both dipoles scatter, since this would otherwise get counted twice. What we are really doing here is using the Mueller dipole formalism [64], where all of QCD at high energy is formulated in terms of dipoles that can split into other dipoles.

$$\begin{aligned} \mathcal{N}_{q\bar{q}}^{y+\Delta y} &= \mathcal{N}_{q\bar{q}}^y + \frac{\alpha_s}{\pi^2} \frac{N_c^2 - 1}{2N_c} \int_y^{y+\Delta y} d \ln 1/z' \int d^2 \mathbf{z} \frac{(\mathbf{x} - \mathbf{y})^2}{(\mathbf{x} - \mathbf{z})^2 (\mathbf{z} - \mathbf{y})^2} \\ &\quad \times \left[\mathcal{N}_{q\bar{q}}^{\ln 1/z'}(\mathbf{x}, \mathbf{z}) + \mathcal{N}_{q\bar{q}}^{\ln 1/z'}(\mathbf{z}, \mathbf{y}) - \mathcal{N}_{q\bar{q}}^{\ln 1/z'}(\mathbf{x}, \mathbf{z})\mathcal{N}_{q\bar{q}}^{\ln 1/z'}(\mathbf{z}, \mathbf{y}) - \mathcal{N}_{q\bar{q}}^{\ln 1/z'}(\mathbf{x}, \mathbf{y}) \right] \end{aligned} \quad (4.114)$$

Differentially in Δy

$$\partial_y \mathcal{N}(\mathbf{r}) = \frac{\alpha_s N_c}{2\pi^2} \int d^2 \mathbf{r}'_{\perp} \frac{\mathbf{r}^2}{\mathbf{r}'_{\perp}{}^2 (\mathbf{r}'_{\perp} - \mathbf{r})^2} [\mathcal{N}(\mathbf{r}'_{\perp}) + \mathcal{N}(\mathbf{r} - \mathbf{r}'_{\perp}) - \mathcal{N}(\mathbf{r}'_{\perp})\mathcal{N}(\mathbf{r} - \mathbf{r}'_{\perp}) - \mathcal{N}(\mathbf{r})] \quad (4.115)$$

This is the BK equation (1995) [41, 43, 42]. I personally like to call this the holy grail of small x physics. It is the basic tool for a lot of practical phenomenology.

- Given initial condition $\mathcal{N}(\mathbf{r})$ at $y = y_0$ the equation predicts the scattering amplitude at larger $y =$ smaller $x =$ higher \sqrt{s} .
- If one drops the nonlinear term one gets the BFKL (Balitsky-Fadin-Kuraev-Lipatov) equation (in the form (2.176), see e.g. [65]), which was derived by summing normal Feynman diagrams for the scattering, already a longer time ago.
- The divergences of the kernel at $\mathbf{r}'_{\perp} \rightarrow 0$ and $\mathbf{r}'_{\perp} \rightarrow \mathbf{r}$ are regulated because $\mathcal{N}(0) = 0$. This feature is referred to as “color transparency”: a dipole is a color neutral object as a whole, and if its size is zero it should not scatter at all.
- The equation enforces the black disk limit (unitarity) $\mathcal{N} < 1$
- For practical work the coupling α_s should not be fixed, but depend on a distance scale, which can be some combination of $\mathbf{r}, \mathbf{r}'_{\perp}, \mathbf{r} - \mathbf{r}'_{\perp}$. What, in the end, is both theoretically and practically the correct way to do this is still a matter of discussion in the field.

The equation can be solved numerically, let us look at a few features of the solution

- Small dipoles $r \lesssim 1/Q_s$ scatter very little, color transparency is satisfied.
- Large dipoles $r \gtrsim 1/Q_s$ scatter with probability almost one, but not more. This is *gluon saturation* in action, although in this calculation gluon saturation does not appear as some mystical complicated phenomenon, but just the obvious fact that the scattering can only happen with a probability of at most one.
- When going towards smaller x , the “front” of the solution moves towards the left. This means that the density of gluons in the target increases, justifying a posteriori our assumption that at smaller x the classical field picture of the target gets better and better.

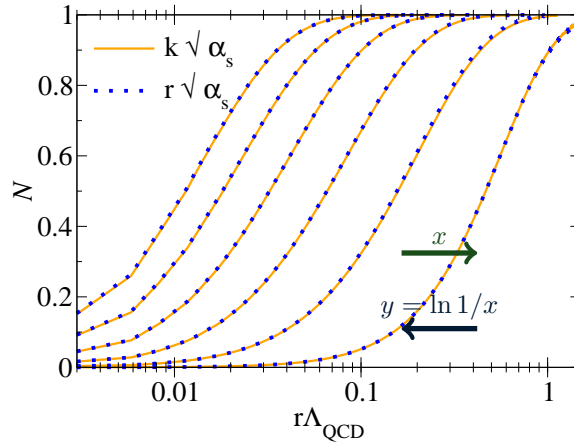


Figure 4.2: Solution of the BK equation from a numerical calculation. (Actually cheating, this particular plot from [66] is a solution of JIMWLK, which generalizes BK)

To set this in context remember that for the DIS cross sections F_2, F_L this solution of the BK equation has to be convoluted with the (known) γ^* wavefunction.

$$\sigma_{T,L}^{\gamma^* p} = \int d^2\mathbf{b} d^2\mathbf{r} dz \left| \psi^{\gamma^* \rightarrow q\bar{q}}(r, z)_{T,L} \right|^2 2\mathcal{N}(\mathbf{r}, \mathbf{b}, x) \quad (4.116)$$

Fits HERA data ($x < 0.01$ Q^2 moderate) with this formula work extremely well, although this depends on a specific way to model the b -dependence of the dipole amplitude.

The JIMWLK equation is a generalization of the BK equation, in the sense of giving up the mean field approximation that we had to use. In fact, even without this approximation and at finite N_c it turns out,

after some color algebra magic, that the dipole amplitude satisfies an equation that has the form (4.115). However, the amplitudes \mathcal{N} are replaced by expectation values of the amplitudes in some distribution. In general, the expectation value of the product of amplitudes $\langle \mathcal{N}\mathcal{N} \rangle$ cannot be expressed in terms of the expectation value of the amplitude $\langle \mathcal{N} \rangle$. Thus the resulting equation does not close. One can then derive an additional evolution equation for the x -dependence of $\langle \mathcal{N}\mathcal{N} \rangle$, but this will involve a new quantity $\langle \mathcal{N}\mathcal{N}\mathcal{N} \rangle$, and so on ad infinitum. This set of evolution equations is known as the *Balitsky hierarchy*. It is equivalent to the JIMWLK equation, which is written as an evolution equation for the probability distribution of the Wilson lines from which the amplitudes are constructed. Knowing the probability distribution is equivalent to knowing all possible expectation values.

Chapter 5

Heavy ion collisions

5.1 Gluon saturation & CGC

5.1.1 Spacetime structure in 2 gauges

Let us now reflect the z -axis and consider a nucleus (in stead of the probe) moving in the $+$ -direction, just to confuse the reader. . . This means that the color field of the nucleus has a large A^+ component.

Until now we have been describing the high energy nucleus as a classical field with one Lorentz-component (which was A^- and is now A^+), which we then developed into a path-ordered exponential or Wilson line, which is the eikonal scattering amplitude for a high energy probe passing through the nucleus. What does this picture imply in terms of the partonic content of the nucleus, i.e. the gluon distribution? For this we need some kind of a microscopical picture of where the classical field comes from. We know that it should represent small- x gluonic degrees of freedom. We also remember from our discussion of the eikonal vertex that a gluon carrying only a small longitudinal momentum fraction (a soft gluon) is essentially *classical* radiation, that only cares about color charge. This leads to the basic idea of the CGC: a classical field approximation for small x gluons, radiated by classical color charges representing the large- x degrees of freedom.

The basic idea of the CGC is that we separate the microscopic degrees of freedom inside a high energy nucleus into two things:

CGC separation of scales:

- small x : classical field
- large x : color charge

For a first simplistic picture one can think of the color charge as valence quarks, which then radiate gluons, represented by the classical field. A classical field radiated by a classical current follows the classical equation of motion. For Yang-Mills theory this is given by

$$[D_\mu, F^{\mu\nu}] = J^\nu \quad (5.1)$$

Note that here we are using a matrix notation, with

$$J^\mu = J_a^\mu t^a \quad F_{\mu\nu} = F_{\mu\nu}^a t^a \quad D_\mu = \partial_\mu + igA_\mu \quad (5.2)$$

so that the commutator of the generators

$$[t^a, t^b] = if^{abc}t^c \quad (5.3)$$

provides just a short way of writing

$$\partial_\mu F_a^{\mu\nu} - gf^{abc}A_\mu^b F_c^{\mu\nu} = J_a^\mu \quad (5.4)$$

Equation (5.1) involves some yet unspecified color current J^μ . The commutator in (5.1) refers to the fact that the gauge potential A_μ , field strength $F_{\mu\nu}$ and color current J^μ are matrices in color space. Incidentally,

note that since the field strength is a commutator of covariant derivatives, $F_{\mu\nu} = -i/g[D_\mu, D_\nu]$, one can show using the Jacobi identity that the color current must be *covariantly conserved*,

$$[D_\nu, J^\nu] = 0 \quad (5.5)$$

in stead of the usual abelian charge conservation $\partial_\mu J^\mu = 0$. This means that the conservation of color charge actually requires J^μ to rotate in color space.

For a nucleus moving in the $+z$ -direction, the classical current should be proportional to the momenta of the large- x degrees of freedom. We therefore expect that the most important (or, only nonzero) component of the current should be a J^+ -component.



Now we have to somehow implement the statement that the charge is supposed to correspond to large x and the fields to small x in a spacetime picture. The consequence of this is that we can treat the color current J^+ as a very thin sheet in x^- . Sometimes one quotes a somewhat naive justification for this approximation in terms of a Lorentz-contraction of the nucleus from its rest frame thickness $2R_A$ to $\Delta z \sim 2R_A m_A / \sqrt{s}$ by the boost from the rest frame energy m_A to the large energy \sqrt{s} . However, the more proper argument for this assumption is the combination of the uncertainty principle with the assumption about a scale separation. The current represents large x degrees of freedom, which for a fast nucleus have a large p^+ momentum. The classical field, on the other hand, corresponds to degrees of freedom with smaller p^+ . As a consequence of this the charges are better localized x^- than the field, so the field (which is what we are interested in) sees the charges as localized in x^- .

Charges are thin sheet in x^-

1. Naive explanation: Lorentz-contraction
2. Real explanation: Heisenberg $\Delta x^- \sim 1/p^+$, charges have large p^+

A similar argument must be made for the dependence of the current on the light cone time coordinate x^+ . A simplistic argument states that for a fast-moving nucleus time is Lorentz-dilated so that all the internal dynamics happens very slowly in x^+ . A more detailed statement of the same effect is that any probe of the small x (small p^+) degrees of freedom will have a larger $p^- \sim p_T^2/p^+$ than the light cone energies p^- of the color charges. Since the color charges have a small p^- , they evolve more slowly in x^+ than the fields, or an external probe of the system operating at the timescale of the small- x fields. Therefore from the point of view of the field, or of this external probe, the charges appear as slowly dependent of x^+ . The extreme limit of this argument is that we can consider the charge density to be independent of the light cone time x^+ , i.e. static.

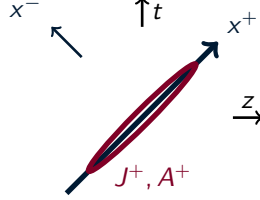
Digression: Glass

A system that is dimer dependent, but whose time dependence is unnaturally slow compared to the timescales that one is probing it with, is known as a glass in statistical physics. An actual glass is a "glass" in the statistical physics sense, because glasses are non-crystalline like liquids, but nevertheless do not flow. In a loose (and not technically correct) sense one can describe a glass as a liquid that flows so slowly that on the timescales of interest it behaves like a solid.

Taking these energy- and momentum scale arguments to the extreme now arrive at the desired form for the color current as a δ -function in x^- , independent of x^+ , which leaves us with a purely 2-dimensional transverse color charge density. The notation $\delta(x^-)$ should be thought of as a somewhat formal limit, we will still need to maintain the concept of path ordering (now in x^- because we switched the direction of motion of the nucleus): so we should still think of the nucleus as slightly elongated in x^- , but very thin compared to any other x^- -scale in the scattering problem.

Current *static*, independent of x^+ \Rightarrow *glass*

1. Time is dilated for the nucleus
2. Charges: small p^- : slow dependence on x^+



We can now easily find a solution to the equation of motion (5.1), in which there is only one component in the gauge field, A^+ , with

$$J^+(x^-, \mathbf{x}) \approx \delta(x^-) \rho(\mathbf{x}) \quad (5.6)$$

$$A^+(x^-, \mathbf{x}) \approx -\delta(x^-) \frac{1}{\nabla_{\perp}^2} \rho(\mathbf{x}) \quad (5.7)$$

$$F^{+i} = \partial_i A^+ \quad (5.8)$$

This looks very nice, the big $+$ -component of the field corresponds to a color current in the $+$ -direction. This is precisely what we would expect in the physical situation of a color charged object (which the nucleus is, if you only look at it locally within a region of size $\ll 1/\Lambda_{\text{QCD}}$ in the transverse plane) moving in the $+z$ -direction, and generating a field A^+ that a leftmoving high energy probe would like to couple to. It is easy to see that the current is covariantly conserved, because it is independent of x^+ , and simultaneously $A^- = 0$.

Note that the only nonzero component of the field strength tensor $F^{\mu\nu}$ is F^{+i} , which corresponds to F^{0i} and F^{zi} , i.e. chromoelectric and - magnetic fields perpendicular to the z -axis. This is the same as the Weizsäcker-Williams field of an electric charge boosted to the speed of light, which can be thought of as an “equivalent photon” cloud accompanying the photon.

The physical picture of “gluons as partons” requires two things

- Infinite momentum frame: we have to boost to a frame where the nucleus is moving fast, so that the partons are collinear (at least approximately) to the nucleus.
- Light cone gauge: in order to have a partonic interpretation we also have to gauge transform to *light cone gauge* $A^+ = 0$.

The choice of the light cone gauge is often just stated without any particular justification or deep reason. We can give two reasons for why we need to work in light cone gauge (this was also discussed in Sec. 4.2.1).

1. In order to talk about gluons as partons we need to quantize the gluon field. In high energy scattering one is probing the hadron or nucleus at an instant in light cone time, with an approximately light-like probe. This means that we want to light cone quantize the gluon field. Canonical quantization proceeds by imposing canonical commutation relations between fields $\phi(x)$ and their canonical conjugate variables. The canonical conjugate of a generalized coordinate is the derivative of the action with respect to the time derivative of the variable, so in light cone quantization

$$\pi = \frac{\delta}{\delta(\partial_+ \phi)} \int d^4x \mathcal{L}. \quad (5.9)$$

But since the QCD Lagrangian is built from the antisymmetric field tensor $F_{\mu\nu}$, the light cone time x^+ derivative of the component A^- is not present in the Lagrangian. In stead, $A^- = \dots$ will be a constraint. We want to solve this constraint equation explicitly so that we can completely eliminate A^- from the theory and only work with physical degrees of freedom. This can be achieved using the $\nu = +$ component of the gauge field equation of motion

$$[D_\mu, F^{\mu\nu}] = J^\nu, \quad (5.10)$$

where J^ν is the color current from the matter fields. Writing the $\nu = +$ component out we get

$$[D_-, F^{-+}] + [D_i, F^{i+}] = J^+. \quad (5.11)$$

Now by choosing the gauge $A^+ = 0$ we see that $F^{-+} = -\partial_- A^-$ is a simple function of A^- and does not even depend on its time derivative. Likewise the covariant derivative D_- is just a normal (spatial, so does not interfere with the dynamics) derivative, and altogether we have

$$(\partial_-)^2 A^- = [D_i, F^{i+}] - J^+, \quad (5.12)$$

from which we can solve, at any light cone time x^+ the constrained field A^- in terms of the physical degrees of freedom: A_i and the matter particle fields. Thus the light cone gauge $A^+ = 0$ conveniently enables a complete reduction of the 4 components of the gauge field to 2 dynamical degrees of freedom. This is similar to the way the Coulomb gauge $\nabla \cdot \mathbf{A} = 0$ enables one to solve A^0 as an explicit constraint in terms of the matter fields in the canonical quantization of QED.

2. In order to talk about partons, we need to be able to look at their longitudinal momentum p^+ , which is some fraction of the longitudinal momentum of the proton or nucleus, $p^+ = xP^+$. Because p^+ is the conjugate variable to x^- , a parton distribution will be defined as a Fourier-transform from x^- to p^+ of a two-point function of fields. Schematically: the parton distribution for partons ϕ , characterized by some field operator $\hat{\phi}$ in a hadron h with momentum P^+ will be

$$f_\phi(x) \stackrel{?}{\sim} \int dx^- e^{ixP^+x^-} \langle h | \hat{\phi}^\dagger(x^-) \hat{\phi}(0) | h \rangle \quad (5.13)$$

For the parton $\phi = \text{gluon}$, the relevant operator would be $\hat{\phi} \sim F^{i+}$, where $i = 1, 2$ is connected to the polarization of the gluon. Now if the particle ϕ carries color, such a two-point function is not gauge invariant, because the gauge transformations of the field operators $\hat{\phi}^\dagger(x^-) \hat{\phi}(0)$ at different values of x^- do not cancel. Thus the proper, physical, measurable definition must include a Wilson line between the coordinates of the operators:

$$f_\phi(x) \sim \int dx^- e^{ixP^+x^-} \langle h | \hat{\phi}^\dagger(x^-) \left[\mathbb{P} \exp \left\{ ig \int_0^{x^-} dy^- A^+(y^-) \right\} \right] \hat{\phi}(0) | h \rangle. \quad (5.14)$$

A consequence of this is that in an arbitrary gauge, the parton distribution for a parton ϕ does not have a clear interpretation as measuring just partons ϕ , but depends in a complicated way also on the gluon fields. But *if*, and only if, we choose the gauge $A^+ = 0$, the parton distribution of parton ϕ is just a two-point function of the field operator $\hat{\phi}$, and thus has (at least roughly) a physical interpretation as measuring the distribution of partons ϕ in the hadron.

So, let us now transform our field to the light cone gauge $A^+ = 0$. In addition to satisfying the requirement of a formal partonic interpretation in terms of a light cone quantization of the degrees of freedom in the nucleus, this gauge transformation will be required to calculate what happens in the collision of our nucleus with another one. We will come back to this in Sec. 5.2. But already at this stage it is useful to note that the other colliding nucleus will have a color current J^- , and if our color field has a A^+ -component it will cause the color current of the other nucleus to precess in color space. But if we transform our field to $A^+ = 0$ -gauge, the current of the other nucleus can stay unaffected by it, leaving only the fields to interact. This is easier to deal with, in fact a major reason for using the classical field approximation in the first place is that classical fields are easier to deal with.

So let us now make this gauge transformation to $A^+ = 0$. We will keep our static approximation, nothing depends on x^+ , but maintain a general x^- -dependence remembering that the support of our color current in x^- is very narrow. Note that since there is no dependence on x^+ , the gauge transform will not generate an A^- -component. This should not be seen as a gauge choice, but as a result of the high energy kinematics.

Gauge transform:

$$A^+ \Rightarrow V^\dagger(\mathbf{x}, x^-) A^+ V(\mathbf{x}, x^-) - \frac{i}{g} V^\dagger(\mathbf{x}, x^-) \partial_- V(\mathbf{x}, x^-) = 0 \quad (5.15)$$

$$A^- \Rightarrow -\frac{i}{g} V^\dagger(\mathbf{x}, x^-) \partial_+ V(\mathbf{x}, x^-) = 0, \text{ still} \quad (5.16)$$

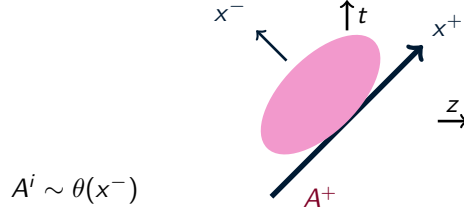
$$A^i \Rightarrow \frac{i}{g} V^\dagger(\mathbf{x}, x^-) \partial_i V(\mathbf{x}, x^-) \quad \text{transverse pure gauge} \quad (5.17)$$

(5.15) solved by

$$V(\mathbf{x}, x^-) = \mathbb{P} \exp \left[-ig \int_{-\infty}^{x^-} dy^- A^+ \right]$$

\Rightarrow Wilson line!

Now since for $A^+(y^-)$ is very localized around $y^- = 0$, the Wilson line V jumps very rapidly from unity (independently of the transverse coordinate) to a nontrivial \mathbf{x} -dependent value around $y^- = 0$. Thus its derivative, which gives A^i , has a $\sim \theta(x^-)$ -function like discontinuity around $x^- = 0$. Now our small- x gluons look like we would expect them to look like based on the Heisenberg uncertainty principle: they are small p^+ gluons and thus should be delocalized in x^- . This was not the case in the covariant gauge.



The current also is gauge transformed as

$$J^\mu \rightarrow V^\dagger J^\mu V. \quad (5.18)$$

This, however, does not change the region of support in x^- : the charges are still localized as $\sim \delta(x^-)$ as we want. Usually practical calculations are in fact (implicitly) done in terms of the covariant gauge charge density ρ that determines the Wilson lines, even if for the gauge fields one uses light cone gauge.

5.1.2 McLerran-Venugopalan model

In order to be able to actually calculate things we will now need a concrete model for what the charge density ρ in Eqs. (5.6), (5.7) could look like. Such a model is provided by the McLerran-Venugopalan (MV) model [39, 38, 40]. The MV model is not the same thing as the CGC, but it is a model that makes sense within the CGC classical field picture.

Let us briefly review the physics argument behind this model. The situation one is thinking about is that of small enough x so that the CGC spacetime picture discussed above is valid; but not necessarily asymptotically small. Instead, we are working in the limit where the nuclear mass number A is very large. This implies that at a fixed coordinate in the transverse plane there is a parametrically large number $\sim A^{1/3}$ of valence quark-like colored degrees of freedom. Since these color charges come from separate nucleons, they should be uncorrelated with each other in the longitudinal direction. Also in the transverse plane, at two different coordinates, the total color charge comes from a sum of at only partially overlapping color charges in the different nucleons, and is therefore different. Thus one can also assume the color charges at different transverse coordinates to be uncorrelated. Finally, since the color charge at one coordinate is a sum of many uncorrelated color charges, the central limit theorem states that its distribution should be Gaussian.

MV model: charge density $\rho(\mathbf{x})$ is

- stochastic, Gaussian random
- local in x^- and \mathbf{x}

$$\langle \rho^a(\mathbf{x}, x^-) \rho^b(\mathbf{y}, y^-) \rangle = g^2 \delta^{ab} \mu^2(x^-) \delta(x^- - y^-) \delta^{(2)}(\mathbf{x} - \mathbf{y}) \quad (5.19)$$

The importance of this model is that it is based on a very general physical argument, but is nevertheless very explicit, enabling one to calculate a large variety of things in various approximations. It is also simple in terms of parameters. So far $\mu^2(x^-)$ is just some unknown function, but should be thought of as being rather narrowly peaked in x^- : $\mu^2(x^-) \sim \delta(x^-)$. It will turn out that the physics in the high energy limit does not care about the functional form, but everything will just depend on the integral of $\mu^2(x^-)$ over x^- , which is essentially the saturation scale

$$Q_s^2 \sim g^4 \int_{-\infty}^{\infty} dx^- \mu^2(x^-). \quad (5.20)$$

gression: Powers of g

There are different conventions for where to put powers of g . Here, μ^2 is a number density. From this we construct ρ as a charge density, thus $\rho \sim g\mu$. Then, from the gluon field $A^+ \sim \rho/\nabla_\perp^2 \sim g\mu$, one calculates the Wilson line which involves $gA^+ \sim g^2\mu$. Thus in fact physics only depends on the combination $g^2\mu$ in the end.

For further developments it is important to note that one is making two independent approximations that need to be considered separately.

- We assumed that the charge density correlator is proportional to $\delta^{(2)}(\mathbf{x}-\mathbf{y})$. This, as we will see, leads to a very specific dependence of the unintegrated gluon distribution $\varphi^{\text{WW}}(\mathbf{k})$ on k_T at high momentum. The resulting distribution is roughly consistent with a DGLAP-like behavior of the gluon distribution, but not for example with the solution of the BK equation at very small- x . This assumption is therefore usually thought of as appropriate for moderately small x and large A , but not parametrically small x .
- The other assumptions; namely that the charges at different x^- are uncorrelated, and that the distribution is Gaussian (which implies a specific relation between the higher 4-, 6- etc. correlators and the 2-point function (5.19)) are much more general. These assumptions can be used to calculate relations between different Wilson line correlators, and in the cases where this has been checked (see e.g. [67]) this assumption has been found to be consistent with JIMWLK evolution. What this implies in practice is that one can use the assumption of locality in x^- and Gaussian correlators to calculate multiparticle correlations, and combine this with a transverse coordinate structure that is not given by $\delta^{(2)}(\mathbf{x}-\mathbf{y})$, but taken e.g. from the solution of the BK equation. This procedure or approximation is often used in the literature (see e.g. [68, 69, 70, 71, 72]). Depending on the authors it is referred to in the literature as the “nonlinear Gaussian” [67], “nonlocal Gaussian” [70] or “Gaussian truncation” [11] approach.

5.1.3 Dipole cross section

In order to get a more physical picture of what the MV model means, let us now use it to calculate two kinds of unintegrated gluon distributions, the dipole distribution or dipole amplitude (appearing in the hybrid formalism in Sec. 3.3), and the so-called Weizsäcker-Williams (WW) distribution.

Dipole

$$S(r = |\mathbf{x} - \mathbf{y}|) \equiv \frac{1}{N_c} \langle \text{tr } V(\mathbf{x}) V^\dagger(\mathbf{y}) \rangle \quad V(\mathbf{x}, x^-) = \mathbb{P} \exp \left[-ig \int_{-\infty}^{x^-} dy^- A^+ \right] \quad (5.21)$$

$$\langle A_a^+(\mathbf{x}, x^-) A_b^+(\mathbf{y}, y^-) \rangle = g^2 \delta^{ab} \mu^2(x^-) \delta(x^- - y^-) L(\mathbf{x} - \mathbf{y}) \quad (5.22)$$

Here we have introduced a notation $L(\mathbf{x} - \mathbf{y})$ for the two-point function of the covariant gauge field A^+ , which is related to the color charge density by Eq. (5.7). Since our MV model color charge density has a two-point function $\sim \delta(x^- - y^-)$, also the two point function of the fields will be proportional to the same delta function. The transverse coordinate dependence is more complicated because of the 2-dimensional Laplacian, therefore we just denote it by L and come back to it later.

In order to make sense of the path ordered exponential, it is not in practice very convenient to use the path-ordered product definition (3.60). Instead, we will discretize the integral over x^- into many infinitesimally thin pieces of width $\Delta^- \rightarrow 0$. Now a path ordered exponential of an integral turns into a path ordered exponential of a sum, which is nicely interpreted as a path ordered product of exponentials of individual terms in the sum.

Discretize

$$x^- = n\Delta^- \implies \langle A_{ma}^+(\mathbf{x}) A_{nb}^+(\mathbf{y}) \rangle = g^2 \delta^{ab} \mu_n^2 \overbrace{\frac{1}{\Delta^-} \delta_{mn}}^{\delta(x^- - y^-)} L(\mathbf{x} - \mathbf{y}) \quad (5.23)$$

$$V(\mathbf{x}) = \lim_{N \rightarrow \infty} e^{-ig\Delta^- A_N^+(\mathbf{x})} \dots e^{-ig\Delta^- A_n^+(\mathbf{x})} \dots e^{-ig\Delta^- A_{-N}^+(\mathbf{x})} \quad (5.24)$$

Plugging the infinite produce representation of the Wilson lines into the dipole operator (5.21) we obtain

$$S(r) = \lim_{N \rightarrow \infty} \frac{1}{N_c} \text{tr} \left\langle e^{-ig\Delta^- A_N^+(\mathbf{x})} \dots e^{-ig\Delta^- A_n^+(\mathbf{x})} \dots e^{-ig\Delta^- A_{-N}^+(\mathbf{x})} \right. \\ \left. \times e^{ig\Delta^- A_{-N}^+(\mathbf{y})} \dots e^{ig\Delta^- A_n^+(\mathbf{y})} \dots e^{ig\Delta^- A_N^+(\mathbf{y})} \right\rangle \quad (5.25)$$

Notice that if the path ordering in the Wilson line is from right to left, in the hermitian conjugate the corresponding ordering is from left to right. Thus in the trace (5.25) the elements at the lower limit in x^- are next to each other.

Now according to the MV model assumption the color fields at different steps in x^- are independent of each other. This means that the expectation value of the product is the product of expectation values, and we can start calculating the expectation values one rapidity step at the time, starting with the innermost $n = -N$. Now we also use the fact that Δ^- is small and expand

$$\left\langle e^{-ig\Delta^- A_n^+(\mathbf{x})} e^{ig\Delta^- A_n^+(\mathbf{y})} \right\rangle \approx \left\langle 1 - ig\Delta^- A_n^+(\mathbf{x}) + ig\Delta^- A_n^+(\mathbf{y}) + g^2(\Delta^-)^2 A_n^+(\mathbf{x}) A_n^+(\mathbf{y}) \right. \\ \left. - \frac{1}{2} g^2(\Delta^-)^2 \left((A_n^+(\mathbf{x}))^2 + (A_n^+(\mathbf{y}))^2 \right) \right\rangle + \mathcal{O}(\Delta^-)^{3/2} \quad (5.26)$$

Here the power counting combines the explicit Δ^- in the exponent with

$$A^+ \sim \frac{1}{\sqrt{\Delta^-}}, \quad (5.27)$$

which is to be understood as following in a r.m.s. sense from the discretized two-point function (5.23).

The expectation value of a single A^+ vanishes and we use (5.23) for the two point function:

$$\left\langle e^{-ig\Delta^- A_n^+(\mathbf{x})} e^{ig\Delta^- A_n^+(\mathbf{y})} \right\rangle \\ \approx 1 + g^4(\Delta^-)^2 \frac{\mu_n^2}{\Delta^-} \left[L(\mathbf{x} - \mathbf{y}) - \frac{1}{2} L(\mathbf{x} - \mathbf{x}) - \frac{1}{2} L(\mathbf{y} - \mathbf{y}) \right] \overbrace{t^a t^a}^{=C_F \mathbb{I}_{N_c \times N_c}} \\ \approx \exp \left\{ g^4 \Delta^- C_F \mu_n^2 \underbrace{\left[L(\mathbf{x} - \mathbf{y}) - \frac{1}{2} L(\mathbf{x} - \mathbf{x}) - \frac{1}{2} L(\mathbf{y} - \mathbf{y}) \right]}_{-\Gamma(\mathbf{x} - \mathbf{y})} \right\} \mathbb{I}_{N_c \times N_c} \quad (5.28)$$

Here we have defined a new notation Γ for the field-field correlator L minus its value at the origin. As we will see, the value of L at zero has a power law (=bad) IR divergence. This subtraction removes this leading divergence.

Now that this expectation value is just a number times the identity matrix, it commutes with all the other infinitesimal Wilson line factors in the infinite product (5.25). We can therefore pull it out and repeat the same procedure for the next factor (next n). Doing this one by one we finally get just a product of terms like (5.28), each of them proportional to the identity matrix. The overall trace now just gives a factor N_c that cancels with the normalization. We can now return from the discrete to the continuous notation as

$$S(r) = \exp \left\{ -g^4 C_F \int_{-\infty}^{\infty} dx^- \mu^2(x^-) \Gamma(\mathbf{x} - \mathbf{y}) \right\} \quad (5.29)$$

This is now practically our final result. Note that, as advertized, the Wilson line correlator only depends on the integral of $\mu^2(x^-)$ over x^- ; at this stage the functional form (which we never specified) of the dependence on x^- does not matter any more.

The only thing we have used so far from the MV model is the more general of the two approximations

involved: the independence of different x^- color charges and the Gaussian expectation value¹. We have not yet actually used the assumption that the correlator (5.19) is proportional to $\delta^{(2)}(\mathbf{x} - \mathbf{y})$ at all. Therefore the result (5.29) can be used independently of the MV model assumption. In particular, we can take a solution of the BK equation for $S(r)$, and consider (5.29) as the definition of the correlator $\Gamma(\mathbf{x} - \mathbf{y}) \equiv -L(\mathbf{x} - \mathbf{y}) + L(\mathbf{0})$. But in order to see what the more restrictive local charge correlation assumption gives us, let us now calculate $\Gamma(\mathbf{x} - \mathbf{y})$ in the actual model, recalling that physically we expect this to be a good approximation in the limit of smallish x and very large A . In order to get the A^+ correlator from the MV model assumption for the correlator of ρ 's we need to solve the Poisson equation (5.7). This is done by Fourier-transforming; we also need to introduce an additional IR cutoff to deal with the very divergent integrals in intermediate stages of our calculation. For now we will suppress the argument x^- for brevity, the following steps happen locally in x^- .

The covariant gauge field A^+ is related to the color charge by the Poisson equation (5.7). This equation is best solved by Fourier-transforming:

At each x^-

$$A^+(k_T) = \frac{1}{\mathbf{k}^2} \rho(\mathbf{k}) \quad (5.30)$$

To work in momentum space we also need the Fourier-transform of the color charge 2-point function (5.19)

$$\begin{aligned} \langle \rho^a(\mathbf{k}) \rho^b(\mathbf{p}) \rangle &= g^2 \delta^{ab} \mu^2 \int d^2\mathbf{x} d^2\mathbf{y} e^{i\mathbf{k} \cdot \mathbf{x} + i\mathbf{p} \cdot \mathbf{y}} \delta^{(2)}(\mathbf{x} - \mathbf{y}) \\ &= g^2 \delta^{ab} \mu^2 (2\pi)^2 \delta^{(2)}(\mathbf{k} + \mathbf{p}) \end{aligned} \quad (5.31)$$

Combining the relation between A^+ and ρ , and the two-point function of ρ 's, we get

$$\begin{aligned} \Gamma(\mathbf{x} - \mathbf{y}) &= \int \frac{d^2\mathbf{k}}{(2\pi)^2} \frac{d^2\mathbf{p}}{(2\pi)^2} (2\pi)^2 \frac{\delta^{(2)}(\mathbf{k} + \mathbf{p})}{\rho_T^2 k_T^2} [1 - e^{-i\mathbf{k} \cdot \mathbf{x} - i\mathbf{p} \cdot \mathbf{y}}] \\ &= \frac{1}{2\pi} \int d\mathbf{k} \frac{1 - J_0(kr)}{k^3} \approx \frac{1}{8\pi} r^2 \ln \frac{1}{r\Lambda} \quad \gg 1 \end{aligned} \quad (5.32)$$

This integral is still IR divergent at $k = 0$, but only logarithmically so. The leading power law divergence cancels² in the combination $\Gamma(\mathbf{x} - \mathbf{y}) \equiv -L(\mathbf{x} - \mathbf{y}) + L(\mathbf{0})$. This is true generally: expectation values of nonsinglet operators are very very sick because they depend on $L(\mathbf{x} - \mathbf{y})$ alone. They diverge (or vanish) as an exponential function of a power of the IR cutoff; they do not describe meaningful physical quantities. Expectation values of singlet operators, such as the dipole that we are calculating here, depend always on the combination $\Gamma(\mathbf{x} - \mathbf{y})$ which, in the MV model, is only logarithmically divergent. One can always argue away the logarithm for coordinate space quantities like $S(r)$, but it does affect the analytical properties and therefore the momentum space behavior, so it is better to keep it for now. Note that since Λ in Eq. (5.32) is an IR cutoff in the k -integral, we should assume that it is always small compared to any coordinate value that we are interested in: $r\Lambda \ll 1$. The full $\Gamma(r)$ is, however finite, because of the power of r multiplying the logarithm.

Different ways of regulating the IR divergence lead to different values for the remaining finite term. The leading log, however, is universal. Our result is for the dipole cross section is now:

$$S_{MV}(r) \equiv \frac{1}{N_c} \langle \text{tr } V(\mathbf{x}) V^\dagger(\mathbf{y}) \rangle = \exp \left\{ -\frac{g^4 C_F}{8\pi} \left[\int_{-\infty}^{\infty} dx^- \mu^2(x^-) \right] r^2 \ln \frac{1}{r\Lambda} \right\} \quad (5.33)$$

$$Q_s^2 \sim \frac{g^4 C_F}{4\pi} \left[\int_{-\infty}^{\infty} dx^- \mu^2(x^-) \right] \quad (5.34)$$

¹In fact we did not even use the Gaussian property, because we expanded in powers of Δ^- and only used the two-point function. At least for a Gaussian correlator some anomalously large expectation values of higher orders in the series in powers of Δ^- do not matter, but for this it is enough that the higher point correlators are not too large, they don't need to be exactly Gaussian. In fact it is probably better to think of the Gaussianity as arising via the central limit theorem; a color charge that is built up of layers in x^- that are independent of each other will behave as a Gaussian.

²It is curious that a small-momentum, i.e. IR, divergence manifests itself in the short-distance behavior of the two-point function.

This provides a concrete link between the MV model variable μ^2 (as already promised, this only enters as the integral over x^-) and the dipole cross section, e.g. the quar-nucleus scattering or DIS cross sections. We can now make a fit to DIS data, use that to extract a value for μ^2 , and apply this to calculating heavy ion collisions: this is indeed what is done in the very successful IPglasma model for the initial stage of a heavy ion collision [73].

The dipole cross section interpolates between 1 at $r = 0$ and 0 at $r \rightarrow \infty$ as it should, satisfying the expectations for a SU(3) matrix correlator. We can identify the saturation scale Q_s from the characteristic scale in this r -dependence. Here we calculated the dipole amplitude in the fundamental representation, which is why our result has the Casimir operator C_F , overall the saturation scale should have *Casimir scaling*, i.e. be proportional to the relevant Casimir. The glasma fields in the initial stage of a heavy ion collision are gluons, there the relevant scale is the adjoint Casimir $C_A = N_c$ which, in the MV model, is larger than the saturation scale measured e.g. in DIS. In addition to the color factor, the value of Q_s depends on the precise convention chosen to determine it from the dipole correlator (there are many ways to extract something so vaguely defined as “the” characteristic scale from a function). In the MV model specifically, it also depends on the details of how one regularized the IR divergence in the momentum integral, this adds another uncertainty factor into the interpretation of MV model calculations [74].

In momentum space, the Fourier-transform of the dipole expectation value, multiplied by k_T^2 , is known as the dipole gluon distribution

$$\varphi_{\text{dip.}}(k_T) \sim k_T^2 \int d^2\mathbf{r} e^{i\mathbf{r} \cdot \mathbf{k}} S(r) \quad (5.35)$$

Thanks to the logarithm of r in the MV model expression, it behaves [Exercise!] like $1/k_T^2$ at large k_T . At small k_T , the dipole distribution behaves as $\sim k_T^2$ (this is easy to see, since the integral of $S(r)$ over \mathbf{r} is finite, therefore $S(k_T = 0)$ is a constant and $\varphi_{\text{dip.}}(k_T) \sim k_T^2 S(k)$).

5.1.4 Weizsäcker-Williams distribution

To characterize the number distribution of gluons in the nucleus one needs, as discussed above, to look at a 2-point function of the gluon field in the light cone gauge. Note that now (contrary to the dipole picture of DIS or the hybrid formulation of proton-nucleus scattering) we trying to analyze gluons, quanta, in the target nucleus, not the probe. It would be difficult to light cone quantize both at the same time because we cannot simultaneously fix the gauge to be both $A^+ = 0$ and $A^- = 0$.

This gluon number density corresponds to what is know as the Weizsäcker-Williams gluon distribution. The full calculation in the MV model was first done in [75], following a procedure very similar to the above. Repeating this would take up too much time in this lecture, so we will just quote the result below. But before that it is useful to look at the *dilute limit* of the calculation. This can be derived by assuming that $\rho \sim g^2\mu$ is small, in which case one can expand the Wilson lines to lowest order. Since in the MV model everything is expressed in terms of $A^+ \sim \rho/\nabla_\perp^2$, the dilute limit of small $g^2\mu$ is at the same time the limit of large transverse momenta.

High \mathbf{k} — small μ :

$$\frac{dN}{d^2\mathbf{k} d\mathbf{y}} = \varphi^{\text{WW}}(\mathbf{k}) \sim \langle A_a^i(\mathbf{k}) A_a^i(-\mathbf{k}) \rangle \quad (5.36)$$

$$A_a^i(\mathbf{k}) = \frac{k^i}{k_T^2} \rho^a(\mathbf{k}) \implies \langle A_a^i(\mathbf{k}) A_a^i(-\mathbf{k}) \rangle = \frac{1}{g^2} \overbrace{(2\pi)^2 \delta^{(2)}(\mathbf{k} = \mathbf{0})}^{\pi R_A^2} (N_c^2 - 1) \overbrace{\frac{g^4 \mu^2}{\mathbf{k}^2}}^{\sim Q_s^2} \quad (5.37)$$

Here we used the momentum space correlator (5.31) and the fact that in the dilute limit the light cone gauge transverse gauge field in (5.17) reduces to just a derivative of covariant gauge A^+ field. This gluon distribution reduced in a very natural way to the DGLAP-evolved integrated gluon distribution, for which the definition in terms of the quantized light cone gauge gluonic field operators leads to

$$xG(x, Q^2) = \int^{Q^2} d^2\mathbf{k} \frac{dN}{d^2\mathbf{k} d\mathbf{y}} \sim \pi R_A^2 (N_c^2 - 1) \frac{Q_s^2}{g^2} \ln Q^2, \quad (5.38)$$

i.e. a function that grows logarithmically with Q^2 . This growth can be identified with the growth in the number of gluons in DGLAP evolution when increasing the resolution scale Q^2 .

The result from [75] (see e.g. [76] for a mathematically clearer but more formal derivation) for the Weizsäcker-Williams gluon distribution is

WW distribution

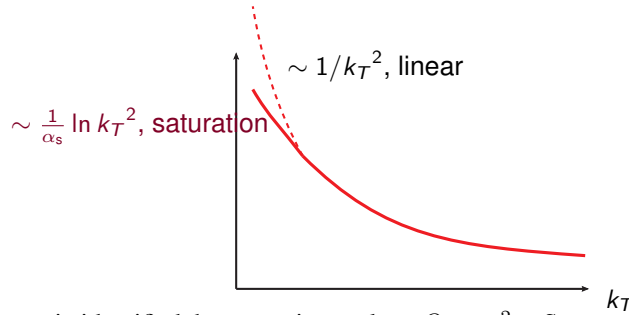
$$A^i = \frac{i}{g} V(\mathbf{x}) \partial_i V(\mathbf{x}) \quad (5.39)$$

\Rightarrow

$$\langle A_a^i(\mathbf{x}) A_b^j(\mathbf{y}) \rangle = \delta^{ab} \frac{N_c}{g^2} \frac{\nabla_{\perp}^2 \Gamma(\mathbf{x} - \mathbf{y})}{\Gamma(\mathbf{x} - \mathbf{y})} \left(\exp \left\{ -g^4 N_c \int_{-\infty}^{\infty} dx^- \mu^2(x^-) \Gamma(\mathbf{x} - \mathbf{y}) \right\} - 1 \right) \quad (5.40)$$

\Rightarrow

$$\varphi_{WW}(k_T) \sim \begin{cases} \frac{1}{\alpha_s} \ln k_T, & k_T \ll Q_s^2 \\ \frac{1}{\alpha_s} \frac{Q_s^2}{k_T^2}, & k_T \gg Q_s^2. \end{cases} \quad (5.41)$$



Here we have again identified the saturation scale as $Q_s \sim g^2 \mu$. Some points to note about the expression (5.41):

- The factor in the exponent is an adjoint representation Casimir C_A , compared to the fundamental Casimir $C_F = (N_c^2 - 1)/(2N_c)$ in the fundamental representation dipole (5.33). This is what one would expect for gluons as opposed to a fundamental representation probe.
- Both the dipole gluon distribution (5.35) and the WW distribution (5.41) have (when properly normalized) the same large k_T limit. However, they look quite different at small k_T . Both exhibit saturation: the behavior changes at $k_T \lesssim Q_s$; the dipole distribution changes to $\sim k_T^2$ and the WW distribution to $\sim \ln k_T$. You can deduce the latter property by noting that due to the 1 inside the bracket in (5.39), the integral over r of the coordinate space distribution diverges logarithmically; this would be the $k_T = 0$ value of the momentum space distribution.
- In a strict operatorial sense the dipole and WW distributions are independent quantities, some cross sections depend on one, some on the other. Without evoking a model such as MV one has to measure both of them separately experimentally. The MV model (or in general the nonlinear Gaussian assumption) provides an additional physical model that allows one to relate them to each other. For a discussion explaining how these two distributions result in the small x limit from transverse momentum distributions (TMD's) that have explicitly gauge invariant operatorial definitions, see [72].
- The WW distribution is, when one writes it in terms of the saturation scale Q_s in stead of the model parameter μ , proportional to $1/g^2$ or $1/\alpha_s$. The WW distribution is the best we can do if we try to make a bona fide effort to count gluons. In the CGC field the result is that, at weak coupling $\alpha_s \rightarrow 0$, there is a nonperturbatively large number of them. This is the justification for the word *condensate* in the CGC.

5.2 Glasma

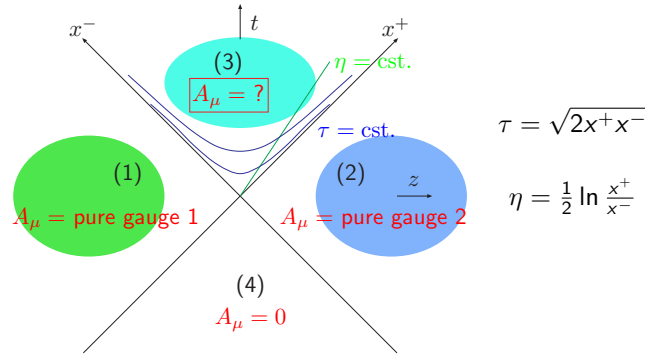
5.2.1 Heavy ion collision: initial condition

Now let us finally move to the collision of two high energy nuclei. We follow here a calculation that was originally done in Ref. [77]. We will represent both nuclei in a symmetrical way, by their own classical

color currents and radiated fields, with nucleus (1) moving in the positive z -direction and nucleus (2) in the negative one.

$$J^\mu = \underbrace{\delta^{\mu+} \rho_{(1)}(\mathbf{x}) \delta(x^-)}_{A^i \sim \theta(x^-)} + \underbrace{\delta^{\mu-} \rho_{(2)}(\mathbf{x}) \delta(x^+)}_{A^i \sim \theta(x^+)} \quad (5.42)$$

For each of these currents separately, we already know the solution of the field in the light cone gauge of each of the currents $A^\pm = 0$, and these solutions have the nice property that also the other longitudinal component vanishes: $A^\mp = 0$. I.e. the light cone field of nucleus (1) also “accidentally” satisfies the light cone gauge condition of the other one. Thus in some region of spacetime, which is causally connected to only one of the nuclei (we chose the boundary conditions for the Yang-Mills equation to be causal, so that one gets a color field only in the region after the passage of the nucleus).



Let us recall the expressions for these “transverse pure gauge” fields without the θ -functions, which we will deal with separately.

$$A_{(1,2)}^i = \frac{i}{g} V_{(1,2)}(\mathbf{x}) \partial_i V_{(1,2)}^\dagger(\mathbf{x}) \quad (5.43)$$

$$V_{(1,2)}(\mathbf{x}) = P e^{ig \int d\mathbf{x}^\mp \frac{\rho(\mathbf{x}, \mathbf{x}^\mp)}{\nabla_\perp^2}} \quad (5.44)$$

Digression: Conventions for $\pm ig$

In my conventions in this Section (note necessarily everywhere in this lecture note) the covariant derivative is

$$D_\mu = \partial_\mu + ig A_\mu \quad (5.45)$$

the field strength tensor

$$F_{\mu\nu} = \partial_\mu A_\nu - \partial_\nu A_\mu + ig [A_\mu, A_\nu]. \quad (5.46)$$

A gauge transformation is

$$A_\mu \rightarrow V A_\mu V^\dagger - \frac{i}{g} V \partial_\mu V^\dagger \quad (5.47)$$

and a pure gauge

$$-\frac{i}{g} V \partial_\mu V^\dagger. \quad (5.48)$$

All the signs of the ig 's in these expressions are correlated with each other, and it becomes hard to keep one's conventions consistent. For the transverse pure gauge in Eq. (5.43) one has to note that $A^i = -A_i$, and thus the sign is

$$A^i = -A_i = \frac{i}{g} V \partial_i V^\dagger. \quad (5.49)$$

Equations (5.43) and (5.44) provide valid solutions to the equations of motion in the regions (1) and (2) in the figure above, which are causally connected to only one of the two nuclei. Let us now derive an initial condition for the field inside the future light cone, which is causally connected to both. Inside the region (3) there is no current (since the color currents are proportional to delta functions)

Region (3):

- Inside: $[D_\mu, F^{\mu\nu}] = 0$; no source

- Need initial conditions at $\tau = 0$
- $\sqrt{s} \rightarrow \infty$: should be boost invariant: $A_\mu(\tau, \mathbf{x})$

Gauge choice:

- Avoid color precession: $A^- = 0$ at $x^- = 0$ where J^+ lives, + vice versa
- Boost invariant: τ, η -components

⇒ Fock-Schwinger $A_\tau = (x^+ A^- + x^- A^+) / \tau = 0$

The Fock-Schwinger or temporal gauge condition has the very nice property that on the x^+ -axis, i.e. $x^- = 0$, it reduces to $x^+ A^- = 0$, i.e. $A^- = 0$. Thus the current that lives on this light cone is not only covariantly conserved $[D_\mu, J^\mu] = \partial_+ + ig[A^-, J^+] = 0$, but in fact does not color precess and is constant $\partial_+ J^+ = 0$. This significantly simplifies our following calculation. The other advantage of the $A_\tau = 0$ -condition is that in order to solve the equations of motion numerically in a Hamiltonian formalism, which is the standard thing to do, one needs to choose a temporal gauge condition. There are a few calculations of gluon production inside the forward light cone in another gauge, the covariant gauge, but this is done only in the dilute limit, not including any final state interactions [78, 79]. I am not aware of a numerical implementation of the full equations in another gauge.

Now, as discussed above, we need an initial condition for the field inside the future light cone. For the case of one nucleus we could have two components equal to zero, one as a gauge choice and the other one as a result of our current being independent of the light cone time x^+ . In the case of two nuclei there is a dependence on both x^- and x^+ in the problem, and we cannot have this “accidental” vanishing of one component of the gauge field any more. So we can only make one component of the gauge field vanish with a gauge choice, but our solution inside the future light cone will have nonzero values for the other three. With $A_\tau = 0$, this third component is the longitudinal field orthogonal to it, namely A_η or $A^\eta = -A_\eta / \tau^2$. In the following we will use the latter, because A^η is finite at $\tau = 0$, and consequently $A_\eta(\tau = 0) = 0$.

Since the currents exist only on the light cones, the field can have discontinuities across the light cone. We can write an ansatz for the solution in terms of θ functions. Inserting this into the equations of motion will yield δ -functions arising from derivatives of the θ -functions. We can determine the initial conditions for the field at $\tau = 0^+$ by requiring that the coefficients of these δ -functions vanish. This is enough to determine the initial condition, we do not need the terms that do not have a $\delta(x^\pm)$.

$$\text{Ansatz: } A_i = \overbrace{A_i^{(1)}(\mathbf{x})\theta(-x^+)\theta(x^-) + A_i^{(2)}(\mathbf{x})\theta(x^+)\theta(-x^-)}^{\text{known}} + A_i^{(3)}(\mathbf{x}, \tau)\theta(x^+)\theta(x^-) \quad (5.50)$$

$$A^\pm = \pm\theta(x^+)\theta(x^-)x^\pm A^\eta(\mathbf{x}, \tau) \quad (5.51)$$

$$[D_\mu, F^{\mu\nu}] = J^\nu \quad \text{match} \quad \delta(x^\pm) \quad (5.52)$$



$\delta(x^-)\delta(x^+)$ in:

$$J^i = \partial_- \partial_+ A^i + \dots = \delta(x^-)\delta(x^+)(-A_i^{(1)}(\mathbf{x}) - A_i^{(2)}(\mathbf{x}) + A_i^{(3)}(\mathbf{x})) = 0 \quad (5.53)$$

To get a contribution like $\delta(x^-)\delta(x^+)$ we need two derivatives $\partial_- \partial_+$ acting on the theta functions $\theta(\pm x^\pm)\theta(\pm x^\pm)$. When acting on the transverse component A^- such derivatives appear in the $J^i = 0$ equation. In principle we have derivatives like $\partial_- \partial_+$ acting on $\theta(\pm x^\pm)\theta(\pm x^\pm)$ in A^\pm in the equations with J^\pm . However, in this case the contribution is killed by the additional x^\pm in the relation between A^\pm and A^η , which gives terms like $\delta(x^-)\delta(x^+)x^\pm = 0$. We now have our first equation.

Next, we have to start looking at terms like $\delta(x^\pm)\theta(x^\mp)$, where one derivative is acting on a theta function and other derivatives on something else. There are such terms in the $J^i = 0$ equation too, but it turns out they do not give us new constraints on the fields in region (3). Instead, we have to look at the equations for J^\pm . Since + and - are symmetric, we can look at either J^+ or J^- ; let us look at the first one. Now $J^+ \sim \delta(x^-)$, so we want to be looking for terms $\sim \delta(x^-)$ in the equation for J^+ . There are several:

$\delta(x^-)\theta(x^+)$ in J^+ equation

$$\begin{aligned}\partial_- F^{++} &= [\partial_- \overbrace{\partial_+ (x^+ \theta(x^+) \theta(x^-))}^{A^+} - \partial_- \overbrace{\partial_- (-x^- \theta(x^+) \theta(x^-))}^{A^-}] A^\eta(\mathbf{x}, \tau) \\ &= 2\delta(x^-)\theta(x^+)A^\eta(\mathbf{x}, \tau) + \dots\end{aligned}\quad (5.54)$$

$$\partial_i \overbrace{(\partial_- A_i)}^{F^{i+}} = \delta(x^-)\theta(x^+)\partial_i \overbrace{(-A_i^{(2)}(\mathbf{x}) + A_i^{(3)}(\mathbf{x}))}^{A_i^{(1)}} = J^+|_{x^+>0} - \dots \quad (5.56)$$

$$\begin{aligned}ig[A_i, \overbrace{\partial_- A_i}]^{F^{i+}} &= ig[\theta(-x^-) \overbrace{A_i^{(2)} + \theta(x^-) A_i^{(1)}}^{A_i^{(2)} + \theta(x^-) A_i^{(1)}}, -\overbrace{A_i^{(2)}(\mathbf{x}) + A_i^{(3)}(\mathbf{x})}^{A_i^{(1)}(\mathbf{x})}] \delta(x^-)\theta(x^+) \\ &= ig[A_i^{(2)}, A_i^{(1)}(\mathbf{x})] \delta(x^-)\theta(x^+) + \dots\end{aligned}\quad (5.57)$$

$$(5.58)$$

Here we have only considered the $\theta(x^+)$ part of the $x^- = 0$ light cone, and thus the $A_i^{(1)}$ part of the ansatz (5.50) does not appear immediately, but only after eliminating $A_i^{(3)}$ using the first matching condition (5.53). The \dots on the r.h.s. of Eq. (5.56) are a reminder of the fact that the equation of motion for the nucleus (1) also has a contribution from the nonlinear term $\sim [A_i^{(1)}, \partial_- A_i^{(1)}]$; as discussed in Sec. (5.1) one needs to spread out the δ function in x^- to treat this term properly, which we are not doing here. This does not, however generate a contribution that would affect the initial condition for A^η . In relating F^{i+} to A_i note both the antisymmetry of $F^{\mu\nu}$ and the Lorentz signature $A_i = -A^i$.

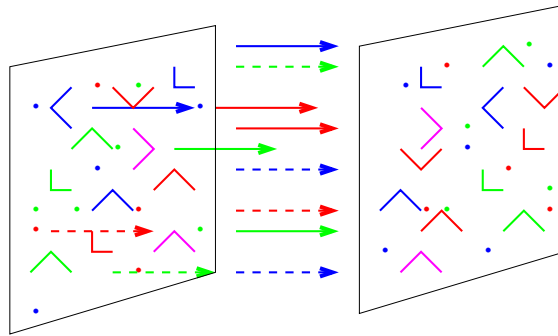
Requiring that all the equations are satisfied leads us to the initial conditions for the glasma fields first derived in Ref. [77]:

$$A_i^{(3)}|_{\tau=0} = A_i^{(1)} + A_i^{(2)} \quad (5.59)$$

$$A^\eta|_{\tau=0} = \frac{ig}{2} [A_i^{(1)}, A_i^{(2)}] \quad (5.60)$$

5.2.2 Properties of glasma fields

Now we have the gauge potentials at $\tau = 0$. From these we can calculate the field strength tensor, i.e. the chromomagnetic and chromoelectric fields. It is quite easy to convince yourself that these are both in the z -direction. These leads to the following often seen picture:



- $\tau = 0$ longitudinal $E^z \sim [A_i^{(1)}, A_i^{(2)}]$ and $B^z \sim \varepsilon^{ij} [A_i^{(1)}, A_j^{(2)}]$
- \perp correlation length $1/Q_s$.

One way to think of the longitudinal initial electric and magnetic fields is to note that in the absence of color charges the fields satisfy the nonabelian Gauss law and Bianchi identities, stating that the covariant divergences of the chromoelectric and -magnetic fields vanish. It is interesting to separate the commutator terms from the linear ones. Then one can interpret the nonlinear terms as kind of effective electric and magnetic field densities generated by the interaction of the electric and magnetic fields of one nucleus with

the pure gauge potential of the other one.

- Gauss

$$[D_i, E^i] = 0 \implies \partial_i E^i = ig[A^i, E^i] \quad (5.61)$$

- Bianchi

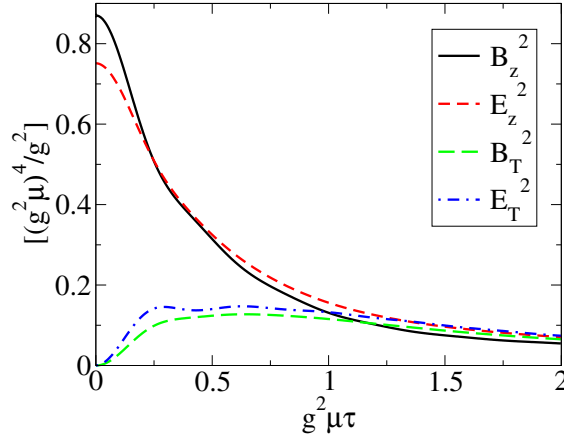
$$[D_i, B^i] = 0 \implies \partial_i B^i = ig[A^i, B^i] \quad (5.62)$$

Loosely quoting L. McLerran, the pure gauge field of one nucleus is a “Color Glass Fairy” that sprinkles magic dust on the Weizsäcker-Williams gluons (transverse fields that only live on the light cone, following the color charges) of the other nucleus. This magic fairy dust generates color charges (and chromomagnetic monopoles) on the gluons of the second nucleus, which serve as the end points of color flux tubes.

Digression: Glasma strings and Lund strings

One might think that this picture is similar to the Lund string model. In some ways it is, but in some important ways it is not. The first seemingly very different feature is that there is also a magnetic field, parametrically (and in fact, if one averages over a rotationally invariant target, exactly) equally large. The second, perhaps more consequential, difference is the length scale. The gluon fields depend on the transverse coordinate with a typical length scale $1/Q_s$, which we are assuming to be a weak coupling momentum scale. This is in contrast to Lund strings, whose width and string tension are understood as confinement scale quantities. This means that for Lund strings, the energy is stored in the potential energy of the string. The beam particles are constantly stretching the string and transferring energy to the central rapidity region. This energy is then eventually released in a nonperturbative mechanism of string breaking via the Schwinger mechanism. For the glasma, on the other hand, the field modes can be interpreted as gluons with typical transverse momenta $k_T \sim Q_s$. They can scatter, turn into a quark-gluon plasma, and then eventually hadronize by some mechanism which a weak coupling calculation cannot capture. The energy is not stored in potential energy, but in the kinetic energy (momentum) of these gluonic modes. After the collision, the beams (the currents) are gone and are no longer transferring energy to the midrapidity region. This means that the energy at an early stage in the collision (say $\tau \sim 1\text{fm}$) is larger in the glasma picture: all the energy is already there, while in the Lund string picture the midrapidity region is still gaining energy by pulling back on the receding beams (and other hard particles) that are stretching the strings.

Inside the future light cone the field equations have to be solved numerically. This can be done with relatively standard real time lattice gauge field methods.



In this plot the transverse field notation means

$$E_T^2 = E_x^2 + E_y^2 \quad (5.63)$$

$$B_T^2 = B_x^2 + B_y^2 \quad (5.64)$$

After at time $\tau \sim 1/Q_s$ the transverse and longitudinal fields become equal $E_T^2 \sim B_T^2 \sim B_z^2 \sim E_z^2$ and start to decrease with time as $\sim 1/\tau$ due to the longitudinal expansion of the system encoded in the boost invariance of the field configurations. Note that the late time behavior $E_T^2 \sim B_T^2 \sim B_z^2 \sim E_z^2$ is not isotropic.

A simple way to think of this behavior is in terms of linear polarization states of the gluons. Because of the boost invariance at the level of field configurations, the momenta of all of these gluons are transverse.

Now think of four polarization states with \vec{k} , \vec{B} and \vec{E} all orthogonal to each other:

$$k_x : B_y E_z \quad (5.65)$$

$$k_x : B_z E_y \quad (5.66)$$

$$k_y : B_x E_z \quad (5.67)$$

$$k_y : B_z E_x, \quad (5.68)$$

with each mode oscillating separately between an electric and a magnetic field. These are perfectly consistent polarization states for a gluon, with polarization vectors orthogonal to the momentum. The curious thing about the glasma is that all of these states start, at $\tau = 0$, with a particular phase in their oscillation; the one with a field, electric or magnetic, in the z -direction. This is essentially dictated by boost invariance, which forces the system to a very coherent state in the beginning. After a time $\tau \sim 1/Q_s$, the different field modes with different \mathbf{k} get out of phase, both because of interactions and because they have some spread in frequency. At this point the system is a democratic superposition of all these kind of modes, which leads to $B_z^2 \sim E_z^2 \sim 2B_x^2 \sim 2B_y^2 \sim 2E_x^2 \sim 2E_y^2$.

It is interesting to see what this means in terms of the energy momentum tensor. For pure gauge Yang-Mills theory the diagonal components are given by

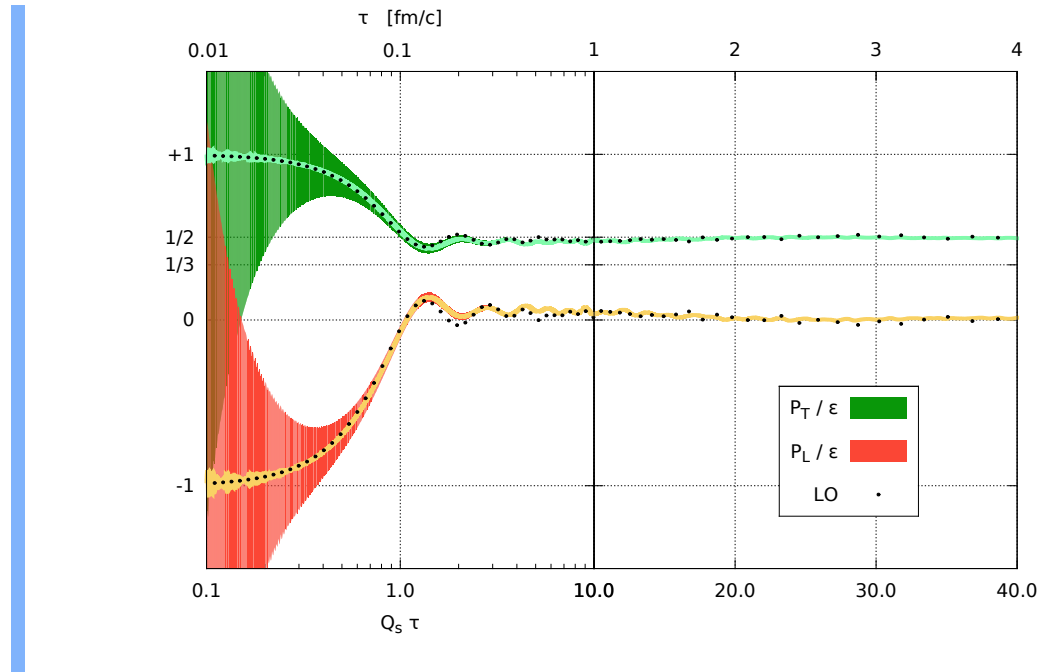
$$\varepsilon = \frac{1}{2} [E_x^2 + E_y^2 + E_z^2 + B_x^2 + B_y^2 + B_z^2] \quad (5.69)$$

$$p_x = \frac{1}{2} [-E_x^2 + E_y^2 + E_z^2 - B_x^2 + B_y^2 + B_z^2] \quad (5.70)$$

$$p_y = \frac{1}{2} [E_x^2 - E_y^2 + E_z^2 + B_x^2 - B_y^2 + B_z^2] \quad (5.71)$$

$$p_z = \frac{1}{2} [E_x^2 + E_y^2 - E_z^2 + B_x^2 + B_y^2 - B_z^2] \quad (5.72)$$

At the initial condition one starts with negative longitudinal pressure $p_z = -p_x = -p_y = -\varepsilon$. This is similar to the longitudinal chromoelectric field in a QCD string, which has a string tension, i.e. negative longitudinal pressure. Here is a plot from [80]:



After a time $\tau \sim 1/Q_s$ the negative pressure approaches zero, and the transverse pressure becomes half of the energy density. This is the starting point for the isotropization of the system, which requires going beyond the classical approximation.

5.2.3 Gluon spectrum

In order to interpret these fields in terms of a number density of gluons (which is possible only after a time $\tau \gtrsim 1/Q_s$), one needs to decompose the solution in Fourier \mathbf{k} -modes. Knowing that this is a one scale problem, with the only dimensionful scale, one knows already beforehand that the gluon number distribution has to have the parametric form

$$\frac{dN_g}{dy d^2\mathbf{x} d^2\mathbf{p}} = \frac{1}{\alpha_s} f\left(\frac{p_T}{Q_s}\right) \quad (5.73)$$

In the dilute limit one can recover a perturbative k_T -factorization result for the gluon density. One first has to transform the fields to transverse Coulomb gauge $\partial_i A_i = 0$; this is done using an additional gauge freedom in the Fock-Schwinger gauge to perform τ -independent gauge transformations. Assuming that the fields are small, one neglects the nonlinear terms in the equations of motion for $\tau > 0$. The linearized equations are then wave equations in an expanding geometry, separately for each transverse momentum mode.

$$(\tau^2 \partial_\tau^2 + \tau \partial_\tau + \tau^2 \mathbf{k}^2) A_i(\tau, \mathbf{k}) = 0 \quad (5.74)$$

$$(\tau^2 \partial_\tau^2 - \tau \partial_\tau + \tau^2 \mathbf{k}^2) A_\eta(\tau, \mathbf{k}) = 0. \quad (5.75)$$

$$\Rightarrow A_i(\tau, \mathbf{k}) = A_i(\tau = 0, \mathbf{k}) J_0(|\mathbf{k}| \tau) \quad A_\eta(\tau, \mathbf{k}) = -\frac{1}{\tau |\mathbf{k}|} A_\eta(\tau = 0, \mathbf{k}) J_1(|\mathbf{k}| \tau). \quad (5.76)$$

- These modes are (boost invariant) plane waves. Thus they can be interpreted as particles, gluons.
- In this approximation (interactions only at $\tau = 0$, free propagation after that), there is no contradiction between a classical field and particle description of the fields. The negative longitudinal pressure at $\tau = 0$ is due to the boost invariance of the situation. This imposes a specific restriction on the two possible linear polarization states for gluons with only transverse momentum. The polarization state with a electric field in the z -direction and a magnetic field in a transverse direction starts in a phase where there is only an electric field, whereas the other polarization state with a magnetic field in the z -direction and an electric field in a transverse direction has to start in a phase where there is only a magnetic field. The different modes present in these two polarization states oscillate in time with slightly different frequencies, and later get out of sync. Thus after a time $\tau \sim 1/Q_s$ the phases of these oscillations are more randomly distributed, and the energy momentum tensor is just dictated by the boost invariance, i.e. absence of longitudinal momentum, i.e. zero longitudinal pressure.
- The initial fields related to Wilson lines, and via that to the dipole amplitude measured in DIS.

In this dilute limit, when we have turned off all the interactions between the gluons after $\tau = 0$ and expanded the color fields of both nuclei to the lowest nontrivial order in their color charge densities, the number distribution is given by a k_T -factorization formula

$$\frac{dN}{dy d^2\mathbf{k}} = \frac{\alpha_s}{S_\perp} \frac{2}{C_F} \frac{1}{k_T^2} \int d^2\mathbf{q} \varphi^{\text{dip}}(\mathbf{q}) \varphi^{\text{dip}}(|\mathbf{k} - \mathbf{q}|), \quad (5.77)$$

with S_\perp the transverse area of the nuclei, and $\varphi^{\text{dip}}(\mathbf{q})$ the dipole distribution obtained from the Fourier-transform of the dipole operator (see Eq. (5.35), exact coefficients convention-dependent, [TBD: need to fix]). This calculation can also be repeated by assuming that *one* of the two colliding objects is dilute (a theorist's "pA" collision) [81].

However, no such analytic calculation exists for a dense-dense system, an "AA" collision. Also in the "AA" case, one can numerically verify that the k_T -factorization formula works for high k_T gluons. However, because of the explicit $1/k_T^2$ in front, it cannot be integrated to give a finite total gluon multiplicity. The full result of the numerical calculation, on the other hand, can. Sometimes this is fixed by an ad hoc cutoff

$$\frac{dN}{d^2\mathbf{p} dy} = \frac{1}{\alpha_s} \frac{1}{\mathbf{p}^2} \int_{\mathbf{k}} \left[\theta(p_T - k_T) \right] \phi_y(\mathbf{k}) \phi_y(\mathbf{p} - \mathbf{k}) \quad (5.78)$$

Figure 5.1 shows a comparison of the k_T -factorized formula (5.77) to the result of the full CYM calculation, and also to the version with the cutoffs (5.78). The calculation for the dilute-dense case is done in the

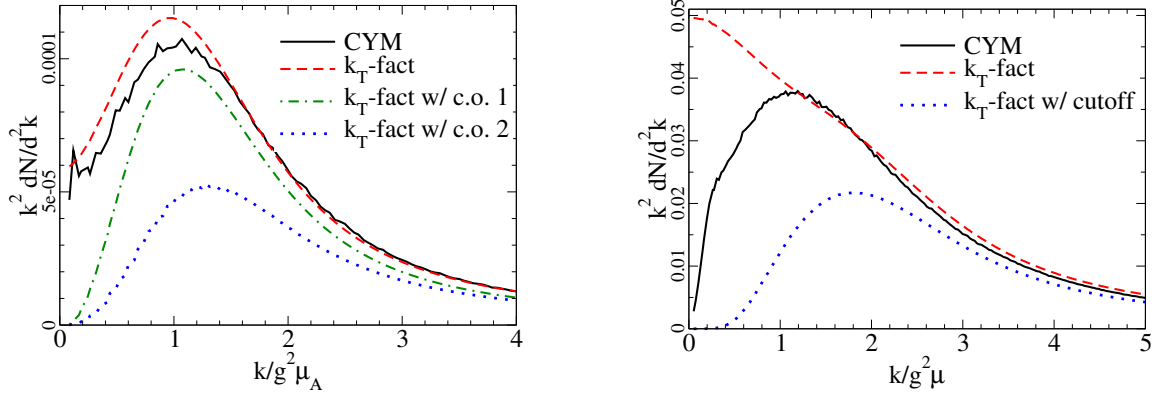


Figure 5.1: Full CYM calculation and different k_T -factorized approximations (with a cutoff on the momentum from one or the other nucleus). Left: dilute-dense case with very small $g^2 \mu$ for one nucleus. Right: dense-dense case with similar $g^2 \mu$ for both nuclei. These plots are from [82].

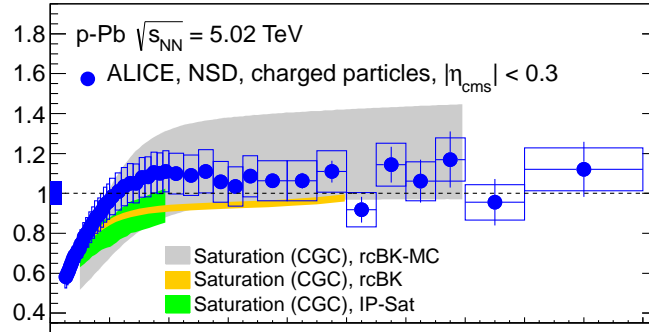


Figure 5.2: Comparison of CGC calculations to ALICE data on midrapidity nuclear modifications to single particle production. The plot is from ALICE [28], the “rcBK” and “IPsat” CGC calculations from [83] and the “rcBK-MC”-calculation from [84]; the difference between these is mostly in how one goes from a unintegrated gluon distribution in a proton to that in a nucleus, less in the formalism of how the particle spectrum is computed.

MV model with two very different values for $g^2 \mu$ in the two colliding nuclei: in this case the result for ad hoc cutoff depends very much on whether one cuts off the spectrum at $k_T < p_T$ or $|\mathbf{p} - \mathbf{k}| < p_T$. The plot on the right in the same figure shows the same comparison in the case of a dense-dense collision, where the k_T -factorization formula does not work for $k_T \lesssim Q_s$.

Figure 5.2 shows a comparison with experimental data from pA collisions; the theory predictions here are calculated with the k_T -factorization formula (5.77), combined with fragmentation functions to turn the produced gluons into hadrons.

5.3 Bottom-up thermalization

5.3.1 Starting point

We have now seen what the “glasma” color fields at the initial stage of a heavy ion collision look like. In particular we have seen that the initial fields are boost invariant. In terms of momenta of gluons this corresponds to an extremely anisotropic momentum space distribution of gluons. This is still very far from a thermal equilibrium that could be matched to hydrodynamics. In particular the important problem is that of *isotropization*. The longitudinal expansion of the system constantly tries to make the momentum distribution more anisotropic, fighting against interactions that try to isotropize the system.

The “extreme” weak coupling parametric analysis of how the interactions eventually isotropize the system is known as the “bottom-up” thermalization scenario, and was developed in Ref. [85]. The qualitative

features of this parametric scenario have later been confirmed in explicit numerical studies both in with Classical Yang-Mills simulations (valid for the first part of the scenario) and in effective kinetic theory. For simplicity this analysis concerns a system that is boost invariant in the longitudinal direction, and infinitely large and homogenous in the transverse ones. Physically this is justified when the collision energy \sqrt{s} is large enough, and when we are interested in times that are early compared to the size of the system πR_A^2

Assumptions:

- $\alpha_s \ll 1$
- Hard scale Q_s , soft $m_D \ll Q_s$
- At $Q_s \tau \sim 1$ overoccupied $f \sim 1/\alpha_s$
- Boost invariance, initially: $p_z \ll p_T \sim Q_s$

At what $Q_s \tau \sim (\alpha_s)^2$ is $p_z \sim p_T$ & $f \sim 1$?

We are describing the system in a kinetic theory language, in terms of gluon phase space distributions f . The kinetic theory setup, at weak coupling, is also based on a separation of hard and soft modes. We start initially with only hard $\sim Q_s$ gluons. The relevant quantities that we want to follow are estimate based on the phase space densities f for hard and soft modes separately:

- The energy density

$$\varepsilon \sim \int d^3\bar{\mathbf{p}} p f(\bar{\mathbf{p}}) \quad (5.79)$$

- The number density

$$n \sim \int d^3\bar{\mathbf{p}} f(\bar{\mathbf{p}}) \quad (5.80)$$

- The Debye mass

$$m_D^2 \sim \alpha_s \int d^3\bar{\mathbf{p}} \frac{f(\bar{\mathbf{p}})}{p} \quad (5.81)$$

In the first stage the hard modes dominate the integrals for all three quantities. The “bottom-up” nature of the thermalization process refers to the fact that we then gradually build up a bath of soft particles, which eventually end up absorbing all the energy of the system. Since the Debye mass is the most infrared sensitive of these three quantities, it will be the first one to become dominated by the soft modes: this marks the end of the first stage. In the second stage the soft modes dominate m_D , but the hard modes the energy density and number density: this stage ends when the number density of soft particles becomes equal to the number density of hard ones. In the third stage the soft modes dominate the Debye mass and the number density, but most of the energy is still in the hard particles. The third stage ends when the hard particles also lose their energy, thus becoming fully absorbed into the thermal bath of soft particles.

5.3.2 First stage: classical fields

Let us first see what happens completely in the absence of interactions. The important feature of this system is that longitudinal momenta are redshifted by the expansion in the longitudinal direction, we have:

$$p_T \sim \text{const.} \quad p_z \sim \frac{1}{\tau} \quad (5.82)$$

To see this formally in kinetic theory we can take the Boltzmann equation for a general Lorentz frame

$$p^\mu \partial_\mu f(p, x) = C[f] \quad (5.83)$$

In the absence of interactions we take the collision term to be zero; $C = 0$. Now we are looking for boost invariant, transversally homogenous solutions for massless particles. In this case we can parametrize the

coordinates and momenta as

$$p^0 = p_T \cosh y \quad (5.84)$$

$$p^z = p_T \sinh y \quad (5.85)$$

$$t = \tau \cosh \eta \quad (5.86)$$

$$z = \tau \sinh \eta \quad (5.87)$$

In terms of these variables the equation (5.83) is

$$\left(\partial_\tau + \tanh(\eta - y) \frac{1}{\tau} \partial_\eta \right) f = 0 \quad (5.88)$$

We must look for a solution of (5.83) that only depends on p_T, τ and $\xi \equiv \eta - y$. For this we can replace $\partial_\eta = \partial_\xi$. The equation is now

$$\left(\partial_\tau + \tanh(\xi) \frac{1}{\tau} \partial_\xi \right) f = 0 \quad (5.89)$$

It is easy to check that this equation is satisfied by any function that only depends on τ and ξ through the combination $\tau \sinh \xi$:

$$f(p_T, \tau \sinh \xi) \quad (5.90)$$

From this it is easy to deduce that the (r.m.s.) average value of the longitudinal momentum $p^z = p_T \sinh \xi$ behaves as $\sqrt{\langle p_z^2 \rangle} \sim 1/\tau$. In the following we simply denote $\sqrt{\langle p_z^2 \rangle}$ by p_z .

A similar behavior is also seen in fully boost invariant classical Yang-Mills simulations, where one observes that the longitudinal pressure (T_{zz} -component of the energy momentum) is much smaller than the transverse one. A physical interpretation in terms of the classical field picture is that the z -momentum component is *redshifted* $p_z \sim 1/\tau$ due to the expansion of the system in the z -direction.

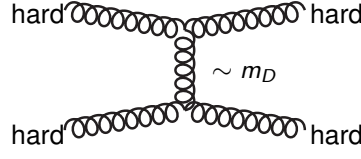
No interactions

- $\text{cst } f \sim 1/\alpha_s$
- $p_T \sim Q_s \sim \text{cst.}$
- $p_z \sim 1/\tau$
- Hard gluon number density

$$n_h \sim \int_{\vec{p}} f \sim p_z p_T^2 \frac{1}{\alpha_s} \sim \frac{1}{\alpha_s} \frac{Q_s^2}{\tau} \quad (5.91)$$

Now let us introduce also elastic collisions, which keep the hard particle number density constant, but start to fight against the redshift from the longitudinal expansion. Note that since we now have collisions that can modify the longitudinal momentum of gluons, the typical longitudinal momentum does not behave like $p_z \sim 1/\tau$ any more. Consequently also the phase space density of the hard gluons, which can be estimated as the total (so far conserved) number density divided by the phase space volume $p_z p_T^2$ occupied by the gluons. However, the number density of hard gluons (the phase space density integrated over the momenta) still continues the $1/\tau$ decrease from Eq. (5.91); the elastic collisions redistribute the hard particles in momentum space but do not change their number, i.e. number density: that is what “elastic” means. Energy and momentum conservation dictates that also the typical transverse momentum of the gluons changes, but this change is of order p_z or m_D , which is so small that it does not change our estimate $p_T \sim Q_s$. An important quantity here is the *Debye mass*, which regulates the otherwise infrared divergent total cross section, and gives the size of the transverse momentum kick received by a particle in a typical collision. The Debye mass is the only dimensionful scale in the scattering cross section in the high-energy (small angle) scattering limit, which dominates the total cross section in QCD (or any gauge theory). To estimate the total scattering cross section between hard particles we count the appropriate power of the coupling constant from the Feynman diagram. This is then multiplied by the appropriate power of the Debye mass using dimensional analysis. Any corrections to this estimate are suppressed by powers of m_D/\sqrt{s} , where for a hard-hard scattering the total energy is of the order of the hard momentum scale $\sqrt{s} \sim Q_s$.

Elastic collisions:



$$\sigma \sim \frac{\alpha_s^2}{m_D^2} \quad (5.92)$$

$$m_D^2 \sim \alpha_s \int \frac{f(\vec{p})}{p} \sim \frac{\alpha_s}{Q_s} n_h \sim \frac{Q_s}{\tau} \quad (5.93)$$

Collision rate

$$\frac{dN_{\text{coll}}}{d\tau} \sim \sigma n_h \overbrace{(1+f)}^{\text{Bose enhancement}} \quad (5.94)$$

$$f \sim \frac{n_h}{p_z Q_s^2} \gg 1 \quad (5.95)$$

In a steady state, the longitudinal momentum p_z gained by the particles per unit time must be the same as the typical p_z divided by the lifetime of the system τ . To see this more formally let us assume quite generally that the typical momentum behaves with a power law in time $p_z^2 \sim \tau^\alpha$, for which $dp_z^2/d\tau \sim p_z^2/\tau$; in a steady state this must be true for the competing contributions of the redshifting that decreases the longitudinal momenta and the collisions that enhance it. The collisional enhancement per unit time is given by the rate of collisions times the typical momentum kick gained in each collision, m_D^2 :

$$\frac{p_z^2}{\tau} \sim \frac{dp_z^2}{d\tau} \sim m_D^2 \frac{dN_{\text{coll}}}{d\tau} \sim m_D^2 \frac{\alpha_s^2}{m_D^2} \frac{Q_s^2}{\alpha_s \tau} \frac{Q_s^2}{\alpha_s \tau Q_s^2 p_z} \sim \frac{Q_s^2}{p_z \tau^2} \implies p_z \sim \frac{Q_s}{(Q_s \tau)^{1/3}} \quad (5.96)$$

Note that $p_z \gg m_D$, which is a necessary consistency requirement, since we estimated the scattering cross section with a 3-dimensional formula, assuming that all the components of the hard momenta are indeed hard compared to the screening scale m_D . Also note that this is a regime when the occupation number is large, and therefore can be described by a classical field approximation. This can be seen also in the fact that the values of the relevant momentum scales $p_T \sim Q_s$, p_z and m_D only depend on the initial hard scale Q_s and τ , but not at all on the coupling. The fact that the coupling scales out of the dynamics completely like this is a feature of the classical field evolution. We can see when this regime ends by checking when the classical high occupation number regime ceases to be valid:

$$f \sim \frac{1}{\alpha_s} \frac{1}{(Q_s \tau)^{2/3}} \sim 1 \implies Q_s \tau \sim \alpha_s^{-3/2} \quad (5.97)$$

5.3.3 Second stage: soft particles start to play a role

As the hard particles at a scale Q_s are happily interacting during the first stage, one starts to create a bath of soft particles at a lower scale, with momenta suppressed by a power of the coupling compared to Q_s . The arguments in the previous section are not fully valid any more, since now it is the 1, and not the f , that dominates in the Bose enhancement factor $1+f$ in the scattering rates. In this next stage of the process, the soft particles will dominate Debye screening, but the hard particles will still carry the dominant part of the gluon number, and energy, of the system. To make the derivation a little bit shorter we will first assume that this is the case, and self-consistently estimate m_D and the number density of soft gluons n_s . One can then, a posteriori, check that indeed the soft gluons dominate m_D but not the total multiplicity.

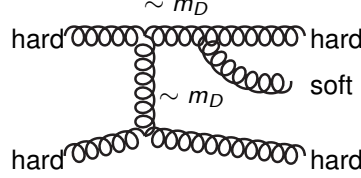
The soft momentum scale (it is isotropic, because the soft sector interacts with itself very strongly) is the product of the number of elastic collisions between soft particles and other (i.e. hard at this stage) particles and the typical momentum obtained by the soft particle in these collisions, which is of the order m_D . The number of collisions is given by the time times the collision rate, and the collision rate is the number density of scattering centers times the cross section. At this stage the scattering centers are still the hard particles, for which the number density (5.91) estimate is still valid. In principle there should be a Bose enhancement factor in (5.98), but now the number density of the hard particles is $f \ll 1$ so it does not matter.

Soft momentum scale

$$k_s^2 \sim N_{\text{coll}} m_D^2 \sim \tau \frac{\alpha_s^2}{m_D^2} \frac{Q_s^3}{\alpha_s Q_s \tau} m_D^2 \sim \alpha_s Q_s^2 \implies \text{indep. of } \tau \quad (5.98)$$

The number density of soft gluons and the Debye scale both depend on each other, so they have to be solved self-consistently:

Producing soft particles (Bethe-Heitler):



$$\sigma \sim \frac{\alpha_s^3}{m_D^2} \quad (5.99)$$

Soft gluon number density

$$n_s \sim \tau \frac{dN^{\text{BH}}}{d\tau} \sim \tau \underbrace{\left(\frac{Q_s^2}{\alpha_s \tau} \right)^2}_{n_h^2} (1 + \underbrace{f_h}_{\ll 1})^2 \frac{\alpha_s^3}{m_D^2} \sim \frac{\alpha_s Q_s^4}{m_D^2 \tau} \quad (5.100)$$

Soft-dominated Debye scale

$$m_D^2 \sim \frac{\alpha_s n_s}{k_s} \quad (5.101)$$

$$n_s \sim \frac{\alpha_s^{1/4} Q_s^3}{(Q_s \tau)^{1/2}} \quad (5.102)$$

$$m_D^2 \sim \frac{\alpha_s^{3/4} Q_s^2}{(Q_s \tau)^{1/2}} \quad (5.103)$$

Comparing these results to the contribution of the hard modes to the Debye mass, eq. (5.93), we can indeed see that now the soft particle contribution to the Debye mass is larger than that of the hard particles, as we anticipated when using Eq. (5.101) to estimate the Debye scale. Comparing the soft momentum scale (5.98) to the Debye scale, remembering that now $Q_s \tau \gg \alpha_s^{-3/2}$, we also see that $k_s \gg m_D$. This means that indeed, as assumed in the estimate (5.98), the soft particles need to accumulate their momentum through several collisions with the hard particles.

On the other hand, we have assumed that although the relative share of hard particles to the total gluon number density is decreasing, they still dominate the particle number density, i.e. $n_h \gg n_s$ (this was assumed e.g. when calculating the production rate for soft particles in eq. (5.100)). Let us now see when this condition ceases to be valid.

Stage ends:

$$n_h \sim \frac{Q_s^2}{\alpha_s \tau} \sim n_s \sim \frac{\alpha_s^{1/4} Q_s^3}{(Q_s \tau)^{1/2}} \implies Q_s \tau \sim \alpha_s^{-5/2} \quad (5.104)$$

Note that during this stage $\alpha_s^{-3/2} \ll Q_s \tau \ll \alpha_s^{-5/2}$ the occupation number of the hard modes has been $f_h \ll 1$ (Exercise: what is the time dependence? Note that this depends on the estimate (5.96) which is now modified both because there is no Bose enhancement and because the Debye mass is determined by the soft modes). The occupation number of the soft modes $f_s \sim n_s/k_s^3$, on the other hand, has been $\gg 1$ during this stage. They are, however, only a small part of the total number density, so overall the system has been underoccupied.

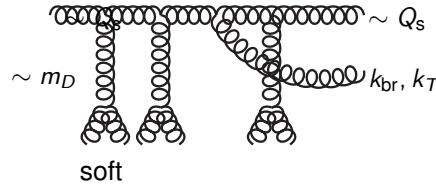
5.3.4 Last stage: energy loss

In the last stage of the development, most of the particle number is in the soft particles, whose momentum distribution is already isotropic. However, there is still a remaining collection of hard particles, which control the energy density. In order to isotropize the energy momentum tensor, they have to lose their energy. This happens when collisions with the soft particles leads to the hard particles losing their energy. In fact, we are doing a calculation of jet energy loss. The physical description of this last stage depends on the destructive interference between gluon emissions, i.e. the Landau-Pomeranchuk-Migdal (LPM) effect.

To get an estimate for how this works we look at a hard gluon, with energy $\sim Q_s$. It goes through a plasma of softer gluons, colliding with scattering centers in this plasma with a cross section $\sigma \sim \alpha_s^2/m_D^2$. The inverse mean free path of the particle in the plasma is the density of scattering centers times the cross section: $\lambda^{-1} \sim n_s \sigma$, this is how often the particle encounters a scattering target per unit time/length. A high energy particle will coherently see many scattering centers. If it propagates a time/distance t_f it will see t_f/λ of them, each time picking up a transverse momentum $\sim m_D^2$. Thus it will pick up a total transverse momentum $k_T^2 = m_D^2 t_f/\lambda$. What is then this formation time t_f ? The emission of a gluon with transverse momentum k_T and longitudinal momentum k_{br} means that one is emitting the gluon at an angle $\theta \approx k_T/k_{br}$. In order for the emission to really take place so that the emitted gluon and its parent are separate particles, the two-particle system has to propagate far enough that the coordinate separation between emitted gluon and parent, $t_f \theta$ is larger than the transverse size or wavelength of the emitted gluon k_T , i.e.

$$t_f \frac{k_T}{k_{br}} \sim k_T \implies t_f \sim \frac{k_{br}}{k_T^2} \quad (5.105)$$

Emitting a very high energy gluon takes a long time, this is what limits how fast you can lose energy by gluon emissions. Within this formation time t_f all the interactions with the target are coherent: the emitted gluon accumulates transverse momentum from all the scattering centers it sees on its way. Within this formation time, one can therefore emit only up to one gluon, in fact one emits one gluon with a probability α_s and zero gluons with probability $1 - \alpha_s$. Therefore the rate for emitting gluons with momentum k_{br} is $1/t_{br} \sim \alpha_s/t_f$, which depends on k_{br} . Since the formation time both determines how much transverse momentum one can accumulate from the medium, and depends on the transverse momentum itself, it has to be determined self-consistently in the following way:



LPM interference: max 1 emission during *formation time*

$$t_f \sim \frac{k_{br}}{k_T^2} \quad (5.106)$$

Mean free path

$$\frac{1}{\lambda} = n_s \sigma = n_s \frac{\alpha_s^2}{m_D^2} \quad (5.107)$$

$$k_T^2 = m_D^2 \frac{1}{\lambda} t_f \implies \frac{1}{t_f} \sim \frac{\alpha_s \sqrt{n_s}}{\sqrt{k_{br}}} \quad (5.108)$$

Emission rate

$$\frac{1}{t_{br}} = \frac{\alpha_s}{t_f} = \frac{\alpha_s^2 \sqrt{n_s}}{\sqrt{k_{br}}} \quad (5.109)$$

Now we have to determine how fast these kind of emissions lead to the hard particles losing all of their energy to the bath of soft particles, which already contains the particle number of the system. Again we have to self-consistently solve for two unknown quantities, the temperature of the bath T and the typical energy loss in a branching, k_{br} . To relate these we need two conditions. One is an equation that, through the medium density in eq. (5.109), relates the branching momentum to the temperature T . For this comparison we again need to equate, similarly to before, the rate of emissions to the lifetime of the system. The other one is

obtained from a comparison of the energy transfer from the hard particle to the medium to the rate of change of the temperature of the medium. In equations:

$$\frac{1}{t_{br}} \sim \frac{1}{\tau} \sim \frac{\alpha_s^2 T^{3/2}}{\sqrt{k_{br}}} \implies k_{br} \sim \alpha_s^4 T^3 \tau^2 \quad (5.110)$$

Energy flow (per unit volume)

$$k_{br} \frac{dN_{br}}{d\tau} = k_{br} \frac{n_h}{t_{br}} \sim k_{br} \frac{1}{\tau} \frac{Q_s^2}{\alpha_s \tau} = \frac{d(T^4)}{d\tau} \sim T^3 \frac{dT}{d\tau} \implies T \sim \alpha_s^3 Q_s^2 \tau \quad (5.111)$$

So the temperature of the soft gluon bath rises very rapidly! The hard gluons have lost all their energy when the temperature of the bath, and thus the energy lost in one branching, is of the same order as the original energy of the hard gluons:

$$k_{br} \sim \alpha_s^4 T^3 \tau^2 \sim Q_s \implies Q_s \tau \sim \alpha_s^{-13/5} \quad (5.112)$$

$$T_{final} \sim \alpha_s^{2/5} Q_s, \quad n_s^{final} \sim \alpha_s^{6/5} Q_s^3 \quad (5.113)$$

Another way to arrive at the same result is to argue in the following way. The energy of the system per unit rapidity, initially in the hard modes is

$$\frac{dE}{d\eta} \sim \frac{Q_s^3}{\alpha_s}. \quad (5.114)$$

The system is isotropic when all of this energy has moved to the soft modes with temperature T , energy density $\sim T^4$ and therefore energy per unit rapidity $\sim T^4 \tau$:

$$\frac{Q_s^3}{\alpha_s} \sim T^4 \tau. \quad (5.115)$$

Combining this equation with the requirement that the branching rate must be the same as the lifetime of the system (5.110) $\tau \sim t_{br}$ and the branching energy the same as the hard scale (5.112) $Q_s \sim k_{br}$, we get

$$\frac{Q_s^3}{\alpha_s} \sim T^4 \tau \quad \frac{1}{\tau} \sim \frac{\alpha_s^2 T^{3/2}}{\sqrt{Q_s}}, \quad (5.116)$$

from which one solves $Q_s \tau \sim \alpha_s^{-13/5}$.

This is a fascinating result: the formal weak coupling result for the isotropization time of the system is given by the fractional power $\alpha_s^{-13/5}$ of the coupling. The nontrivial result is a consequence of many physical processes in gauge theory contributing to different stages of the process. Let us recapitulate some of the necessary ingredients:

- Overoccupied $f \sim 1/\alpha_s$ initial condition dominated by perturbative scale Q_s
- Longitudinal expansion that tends to make the momentum distribution anisotropic
- Development of a softer scale m_D that is initially independent of α_s but later proportional to it, characterizing the collisions.
- Elastic scattering that tries to counteract the expansion and isotropize the momenta
- Inelastic scattering that creates a bath of softer gluons, increasing the particle number
- Interference, i.e. LPM effect, in the scattering of the remaining hard particles with this soft medium

It is nontrivial to build a quantitative calculation that includes all of these effects in a reasonable way. In fact, no one single calculation does so at the moment. Some state of the art methods used in these different stages are

1. Boost invariant CYM up to $Q_s \tau \sim 1$; matched in some way to information from nuclear wavefunctions that can be obtained from DIS.

2. 3-dimensional classical Yang-Mills can go from $Q_s \tau \sim 1$ to $Q_s \tau \sim \alpha_s^{-3/2}$ and has been seen to reproduce the first stage of the evolution process, demonstrating that the “bottom-up” scenario was the right one of several proposed weak coupling scaling solutions see e.g. [86]
3. After $Q_s \tau \gg 1$, when the occupation number has fallen below $1/\alpha_s$ due to some elastic scatterings taking place, one can use an effective kinetic theory description [87] that includes both elastic and inelastic interactions, Debye screening, and LPM interference, to evolve the system towards hydrodynamics. This was done e.g. in the calculation of [88].
4. The kinetic theory takes one close to isotropy so that the deviations from it are small; one can then match to viscous hydrodynamics which is a systematical way to treat systems close to local thermal equilibrium; again there is a common regime of validity for both theories.
5. In the earliest stages of this process, this is not actually the whole story. Anisotropic systems of gauge fields exhibit *plasma instabilities* that were not included in this picture. They affect the transition from stage 1 to 2, which in any case has been by far the sketchiest (i.e. no quantitative description at all) part in these lectures
6. In addition, there have been many studies of thermalization in the limit of strong coupling, but this would take us too far afield from the topic of these lectures.

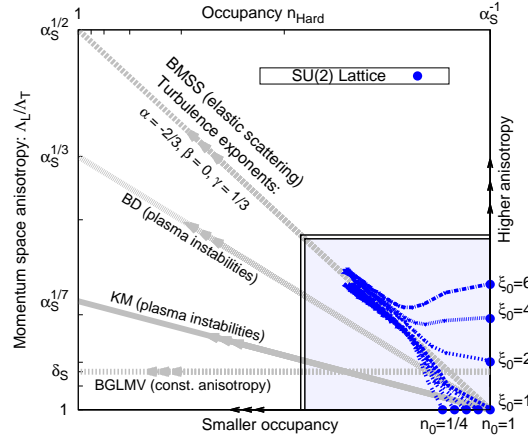
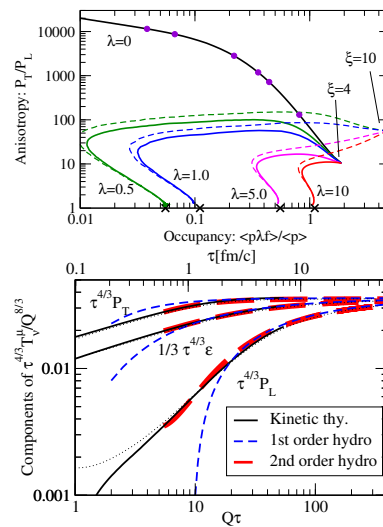


Figure 5.3: Comparison of CYM simulation from [86], compared to several proposed weak coupling scaling laws for the development of the occupation number and anisotropy in the 3-dimensional classical field phase.



These plots are from the effective kinetic theory simulation of [88], tracing the steps of the bottom-up thermalization scenario in an actual calculation.

Bibliography

- [1] Y. V. Kovchegov and E. Levin, *Quantum chromodynamics at high energy*, vol. 33. Cambridge University Press, 2012.
- [2] V. Barone and E. Predazzi, *High-Energy Particle Diffraction*, vol. v.565 of *Texts and Monographs in Physics*. Springer-Verlag, Berlin Heidelberg, 2002.
- [3] J. R. Forshaw and D. A. Ross, *Quantum Chromodynamics and the Pomeron*, vol. 9. Oxford University Press, 1998.
- [4] F. Gelis, *Initial state and thermalization in the Color Glass Condensate framework*, *Int. J. Mod. Phys. E* **24** (2015) 1530008 [[arXiv:1508.07974](#) [hep-ph]].
- [5] J. L. Albacete and C. Marquet, *Gluon saturation and initial conditions for relativistic heavy ion collisions*, *Prog. Part. Nucl. Phys.* **76** (2014) 1 [[arXiv:1401.4866](#) [hep-ph]].
- [6] S. Schlichting and D. Teaney, *The First fm/c of Heavy-Ion Collisions*, *Ann. Rev. Nucl. Part. Sci.* **69** (2019) 447 [[arXiv:1908.02113](#) [nucl-th]].
- [7] J. Berges, M. P. Heller, A. Mazeliauskas and R. Venugopalan, *QCD thermalization: Ab initio approaches and interdisciplinary connections*, *Rev. Mod. Phys.* **93** (2021) 035003 [[arXiv:2005.12299](#) [hep-th]].
- [8] E. Iancu and R. Venugopalan, *The Color glass condensate and high-energy scattering in QCD*, in *Quark-gluon plasma 4* (R. C. Hwa and X.-N. Wang, eds.), pp. 249–3363. 2003. [arXiv:hep-ph/0303204](#) [hep-ph].
- [9] F. Gelis, E. Iancu, J. Jalilian-Marian and R. Venugopalan, *The Color Glass Condensate*, *Ann. Rev. Nucl. Part. Sci.* **60** (2010) 463 [[arXiv:1002.0333](#) [hep-ph]].
- [10] T. Lappi, *Small x physics and RHIC data*, *Int. J. Mod. Phys. E* **20** (2011) 1 [[arXiv:1003.1852](#) [hep-ph]].
- [11] H. Weigert, *Evolution at small $x(bj)$: The Color glass condensate*, *Prog. Part. Nucl. Phys.* **55** (2005) 461 [[arXiv:hep-ph/0501087](#) [hep-ph]].
- [12] J. Jalilian-Marian and Y. V. Kovchegov, *Saturation physics and deuteron-Gold collisions at RHIC*, *Prog. Part. Nucl. Phys.* **56** (2006) 104 [[arXiv:hep-ph/0505052](#) [hep-ph]].
- [13] F. Gelis, T. Lappi and R. Venugopalan, *High energy scattering in Quantum Chromodynamics*, *Int. J. Mod. Phys. E* **16** (2007) 2595 [[arXiv:0708.0047](#) [hep-ph]].
- [14] S. J. Brodsky, H.-C. Pauli and S. S. Pinsky, *Quantum chromodynamics and other field theories on the light cone*, *Phys. Rept.* **301** (1998) 299 [[arXiv:hep-ph/9705477](#) [hep-ph]].
- [15] C. Marquet, *Chromodynamique quantique à haute énergie, théorie et phénoménologie appliquée aux collisions de hadrons*, 2006. PhD thesis, Paris, LPTHE. <https://tel.archives-ouvertes.fr/tel-00096416/fr/>.
- [16] H. Hänninen, *Deep inelastic scattering in the dipole picture at next-to-leading order*. PhD thesis, Jyväskylä U., Jyväskylä U., 2021. [arXiv:2112.08818](#) [hep-ph].

- [17] **Particle Data Group** collaboration, P. A. Zyla *et. al.*, *Review of Particle Physics*, *PTEP* **2020** (2020) 083C01.
- [18] A. Accardi *et. al.*, *Electron Ion Collider: The Next QCD Frontier: Understanding the glue that binds us all*, *Eur. Phys. J. A* **52** (2016) 268 [[arXiv:1212.1701](#) [[nucl-ex](#)]].
- [19] R. Abdul Khalek *et. al.*, *Science Requirements and Detector Concepts for the Electron-Ion Collider: EIC Yellow Report*, [arXiv:2103.05419](#) [[physics.ins-det](#)].
- [20] **LHeC Study Group** collaboration, J. L. Abelleira Fernandez *et. al.*, *A Large Hadron Electron Collider at CERN: Report on the Physics and Design Concepts for Machine and Detector*, *J. Phys. G* **39** (2012) 075001 [[arXiv:1206.2913](#) [[physics.acc-ph](#)]].
- [21] J. D. Bjorken, J. B. Kogut and D. E. Soper, *Quantum Electrodynamics at Infinite Momentum: Scattering from an External Field*, *Phys. Rev.* **D3** (1971) 1382.
- [22] T. Regge, *Introduction to complex orbital momenta*, *Nuovo Cim.* **14** (1959) 951.
- [23] A. Donnachie and P. V. Landshoff, *Total cross-sections*, *Phys. Lett. B* **296** (1992) 227 [[arXiv:hep-ph/9209205](#)].
- [24] P. Desgrolard, M. Giffon, E. Martynov and E. Predazzi, *Exchange degenerate Regge trajectories: A Fresh look from resonance and forward scattering regions*, *Eur. Phys. J. C* **18** (2001) 555 [[arXiv:hep-ph/0006244](#)].
- [25] A. V. Barnes, D. J. Mellema, A. V. Tollestrup, R. L. Walker, O. I. Dahl, R. A. Johnson, R. W. Kenney and M. Pripstein, *Pion Charge Exchange Scattering at High-Energies*, *Phys. Rev. Lett.* **37** (1976) 76.
- [26] E. A. Kuraev, L. N. Lipatov and V. S. Fadin, *The Pomeron Singularity in Nonabelian Gauge Theories*, *Sov. Phys. JETP* **45** (1977) 199.
- [27] I. I. Balitsky and L. N. Lipatov, *The Pomeron Singularity in Quantum Chromodynamics*, *Sov. J. Nucl. Phys.* **28** (1978) 822.
- [28] **ALICE** collaboration, B. Abelev *et. al.*, *Transverse momentum distribution and nuclear modification factor of charged particles in p-Pb collisions at $\sqrt{s_{NN}} = 5.02$ TeV*, *Phys. Rev. Lett.* **110** (2013) 082302 [[arXiv:1210.4520](#) [[nucl-ex](#)]].
- [29] **LHCb** collaboration, R. Aaij *et. al.*, *Measurement of the Nuclear Modification Factor and Prompt Charged Particle Production in p – Pb and pp Collisions at $\sqrt{s_{NN}}=5$ TeV*, *Phys. Rev. Lett.* **128** (2022) 142004 [[arXiv:2108.13115](#) [[hep-ex](#)]].
- [30] **LHCb** collaboration, *Nuclear modification factor of neutral pions in the forward and backward regions in pPb collisions*, [arXiv:2204.10608](#) [[nucl-ex](#)].
- [31] G. Beuf, *Dipole factorization for DIS at NLO: Loop correction to the $\gamma_{T,L}^* \rightarrow q\bar{q}$ light-front wave functions*, *Phys. Rev. D* **94** (2016) 054016 [[arXiv:1606.00777](#) [[hep-ph](#)]].
- [32] G. Beuf, *Dipole factorization for DIS at NLO: Combining the $q\bar{q}$ and $q\bar{q}g$ contributions*, *Phys. Rev. D* **96** (2017) 074033 [[arXiv:1708.06557](#) [[hep-ph](#)]].
- [33] T. Lappi and R. Paatelainen, *The one loop gluon emission light cone wave function*, *Annals Phys.* **379** (2017) 34 [[arXiv:1611.00497](#) [[hep-ph](#)]].
- [34] H. Hänninen, T. Lappi and R. Paatelainen, *One-loop corrections to light cone wave functions: the dipole picture DIS cross section*, *Annals Phys.* **393** (2018) 358 [[arXiv:1711.08207](#) [[hep-ph](#)]].
- [35] G. Beuf, T. Lappi and R. Paatelainen, *Massive quarks in NLO dipole factorization for DIS: Longitudinal photon*, *Phys. Rev. D* **104** (2021) 056032 [[arXiv:2103.14549](#) [[hep-ph](#)]].
- [36] G. Beuf, T. Lappi and R. Paatelainen, *Massive Quarks at One Loop in the Dipole Picture of Deep Inelastic Scattering*, *Phys. Rev. Lett.* **129** (2022) 072001 [[arXiv:2112.03158](#) [[hep-ph](#)]].

- [37] G. Beuf, T. Lappi and R. Paatelainen, *Massive quarks in NLO dipole factorization for DIS: Transverse photon*, *Phys. Rev. D* **106** (2022) 034013 [[arXiv:2204.02486 \[hep-ph\]](#)].
- [38] L. D. McLerran and R. Venugopalan, *Gluon distribution functions for very large nuclei at small transverse momentum*, *Phys. Rev.* **D49** (1994) 3352 [[arXiv:hep-ph/9311205 \[hep-ph\]](#)].
- [39] L. D. McLerran and R. Venugopalan, *Computing quark and gluon distribution functions for very large nuclei*, *Phys. Rev.* **D49** (1994) 2233 [[arXiv:hep-ph/9309289 \[hep-ph\]](#)].
- [40] L. D. McLerran and R. Venugopalan, *Green's functions in the color field of a large nucleus*, *Phys. Rev.* **D50** (1994) 2225 [[arXiv:hep-ph/9402335 \[hep-ph\]](#)].
- [41] I. Balitsky, *Operator expansion for high-energy scattering*, *Nucl. Phys.* **B463** (1996) 99 [[arXiv:hep-ph/9509348](#)].
- [42] Y. V. Kovchegov, *Unitarization of the BFKL pomeron on a nucleus*, *Phys. Rev.* **D61** (2000) 074018 [[arXiv:hep-ph/9905214](#)].
- [43] Y. V. Kovchegov, *Small- x F2 structure function of a nucleus including multiple pomeron exchanges*, *Phys. Rev.* **D60** (1999) 034008 [[arXiv:hep-ph/9901281](#)].
- [44] J. Jalilian-Marian, A. Kovner, L. D. McLerran and H. Weigert, *The intrinsic glue distribution at very small x* , *Phys. Rev.* **D55** (1997) 5414 [[arXiv:hep-ph/9606337 \[hep-ph\]](#)].
- [45] J. Jalilian-Marian, A. Kovner, A. Leonidov and H. Weigert, *The BFKL equation from the Wilson renormalization group*, *Nucl. Phys.* **B504** (1997) 415 [[arXiv:hep-ph/9701284](#)].
- [46] J. Jalilian-Marian, A. Kovner, A. Leonidov and H. Weigert, *The Wilson renormalization group for low x physics: Towards the high density regime*, *Phys. Rev.* **D59** (1998) 014014 [[arXiv:hep-ph/9706377](#)].
- [47] J. Jalilian-Marian, A. Kovner and H. Weigert, *The Wilson renormalization group for low x physics: Gluon evolution at finite parton density*, *Phys. Rev.* **D59** (1998) 014015 [[arXiv:hep-ph/9709432](#)].
- [48] J. Jalilian-Marian, A. Kovner, A. Leonidov and H. Weigert, *Unitarization of gluon distribution in the doubly logarithmic regime at high density*, *Phys. Rev.* **D59** (1999) 034007 [[arXiv:hep-ph/9807462](#)].
- [49] E. Iancu, A. Leonidov and L. D. McLerran, *Nonlinear gluon evolution in the color glass condensate. I*, *Nucl. Phys.* **A692** (2001) 583 [[arXiv:hep-ph/0011241](#)].
- [50] E. Ferreiro, E. Iancu, A. Leonidov and L. McLerran, *Nonlinear gluon evolution in the color glass condensate. II*, *Nucl. Phys.* **A703** (2002) 489 [[arXiv:hep-ph/0109115](#)].
- [51] A. H. Mueller, *A simple derivation of the JIMWLK equation*, *Phys. Lett.* **B523** (2001) 243 [[arXiv:hep-ph/0110169](#)].
- [52] C. Marquet, *Forward inclusive dijet production and azimuthal correlations in $p(A)$ collisions*, *Nucl. Phys. A* **796** (2007) 41 [[arXiv:0708.0231 \[hep-ph\]](#)].
- [53] A. Dumitru, A. Hayashigaki and J. Jalilian-Marian, *The Color glass condensate and hadron production in the forward region*, *Nucl. Phys. A* **765** (2006) 464 [[arXiv:hep-ph/0506308](#)].
- [54] G. A. Chirilli, B.-W. Xiao and F. Yuan, *One-loop Factorization for Inclusive Hadron Production in pA Collisions in the Saturation Formalism*, *Phys. Rev. Lett.* **108** (2012) 122301 [[arXiv:1112.1061 \[hep-ph\]](#)].
- [55] G. A. Chirilli, B.-W. Xiao and F. Yuan, *Inclusive Hadron Productions in pA Collisions*, *Phys. Rev. D* **86** (2012) 054005 [[arXiv:1203.6139 \[hep-ph\]](#)].
- [56] B. Ducloué, T. Lappi and Y. Zhu, *Implementation of NLO high energy factorization in single inclusive forward hadron production*, *Phys. Rev. D* **95** (2017) 114007 [[arXiv:1703.04962 \[hep-ph\]](#)].

- [57] E. Iancu, A. H. Mueller and D. N. Triantafyllopoulos, *CGC factorization for forward particle production in proton-nucleus collisions at next-to-leading order*, *JHEP* **12** (2016) 041 [[arXiv:1608.05293 \[hep-ph\]](#)].
- [58] R. K. Ellis, W. J. Stirling and B. R. Webber, *QCD and collider physics*, vol. 8. Cambridge University Press, 2, 2011.
- [59] M. Li, *Mesons on the light front*, [arXiv:2212.05100 \[hep-ph\]](#).
- [60] P. A. M. Dirac, *Forms of Relativistic Dynamics*, *Rev. Mod. Phys.* **21** (1949) 392.
- [61] W.-M. Zhang and A. Harindranath, *Role of longitudinal boundary integrals in light front QCD*, *Phys. Rev. D* **48** (1993) 4868 [[arXiv:hep-th/9302119](#)].
- [62] M. Tevio, *Quark mass renormalization in perturbative quantum chromodynamics in light-cone gauge*, 2020. <https://jyx.jyu.fi/handle/123456789/73127>.
- [63] H. C. Pauli, *A compendium of light cone quantization*, *Nucl. Phys. Proc. Suppl.* **90** (2000) 259 [[arXiv:hep-ph/0103106 \[hep-ph\]](#)]. [,259(2000)].
- [64] A. H. Mueller, *Soft gluons in the infinite momentum wave function and the BFKL pomeron*, *Nucl. Phys. B* **415** (1994) 373.
- [65] H. Mäntysaari, *Balitsky-Kovchegov equation*, 2011. <https://jyx.jyu.fi/handle/123456789/37095>.
- [66] T. Lappi and H. Mäntysaari, *On the running coupling in the JIMWLK equation*, *Eur. Phys. J. C* **73** (2013) 2307 [[arXiv:1212.4825 \[hep-ph\]](#)].
- [67] A. Dumitru, J. Jalilian-Marian, T. Lappi, B. Schenke and R. Venugopalan, *Renormalization group evolution of multi-gluon correlators in high energy QCD*, *Phys. Lett. B* **706** (2011) 219 [[arXiv:1108.4764 \[hep-ph\]](#)].
- [68] E. Iancu, K. Itakura and L. McLerran, *A Gaussian effective theory for gluon saturation*, *Nucl. Phys. A* **724** (2003) 181 [[arXiv:hep-ph/0212123](#)].
- [69] J. P. Blaizot, F. Gelis and R. Venugopalan, *High-energy pA collisions in the color glass condensate approach. 2. Quark production*, *Nucl. Phys. A* **743** (2004) 57 [[arXiv:hep-ph/0402257](#)].
- [70] F. Gelis, A. M. Stasto and R. Venugopalan, *Limiting fragmentation in hadron-hadron collisions at high energies*, *Eur. Phys. J. C* **48** (2006) 489 [[arXiv:hep-ph/0605087](#)].
- [71] F. Dominguez, C. Marquet and B. Wu, *On multiple scatterings of mesons in hot and cold QCD matter*, *Nucl. Phys. A* **823** (2009) 99 [[arXiv:0812.3878 \[nucl-th\]](#)].
- [72] F. Dominguez, C. Marquet, B.-W. Xiao and F. Yuan, *Universality of Unintegrated Gluon Distributions at small x*, *Phys. Rev. D* **83** (2011) 105005 [[arXiv:1101.0715 \[hep-ph\]](#)].
- [73] B. Schenke, P. Tribedy and R. Venugopalan, *Fluctuating Glasma initial conditions and flow in heavy ion collisions*, *Phys. Rev. Lett.* **108** (2012) 252301 [[arXiv:1202.6646 \[nucl-th\]](#)].
- [74] T. Lappi, *Wilson line correlator in the MV model: Relating the glasma to deep inelastic scattering*, *Eur. Phys. J. C* **55** (2008) 285 [[arXiv:0711.3039 \[hep-ph\]](#)].
- [75] J. Jalilian-Marian, A. Kovner, L. D. McLerran and H. Weigert, *The intrinsic glue distribution at very small x*, in *Phys. Rev.* [44], pp. 5414–5428, [[arXiv:hep-ph/9606337 \[hep-ph\]](#)].
- [76] T. Lappi and S. Schlichting, *Linearly polarized gluons and axial charge fluctuations in the Glasma*, *Phys. Rev. D* **97** (2018) 034034 [[arXiv:1708.08625 \[hep-ph\]](#)].
- [77] A. Kovner, L. D. McLerran and H. Weigert, *Gluon production from nonAbelian Weizsacker-Williams fields in nucleus-nucleus collisions*, *Phys. Rev. D* **52** (1995) 6231 [[arXiv:hep-ph/9502289 \[hep-ph\]](#)].

- [78] Y. V. Kovchegov and D. H. Rischke, *Classical gluon radiation in ultrarelativistic nucleus-nucleus collisions*, *Phys. Rev.* **C56** (1997) 1084 [[arXiv:hep-ph/9704201](#) [hep-ph]].
- [79] J. P. Blaizot, F. Gelis and R. Venugopalan, *High-energy pA collisions in the color glass condensate approach. I. Gluon production and the Cronin effect*, *Nucl. Phys.* **A743** (2004) 13 [[arXiv:hep-ph/0402256](#) [hep-ph]].
- [80] T. Epelbaum and F. Gelis, *Pressure isotropization in high energy heavy ion collisions*, *Phys. Rev. Lett.* **111** (2013) 232301 [[arXiv:1307.2214](#) [hep-ph]].
- [81] A. Dumitru and L. D. McLerran, *How protons shatter colored glass*, *Nucl. Phys. A* **700** (2002) 492 [[arXiv:hep-ph/0105268](#)].
- [82] J. P. Blaizot, T. Lappi and Y. Mehtar-Tani, *On the gluon spectrum in the glasma*, *Nucl. Phys.* **A846** (2010) 63 [[arXiv:1005.0955](#) [hep-ph]].
- [83] P. Tribedy and R. Venugopalan, *QCD saturation at the LHC: Comparisons of models to $p + p$ and $A + A$ data and predictions for $p + Pb$ collisions*, *Phys. Lett.* **B710** (2012) 125 [[arXiv:1112.2445](#) [hep-ph]]. [Erratum: *Phys. Lett.* **B718**, 1154(2013)].
- [84] J. L. Albacete, A. Dumitru, H. Fujii and Y. Nara, *CGC predictions for $p + Pb$ collisions at the LHC*, *Nucl. Phys. A* **897** (2013) 1 [[arXiv:1209.2001](#) [hep-ph]].
- [85] R. Baier, A. H. Mueller, D. Schiff and D. T. Son, *'Bottom up' thermalization in heavy ion collisions*, *Phys. Lett.* **B502** (2001) 51 [[arXiv:hep-ph/0009237](#) [hep-ph]].
- [86] J. Berges, K. Boguslavski, S. Schlichting and R. Venugopalan, *Universal attractor in a highly occupied non-Abelian plasma*, *Phys. Rev.* **D89** (2014) 114007 [[arXiv:1311.3005](#) [hep-ph]].
- [87] P. B. Arnold, G. D. Moore and L. G. Yaffe, *Effective kinetic theory for high temperature gauge theories*, *JHEP* **01** (2003) 030 [[arXiv:hep-ph/0209353](#) [hep-ph]].
- [88] A. Kurkela and Y. Zhu, *Isotropization and hydrodynamization in weakly coupled heavy-ion collisions*, *Phys. Rev. Lett.* **115** (2015) 182301 [[arXiv:1506.06647](#) [hep-ph]].